2013

Polyanhydride particle platform for design of novel influenza vaccines

Lucas Mark Huntimer
Iowa State University

Polyanhydride particle platform for design of novel influenza vaccines

by

Lucas Mark Huntimer

A dissertation submitted to the graduate faculty

in partial fulfillment of the requirements for the degree of

DOCTOR OF PHILOSOPHY

Major: Immunobiology

Program of Study Committee:

Michael Wannemuehler, Major Professor

Balaji Narasimhan

Cathy Miller

Marian Kohut

W. Ray Waters

Iowa State University

Ames, Iowa

2013

TABLE OF CONTENTS

ABSTRACT

Vaccines remain the most effective medical intervention to disease in which effective vaccines are available. Designing vaccines that elicit protective immunity while minimizing adverse events is difficult. Exacerbating the challenges of vaccine design is the increased emphasis on using pure preparation of antigens that alleviate safety concerns but also show decreased potency. Therefore the need for safe adjuvants to boost immunity of subunit immunizations is great. This work demonstrates the capability of a novel bio-erodible polyanhydride particle platform to enhance humoral and cellular immunity. Encapsulation of 25 μg of Ovalbumin (Ova) antigen in microparticles elicits humoral immune responses equivalent to 1600, 400, and 100 μg dosages of Ova. Characterizing the persistence of the nanoparticle platform shows that in vivo persistence and immunomodulatory activity can be tailored by altering copolymer chemistry. Polyanhydride nanoparticle vaccines against Ova show an increased ability to expand $CD8^+$ T cells as compared to Alum and soluble Ova. These same polyanhydride nanoparticle vaccines expand $CD4^+$ T cells and promote a T follicular helper ($CXCR5^{high}$ $PD\text{-}1^{high}$) cell phenotype important for germinal center formation. The polyanhydride platform designed vaccines against H5N1 using a stabilized trimeric H5 antigen were evaluated in multiple dose and route regimens and elicit neutralizing antibody activity and expanded $CD4^+$ cellular recall responses

when administered subcutaneously. These results demonstrate that the polyanhydride particle platform can be used to effectively enhance immune responses in subunit immunizations.

CHAPTER 1: GENERAL INTRODUCTION AND LITERATURE REVIEW

Introduction

Vaccinology

Preventive immunizations remains the most effective therapeutic intervention to disease [1]. In 1742, the modern era of immunization began with crude preparations of cowpox from lesions administered by Edward Jenner to individuals to prevent smallpox. This process was initially termed variolation and this milestone in health history both led to insight into mechanism of the evolved mammalian immune system as well as establishing immunization as a preventive therapy. Using an attenuated cowpox organism to prevent infection by a more virulent smallpox organism was the first designed vaccine and the same basic principle for vaccine design is used today. Attenuated whole organisms replicate in vivo, establish low levels of infection, and train the adaptive immune system to respond to a more virulent version of the attenuated organism. Attenuating organisms present many problems however.

Establishing attenuated organisms can be very difficult due to unforeseen genetic mutations of the organism, safety concerns associated with attenuating the organism in production, reversion to wild-type, and shedding of organisms into the environment [2]. Compounding the difficulties associated with attenuated vaccine strains one must consider the complications presented when using whole cell organisms or lysates as vaccine preparations. For example, whole cell lysates contain a myriad of phlogistic components in addition to the target immunogen

creating problems with purity with the preparation and adverse reactions after administration. Whole cell preparations, whether viable or killed, contain components of the organism that may lead to undesired inflammatory reactions because of conserved microbe associated molecular patterns (MAMPS) that ligate pattern recognition receptors (PRRs) of the innate immune system, masking immunodominant epitopes, and replicating mechanisms that may incorporate into the genome in the cases of attenuated viruses [3-5].

The subsequent 200 years in vaccine design has evolved. Many of the same challenges persist in attempting to recapitulate a low level infection to prevent a more detrimental infection later but at the same time not cause overwhelming harm to the host as a consequence of immunizations. Inactivation of pathogenic organisms was an initial alternative to producing attenuated organisms. Inactivation of organisms leads to complications with antigenic structures, complications of inactivating chemicals (i.e. reactive carbonyl groups on proteins), as well as being unable to alleviate the MAMPS of an organism that cause detrimental inflammation and adverse reactions [6].

There is a trade off in the benefits of whole cell antigenic preparations. Whole cell preparations have the benefit of containing multiple MAMPS that specifically and non-specifically act to activate the innate immune system augmenting downstream adaptive immune responses [7]. Those same ligands may also lead to detrimental non-specific side-effects including inflammation and pain at the site of administration. Whole cell antigen preparations also benefit in activation of the immune system by providing particulate structure for phagocytic antigen presenting

cells (APCs) to uptake the antigen and process for antigen presentation. Finally, whole cell preparations also allow for multiple epitopes to be served up as antigenic targets.

Examining alternatives to the use of crude whole cell antigen preparations led to methods in which pathogenic organisms were essentially lysed or broken apart and components were purified for the purposes of antigenic preparations [8]. These lysed antigenic preparations led to increases in purity, which help to alleviate non-specific adverse events associated with whole cell vaccines as well as focusing immune responses towards the antigens of interest.

Advances in recombinant technology have led to relative ease in production of highly purified proteins. This advance in ability to produce and purify proteins of interest based on sequence has pushed vaccine antigens to be highly purified, essentially having vaccine antigenic preparations consisting of only the antigen of interest and not blanketed with other epitopes as would be the case with whole cell vaccines. These vast improvements in purity, and the subsequent reduction in adverse events associated with the vaccine, have consequently resulted in less robust immune responses because of the elimination of the non-specific immune stimulation provided by MAMPs and limiting the number of epitopes to which the host can respond.

Understanding the immunological mechanisms that elicit lifelong protection following administration of efficacious vaccines like the highly successful yellow fever vaccine or polio virus vaccine [9-11], as well as the vaccine-induced mechanisms that cause deleterious effects following immunization with the

respiratory syncytial virus incidences of increased disease after administration of a formalin inactivated vaccine [12], will pave the road for understanding mechanisms to design next generation vaccines using highly pure antigenic preparations.

History of efficacious vaccines

As stated earlier, vaccines and the subsequent immune responses elicited by them are dependent on different factors in the vaccine preparation (e.g. antigen(s) and adjuvant) as well as the route of immunization and genetics/health of the vaccinee. The earliest vaccine developed was the attenuated smallpox variolation by Edward Jenner, essentially using an attenuated version of a smallpox virus that elicited protection from the lethal smallpox virus [13]. The whole cell *Bordetella pertussis* vaccine against whooping cough best exemplifies the classic structure of many vaccines discovered and employed in the early to mid twentieth century (commonly referred to as first generation vaccines). In 1933, isolated whole cell *B. pertussis* was administered as a preventive and therapeutic treatment against whooping cough and provided a modicum of protection and treatment indicating efficacy [14]. Many adaptations to the whole cell preparation were tested afterwards and the consensus antigenic preparation of the pertussis vaccine consisted of washed, concentrated, and inactivated (either by heat of chemical) whole *B. pertussis* [15]. The pertussis vaccine is now commonly administered in conjunction with toxoids (DTP) prepared from the toxins from *Corynebacterium diphtheriae* and *Clostridium tetani* and the immunization regimen consists of three treatments within the first year of life with booster immunizations recommended at 2 and 4-6 years of

age [16]. This relatively simple vaccine preparation where a pathogenic organism is isolated from a diseased individual, grown, attenuated or inactivated, and administered as vaccine antigen was, and is, employed for many of the vaccines (influenza virus, polio virus, hepatitis A virus, Measels, Mumps, Rubella, Varicella, Rotavirus, *Salmonella typhimurium*, Yellow fever virus, and Bacillus of Calmette and Guerin (BCG)) used today [17].

The pertussis vaccine also presents a great allegory into how our increased understanding of the immune system and the parallel increased emphasis on drug safety has led to a refined focus in next generation vaccine design. Whole cell pertussis vaccines (as would all whole cell bacterin vaccines) contained endotoxin which would induce adverse vaccine events such as fever (and earlier febrile seizures in children), arthus reactions, and pain at the injection site in some people [15, 18]. First occurrences of epileptic seizures is hastened by whole cell pertussis vaccine administration to epileptic children (often times diagnosed after immunization) [19]. These adverse events led to a shift towards use of an acellular pertussis vaccine consisting of purified bacterial components of *B. pertussis*. A randomized controlled trial in Sweden demonstrated increased efficacy with an improved safety profile of a five *B. pertussis* component (glutaraldehyde-inactivated pertussis toxin, filamentous hemagglutinin, 2 and 3 combined, and pertactin) acellular DTP vaccine as compared to a two component acellular DTP and a whole cell DTP vaccine [20].

Next generation vaccine design

First generation vaccine design was relatively simple: isolate pathogenic organism, culture pure organism, attenuate or kill organism, and make a vaccine [21]. We now know that the “crude” method will not continue to fulfill the standards of safety that public and the regulatory agencies governing medical interventions expect and rightly so. The shift in focus towards vaccines of increasing purity to improve safety directs the design of next generation vaccines [22]. The increasing advancements in recombinant technology also push vaccinology to new heights by allowing for manufacture of purified antigens to be used in immunization. This increase in purity often leads to decreases in efficacy of the vaccine as compared to the traditional whole cell formulations. This decrease in efficacy indicates a need for adjuvants (non-specific immune stimulators) and booster immunizations to increase potency and efficacy.

Adjuvants are commonly referred to as immunologists “dirty little secret” because of their use in many first generation vaccine formulations, as well as tools in research, without the knowledge defining the exact mechanisms as to how adjuvants augment an immune response [23]. Many elegant reviews have now outlined general principles of adjuvants and how their use in vaccine design leads to enhanced immune responses [21, 22, 24-26]. Here, we outline the general principles of what adjuvants can do to improve vaccine efficacy.

Particulate antigen

Recombinant technology allows for production of large quantities of purified

proteins from a pathogen that are known, or suspected, to be important for the induction of a protective immune response. The *raison d'être* of immunization is to capitulate an infection to "train" the adaptive immune response (i.e. cellular and humoral immunity) so that there is immunological memory to respond to a much more serious pathogenic infection at a later time. This process is dependent on the antigen(s) and the ability of the antigens to engage with the phagocytic APCs of the innate immune system.

Innate immunity serves as the initial barrier to protect the host from infection. Anatomical and physiologic barriers such as skin, cilia, hair, and degradative enzymes found on mucosal surfaces all serve protective functions of exclusion of pathogens from the host [23, 27]. The cellular component of the innate immune system consists of leukocytes that circulate throughout the host to monitor and maintain homeostasis. These leukocytes consist of mast cells, natural killer cells, basophils, and eosinophils with specialized effector functions which will not be discussed here. The other major components of the innate leukocyte population of interest in vaccine design are the phagocytic macrophages, neutrophils, and dendritic cells. The phagocytic cell populations fulfill varying levels of antigen presentation functions for initiating adaptive immune responses in the secondary lymphoid tissues with the most professional antigen presentation being performed by the dendritic cells (with varying subsets), then the macrophages and some presentation by neutrophils [28-31].

For the initial purpose of targeting the antigen towards these critically important cell populations, it is key for vaccines to have a particulate structure [32,

33]. Recombinant antigens are quite miniscule in scale as compared to the corresponding whole cell or virion that the antigens are derived from. By having the antigen delivered in the context of a particulate structure, the APCs of the innate immune system can phagocytose the antigen similar to the process the APCs would use to clear viruses or bacteria.

Common adjuvants used for many years in immunological research, as well as some current vaccines, do provide a particulate structure when adjuvanting protein antigens. Liposomes, virosomes, synthetic particles (nano, micro), immunostimulatory complexes (ISCOMs), aluminum salts (Alum), water-in-oil emulsions (Freund's adjuvant), and oil-in-water emulsions (MF59) all create a particular structure when combined with antigen that is larger than soluble antigens as well as mimicking the size of the pathogens being targeted against [24].

APCs (dendritic cells (DCs) and macrophages) bridge the chasm between innate and adaptive immunity by continued immune surveillance in the tissues and phagocytosing foreign substances [34]. APC interaction with antigen, whether in the form of the pathogen or particulate structure, can be directly affected by the size. Rettig et al found that particles containing the same Toll-like receptor (TLR) ligand that activates plasmactyoid dendritic cells (pDCs) to mature and secrete pro-inflammatory cytokines show different cytokine profiles when particles are ~220 μm compared to ~1200 μm particles [35]. The smaller particles led to more IFN-α, a typical anti-viral inflammatory cytokine response, and larger particles led to a more TNF-α indicating a more pleiotropic inflammatory response.

Phagocytosis of antigens by APCs leads to intracellular trafficking towards a

phagolysomal compartment where the antigens can be broken down for presentation to the adaptive immune system by lysomal degradative enzymes [36]. The interaction of the phagosome compartment containing the phagocytosed materials and the subsequent lysosome fusion may be effected by the particle size phagocytosed [37]. The optimal size for phagocytosis of particles and antigenic particles is < 500 μm as compared to larger materials [38-42]. Particles of < 200 nm are able to directly drain to secondary lymphoid tissue by lymphatic vessels and arrive in the lymph nodes within minutes while particles 200 to 500 nm in diameter do so less efficiently [43]. In contrast, particles of 200 nm to 2 μm in diameter require APC trafficking for optimal delivery to lymph tissue arriving approximately 24 hours after administration [41].

Particulate antigen also benefits from controlled presentation to T cells and B cells in the secondary lymphoid tissue. The conduit system transfers and shuttles soluble antigen to initiate early primary immune responses (i.e., expansion and differentiation of naïve antigen specific T cells and B cells) in the secondary lymphoid tissue [44-46]. Particulate antigens, while being phagocytosed and trafficked to secondary lymphoid tissues through the traditional APC maturation pathway as well as being captured by macrophages in the medulla, benefit from sustained presentation to follicular B cells by subscapular sinus macrophages [47]. Subscapular sinus macrophages provide a sustained presentation of particulate antigens to follicular dendritic cells, a specialized cell in the secondary lymphoid follicles that retains immune complexes on the surface via complement receptors [48]. These follicular dendritic cells can then retain immune complexes on their

surface for continued antigen presentation resulting in retention of B cells in the germinal center and generation of affinity matured memory B cells and plasma cells [49, 50].

Creating a particulate antigen for design of vaccines produces a larger surface area of the particle for receptor or membrane interaction with the APC(s). Particulate antigens also present charge differences that dictate APC interaction with the particle. Protein opsonins or humoral pattern recognition molecules (PRMs) such as innate natural IgM, complement protein components, pentraxins, and serum amyloid proteins all bind to repetitive structures in vivo which lead to subsequent Fc or complement receptor based interaction and phagocytosis by APCs [51-53]. Particulate antigens provide this repetitive structure. Hydrophobicity of the particulate antigens plays an important role in the binding of the protein opsonins as well [54, 55]. Many of the protein opsonins are thought to be evolutionarily early forms of antibodies, or innate antibodies in the case of natural IgM, that function to bind to hydrophobic residues for targeting to phagocytes for degradation or antigen presentation [43, 56-58].

Repetitive structure

Pathogens, especially viruses, often contain a highly ordered surface structure of proteins, carbohydrates and/or lipids. These highly ordered surface structure are important for engaging the conserved ‘danger’ signaling mechanisms of the innate immune system as the host does not often exhibit such order [59]. Particulate antigens that exploit the repetitive structure show a strong induction of

IgM because they are able to engage B cell receptors directly leading to T cell independent antibody responses solely based on antigen repetition at approximately 5-10 nm apart [60]. All vaccines adjuvanted to create particulate antigens most likely exhibit some antigen repetitiveness as compared to soluble antigens.

Virus-like particles (VLPs) are the most efficient particulate antigen system at achieving this 5 to 10 nm particulate spacing [26]. Translation of the capsid protein in conjunction with the surface proteins, or antigens, of interest results in a virus particle devoid of nucleic acid material making it effectively neutered from replication [61]. Many different VLP constructs have been produced and using molecular genetics techniques allows for many proteins to be expressed on the VLP surface [61, 62].

Emulsion based adjuvants are used to create particulate of varying sizes based on differences in oils and techniques used. Oil based adjuvants have long been used in vaccines with complete Freund's adjuvant (CFA) consisting of a water in mineral oil emulsion with dried and inactivated Mycobacteria added as an immunopotentiator. Incomplete Freund's (IFA) is the water in oil (W/O) emulsion without the Mycobacteria. Presumably the antigen would be ordered in the emulsion particles especially in W/O adjuvants that retain the antigen in the particle for up to 3 weeks in vitro compared to water-oil-water (W/O/W) and oil in water (O/W) (equivalent of MF59) emulsions [63].

Biodegradable particle adjuvant systems could provide the same repetitive antigenic structure. Antigens are often encapsulated into biodegradable materials such as poly(dl-lactic-co-glycolic acid) (PLGA), poly(amino acid)s, and

polyanhydrides all effectively augment the induction of an immune responses [64, 65]. Many different size ranges can effectively be created by altering fabrication processes with these biomaterials thus leading to antigen dispersal within the particle. Small amounts of antigen in a large diameter particle may lead to large gaps between antigens on the surface of the particles while that same amount of antigen in smaller diameter particle will lead to tighter spacing of antigens thus effectively poising the particle for B-cell receptor ligation.

Jegerlehner et al demonstrate that IgG, but not IgM, can be enhanced with this structured spacing of antigen using nanoparticles expressing 60 epitopes at 5 to 10 nm spacing [66]. Structured antigen of inactivated vesicular stomatitis virus glycoprotein (VSV-gP) was able to break tolerance in a mouse model expressing VSV-gP as a self protein while administration of soluble VSV-gP induced no immune activation [60, 67, 68]. Complement activation is enhanced by repetitive antigen structures thus leading to more efficient CD19-21 complex ligation on B cells [69]. The increased ligation of CD19-CD21 decreases the amount of BCR ligation needed to activate transcription factors crucial for plasma cell generation [70-72]. These benefits appear largely T cell independent but as stated earlier, protein opsonins such as complement and natural IgM enhance particulate antigen uptake to APC's. Repetitive antigen structure facilitates enhanced opsonin binding leading to greater uptake of antigen by phagocytic APC's, thus leading to greater T cell activation indicating the benefits of repetitive antigen structure on T cell activation. Complement components C3b and C4b have also been attributed to T cell activation through receptor interactions between T cell co-receptors CD46, CD55, and CD59

again indicating how repetitive antigenic structures can function to enhance cellular immune responses [73].

Innate pathogen recognition receptors

Repetitive structures contributing to immune activation via receptor linking and innate opsonin ligation leading to uptake demonstrate important factors in the host determining non-self components. A burgeoning area of research into initiation of immune responses has been the repetitive structures of pathogen associated molecular patterns (PAMPs) and how these conserved components of pathogens lead to activation of innate immune APCs via evolutionarily conserved intra and extracellular pattern recognition receptors (PRRs). The most familiar PRRs are the Toll-like receptors (TLRs) first described in drosophila [74] but also include the nucleotide oligomerization domain (NOD) like receptors (NLRs), C-type lectin receptors (CLRs), retinoic acid-inducible gene (RIG-I) like receptors (RLRs) [75]. These PRRs sense the cellular environment and, when ligated, begin a cascade of intracellular signaling leading to transcription of inflammatory mediators such as Type I interferons, proinflammatory cytokines like tumor necrosis factor (TNF), IL-1ß, IL-6, and other cytokines and chemokines. These conserved danger receptors of the innate immune system are not only expressed by phagocytic APCs but are also located on the cell surface of T and B cells and non-myeloid epithelial cells, endothelial cells, and fibroblasts.

The PRRs serve to recognize conserved, and most times highly structured, components of pathogens that are relatively static. PRRs also have a self-sensing

component in recognizing damage associated molecular patterns (DAMPs) of cell death leading to immune activation. TLRs remain the most characterized forms of PRRs. TLRs contain a Toll/IL-1R homology (TIR) domain that extends into the cytoplasm from the membrane allowing for downstream signaling after sensing extracellular or intracellular pathogens within membrane bound compartments [76]. TLR2 forms heterodimers on the plasma membrane with either TLR1 or TLR6 recognizing different forms of lipoproteins on bacteria, viruses, and parasites as well as some self components. TLR4, TLR5, and TLR11 are the other extracellular TLRs and recognize lipopolysaccharide (LPS), bacterial flagellin, and a profilin-like protein of protozoa, respectively. Endolysosomal TLRs recognize structural components of viral replication such as dsRNA, ssRNA, and CpG-DNA that ligate TLR3, TLR7 (mouse) or TLR8 (human), and TLR9, respectively. TLR10 is another endolysomal sensor found in humans but is yet uncharacterized as far as ligands recognized but is up-regulated by reactive oxygen species in a human monocyte cell line [77]. The compartmentalization of the endosomal TLRs serves to protect the host from aberrant inflammatory responses to self components that resemble the ligands of those TLRs [78]. TLR ligation leads to signaling cascades dictated by the adaptor molecules recruited to the TIR domains. The major adaptor molecule recruited to most TLRs with the exception of TLR3 is MyD88. MyD88 recruitment leads to an intracellular signaling cascade that concludes with translocation of the transcription factor NF-κB leading to pro-inflammatory cytokine transcription. Type I IFN transcription is also dependent on MyD88 via the translocation of interferon regulatory factor (IRF) 1 and 7 via TLR7 and TLR9 ligation [79]. TIR domain

containing adaptor inducing IFN-β (TRIF) is the other major adaptor protein recruited to TLR3 and TLR4. Recruitment of TRIF leads to a signaling cascade resulting in translocation of NF-κB, IRF3, and IRF7 [79, 80].

The RLR family are intracellular PRRs located in the cytoplasm that are up-regulated by type I IFNs and recognize genomic double stranded RNA (dsRNA) and dsDNA from viral replication [81]. RIG-I, melanoma differentiation-associated gene 5 (MDA5), and LGP2 make up the RLR family and recognize short dsRNA (up to 1kb) and dsDNA, long dsRNA (greater than 2 kb), and modified viral RNA (speculative), respectively [75, 82]. RLR structurally contain a C-terminal regulatory domain, which binds dsRNA ligands, as well as two N-terminal caspase recruitment domains (CARDs) (except in the case of LGP2) and a central DEAD box helicase/ATPase domain. The CARD domain triggers the signaling cascades resulting in transcription of type I IFNs via IRF3 and IRF7 transcription factors and NF-κB.

NLRs are also cytoplasmic PRRs that exhibit leucine rich repeat (LRRs) regions responsible for binding and make up portions of larger signaling complexes termed signalosomes and the inflammasome [83]. The signalosome and inflammasome are part of large inflammatory cytokine regulatory unit used to control inflammatory caspases needed to cleave pro IL-1β into the mature active IL-1β form for subsequent release [84]. There have been 14 genes identified with NALP receptors, non CARD carrying NLRs, and six genes identified with NOD receptors, CARD carrying NLRs, in humans [85]. Much like extracellular surface TLRs, NOD1 and NOD2 recognize conserved structures of the gram positive bacterial cell wall peptidoglycan, specifically g-D-glutamyl-meso-diaminopimelic acid (iE-DAP) and

muramyl dipeptide (MDP) which are often degraded components of the bacteria after phagocytosis. The NOD signalosome essentially consists of NOD receptors engaged with kinases through CARD domain interactions leading to activation of NF-κB [86]. Similarly NALPs provide a framework for the high molecular weight signaling complex termed the inflammasome. Inflammasomes are subsequently responsible for recognizing bacterial toxin components as well as cell wall components similar to NODs. Inflammasome signaling has also been associated with danger associated molecular patterns (DAMPs) of self, indicating cellular damage such as uric acid, extracellular ATP, and reactive oxygen species [87-89].

Finally, CLRs are transmembrane receptors capable of binding conserved carbohydrate sequences of pathogens [90]. CLRs are generally divided into mannose receptor families and the asialoglycoprotein receptor family. CLRs are responsible for signaling uptake by the phagocytic antigen-presenting cell as well as downstream signaling leading to pro-inflammatory cytokine secretion. Signaling mechanisms of CLRs are vague but most CLRs contain an immunoreceptor tyrosine-based activation motif (ITAM) similar to what is found on B cell and T cell receptors that eventually leads to NF-AT and NF-κB dependent transcription of pro-inflammatory cytokines.

A major action of adjuvants is to interact with these innate immune receptors to activate APCs leading to presentation of antigen and initiating a robust adaptive immune response against the antigen of interest by influencing the T cells and B cell polarizations through antigen presentation and cytokine secretion. The interactions with the conserved PRRs to the ligands, either from the pathogen or the host danger

signals, are not exclusively single events but rather elegant events of multiple interactions and thus multiple synergistically signaling events, as evidenced by common vaccine formulations being able to elicit robust immune responses in the absence of TLR signaling mechanisms [91]. Formulations of vaccines, either adjuvanted or non-adjuvanted, interact with these conserved receptors to activate and get past the hurdles of the innate immune system barrier to activate adaptive immunity. Obviously, whole cell vaccines maintain the integrity of the microbe thus interacting with the host (i.e., APCs) in a similar manner as would the target pathogen. As stated before, subunit or purified vaccine preparations lack many of the immune stimulating ligands of the whole cell and, thus, adjuvants are utilized. Documented adjuvant interactions with these conserved PRRs explained earlier are outlined in Table 1 adapted from Takeuchi et al and Coffman et al [33, 75].

Table 1. Pattern recognition receptors and the adjuvants that exploit their mechanism

PRRs	Ligand	Adjuvant	Output
TLR1/2	Triacyl lipoprotein (bacteria)	Pam3CSK4 (synthetic lipoprotein)[92, 93], alkane polymeric particles [94]	Ab, $CD8^+$ (DNA priming)
TLR2/6	Lipoprotein (bacteria, virus, parasites, self)	Macrophage-activating lipopeptide-2 (MALP-2) [95], alginate biomaterials [96], modified vaccinia virus Ankara (MVA) [97]	Ab
TLR3	dsRNA (virus)	Polyriboinosinic:polyribocytidylic acid (Poly I:C) [98]	Ab, $CD4^+$
TLR4	LPS (bacteria, virus, self)	MPL, AS04 (MPL + Alum) [99], Ribi.529 [100], alginate biomaterials [96], hydroxyapatite [101]	Ab, $CD4^+$
TLR5	Flagellin (bacteria)	FliC [102]	Ab, $CD4^+$, $CD8^+$
TLR7	ssRNA (virus, bacteria, self)	Imidazoquinoline [103], SM360320 [104]	Ab, $CD4^+$, $CD8^+$

Table 1 (continued)

TLR9	CpG-DNA (virus, bacteria, protozoa, self)	CpG ODN, CpG 7909 [105], IC31 [106]	Ab, $CD4^+$, $CD8^+$
TLR11	Profilin-like molecule (protozoa)	*Eimeria tenella* profilin-like protein [107]	Ab
RIG-I	Short dsRNA, 5' triphosphate dsRNA (virus)	DNA vaccine vectors alone or expressing RNA [108]	$CD8^+$
MDA5	Long dsRNA (virus)	MVA [97], Poly I:C [109]	
LGP2	(virus)	Inactivated WNV vaccines [110]	
NOD1 and NOD2	Peptidoglycan components (bacteria)	iE-DAP, MDP [111]	
NALP3	β-Glucan	alkane polymeric particles [94], poly(lactide-co-glycolide) (PLG) [112], MVA [97], Alum [113]	
Dectin-1	β-Glucan (fungi)	Curdlan [114]	$CD8^+$
Dectin-2	β-Glucan (fungi)	Ara h 1 [115]	
MINCLE	SAP130 (self, fungi)	CFA (trehalose dimycolate (cord factor) of Mycobacteria [33], CAF01 [116]	Ab

Table 1.
Table outlines common PRRs, the ligands they bind of pathogens, the adjuvants that exploit the receptors, and the enhanced immune phenotype.

Antigen exposure kinetics

The final hallmark of next generation vaccine design is to recapitulate the kinetics of antigen exposure similar to a pathogenic infection. Killed, attenuated, or subunit vaccines face the greatest hurdle in this arena because the antigen does not replicate resulting in an antigen exposure curve where the peak amount of antigen presented to the immune system occurs very quickly and then rapidly wanes (Figure 1). For soluble antigens, that antigen exposure is lost very quickly as the antigen is

cleared from the system often resulting in the induction of poor protective immune responses. Replicating pathogens provide a sustained antigen exposure resulting in a continued training regimen for the immune response to establish quality immune memory. A major mechanism of adjuvants in vaccines is to provide a controlled release of antigen either through depot effect or mechanisms of antigen exclusion. The prolonged antigenic exposure curve (Fig. 1, red line) is a major mechanism associated with establishing and maintaining protective immunity to viral infections [117, 118]. Low dose injections of a total fixed 125 μg dose of antigen amount given in daily dosing regimen of increasing amount of antigen, thus, replicating a replicating pathogenic infection, has been shown to be more effective in eliciting T cell responses compared to injections involving the same amount of antigen at each time [119]. These extended antigen exposures also lead to improved T cell memory that can overcome the need for T cell co-stimulation [120, 121].

Immunization schedules involving multiple injections to replicate this antigen exposure are often not feasible because of decreased patient compliance and increased cost. Single dose vaccines that are able to provide protective immunity through alteration of these antigen release kinetics are ideal. The feasibility of single dose immunizations is dependent on the ability of the adjuvant to provide particulate and repetitive structure, immunomodulatory activity of innate immune receptors and altering in vivo antigen kinetics, as well as the immunogenicity of the antigen, protective epitopes being targeted, and immune phenotypes elicited by the vaccine.

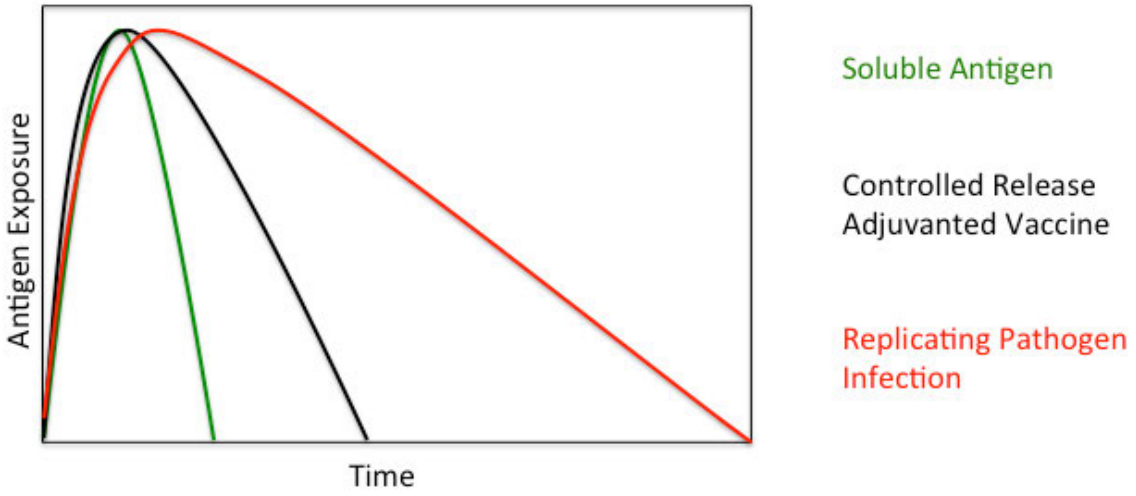

Figure 1. Antigen exposure kinetics of vaccines and how similar those kinetics can be altered with adjuvants to mimic a replicating pathogen infection. A theoretic table outlining the kinetics of soluble antigen vaccine (green curve) in which the peak amount of antigen is exposed immediately after administration. A mechanism of adjuvants allows for sequestration of antigen for continued exposure altering the kinetics of clearance by the immune system. This shift comes closer to the kinetics of antigen exposure of a pathogen in which replication occurs allowing for a continued antigen exposure until the immune system can eliminate the infection.

The designing of next generation vaccines, using the principles outlined above, will be driven by the need to develop efficacious vaccines against eminent pandemic pathogens. One pandemic pathogen that is heavily studied and speculated to become the next pandemic is the highly pathogenic influenza A virus H5N1 emerging from Asia. The following review outlines the pathogenesis of H5N1 and how the potential pandemic potential of the virus has led to innovation in vaccine and post-exposure therapeutic design deviating from traditional seasonal influenza.

CHAPTER 2: THE REQUISITE OF PREPAREDNESS DRIVING INNOVATION IN PANDEMIC H5N1 INFLUENZA VACCINES AND PREVENTIVE THERAPIES

A review paper to be submitted to *Vaccine*

Lucas Huntimer, Kathleen Ross, Balaji Narasimhan, and Michael Wannemuehler

Abstract

The potential human pandemic resulting from highly pathogenic avian influenza (HPAI) H5N1 has been rigorously studied since the identification of the virus in the Guangdong province of China. The majority of research has focused on the unique and severe tissue damage induced by the viral infection. These severe pathological lesions have also prompted investigators to evaluate various immunological approaches to induce protective immunity against HPAI, which will be discussed in this review.

Introduction

Influenza A virus is a single strand negative sense RNA virus of the Orthomyxoviridae family. The genome of influenza contains eight segmented RNA strands. The negative sense orientation of the RNA in the genome leads to replication dependence on a low fidelity RNA polymerase allowing a myriad of mutations contributing to antigenic diversity, which is called genetic drift [122]. The segmented genome also allows for re-assortment of the segments to take place between different viruses infecting the same host cell leading to genetic shift [123]. Genetic shift is the basis for the sub-classification of the influenza virus based on the

sixteen subtypes of hemagglutinin (HA) surface proteins, which bind the sialic acid (SA) receptors on epithelial cells of the host's respiratory tract, and the nine subtypes of neuraminidase (NA) surface proteins, which cleave the SA of the host cell allowing release of the virus. These surface proteins are the primary neutralizing antigens towards which host antibody responses are directed.

A distinct classification of avian H5N1 influenza viruses based on their pathogenicity in chickens was first identified from a geese population in the Guandong province of China in 1996 [124]. This lineage of highly pathogenic avian influenza (HPAI) H5N1 viruses has since been detected in over 60 countries. Because of the genetic drift of influenza viruses, genetic sub-classifications of clades of HPAI viruses have been created based upon their hemagglutinin sequence [125, 126]. The evolution of the HPAI viruses has led to classification of a particular HPAI genotype into clades of heterogeneity.

The avian H5N1 influenza binds preferentially to SA linked to galactose with α 2-3 linkages that are characteristic of avian cells in comparison with α 2-6 SA linkages to galactose in the upper human respiratory tract (that bind typical seasonal H3N2 and H1N1 viruses) and both α 2-6 SA and O-linked α 2-3 SA linkages that bind both human and avian influenza viruses [127-129]. Because of the preferential binding of avian SA, HPAI H5N1 has not been able to efficiently spread from human to human although suspected human to human transmission has been reported [130]. The swine respiratory tract contains both α 2-3 and α 2-6 SA making the pig a potential mixing vessel for genetic re-assortment [131]. Because of the ability of influenza to mutate very quickly, there are concerns that the mutations needed to

change binding preferences for SA linkages from the avian α 2-3 to the human α 2-6 could lead to a global pandemic, similar to the global spread of the H1N1 pandemic of 2009 [129]. Recent work with serial passage of the wild type virus in ferrets, the preferred animal model for recapitulating human responses to influenza because of sialic acid receptor distribution and pathological similarities, has demonstrated that the virus will adapt to airborne transmission albeit with a loss in pathogenicity [132-134]. These studies, while generating controversy within the scientific community, are essential to the understanding of the virus and the capabilities of the HPAI H5N1 to evolve and adapt if sufficient selective pressure is placed on the virus.

HPAI H5N1 influenza infection in humans is attributed to extended viral replication in tissue sites beyond the respiratory tract as well as increased host inflammatory responses as compared to seasonal influenza infections [135-137]. Mutations in the HA viral sequence leading to multiple basic amino acids at the HA cleavage site of HPAI viruses skews the ability of the virus to replicate in multiple tissue sites as compared to other influenza viruses being restricted to the respiratory

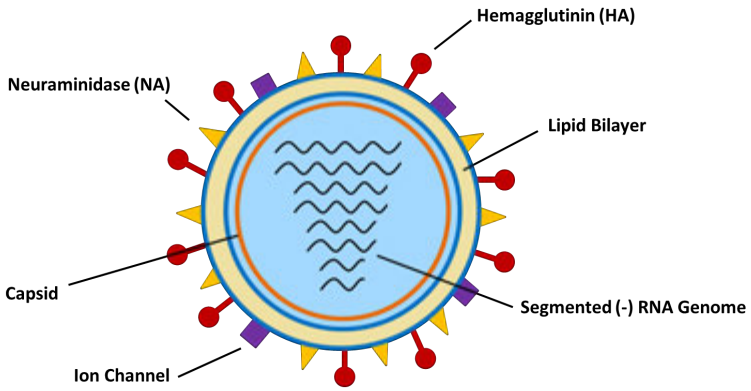

Figure 2.
The H5N1 virion capsid encloses an eight segmented, negative sense RNA genome. The virion also contains a lipid envelope with several major glycoproteins: hemagglutinin (HA), neuraminidase (NA), and ion channels (M2 proton channels).

tract [138, 139]. The multibasic cleavage site leads to an increased ability for cleavage needed for viral attachment. The ubiquitous distribution of replicating HPAI virus contributes to an overabundant antiviral immune response. Human peripheral blood derived macrophages infected *in vitro* with H5N1 exhibited increased release of the cytokines TNF-α, IL-6, IL-1β, IL-10, and IFN α and β as well increased release of the chemokines RANTES, MCP-1, MCP-3, MIP-1α, and MIP-1β [140-142]. *In vitro* infection of bronchial alveolar epithelial cells showed an increase in IFN-β, RANTES, and CXCL10 early in infection as compared to a seasonal H1N1 virus [143]. These detrimental inflammatory responses were attributed to the increased cytokine (IL-6, IL-8, and IL-10) and chemokine responses (CXCL10 and MCP-1) measured in the plasma of patients with increased viral load [91, 136, 137]. Approximately half of the cases of human H5N1 infections demonstrated the wide tissue tropism of viral replication [144]. Primate studies have disputed the wide tissue tropism of H5N1 replication seen in the liver and intestines of human patients in that the virus was only demonstrated to replicate in the lung but little in other tissue sites [145]. Nevertheless, the increased systemic viral loads as well as the hypercytokinemia and hyperchemokinemia in the respiratory tract are believed to be root cause of the severe tissue damage associated with H5N1 infection compared to seasonal influenza.

The histopathological changes associated with H5N1 influenza infection are characteristic of acute respiratory distress syndrome (ARDS) in which there is pulmonary congestion caused by cellular infiltrate of innate and activated adaptive immune cells as well as alveolar epithelial cell apoptosis [127]. Leukopenia,

gastrointestinal symptoms, renal dysfunction, and liver dysfunction have also been reported [144, 146, 147]. Traces of virus sequence and antigens have also appeared in brain and cerebrospinal fluid [136, 139]. Evidence of HPAI infecting the placenta and subsequently the virus is able to be vertically transmitted [139, 148].

Immune surveillance is still lacking concerning the prevalence of H5N1 in the human population. Recent epidemiological surveillance studies suggested that 9.1% of rural Thai villagers have antibodies against one of two H5N1 viruses suggesting subclinical prevalence [149]. Although the severity of disease associated with H5N1 human infections can be disputed based on this limited evidence of subclinical infections, it is very important to be prepared against a pandemic due to the unfamiliarity of the H5 HA to the human population.

The severe tissue damage associated with H5N1 infections in humans, the increased risk of secondary infections due to subsequent immunocompromise, as well as the high frequency of mutation of influenza virus which could lead to human to human transmission, have motivated research in the realm of preventive therapeutic approaches against HPAI. This section will focus on the traditional seasonal influenza vaccines and the possibility of using those approaches for pandemic preparedness to H5N1 as well as emerging vaccine and anti-viral technologies being explored to which may facilitate pandemic preparedness.

Inactivated viral vaccines

The traditional seasonal influenza vaccine consists of formaldehyde or β-propiolactone inactivated virus propagated in embryonated hen eggs [150], and

more recently, propagation of influenza virus in Vero cell cultures to replace hen egg propagation [151]. The antigenic components of the vaccine are either administered as whole inactivated virion, purified subunit of surface glycoproteins, or chemically split virus vaccine consisting of viral components. These different formulations of seasonal influenza vaccines may, therefore, be applied towards stockpiling H5N1-specific vaccines for pandemic preparedness. Production and distrubution of seasonal influenza vaccines are based on epidemiological studies to closely match antigenic profiles and previous exposure to influenza [152]. With respect to HPAI H5N1, the human population will be immunologically naive due to the fact that seasonal influenza A virus vaccines contain H1 and H3 (and not H5) HA [4].

Inactivated influenza virus vaccines can result in rubor and tumor at injection sites with frequency of incidence dictated by age but no differences from placebo were observed [153-155]. People with egg albumin allergies are also not able to be administered the traditional mass-produced inactivated vaccines because of hen egg virus propagation. The main conundrum of using traditional seasonal inactivated influenza virus vaccine technologies to produce pandemic vaccines is the time needed for production of the virus and manufacturing of the vaccines. Typical mass production timelines are estimated to be 6-9 months [156]. A dominant pandemic strain would need to be identified prior to vaccine production which would delay when the vaccine could make it to clinics and undermine the benefits of prophylactic immunization programs.

The immune response elicited by inactivated influenza virus vaccines is predominately humoral. Antibody responses are typically directed towards the

surface glycoproteins HA and NA. Systemic antibody specific for HA and NA is predominately IgG1 with some IgM and IgA being identified and protective antibody responses being elicited within two weeks post-vaccination [157]. IgG and IgA specific antibody secreting cells have been identified in peripheral blood following vaccination [158]. The IgG isotypes associated with these humoral responses can be attributed to the prime/boost benefits provided by the previous year's vaccinations [159]. Combinations of antiviral NA inhibitors with inactivated virus vaccines may also be an effective treatment regimen during an influenza pandemic disease outbreak due to little interference with the humoral response in clinical studies [160]. Inactivated viral vaccines can also elicit stronger influenza antigen-specific proliferative responses of T cells isolated from the palatine tonsils or peripheral blood, although this may also be attributed to the prime/boost responses subsequent to either natural seasonal influenza infection or previous vaccinations [157, 161-163].

Studies with inactivated HPAI H5N1 prepared and administered similarly to licensed seasonal vaccines still present the most viable option for pandemic formulations due to the vaccine not having to undergo licensure but rather be considered a new strain of influenza added to an existing licensed product to alleviate regulatory delays. Inactivated subvirion (chemically split measured by HA units) H5N1 virus vaccines were shown to provide virus neutralization titers in 54 percent of individuals receiving two doses of 90 μg of HA units, which is approximately six times the dose of seasonal influenza vaccines [164, 165]. A TLR7 dependent mechanism associated with increased immunogenicity of inactivated

H5N1 vaccines, because of residual viral RNA in the preparation, has been identified [166]. Aluminum salt adjuvanted inactivated split virion H5N1 vaccines were able to elicit 67% HA inhibition in patients after two doses of 30 μg HA [167]. After vaccination, immunological responses to split virion H5N1 were greater in infants and children [168]. Additionally, inactivated, whole virion H5N1 vaccines were able to produce 78 % seroconversion when administered in a two dose regimen with aluminum salts at a dosage of 10 μg of HA [169]. Vero cell derived and inactivated H5N1 vaccines induced similar humoral immune responses with and without $Al(OH)_3$ adjuvant [170].

Cold adapted attenuated viral vaccines

Influenza vaccine options were expanded by the licensure of a cold adapted live seasonal influenza vaccine (Flumist®, Aviron Gaithersberg, MD). Cold adapted live influenza viruses are based on the master strain A/Ann Arbor/6/60 (H2N2) being attenuated by passaging the virus through decreasing temperatures in embryonated hen eggs. The continuous passage through decreasing temperatures allows for mutational adaptations in the polymerase (PA), PB1, PB2, and M genes of influenza leading to the cold adapted phenotype in which replication is restricted to 33^{o}C in the upper respiratory tract [171]. The cold adapted virus expressing the HA and NA of interest, either the seasonal influenza strains or pandemic strains, is produced by genetic reassortment [172]. The modified live cold adapted influenza virus allows for an intranasal vaccination that mimics the natural infection in both site and mode of infection but under the virus replicative constraints of the upper respiratory tract. The

upper respiratory replication of the virus allows for lower doses of influenza antigen to be administered in order to induce an effective immune response.

The cold adapted influenza virus seasonal vaccines have shown cross-reactive immune responses to other antigenically drifted H1N1 and H3N2 strains [173-175]. This cross reactivity could prove extremely beneficial in the stockpiling of pandemic influenza vaccines because prediction of the antigenically drifted strain of influenza will be difficult [176]. The intranasal route also allows for ease of administration by individuals with minimal professional training during a pandemic situation.

Cold adapted H5N1 virus vaccines were able to provide incomplete protection after single dose vaccinations with homologous and heterologous viral challenge but two dose regimens (prime/boost) provided heterologous cross protection in laboratory models [177]. Safety and toxicological profiles of the cold adapted H5N1 vaccines were favorable in the ferret model [178]. Clinical evaluations of a cold adapted influenza vaccine containing the H5 and N1 outer glycoproteins of two H5N1 isotypes A/Vietnam/1203/2004 and A/Hong Kong/213/2003 on the A/Ann Arbor/6/60 show limited viral replication leading to nominal neutralizing humoral immune response [176]. Immune responses were elicited using a low pathogenicity avian influenza A/Duck/Potsdam/1402-6/86 (H5N2) genetically reassorted to a cold adapted A/Leningrad/134/17/57(H2N2) that show cross reactivity to an H5N1 strain in a HA inhibition test [179]. Interestingly, a cold adapted vaccine consisting of HA and NA of the 2009 pandemic H1N1 was able to protect mice from lethal H5N1 challenge [180, 181].

Reverse genetics derived virus

The traditional method of genetic re-assortment of influenza virus for vaccines in embryonated hen eggs can be inefficient and variable. Recent advances in molecular biological techniques have allowed for the formation of infectious influenza A virus completely from plasmid cDNA expression of the viral RNA segments transfected in human embryonic kidney cells (293T) or Madin-Darby canine kidney (MDCK) cells [182, 183]. The reverse genetics system of creation and propagation of influenza virus allows for molecular manipulation of the genetic elements to decrease pathogenicity, a more targeted approach for creation of genetically reassorted viruses, and alleviation of propagation validation issues associated with production of virus for vaccine purposes.

The initial reverse genetics systems demonstrated the rescue of seasonal influenza variants containing the HA and NA of A/New Caledonia/20/99 (H1N1), A/Panama/2007/99 (H3N2), A/teal/HK/W312 (H6N1), and A/quail/HK/G1/97 (H9N2) and the six internal genes of PR8, a high growth lab strain of influenza [184]. Subsequently, reverse genetics derived strains containing the HA and NA of H5N1 were created [185, 186] and adapted for expression in Vero cells, which have been previously validated for the production of polio vaccine [187-189]. The reverse genetics derived system for production of re-assorted viruses verified the decreased timeline needed for reverse genetics derivation compared to the traditional embryonated hen egg re-assortment method. Vero cells present difficulties in transfection efficiency compared to non-production validated cell lines such as 293T cells. Adenovirus vectors that, when transduced in Vero cells, produce the viral RNA

needed for creation of the viral ribonucleoprotein complex by transfecting the same cells with plasmids encoding the PB1, PB2, and PA subunits of the viral polymerase increased the viral production efficiency from the traditional eight plasmid method [190].

Reverse genetics derived inactivated virus was used for immunization and elicited cross neutralization to several H5N1 strains isolated from human infections in a guinea pig model and protection from challenge with three different H5N1 viruses in mice vaccinated with a prime/boost regimen [191]. A H5N3 reverse genetics derived virus was used for an inactivated vaccination challenge model in ducks and chickens that provided protection in a single dose and a two dose regimen [192]. Finally, a formalin inactivated reverse genetics derived H5N1 oil emulsion vaccine also showed protection 43 weeks post vaccination in chickens [193].

The reverse genetics platform allows for a more targeted approach towards generation of cold adapted influenza virus with the A/Ann Arbor/6/60 (H2N2) backbone and the H5N1 glycoproteins of HPAI H5N1 as well. Reverse genetics derivation of cold adapted influenza virus for modified live vaccines have shown potential in two dose intranasal administrations in reducing wild type virus replication [194]. Protection from homologous and heterologous virus challenge in mice, ferrets, and macaques has also been reported when boosted with a second immunization [177, 195].

DNA vaccines

DNA vaccination, in general, refers to the initiation of an immune response against an antigen introduced via purified DNA in supercoiled plasmids that encode for the antigen (poly)peptide sequence [196]. The plasmid DNA incorporates into the host cells via direct gene transfer and the host cells produce the protein antigen. Mass production of plasmid DNA is less labor intensive than protein antigens and DNA storage conditions are less intense when proper techniques are used, providing advantages in stockpiling pandemic vaccines [197].

The immune response elicited to DNA vaccines is primarily skewed to the Th1 type of immune response, in which cell-mediated immunity (CMI) to the DNA encoded antigen is more prevalent with IFN-γ and IL-12 being the predominant cytokines reported in the vaccine response [198]. Although the entirety of the plasmid DNA in the vaccine is non-immunogenic, the plasmid DNA can be a non-specific immunostimulatory component through pattern recognition receptors (PRRs) thus providing an innate adjuvant response [199, 200]. The proposed mechanism of DNA vaccines mimics the cellular pathogenesis of viruses. The post-transcriptional and -translational proteins are split into smaller peptides by intracellular proteasomes of either muscle, epithelial, or APCs [201, 202]. The peptides are presented by MHC class I molecules after trafficking through the endoplasmic reticulum of the host cell. The MHC class I molecule containing the peptide then elicits the appropriate $CD8^+$ T cell responses.

The stability and ease of manipulation of plasmid DNA allows for encoding of additional immunostimulatory components to be transcribed and translated by the

host cell. Some components that have been encoded to be co-expressed with the antigen of interest include the cytokines IFN-γ, IL-2, IL-12, and/or GM-CSF, co-stimulatory molecules such as B7 (CD80 and CD86) and CTLA4-Ig, as well as DNA sequences that are specifically immunostimulatory [203-208].

The molecular techniques developed in the last decade and the antigenic drift associated with influenza have provided resources to enable fast production of a pandemic H5N1 vaccine. Protection from lethal challenge of heterologous strains of H5N1 influenza with DNA vaccines encoding HA proteins as well as protection from homologous strains encoding for NA, NP, or M2 have been demonstrated [209-211]. Dependency on the HA protein needing to be encoded in the formulation for humoral and cellular immunity is evident when combinations of all of the antigenic targets are used [212-214]. Addition of a virus induced signaling adaptor (VISA) molecule in the DNA antigenic preparation of an H5 HA peptide was able to convey protection from lethal challenge in a mouse model [215]. Heterotypic immunity against different clades of HPAI viruses has been reported thus validating the approach [216]. Clinical trials of H5N1 DNA vaccines have begun [217].

Virus like particles (VLPs)

Responding to the need for enhanced immunity and novel approaches for potential pandemics, VLPs present viral antigens in a more native and, therefore, immunogenic fashion [218, 219]. VLPs are self-assembled virion shells containing relevant viral proteins such as HA, NA, nucleoprotein (NP), and matrix protein 1 and 2 (M1, M2) [220-222]. The presented proteins are active and remain in their native

structures similar to live virions.

VLPs are immunogenic due to their ability to mimic live virions at the cellular level [220]. Due to the lack of the viral genome, VLPs are non-replicating and non-infectious and, therefore, remain immunogenic and safe to those in high-risk groups such as the elderly, even after several administrations [218, 220, 221, 223]. Immunogenicity of VLPs can be further enhanced due to the particle's adjuvant properties to stimulate both humoral and cellular immune responses, including cross-reactive antibodies that protect against the variability of influenza strains [218, 221, 222, 224].

VLP proteins are commonly recombinant based, produced by the baculovirus system in yeast, insect, or mammalian cells [219, 220, 222]. Independence from egg-derived vaccines is especially important for an avian influenza vaccine, due to the limited egg supply and the H5N1's ability to kill egg embryos [224]. Egg independence also eliminates the need for live viruses during production and manufacturing, and is, therefore, very favorable for production without the need for chemical inactivation or biosafety containment.

VLP's against H5N1 have been successful in eliciting cross-reactive responses between subtypes [218, 219, 224, 225]. H1N1 VLP intranasal vaccinations in mice and ferrets induced high levels of cross-reactive IgG and IgA and had two to three fold greater amounts of IL-2, IL-9, IL-10, and IL-17 than other vaccinations, while remaining protective against a heterologous H5N1 challenge [218]. VLPs using HA and NA surface proteins, while internalizing the conserved epitopes of the M1 protein, stimulated the activation and proliferation of $CD8^+$ T cells

that increase production of IFN-γ, TNF-α, and IL-2 when compared to recombinant protein subunit vaccines [219, 223]. Although the HA protein is mainly responsible for inducing H5N1 specific antibodies, the M1 protein's conserved epitopes are generally accountable for cellular immunity and cross-protection [219, 223]. This increase in cellular immunity was also apparent in the ratios of antibodies found with H5N1 VLP vaccine responses. Post-vaccination, IgG2a and IgG2b titers were largely increased resulting in a balanced IgG1:IgG2 ratio [224, 226]. H5N1 vaccines using VLP technology showed long lasting memory responses in challenge with single does as low as 0.4 μg [219, 227] and utilized needle-free technologies for inoculation [219, 226-228]. Protective efficacy of VLP vaccines against H5N1 have been shown in poultry and a computationally optimized broadly reactive antigen (COBRA) H5 VLP vaccine showed protection from challenge in a non-human primate model challenged with clade 2.2 A/Whooper Swan/Mongolia/244/05 (WS/05) [229, 230].

Subunit vaccines

Recombinant subunit protein-based vaccines, using a single protein antigen, have also been examined due to the increased purity and safety profiles [220, 231-233]. Using this system, individual viral proteins, most commonly HA and NA, are recombinantly synthesized in mammalian or insect cells that support post-translational modifications such as glycosylation, allowing the production of correctly folded proteins [220, 232-234].

While the baculovirus technology allows rapid production of recombinant

proteins, there is some debate on using insect or mammalian cultures [220, 231-233]. During translation of recombinant H5 HA protein, mammalian cells commonly produced a high-molecular weight oligomer or trimer form of HA [231-233]. Insect cells have been more likely to produce cleaved or monomer forms of the HA protein, although some studies have shown stable production of trimer HA in insect cultures [231-233]. In most cases, the immunogenicity of the H5 HA protein was highly dependent on its oligomer and trimer forms showing that in a weakly immunogenic protein it is optimal to present it in its natural trimeric state [231-233].

Besides the challenges associated with the protein's production, H5 HA is a weak antigen that degrades quickly in the body. Therefore, several large doses (up to 90 μg) are needed to achieve suitable protection. However, with the help of novel adjuvants and/or protein carriers, the immunogenicity of HA can be greatly improved to reduce both the number and size of vaccine doses [220, 232, 235, 236]. H5 HA has been shown to be the dominant protein for subunit immunizations for the obvious reasons of inducing H5N1 specific neutralizing antibodies, however other proteins that have not shown to be protective on their own, such as NA, are also included in protein-based vaccinations. When used in tandem with HA protein, NA enhances cross-reactive protection between H5N1 clades [231, 232, 234, 235].

Like DNA vaccines and VLPs, recombinant proteins can be produced quickly in mass quantities without the dependence on a limited egg supply [231, 233]. Large scale production of recombinant proteins is feasible because no live viruses are required, eliminating the need for bio-containment facilities [231, 233]. Novel recombinant production techniques that use plant-based systems are being

developed for influenza HA antigens [237]. Likewise, recombinant proteins can be highly purified and don't utilize chemicals to inactivate the antigen, reducing contamination and adverse effects on patients [231].

Oral and intranasal vaccinations of baculovirus produced H5 HA led to effective, long-lived production of IgA in mucosal tissues, as well as protection in mice [233, 235]. Likewise, H5N1 proteins such as M2, NP, and NA have also been used to induce cross-protection between clades of avian influenza [234, 238, 239]. As mentioned previously, HA is the primary antigen that stimulates neutralizing antibody in H5N1 [238] . However, by using more conserved proteins, studies have shown an increase in HA-specific neutralizing antibodies, as well as IFN-γ producing $CD8^+$ T cells, especially in the presence of an adjuvant [234, 238-240]. Recombinant production of HA proteins of H5 allows for manipulation of the antigen, specifically in the creation of stabilized trimeric forms of the antigen that increase the immunogenicity of the protein [241-243]. Licensure of a recombinant HA vaccine, FluBlok, grown in insect cells has been a recent advancement in this area [244].

Immune refocusing

Immune refocusing, also termed as deceptive imprinting or epitope masking, is a new advance in influenza vaccine technology. Immune refocusing targets class II pathogens, such as influenza, or pathogens that have immune responses to strain specific epitopes, yet high rates of mutation within these epitopes [245]. Tobin et al. theorize that pathogens, such as H5N1 avian influenza, have immunodominant epitopes, such as the globular head of the HA trimer, and subdominant epitopes, or

more conserved proteins [245]. These dominant epitopes are distractions to obstruct the immune system from recognizing and manufacturing antibodies against more protective or cross-reactive epitopes [246]. This concept arises from the theory of original antigenic sin [247]. For example, a secondary influenza infection containing epitopes previously recognized from a former strain as well as new epitopes will only produce antibodies against the previous epitopes, eliminating the infection quickly during a memory response [247]. However, in the cases of HPAI, strain specific epitopes dominate the immune response and block reactions to epitopes that appear from strain to strain. In this case, the immune system must respond to each infection as a primary infection, with no memory response [247].

Recent evidence has identified wide cross reaction of the influenza HA immune responses by constructing a headless HA molecule that retains the correct conformation of the stalk structure [248]. The HA protein has two subunits: the globular head and immunodominant HA1, and the more conserved and cross-reactive HA2 [35]. By removing a portion of the HA1 globular head, the most variable and strain specific subunit, the remaining portion of HA1 and conserved HA2 is retained and exposed to the immune response allowing cross-reactive antibodies to form [248]. Immunizations with the headless HA allowed complete protection and partial prevention of weight loss during a lethal homologous challenge and cross-reactive antibodies to different HA subtypes. This advancement could be exploited for a prospective pandemic platform for cross-reactive influenza vaccines [248].

Vectors

An increasing focus on utilizing vectors (i.e. bacteria or viruses) to deliver antigen to the appropriate cellular compartments has been identified with emphasis on production in poultry medicine. A commercially available fowlpox vectored avian influenza vaccine administered parenterally has demonstrated extensive efficacy in poultry against HPAI although administration requires handling of each individual bird [249, 250]. Subsequent studies looked at improving efficacy by overcoming immune suppressive effects of the fowlpox vector by including genes encoding for the cytokine IL-18 [251]. Modified Vaccinia virus Ankara (MVA) encoding H5 HA showed protective efficacy in mice [252]. Vaccinia virus, smallpox and fowlpox viral vector vaccines encoding A/chicken/Indonesia/7/03 H5 hemagglutinin were examined in a swine model of vaccination and elicited protection from challenge with low pathogenic H5N1 virus [253]. Replication defective human adenovirus vectors effectively delivered DNA encoding influenza antigens to host cells while being well tolerated in human trials [254]. The adenovirus technology ensures a targeted approach towards delivery of the H5 HA DNA over the intramuscular injection of DNA discussed earlier and demonstrated protection in mouse and poultry models of HPAI challenge [255-257]. A poultry specific attenuated live vaccine strain of Newcastle Disease Virus (NDV) was genetically modified to express HA of HPAI and showed protection from lethal challenge of both HPAI and NDV in poultry [258]. Wang et al. have demonstrated that a common poultry *Lactobacillus* that colonizes the gut of poultry delivered H5 antigen to mucosal tissues and elicited specific IgA and cell mediated immune responses [259].

Table 2. Clinic trials of H5N1 vaccines

Vaccine	Unique Clinical Trial Identifier	Phase Clinical Trial	Route	Dose	Regimen
Inactivated (A/Vietnam/1194/2004 HA and NA or A/Vietnam/1203/2004 x A/PR/8/34) grown in embryonated hen's egg adjuvanted with or without MF59 [260-267]	20	I, II, III	IM	3.75, 7.5, 15, 30, or 45 µg	Prime/Boost 1, 2, 3, 4, or 6 weeks post-primary immunization
DNA plasmid encoding H5 A/Indonesia/05/2006 with CMV/R promotor [268]	4	I, II, III	ID (w/ or w/o needle free technology)	500 and 1000 µg	Prime/boost 4 weeks and 8 weeks post-primary immunization
Inactivated H5N1 (A/Vietnam/1194/2004 or A/Vietnam/1203/2004 HA and NA x A/PR/8/34 (NIBRG-14)) grown in embryonated hen's egg adjuvanted with or without Alum [164, 168, 169, 262, 269-275]	36	I, II	IM or ID	1.25, 2.5, 3, 5, 7.5, 9, 10, 15, 45, 90 , or 300 µg	Prime/Boost 28 days post-primary immunization Third dose 6 months post second dose *Up to 4 doses with in 4 weeks of primary immunization
Purified recombinant H5 HA A/Vietnam/1203/2004 produced using baculovirus expression system in insect cells adjuvanted with or without Alum	2	I, II	IM	45, 90, or 135 µg	Prime/Boost 21 days post-primary immunization
Purified recombinant H5 HA A/Indonesia/05/2006 produced using baculovirus expression system in insect cells adjuvanted with or without Glucopyranosyl Lipid A (GLA-SE)	3	I, II	IM	3.8, 7.5, 15, 45, 90, or 135 µg	Prime/Boost 21 days post-primary immunization
Inactivated split virion A/Indonesia/5/05 adjuvanted grown in embryonated hen's egg with tocopherol (AS03) [268, 273, 276-278]	11	I, II, III	IM	3.75, 7.5, 15, 45, or 90 µg	Prime/Boost 21 or 28 days post-primary immunization
Inactivated split virion A/Vietnam/1194/2004-like strain grown in embryonated hen's egg adjuvanted with tocopherol (AS03(A) 11.86 mg) [278-280]	10	III	IM	3.75 µg of HA	Prime/Boost 21 days post-primary immunization
Inactivated pre-pandemic H5N1 Vero cell derived A/Vietnam/1203/2004 adjuvanted with or without Alum [151, 170, 281]	11	I, II, III	IM or SC	3.75, 7.5, 15, or 45 µg	Prime/Boost 21 or 28 days post-primary immunization Third dose 6 months, 12 months, or 24 months

Table 2 (Continued).

Inactivated pre-pandemic H5N1 Vero cell derived A/Indonesia/05/2005 unadjuvanted Baxter Healthcare Corp.	2	I, II	IM	3.75, 7.5, 15, or 45 µg	Prime/Boost 21 days post-primary immunization
Inactivated split virion A/Vietnam/1194/2004 grown in embryonated hen's egg adjuvanted with proprietary oil-in-water emulsion (AS) [282]	2	I, II, III	IM	3.8 or 15 µg	Prime/Boost 21 days post-primary immunization
Inactivated split virion A/Indonesia/5/2005 grown in embryonated hen's egg adjuvanted with proprietary oil-in-water emulsion (AS) [282]	1	I	IM	3.8 or 15 µg	Prime/Boost 21 days post-primary immunization
Inactivated subvirion A/Indonesa/5/05 grown in embryonated hen's eggs adjuvanted with or without MF59	3	I, II	IM	3.75, 7.5, 15 or 90 µg	Prime only or Prime/Boost 28 days post-primary immunization
Recombinant H5 HA A/Indonesia/5/2005 produced in plant based expression system assembled into VLP adjuvanted with glucopyranosyl lipid adjuvant (GLA-AF) or Alhydrogel® or without adjuvant [283]	3	I	IM or ID	5, 10, 15, 20, 45, or 90 µg	Prime/Boost 21 days post-primary immunization
Replication competent Adenovirus expressing H5 HA A/Vietnam/1194/2004 adjuvanted with or without dsRNA	4	I	Oral, IN, or tonsillar (mouth spray)	10^7, 10^8, 10^9 10^10, 10^11	Prime/boost 56 days post primary/boost 112 post primary immunization
HA and NA of A/Vietnam/1194/2004 (H5N1) x A/Puerto Rico/8/34, purified and coupled with phospholipids to create virosomes with or without Matrix M™ adjuvant [284]	1	I	IM	1.5, 7.5, or 30 µg of HA	Prime/Boost 21 days post-primary immunization
Cold adapted live attenuated HA and NA of A/Vietnam/1203/2004 or A/HongKong/213/2003 x A/AnnArbor/6/60/ca [176]	2	I	IN	10^3, 10^5, or 10^7 TCID50	Prime/Boost 4-8 weeks post-primary immunization
Inactivated cell based H5 A/Vietnam/1203/2004 vaccine adjuvanted with GelVac™ a plant polysaccharide gel that encapsulates the antigen	1	I	IN	30 µg	Primary
Inactivated H5N1 (A/Vietnam/1194/2004 HA and NA x A/PR/8/34) grown in embryonated hen's egg adjuvanted with or without oil-in-water emulsion [285]	1	I	IM	1.9, 3.8, 7.5, or 15 µg	Prime/Boost 21 days post-primary immunization
Inactivated H5N1 A/Vietnam/1194/2004 Madin-Darby canine kidney (MDCK) cell derived unadjuvanted Baxter Healthcare Corp.	1	I	IM	7.5, 15, or 30 µg	Prime/Boost 21 days post-primary immunization

Table 2 (Continued).

Recombinant H5 HA A/Indonesia/5/2005 produced in baculovirus/insect cell expression system assembled into VLP	3	I, II	IM	15, 45, of 90	Prime/Boost 21 or 28 days post-primary immunization
Globular head domain of H5 hemagglutinin A/Indonesia/5/2005 fused with Salmonella typhimurium flagellin type 2 (STF2) TLR5 agonist	2	I	IM	1, 2.5, 4, 6, 8 or 12 µg	Prime/Boost 21 days post-primary immunization
DNA plasmid encoding H5 protein VGX-3400X	3	I	IM, or ID + electroporation Day 0 and 1 month	0.6, 0.9, 2, or 6 mg of DNA/dose	Prime/Boost 28 days post-primary immunization
Live attenuated H5N2 A/17/Turkey/05/133	1	I	IN		Prime/Boost 21 days post-primary immunization
Replication competent Adenovirus expressing H5 HA A/Vietnam/1194/2004 adjuvanted with or without dsRNA Ad4-H5-Vtn for delivery to the ileum by a radio controlled capsule (ND1.1)	1	I	Oral		
Inactivated H5N1 vaccine adjuvanted with 50 µg of E. coli heat-labile toxin (LT) patch at immunization site	3	I, II	IM + LT Patch	15 or 30 µg	Prime/Boost 21 days post-primary immunization

Table 2.
Pandemic preparedness leading to design of standard (based on seasonal influenza vaccines) and novel vaccines has led to 131 unique clinical trial identifiers at clinicaltrials.gov.

Adjuvants

HPAI vaccines are confronted with the same problems that hinder seasonal influenza vaccines in that the immunogenicity of the antigens is mediocre [286]. Including adjuvants with immunostimulatory compounds in vaccine formulations has long been a proven technique for increasing the immune response towards the antigens of interest [23]. However, the use of adjuvants heighten safety concerns as vaccinologists and immunologists attempt to balance between sufficiently engaging the immune system to mount a robust response without crossing the line into a

deleterious immune event. Because of the potential for adverse events associated with adjuvants, very few vaccines containing adjuvants have been approved for use in humans [287, 288]. Seasonal as well as pandemic influenza vaccine research has led to significant advances in adjuvant development, leading to novel adjuvants like MF59, an oil-in-water emulsion, being approved for human use in the European Union [289].

As mentioned in earlier sections, many vaccine formulations for HPAI under investigation contain adjuvants. Here, we highlight the advances in adjuvant research in the context of HPAI vaccines. Alum remains the principal adjuvant studied because of its approval for human use while maintaining favorable safety profiles [290-292]. MF59 and AS03 (another oil-in-water emulsion) appear to more effectively increase efficacy as compared to Alum, although vaccines using these adjuvants are limited in their approval for use world-wide [293-297]. Evidence has pointed to the induction of serum antibody recognizing more epitopes of H5N1 following immunization with a MF59 adjuvanted H5N1 vaccine versus non-adjuvanted vaccines providing insight into a basis for vaccine efficacy [298].

The pandemic possibility of HPAI has pushed other avenues of adjuvant research. Inactivated whole virus adjuvanted with CoVaccine HT^{TM}, a mixture of squalene, polysorbate 80, sucrose fatty acid sulphate ester in water, demonstrated favorable HA inhibition titers in ferrets and macaques with a single dose regimen [299, 300]. A purified derivative of the saponin from *Quillaja saponaria*, QS-21, has been identified as another potential adjuvant in pandemic HPAI vaccines [195]. The addition of QS-21 along with Alum in H5N1 vaccines greatly increased antibody

responses to the M2 protein in rhesus monkeys [195]. Immune stimulating complexes (ISCOMs) are 40 nm structures containing glycosides from *Quillaja saponaria* and lipids for which immunogens can attach via hydrophobic interactions. These compounds have shown promising protection data upon lethal challenge in avian models [301, 302]. Platycodin D, another saponin derived from *Platycodon grandiflorum*, has shown adjuvant potential when combined with recombinant H5 [303].

Recent advances in molecular and structural biology have led to targeted approaches to stimulate innate immune cells through pattern recognition receptors (PRRs) such as Toll-like receptors (TLRs), RIG-1-like receptors, NOD-like receptors, and C-type lectin receptors (CLRs) [304, 305]. Stimulating PRRs with ligands in conjunction with delivering antigens enhances immune responses [306]. Stimulation of endosomal TLR3 or TLR9 with poly IC:LC or CpG DNA, respectively, during HPAI infections led to protection and viral clearance [307]. The adjuvant effect of TLR3 ligands was also demonstrated in intranasal (IN) HPAI vaccines in primates [308]. IN administration of poly I:C with H5N1 HA as well as with using chitin microparticles concurrently with poly I:C induced immune protection upon lethal challenge [309, 310]. PIKA, a dsRNA analog that functions through ligation of TLR3 showed adjuvant effects to subunit H5N1 vaccines administered intranasally in mice as well as protection from heterologous challenge [311]. Incorporation of monophosphoryl lipid A (MPLA), a non-toxic derivative of LPS that signals through TLR4, combined with Alum induced higher HAI antibody responses characterized by a balanced HA-specific IgG1 and IgG2a isotypes using a dose a 3.8 μg HA combined with a split

virion vaccine [312].

Cholera toxin (CT) has demonstrated mucosal adjuvant capabilities that appear to be STAT3 signaling dependent [313]. Recombinant CT demonstrated more favorable safety profiles due to engineering the absence of the catalytic subunit [314]. Recombinant CT used as an adjuvant in combination with inactivated H5N1 viral vaccines showed similar antibody titers to other adjuvanted inactivated H5N1 vaccines but with diminished protection [315]. Another bacterially derived adjuvant, the heat labile enterotoxin from *E. coli* (LT) administered, proved to be safe and provided enhanced mean HA inhibition (HI) titer in a randomized clinical trial in a prime boost immunization regimen [316].

Combinations of adjuvants, as alluded to earlier with MPLA and Alum, are also an exciting avenue of vaccine research. A synthetic bioresorbable diblock tri-component copolymer poly(ethylene glycol)-block-poly(lactide-co-ε-caprolactone)(PEG-*b*-PLACL) was used to create a novel emulsion delivery system (PELC) that when combined with CpG DNA, a TLR9 agonist induced higher antibody responses in single dose applications using inactivated H5N1 virus and elicited cross reactive antibodies to heterologous virus [317, 318]. These increased immune responses with a particulate adjuvant, as well as other studies using micelle-based carriers administered orally [319] indicate the importance of size and shape in designing adjuvants [24].

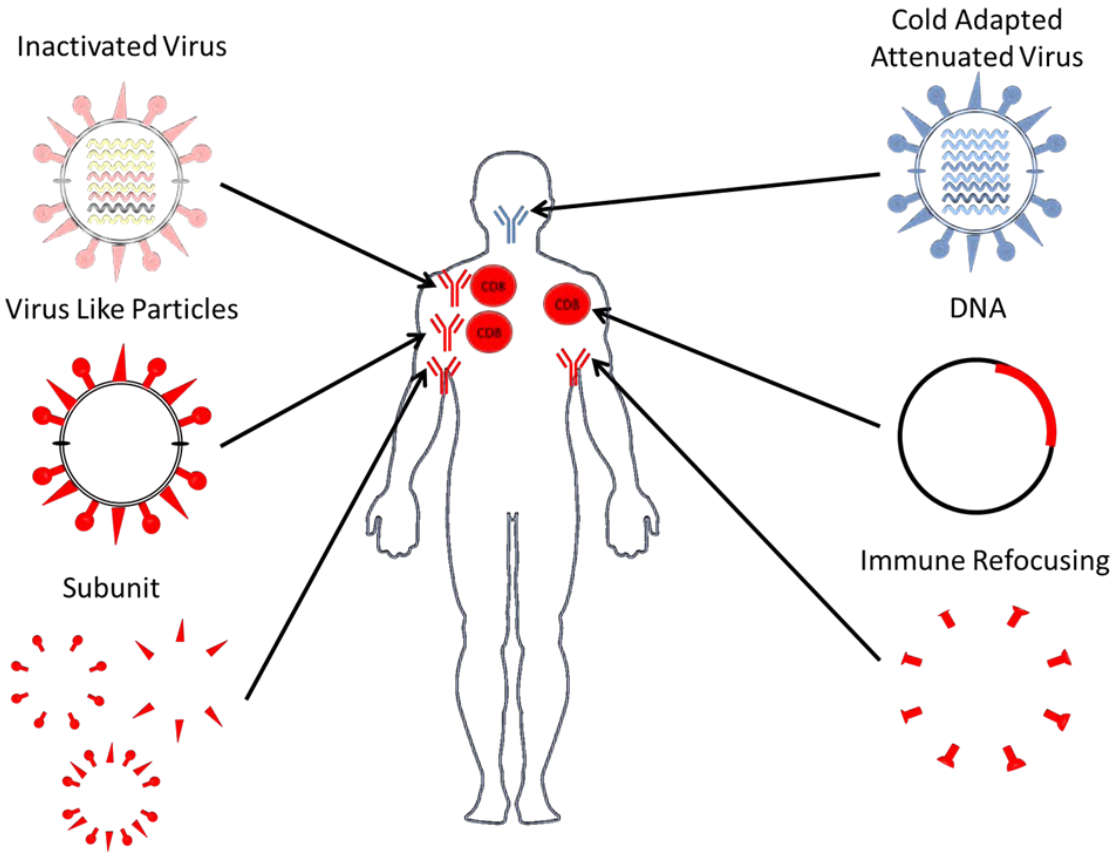

Figure 3.
The looming influence of a possible pandemic of HPAI has pushed research into refining, improving and generating novel vaccine approaches. A simplified overview of the immune responses generated from the different antigens used in the vaccines discussed in this paper. Arrows are indicative of the route of administration being used for the discussed vaccines.

Anti-viral drugs

Besides vaccines, stockpiling of anti-viral drugs for use in a possible H5N1 pandemic is also critical for treatment of infected individuals. These drugs are focused on inhibiting specific functions of viral replication and can be used prophylactically or therapeutically against viral infection [320]. Drugs such as oseltamivir and zanamivir act as NA inhibitors of influenza virus by binding to the

functional binding site of NA [321]. Oseltamivir treatments studied in HPAI H5N1 mouse and ferret models show incomplete virus inhibition when not given early (within 4 hours) in the infection cycle [322, 323]. Oseltamivir resistant H5N1 viruses have also been identified in clinical studies of infected individuals [91, 324, 325]. Small animal models studying the effects of therapeutic zanamivir on reducing HPAI viral load showed promise in decreasing morbidity and mortality [322, 326]. Zanamivir when administered prophylactically in a non-human primate model showed promising antiviral effects by reducing viral load but therapeutic doses given post HPAI infection showed less effect [327].

Ion channel inhibitors such as amantadine and rimantidine are viable options for anti-viral treatment in pandemic HPAI situations. Amantadine and rimantidine form a barrier at the M2 influenza viral protein that functions to enable the entry of H^+ ions [328]. Inhibition of the ion flux hinders viral entry and prevents release of viral genome segments from matrix protein. Older HPAI isolates from human infections showed resistance to amantadine and rimantidine but new isolates showed susceptibility to amantadine, making stockpiling for combination anti-viral therapies useful [329, 330].

Type I IFNs and corticosteroids could also be utilized as broad-spectrum anti-viral therapies in the case of pandemics. IFNs are cytokines produced by viral infected cells that help facilitate resistance to viral replication, increase class I antigen presentation, and activate innate antigen presenting cells and natural killer cells [23]. Synthetic IFNs have shown efficacy in therapeutic applications of influenza infection however only prophylactic treatments have shown efficacy with

HPAI [331, 332]. Corticosteroid treatments have also been examined in the context of HPAI infection because of the multi-system cytokine storm associated with pathogenesis. Corticosteroids provided little improvement from the pathogenic traits in animal models and in clinical patients [333-335].

Prophylactic anti-viral treatment appears to be the most effective anti-viral approach in the midst of pandemic influenza. Speculation has occurred as to what may be the most effective combination of therapies for infected individuals, however, truly definitive studies examining HPAI may be unable to be performed [330, 335, 336].

Table 4. An outline of the typical factors needed to be considered towards designing and producing a pandemic vaccine against HPAI.

Vaccine	Potency	Production Speed	Purity	Safety
Inactivated Viral	**	*	*	*
Cold Adapted Attenuated Viral	**	*	**	*
Reverse Genetics Derived	**	**	*	*
DNA	**	***	***	**
Virus Like Particles	***	**	**	**
Immune Refocusing	*	**	***	***

Table 4.
Efficacy is often the major consideration but production speed, purity, and safety of the vaccines are all important aspects of vaccines to undergo and pass aspects of governmental regulations to be used in the population. Safety in the context of this table is considering only the antigen. Safety of many of these vaccines can be altered by the use of adjuvants which may present more adverse events at the time of or after vaccination. One * represents low value and *** represents higher value in the context of the vaccines discussed.

Discussion

The 2009 H1N1 influenza pandemic has reinforced the speed and aggressiveness of global influenza virus spread. Technological advancements in media and virus detection allowed the public to witness the virus distribution in real time. This public awareness as to how quickly influenza virus can be transmitted to

different populations globally has emphasized the need for pandemic preparedness and preventative therapeutics.

Highly pathogenic avian influenza H5N1 poses great concern to dense human populations because of the disease severity associated with this variant not typically associated with seasonal influenza virus. Although the H5N1 influenza has yet to acquire the ability to be transmitted from human to human, significant efforts have been focused on studying the viral pathogenicity as well as investigating prophylactic treatments in case of pandemic spread.

Traditional seasonal influenza vaccine preparations involving inactivated virus have shown efficacy, but are limited by the production constraints associated with seasonal influenza vaccines grown in embryonated hen eggs. New techniques using viral propagation in cell culture as well as the development of reverse genetics systems where an entire virus can be produced from plasmid DNA *in vitro* can help alleviate the production constraints with traditional methods. These inactivated viral vaccines from non-egg origins still face licensure scrutiny from the governing oversight committees, however, the increased turnaround time of propagating the virus as well as the lack of egg products negating the allergic effects observed in traditional seasonal vaccines provides these technologies with advantages.

Cold adapted viral vaccines present another promising option for H5N1 pandemic vaccines. Because of the restrictive replicative abilities of the modified live virus in the upper respiratory tract, low quantities of antigen are needed. Cold adapted viral vaccines are also advantageous for pandemic situations because of the ease of intranasal administration as well as not being constrained by the need

for medical professionals for administration.

DNA vaccines are an attractive option in vaccine development because of the low cost of production of DNA in contrast to protein antigen. DNA vaccines are also very stable and are not restricted by cold chain storage when produced, thus providing a significant advantage in pandemic situations. However, DNA vaccines may suffer from the specialized regimens needed, such as electroporation, which may not be readily executable. To get around these specialized regimens, DNA vaccines have been examined in the form of viral vectored vaccines encoding genes of influenza virus. Regulatory approval for viral vectored vaccines in humans is still a challenge.

Subunit vaccines for HPAI H5N1 present one of the better safety profiles of pandemic influenza vaccines due to the purity of the single or tandem antigens used. Efficacy of subunit vaccines remains a consistent hurdle that needs to be overcome especially in the context of H5N1 vaccines. The HA trimer is the target of a neutralizing antibody response due to the antibody being able to block the binding of virus to host epithelial cells. The HA molecules are under constant selective pressure to evade adaptive immune responses and as such are one of the most rapidly mutagenic proteins of influenza virus that allow the virus to undergo antigenic drift or shift precipitously.

Adjuvants such as aluminum salts, TLR agonists, and MF59^{TM} have been commonly used to enhance the immune response to the subunit protein antigens of H5N1 [238, 261, 265, 298, 311, 337-339]. Co-administration of HA and NA antigens as well as the vaccination of VLPs improves the protective immune responses due

to the increased resemblance to an infectious event compared with a single antigen. Although protective efficacy associated with the use of recombinant proteins may be less than with other immunogen formats, the labor and cost of producing recombinant proteins are reducing with technological advances in protein engineering.

Cross protective influenza vaccines against distinct strains remains one of the biggest obstacles in influenza vaccine design. Recent insights into examining the immunological map of where the immune responses are directed to on the HA are raising exciting possibilities in obtaining cross strain protection. Antigens that refocus the immune response to more conserved regions in the stalk of the HA molecule of a lab strain of influenza have induced antibodies that cross react with other strains [248]. Although in its infancy, this technology could prove to be the ultimate fail safe in protecting against a pandemic by eliciting protection against both seasonal and pandemic strains of influenza.

Prophylactic or therapeutic anti-viral drugs also need be evaluated when examining influenza pandemic preparedness. Prophylactic anti-viral treatments appear to be the most effective approach to prevent infection [336]. Combination therapies have also been examined to tackle the issues associated with genetic resistance to anti-viral drugs.

Polyanhydride particle platform

The main principle supporting the use of polyanhydrides as biomaterial drug delivery vehicles was the ability of these materials to provide a controlled release of

a payload encapsulated within the particle by a unique surface erosion mechanism [340]. The erosion kinetics can be tailored by purposeful selection of copolymer combinations of aromatic polyanhydrides such as 1,6-bis(*p*-carboxyphenoxy) hexane (CPH), and 1,8-bis(*p*-carboxyphenoxy)-3,6-dioxaoctane (CPTEG) either in combination with each other or in combination with sebacic acid (SA) to increase or decrease the rate of degradation and thus the release of protein. Combinations consisting of CPH and SA erode relatively quicker than combinations of CPH and CPTEG [341]. The amount of CPH in copolymer dictates longer erosion kinetics as well for example 50:50 CPTEG:CPH erodes quicker than 20:80 CPTEG:CPH. Differences in size of proteins and chemistry of particles of particles all lead to unique erosion and release kinetics from particles but the principle of controlled release is maintained.

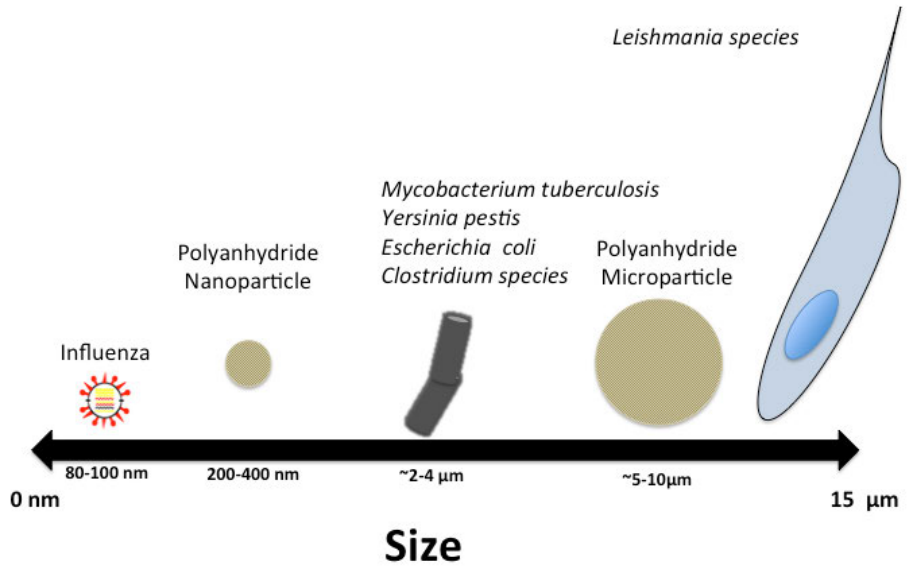

Figure 4. Size comparisons of the synthetic polyanhydride nanoparticle platform compared to common pathogens. A continuous size comparison of common pathogen sizes expressed in nanometers to microns.

Using different fabrication techniques allows for manipulation of particle size creating ~15 µm diameter particles when using solid/oil/oil emulsion methods or cryogenic atomization based methods outlined in Lopac et al [342] and ~300 nm diameter particles when using an anti-solvent nanoprecipitation technique outlined in Ulery et al [343]. The CPTEG containing polyanhydride particles allow for an amphiphilic and an environment that serves to maintain structural integrity and immunogenicity of the encapsulated immunogen [344-346] while mimicking pathogen sizes (Figure 3). These microparticles or nanoparticles provide a particulate context for phagocytic APCs enhance activation markers of antigen presenting cells [343, 347].

Using these attributes of size optimized for phagocytosis [343, 347], innate immunomodulatory activity of APCs [344, 347-349], controlled release of encapsulated antigen to continually provide antigen for an extended period of time

post-immunization [340, 342, 345, 350-354], and theoretical repetitive structure of an antigen loaded in particles helping to provide crosslinking of B cell receptors, the polyanhydride particle platform provides a unique base for vaccine design.

Efficacy of vaccines designed using the polyanhydride particle platform has been characterized by the induction of long-lived antibody responses of high titer and high avidity [65, 355, 356]. Fully encapsulating tetanus toxoid into polyanhydride microparticles composed of 20:80 CPH:SA or 50:50 CPH:SA was capable of inducing high titer IgG1 as well as IgG2a in the case of the 50:50 CPH:SA groups indicating presence of IFN-γ elicited post-immunization [357]. Building from that information as well as other studies, an intranasal polyanhydride nanoparticle vaccine against *Yersinia pestis* was designed using the F1-V fusion protein, a protective antigen consisting of the Fraction 1 capsular antigen (F1) and the V protein portion of the type III secretion system [358]. The vaccine regimen consisted of a soluble antigen administered along with F1-V encapsulated into 50:50 CPTEG:CPH polyanhydride nanoparticles. After a single intranasal dose, protective immunity from *Y. pestis* challenge was observed at 26 and 40 weeks post-immunization that was characterized by the presence of high titer and highly avid F1-V-specific IgG1 [65, 356].

Overview of thesis and project objectives

Based on previous studies, elucidating the cellular mechanisms underlying the efficacious adjuvant activity of the polyanhydride particle platform was warranted. The following chapters of this dissertation attempt to define those

mechanisms and to use that knowledge for design of a novel vaccine using the polyanhydride particle platform against the H5N1 influenza virus. Specifically, the aims were to (1) provide a proof of concept of encapsulation of antigen into polyanhydride particles facilitates antigen sparing and induction of antigen-specific IgG1 and IgG2a antibodies, (2) define biocompatibility, reactogenicity, and in vivo kinetics of particle persistence after administration, (3) define the $CD4^+$ and $CD8^+$ T cell responses after immunization, and (4) test the efficacy of polyanhydride nanoparticle designed vaccines to induce neutralizing antibody against the H5N1 influenza virus. By defining these host response characteristics and tailoring the platform to induce neutralizing antibody against a viral pathogen, this will further define the host response characteristics needed for translating the polyanhydride platform to use in human and veterinary medicine as well as demonstrate the capabilities of the platform for other vaccinological applications.

References:

[1] Jones G, Steketee RW, Black RE, Bhutta ZA, Morris SS. How many child deaths can we prevent this year? The Lancet 2003;362(9377):65-71.

[2] Arnon R, Ben-Yedidia T. Old and new vaccine approaches. International Immunopharmacology 2003;3(8):1195-204.

[3] Edwards Km LEWPF. Diphtheria, tetanus, and pertussis vaccine: A comparison of the immune response and adverse reactions to conventional and acellular pertussis components. Archives of Pediatrics & Adolescent Medicine 1986;140(9):867-71.

[4] Dormitzer PR, Galli G, Castellino F, Golding H, Khurana S, Del Giudice G, et al. Influenza vaccine immunology. Immunological Reviews 2011;239(1):167-77.

[5] Vignuzzi M, Wendt E, Andino R. Engineering attenuated virus vaccines by controlling replication fidelity. Nature Medicine 2008;14(2):154-61.

[6] Moghaddam A, Olszewska W, Wang B, Tregoning JS, Helson R, Sattentau QJ, et al. A potential molecular mechanism for hypersensitivity caused by formalin-inactivated vaccines. Nature Medicine 2006;12(8):905-7.

[7] Buonaguro L, Pulendran B. Immunogenomics and systems biology of vaccines. Immunological Reviews 2011;239(1):197-208.

[8] Zepp F. Principles of vaccine design--lessons from nature. Vaccine 2010;28(Supplement 3):C14-C24.

[9] Barrett ADT, Teuwen DE. Yellow fever vaccine - how does it work and why do rare cases of serious adverse events take place? Current Opinion in Immunology 2009;21(3):308-13.

[10] Hepburn MJ, Kortepeter MG, Pittman PR, Boudreau EF, Mangiafico JA, Buck PA, et al. Neutralizing antibody response to booster vaccination with the 17d yellow fever vaccine. Vaccine 2006;24(15):2843-9.

[11] Querec TD, Akondy RS, Lee EK, Cao W, Nakaya HI, Teuwen D, et al. Systems biology approach predicts immunogenicity of the yellow fever vaccine in humans. Nature Immunology 2009;10(1):116-25.

[12] Becker Y. Respiratory syncytial virus (rsv) evades the human adaptive immune system by skewing the th1/th2 cytokine balance toward increased levels of th2 cytokines and ige, markers of allergy—a review. Virus Genes 2006;33(2):235-52.

[13] Barquet N, Domingo P. Smallpox: The triumph over the most terrible of the ministers of death. Annals of Internal Medicine 1997;127(1):635-42.

[14] Cherry JD, Brunell PA, Golden GS, Karzon DT. Report of the task force on pertussis and pertussis immunization-1988. Pediatrics 1988;81(6):933-84.

[15] Cherry JD. Historical review of pertussis and the classical vaccine. Journal of Infectious Diseases 1996;174(Supplement 3):S259-S63.

[16] Cherry JD. The epidemiology of pertussis and pertussis immunization in the united kingdom and the united state: A comparative study. Current Problems in Pediatrics 1984;14(2):7-77.

[17] Complete list of vaccines licensed for immunization and distribution in the us. Vaccines, Blood and Biologics 2012 [cited 2012 6/28/2012]; Available from: http://www.fda.gov/BiologicsBloodVaccines/Vaccines/ApprovedProducts/UCM093833

[18] Howson Cp FHV. Adverse events following pertussis and rubella vaccines: Summary of a report of the institute of medicine. JAMA: The Journal of the American Medical Association 1992;267(3):392-6.

[19] Bellman MH, Ross EM, Miller DL. Infantile spasms and pertussis immunisation. The Lancet 1983;321(8332):1031-4.

[20] Gustafsson L, Hallander HO, Olin P, Reizenstein E, Storsaeter J. A controlled trial of a two-component acellular, a five-component acellular, and a whole-cell pertussis vaccine. New England Journal of Medicine 1996;334(6):349-56.

[21] O'Hagan DT, De Gregorio E. The path to a successful vaccine adjuvant- 'the long and winding road'. Drug Discovery Today 2009;14(11 & 12):541-51.

[22] Bachmann MF, Jennings GT. Designing recombinant vaccines with viral properties: A rational approach to more effective vaccines. Current Molecular Medicine 2007;7(2):143-55.

[23] Murphy K, Travers P, Walport M. Janeway's immunobiology. In: Lawrence E, editor. Janeway's immunobiology. Seventh ed. New York, NY: Garland Science, 2008: 111-77.

[24] Bachmann MF, Jennings GT. Vaccine delivery: A matter of size, geometry, kinetics and molecular patterns. Nature Reviews Immunology;10(11):787-96.

[25] Blander JM, Sander LE. Beyond pattern recognition: Five immune checkpoints for scaling the microbial threat. Nature Reviews Immunology 2012;12(3):215-25.

[26] Spohn G, Bachmann MF. Exploiting viral properties for the rational design of modern vaccines. Expert Review of Vaccines 2008;7(1):43-54.

[27] Janeway CA, Medzhitov R. Innate immune recognition. Annual Review of Immunology 2002;20(1):197-216.

[28] Villadangos JA, Schnorrer P. Intrinsic and cooperative antigen-presenting functions of dendritic-cell subsets in vivo. Nature Reviews Immunology 2007;7(7):543-55.

[29] Steinman RM. Decisions about dendritic cells: Past, present, and future. Annual Review of Immunology 2012;30(1):1-22.

[30] Junt T, Moseman EA, Iannacone M, Massberg S, Lang PA, Boes M, et al. Subcapsular sinus macrophages in lymph nodes clear lymph-borne viruses and present them to antiviral b cells. Nature 2007;450(7166):110-4.

[31] Abi Abdallah DS, Egan CE, Butcher BA, Denkers EY. Mouse neutrophils are professional antigen-presenting cells programmed to instruct th1 and th17 t-cell differentiation. International Immunology 2011;23(5):317-26.

[32] Heath WR, Belz GT, Behrens GMN, Smith CM, Forehan SP, Parish IA, et al. Cross-presentation, dendritic cell subsets, and the generation of immunity to cellular antigens. Immunological Reviews 2004;199(1):9-26.

[33] Coffman RL, Sher A, Seder RA. Vaccine adjuvants: Putting innate immunity to work. Immunity 2010;33(4):492-503.

[34] Banchereau J, Steinman RM. Dendritic cells and the control of immunity. Nature 1998;392(6673):245-52.

[35] Rettig L, Haen SP, Bittermann AG, von Boehmer L, Curioni A, Kramer SD, et al. Particle size and activation threshold: A new dimension of danger signaling. Blood;115(22):4533-41.

[36] Touret N, Paroutis P, Terebiznik M, Harrison RE, Trombetta S, Pypaert M, et al. Quantitative and dynamic assessment of the contribution of the er to phagosome formation. Cell 2005;123(1):157-70.

[37] Underhill DM, Goodridge HS. Information processing during phagocytosis. Nature Reviews Immunology 2012;12(7):492-502.

[38] Foged C, Brodin B, Frokjaer S, Sundblad A. Particle size and surface charge affect particle uptake by human dendritic cells in an in vitro model. International Journal of Pharmaceutics 2005;298(2):315-22.

[39] Clausi A, Cummiskey J, Merkley S, Carpenter JF, Braun LJ, Randolph TW. Influence of particle size and antigen binding on effectiveness of aluminum salt adjuvants in a model lysozyme vaccine. Journal of Pharmaceutical Sciences 2008;97(12):5252-62.

[40] Champion J, Walker A, Mitragotri S. Role of particle size in phagocytosis of polymeric microspheres. Pharmaceutical Research 2008;25(8):1815-21.

[41] Manolova V, Flace A, Bauer M, Schwarz K, Saudan P, Bachmann MF. Nanoparticles target distinct dendritic cell populations according to their size. European Journal of Immunology 2008;38(5):1404-13.

[42] Lu F, Wu S-H, Hung Y, Mou C-Y. Size effect on cell uptake in well-suspended, uniform mesoporous silica nanoparticles. Small 2009;5(12):1408-13.

[43] Reddy ST, van der Vlies AJ, Simeoni E, Angeli V, Randolph GJ, O'Neil CP, et al. Exploiting lymphatic transport and complement activation in nanoparticle vaccines. Nature Biotechnology 2007;25(10):1159-64.

[44] Catron DM, Itano AA, Pape KA, Mueller DL, Jenkins MK. Visualizing the first 50 hr of the primary immune response to a soluble antigen. Immunity 2004;21(3):341-7.

[45] Pape KA, Catron DM, Itano AA, Jenkins MK. The humoral immune response is initiated in lymph nodes by b cells that acquire soluble antigen directly in the follicles. Immunity 2007;26(4):491-502.

[46] Catron DM, Pape KA, Fife BT, van Rooijen N, Jenkins MK. A protease-dependent mechanism for initiating t-dependent b cell responses to large particulate antigens. The Journal of Immunology 2010;184(7):3609-17.

[47] Carrasco YR, Batista FD. B cells acquire particulate antigen in a macrophage-rich area at the boundary between the follicle and the subcapsular sinus of the lymph node. Immunity 2007;27(1):160-71.

[48] Phan TG, Green JA, Gray EE, Xu Y, Cyster JG. Immune complex relay by subcapsular sinus macrophages and noncognate b cells drives antibody affinity maturation. Nat Immunol 2009;10(7):786-93.

[49] Wang X, Cho B, Suzuki K, Xu Y, Green JA, An J, et al. Follicular dendritic cells help establish follicle identity and promote b cell retention in germinal centers. The Journal of Experimental Medicine 2011;208(12):2497-510.

[50] El Shikh MEM, El Sayed RM, Sukumar S, Szakal AK, Tew JG. Activation of b cells by antigens on follicular dendritic cells. Trends in Immunology 2010;31(6):205-11.

[51] Bottazzi B, Doni A, Garlanda C, Mantovani A. An integrated view of humoral innate immunity: Pentraxins as a paradigm. Annual Review of Immunology 2010;28(1):157-83.

[52] Inforzato A, Bottazzi B, Garlanda C, Valentino S, Mantovani A. Pentraxins in humoral innate immunity current topics in innate immunity ii. In: Lambris JD, Hajishengallis G, editors.: Springer New York, 2012: 1-20.

[53] Gasque P. Complement: A unique innate immune sensor for danger signals. Molecular Immunology 2004;41(11):1089-98.

[54] Seifert PS, Hugo F, Tranum-Jensen J, Zâhringer U, Muhly M, Bhakdi S. Isolation and characterization of a complement-activating lipid extracted from human atherosclerotic lesions. The Journal of Experimental Medicine 1990;172(2):547-57.

[55] Seong S-Y, Matzinger P. Hydrophobicity: An ancient damage-associated molecular pattern that initiates innate immune responses. Nature Reviews Immunology 2004;4(6):469-78.

[56] Holmskov U, Thiel S, Jensenius JC. Collectins and ficolins: Humoral lectins of the innate immune defense. Annual Review of Immunology 2003;21(1):547-78.

[57] Kairies N, Beisel H-G, Fuentes-Prior P, Tsuda R, Muta T, Iwanaga S, et al. The 2.0-å crystal structure of tachylectin 5a provides evidence for the common origin of the innate immunity and the blood coagulation systems. Proceedings of the National Academy of Sciences 2001;98(24):13519-24.

[58] Walport MJ. Complement. New England Journal of Medicine 2001;344(14):1058-66.

[59] Bachmann MF, Zinkernagel RM. The influence of virus structure on antibody responses and virus serotype formation. Immunology Today 1996;17(12):553-8.

[60] Bachmann MF, Hengartner H, Zinkernagel RM. T helper cell-independent neutralizing b cell response against vesicular stomatitis virus: Role of antigen patterns in b cell induction? European Journal of Immunology 1995;25(12):3445-51.

[61] Noad R, Roy P. Virus-like particles as immunogens. Trends in Microbiology 2003;11(9):438-44.

[62] Roy P, Noad R. Virus-like particles as a vaccine delivery system: Myths and facts. Human Vaccines 2008;4(1):5-12.

[63] Jansen T, Hofmans MPM, Theelen MJG, Manders F, Schijns VEJC. Structure- and oil type-based efficacy of emulsion adjuvants. Vaccine 2006;24(26):5400-5.

[64] Akagi T, Baba M, Akashi M. Biodegradable nanoparticles as vaccine adjuvants and delivery systems: Regulation of immune responses by nanoparticle-based vaccine polymers in nanomedicine. In: Kunugi S, Yamaoka T, editors.: Springer Berlin / Heidelberg, 2012: 31-64.

[65] Ulery BD, Petersen LK, Phanse Y, Kong CS, Broderick SR, Kumar D, et al. Rational design of pathogen-mimicking amphiphilic materials as nanoadjuvants. Scientific Reports 2011;1.

[66] Jegerlehner A, Storni T, Lipowsky G, Schmid M, Pumpens P, Bachmann MF. Regulation of IgG antibody responses by epitope density and CD21-mediated costimulation. European Journal of Immunology 2002;32(11):3305-14.

[67] Zinkernagel RM, Cooper S, Chambers J, Lazzarini RA, Hengartner H, Arnheiter H. Virus-induced autoantibody response to a transgenic viral antigen. Nature 1990;345(6270):68-71.

[68] Bachmann MF, Zinkernagel RM. Neutralizing antiviral B cell responses. Annual Review of Immunology 1997;15(1):235-70.

[69] Barrington R, Zhang M, Fischer M, Carroll MC. The role of complement in inflammation and adaptive immunity. Immunological Reviews 2001;180(1):5-15.

[70] Carter RH, Myers R. Germinal center structure and function: Lessons from CD19. Seminars in Immunology 2008;20(1):43-8.

[71] Gatto D, Pfister T, Jegerlehner A, Martin SW, Kopf M, Bachmann MF. Complement receptors regulate differentiation of bone marrow plasma cell precursors expressing transcription factors blimp-1 and xbp-1. The Journal of Experimental Medicine 2005;201(6):993-1005.

[72] Rickert RC. Regulation of b lymphocyte activation by complement c3 and the B cell coreceptor complex. Current Opinion in Immunology 2005;17(3):237-43.

[73] Bohana-Kashtan O, Ziporen L, Donin N, Kraus S, Fishelson Z. Cell signals transduced by complement. Molecular Immunology 2004;41(6-7):583-97.

[74] Chtarbanova S, Imler J-L. Microbial sensing by toll receptors. Arteriosclerosis, Thrombosis, and Vascular Biology 2011;31(8):1734-8.

[75] Takeuchi O, Akira S. Pattern recognition receptors and inflammation. Cell 2010;140(6):805-20.

[76] Akira S, Uematsu S, Takeuchi O. Pathogen recognition and innate immunity. Cell 2006;124(4):783-801.

[77] Kim D, Kim YJ, Koh HS, Jang TY, Park HE, Kim JY. Reactive oxygen species enhance tlr10 expression in the human monocytic cell line thp-1. International Journal of Molecular Sciences 2010;11(10):3769-82.

[78] Barton GM, Kagan JC. A cell biological view of toll-like receptor function: Regulation through compartmentalization. Nature Reviews Immunology 2009;9(8):535-42.

[79] Schmitz F, Heit A, Guggemoos S, Krug A, Mages J, Schiemann M, et al. Interferon-regulatory-factor 1 controls toll-like receptor 9-mediated IFN-β production in myeloid dendritic cells. European Journal of Immunology 2007;37(2):315-27.

[80] Takahasi K, Yoneyama M, Nishihori T, Hirai R, Kumeta H, Narita R, et al. Nonself RNA-sensing mechanism of RIG-I helicase and activation of antiviral immune responses. Molecular Cell 2008;29(4):428-40.

[81] Takeuchi O, Akira S. Innate immunity to virus infection. Immunological Reviews 2009;227(1):75-86.

[82] Kato H, Takeuchi O, Sato S, Yoneyama M, Yamamoto M, Matsui K, et al. Differential roles of MDA5 and RIG-I helicases in the recognition of RNA viruses. Nature 2006;441(7089):101-5.

[83] Martinon F, Mayor A, Tschopp J. The inflammasomes: Guardians of the body. Annual Review of Immunology 2009;27(1):229-65.

[84] Dinarello CA. Unraveling the NALP-3/IL-1beta inflammasome: A big lesson from a small mutation. Immunity 2004;20(3):243-4.

[85] Tschopp J, Martinon F, Burns K. Nalps: A novel protein family involved in inflammation. Nature Reviews Molecular Cell Biology 2003;4(2):95-104.

[86] Tattoli I, Travassos L, Carneiro L, Magalhaes J, Girardin S. The nodosome: Nod1 and nod2 control bacterial infections and inflammation. Seminars in Immunopathology 2007;29(3):289-301.

[87] Mariathasan S, Weiss DS, Newton K, McBride J, O'Rourke K, Roose-Girma M, et al. Cryopyrin activates the inflammasome in response to toxins and atp. Nature 2006;440(7081):228-32.

[88] Shi Y, Evans JE, Rock KL. Molecular identification of a danger signal that alerts the immune system to dying cells. Nature 2003;425(6957):516-21.

[89] Dostert C, Pétrilli V, Van Bruggen R, Steele C, Mossman BT, Tschopp J. Innate immune activation through NALP3 inflammasome sensing of asbestos and silica. Science 2008;320(5876):674-7.

[90] Geijtenbeek TBH, Gringhuis SI. Signalling through c-type lectin receptors: Shaping immune responses. Nature Reviews Immunology 2009;9(7):465-79.

[91] de Jong MD, Thanh TT, Khanh TH, Hien VM, Smith GJD, Chau NV, et al. Oseltamivir resistance during treatment of influenza a (H5N1) infection. New England Journal of Medicine 2005;353(25):2667-72.

[92] Caproni E, Tritto E, Cortese M, Muzzi A, Mosca F, Monaci E, et al. MF59 and pam3csk4 boost adaptive responses to influenza subunit vaccine through an IFN type I-independent mechanism of action. The Journal of Immunology 2012;188(7):3088-98.

[93] Jayakumar A, Castilho TM, Park E, Goldsmith-Pestana K, Blackwell JM, McMahon-Pratt D. TLR1/2 activation during heterologous prime-boost vaccination (DNA-mva) enhances $CD8^+$ T cell responses providing protection against *leishmania (viannia)*. PLoS Neglected Tropical Diseases 2011;5(6):e1204.

[94] Maitra R, Clement CC, Scharf B, Crisi GM, Chitta S, Paget D, et al. Endosomal damage and TLR2 mediated inflammasome activation by alkane particles in the generation of aseptic osteolysis. Molecular Immunology 2009;47(2-ì3):175-84.

[95] Borsutzky S, Kretschmer K, Becker PD, Mühlradt PF, Kirschning CJ, Weiss S, et al. The mucosal adjuvant macrophage-activating lipopeptide-2 directly stimulates B lymphocytes via the TLR2 without the need of accessory cells. The Journal of Immunology 2005;174(10):6308-13.

[96] Flo TH, Ryan L, Latz E, Takeuchi O, Monks BG, Lien E, et al. Involvement of toll-like receptor (TLR) 2 and TLR4 in cell activation by mannuronic acid polymers. Journal of Biological Chemistry 2002;277(38):35489-95.

[97] Delaloye J, Roger T, Steiner-Tardivel Q-G, Le Roy D, Knaup Reymond M, Akira S, et al. Innate immune sensing of modified vaccinia virus ankara (MVA) is mediated by TLR2-TLR6, MDA-5 and the NALP3 inflammasome. PLoS Pathogens 2009;5(6):e1000480.

[98] Trumpfheller C, Caskey M, Nchinda G, Longhi MP, Mizenina O, Huang Y, et al. The microbial mimic poly IC induces durable and protective $CD4^+$ T cell immunity together with a dendritic cell targeted vaccine. Proceedings of the National Academy of Sciences 2008;105(7):2574-9.

[99] Didierlaurent AM, Morel S, Lockman L, Giannini SL, Bisteau M, Carlsen H, et al. AS04, an aluminum salt- and TLR4 agonist-based adjuvant system, induces a transient localized innate immune response leading to enhanced adaptive immunity. The Journal of Immunology 2009;183(10):6186-97.

[100] Evans JT, Cluff CW, Johnson DA, Lacy MJ, Persing DH, Baldridge JR. Enhancement of antigen-specific immunity via the TLR4 ligands MPL™ adjuvant and Ribi.529. Expert Review of Vaccines 2003;2(2):219-29.

[101] Grandjean-Laquerriere A, Tabary O, Jacquot J, Richard D, Frayssinet P, Guenounou M, et al. Involvement of toll-like receptor 4 in the inflammatory reaction induced by hydroxyapatite particles. Biomaterials 2007;28(3):400-4.

[102] Mizel SB, Bates JT. Flagellin as an adjuvant: Cellular mechanisms and potential. The Journal of Immunology 2010;185(10):5677-82.

[103] Johnston D, Zaidi B, Bystryn J-C. TLR7 imidazoquinoline ligand 3m-019 is a potent adjuvant for pure protein prototype vaccines. Cancer Immunology, Immunotherapy 2007;56(8):1133-41.

[104] Dharmapuri S, Aurisicchio L, Neuner P, Verdirame M, Ciliberto G, La Monica N. An oral TLR7 agonist is a potent adjuvant of DNA vaccination in transgenic mouse tumor models. Cancer Gene Therapy 2008;16(5):462-72.

[105] Cooper CL, Davis HL, Morris ML, Efler SM, Adhami MA, Krieg AM, et al. Cpg 7909, an immunostimulatory TLR9 agonist oligodeoxynucleotide, as adjuvant to engerix-b® HBV vaccine in healthy adults: A double-blind phase I/II study. Journal of Clinical Immunology 2004;24(6):693-701.

[106] Schellack C, Prinz K, Egyed A, Fritz JrH, Wittmann B, Ginzler M, et al. Ic31, a novel adjuvant signaling via TLR9, induces potent cellular and humoral immune responses. Vaccine 2006;24(26):5461-72.

[107] Hedhli D, Dimier-Poisson I, Judge JW, Rosenberg B, Mévélec MNl. Protective immunity against toxoplasma challenge in mice by coadministration of T. gondii antigens and eimeria profilin-like protein as an adjuvant. Vaccine 2009;27(16):2274-81.

[108] Luke JM, Simon GG, Söderholm J, Errett JS, August JT, Gale M, et al. Coexpressed RIG-I agonist enhances humoral immune response to influenza virus DNA vaccine. Journal of Virology 2011;85(3):1370-83.

[109] Wang Y, Cella M, Gilfillan S, Colonna M. Cutting edge: Polyinosinic:Polycytidylic acid boosts the generation of memory CD8 T cells through melanoma differentiation-associated protein 5 expressed in stromal cells. The Journal of Immunology 2010;184(6):2751-5.

[110] Suthar MS, Ramos HJ, Brassil MM, Netland J, Chappell CP, Blahnik G, et al. The RIG-I-like receptor lgp2 controls $CD8^+$ T cell survival and fitness. Immunity;37(2):235-48.

[111] Wischke C, Mathew S, Roch T, Frentsch M, Lendlein A. Potential of NOD receptor ligands as immunomodulators in particulate vaccine carriers. Journal of Controlled Release;164(3):299-306.

[112] Sharp FA, Ruane D, Claass B, Creagh E, Harris J, Malyala P, et al. Uptake of particulate vaccine adjuvants by dendritic cells activates the NALP3 inflammasome. Proceedings of the National Academy of Sciences 2009;106(3):870-5.

[113] Eisenbarth SC, Colegio OR, O'Connor W, Sutterwala FS, Flavell RA. Crucial role for the NALP3 inflammasome in the immunostimulatory properties of aluminium adjuvants. Nature 2008;453(7198):1122-6.

[114] LeibundGut-Landmann S, Osorio F, Brown GD, Reis e Sousa C. Stimulation of dendritic cells via the dectin-1/syk pathway allows priming of cytotoxic T-cell responses. Blood 2008;112(13):4971-80.

[115] Shreffler WG, Castro RR, Kucuk ZY, Charlop-Powers Z, Grishina G, Yoo S, et al. The major glycoprotein allergen from arachis hypogaea, ara h 1, is a ligand of dendritic cell-specific icam-grabbing nonintegrin and acts as a Th2 adjuvant in vitro. The Journal of Immunology 2006;177(6):3677-85.

[116] Gram GJ, Karlsson I, Agger EM, Andersen P, Fomsgaard A. A novel liposome-based adjuvant caf01 for induction of $CD8^+$ cytotoxic T-lymphocytes (CTL) to HIV-1 minimal CTL peptides in hla-a*0201 transgenic mice. PLoS ONE 2009;4(9):e6950.

[117] Zinkernagel RM. On differences between immunity and immunological memory. Current Opinion in Immunology 2002;14(4):523-36.

[118] Zinkernagel RM. On natural and artificial vaccinations. Annual Review of Immunology 2003;21(1):515-46.

[119] Johansen PI, Storni T, Rettig L, Qiu Z, Der-Sarkissian A, Smith KA, et al. Antigen kinetics determines immune reactivity. Proceedings of the National Academy of Sciences 2008;105(13):5189-94.

[120] Bachmann MF, Beerli RR, Agnellini P, Wolint P, Schwarz K, Oxenius A. Long-lived memory $CD8^+$ T cells are programmed by prolonged antigen exposure and low levels of cellular activation. European Journal of Immunology 2006;36(4):842-54.

[121] Iezzi G, Karjalainen K, Lanzavecchia A. The duration of antigenic stimulation determines the fate of naive and effector t cells. Immunity 1998;8(1):89-95.

[122] Sallie R. Replicative homeostasis II: Influence of polymerase fidelity on RNA virus quasispecies biology: Implications for immune recognition, viral autoimmunity and other "virus receptor" diseases. Virology Journal 2005;2(1):70.

[123] Cox NJ, Subbarao K. Global epidemiology of influenza: Past and present. Annual Review of Medicine 2000;51(1):407-21.

[124] Duan L, Bahl J, Smith GJD, Wang J, Vijaykrishna D, Zhang LJ, et al. The development and genetic diversity of H5N1 influenza virus in China, 1996-2006. Virology 2008;380(2):243-54.

[125] Chen H, Smith GJD, Li KS, Wang J, Fan XH, Rayner JM, et al. Establishment of multiple sublineages of H5N1 influenza virus in Asia: Implications for pandemic

control. Proceedings of the National Academy of Sciences of the United States of America 2006;103(8):2845-50.

[126] Webster RG, Govorkova EA. H5N1 influenza continuing evolution and spread. New England Journal of Medicine 2006;355(21):2174-7.

[127] Peiris JSM, Cheung CY, Leung CYH, Nicholls JM. Innate immune responses to influenza a H5N1: Friend or foe? Trends in Immunology 2009;30(12):574-84.

[128] Shinya K, Ebina M, Yamada S, Ono M, Kasai N, Kawaoka Y. Avian flu: Influenza virus receptors in the human airway. Nature 2006;440(7083):435-6.

[129] Yamada S, Suzuki Y, Suzuki T, Le MQ, Nidom CA, Sakai-Tagawa Y, et al. Haemagglutinin mutations responsible for the binding of H5N1 influenza A viruses to human-type receptors. Nature 2006;444(7117):378-82.

[130] Ungchusak K, Auewarakul P, Dowell SF, Kitphati R, Auwanit W, Puthavathana P, et al. Probable person-to-person transmission of avian influenza a (h5n1). New England Journal of Medicine 2005;352(4):333-40.

[131] Ma W, Kahn RE, Richt JA. The pig as a mixing vessel for influenza viruses: Human and veterinary implications. Journal of Molecular and Genetic Medicine 2009;3(1):158-66.

[132] O'Donnell CD, Subbarao K. The contribution of animal models to the understanding of the host range and virulence of influenza A viruses. Microbes and Infection 2011;13(5):502-15.

[133] Herfst S, Schrauwen EJA, Linster M, Chutinimitkul S, de Wit E, Munster VJ, et al. Airborne transmission of influenza A/H5N1 virus between ferrets. Science 2012;336(6088):1534-41.

[134] Imai M, Watanabe T, Hatta M, Das SC, Ozawa M, Shinya K, et al. Experimental adaptation of an influenza H5 HA confers respiratory droplet transmission to a reassortant H5 HA/H1N1 virus in ferrets. Nature 2012; advance online publication.

[135] Buchy P, Mardy S, Vong S, Toyoda T, Aubin J-T, Miller M, et al. Influenza A/H5N1 virus infection in humans in Cambodia. Journal of Clinical Virology 2007;39(3):164-8.

[136] de Jong MD, Cam BV, Qui PT, Hien VM, Thanh TT, Hue NB, et al. Fatal avian influenza A (H5Ne1) in a child presenting with diarrhea followed by coma. New England Journal of Medicine 2005;352(7):686-91.

[137] de Jong MD, Simmons CP, Thanh TT, Hien VM, Smith GJD, Chau TNB, et al. Fatal outcome of human influenza A (H5N1) is associated with high viral load and hypercytokinemia. Nature Medicine 2006;12(10):1203-7.

[138] Peiris JSM, de Jong MD, Guan Y. Avian influenza virus (H5N1): A threat to human health. Clinical Microbiology Reviews 2007;20(2):243-67.

[139] Gu J, Xie Z, Gao Z, Liu J, Korteweg C, Ye J, et al. H5N1 infection of the respiratory tract and beyond: A molecular pathology study. The Lancet;370(9593):1137-45.

[140] Cheung CY, Poon LLM, Lau AS, Luk W, Lau YL, Shortridge KF, et al. Induction of proinflammatory cytokines in human macrophages by influenza A (H5N1) viruses: A mechanism for the unusual severity of human disease? The Lancet 2002;360(9348):1831-7.

[141] Hofmann P, Sprenger H, Kaufmann A, Bender A, Hasse C, Nain M, et al. Susceptibility of mononuclear phagocytes to influenza a virus infection and possible role in the antiviral response. Journal of Leukocyte Biology 1997;61(4):408-14.

[142] Matikainen S, Pirhonen J, Miettinen M, Lehtonen A, Govenius-Vintola C, Sareneva T, et al. Influenza A and sendai viruses induce differential chemokine gene expression and transcription factor activation in human macrophages. Virology 2000;276(1):138-47.

[143] Chan RWY, Yuen KM, Yu WCL, Ho CCC, Nicholls JM, Peiris JSM, et al. Influenza H5N1 and H1N1 virus replication and innate immune responses in bronchial epithelial cells are influenced by the state of differentiation. PLoS ONE;5(1):e8713.

[144] Yuen KY, Chan PKS, Peiris M, Tsang DNC, Que TL, Shortridge KF, et al. Clinical features and rapid viral diagnosis of human disease associated with avian influenza a H5N1 virus. The Lancet 1998;351(9101):467-71.

[145] Rimmelzwaan GF, Kuiken T, van Amerongen G, Bestebroer TM, Fouchier RAM, Osterhaus ADME. Pathogenesis of influenza A (H5N1) virus infection in a primate model. Journal of Virology 2001;75(14):6687-91.

[146] To K-F, Chan PKS, Chan K-F, Lee W-K, Lam W-Y, Wong K-F, et al. Pathology of fatal human infection associated with avian influenza A H5N1 virus. Journal of Medical Virology 2001;63(3):242-6.

[147] Writing Committee of the Second World Health Organization Consultation on Clinical Aspects of Human Infection with Avian Influenza A Virus. Update on avian influenza A (H5N1) virus infection in humans. New England Journal of Medicine 2008;358(3):261-73.

[148] Korteweg C, Gu J. Pathology, molecular biology, and pathogenesis of avian influenza A (H5N1) infection in humans. American Journal of Pathology 2008;172(5):1155-70.

[149] Khuntirat BP, Yoon I-K, Blair PJ, Krueger WS, Chittaganpitch M, Putnam SD, et al. Evidence for subclinical avian influenza virus infections among rural thai villagers. Clinical Infectious Diseases 2011;53(8):e107-e16.

[150] Cox RJ, Brokstad KA, Ogra P. Influenza virus: Immunity and vaccination strategies. Comparison of the immune response to inactivated and live, attenuated influenza vaccines. Scandinavian Journal of Immunology 2004;59(1):1-15.

[151] Ehrlich HJ, Muller M, Oh HML, Tambyah PA, Joukhadar C, Montomoli E, et al. A clinical trial of a whole-virus H5N1 vaccine derived from cell culture. New England Journal of Medicine 2008;358(24):2573-84.

[152] McCullers JA, Van De Velde L-A, Allison KJ, Branum KC, Webby RJ, Flynn PM. Recipients of vaccine against the 1976 "swine flu" have enhanced neutralization responses to the 2009 novel H1N1 influenza virus. Clinical Infectious Diseases 2010;50(11):1487-92.

[153] Nichol KL, Margolis KL, Lind A, Murdoch M, McFadden R, Hauge M, et al. Side effects associated with influenza vaccination in healthy working adults: A randomized, placebo-controlled trial. Archives of Internal Medicine 1996;156(14):1546-50.

[154] Margolis KL, Nichol KL, Poland GA, Pluhar RE. Frequency of adverse reactions to influenza vaccine in the elderly. JAMA: The Journal of the American Medical Association 1990;264(9):1139-41.

[155] Beyer W, Palache A, Osterhaus A. Comparison of serology and reactogenicity between influenza subunit vaccines and whole virus or split vaccines:

A review and meta-analysis of the literature. Clinical Drug Investigation 1998;15(1):1-12.

[156] Fleming D. Influenza pandemics and avian flu. British Medical Journal (BMJ) 2005;331(7524):1066-9.

[157] Cox RJ, Haaheim LR, Ericsson J-C, Madhun AS, Brokstad KA. The humoral and cellular responses induced locally and systemically after parenteral influenza vaccination in man. Vaccine 2006;24(44-46):6577-80.

[158] Karl A. Brokstad RJC, Jan Olofsson, Roland Jonsson, and Lars R. Haaheim. Parenteral influenza vaccination induces a rapid systemic and local immune response. The Journal of Infectious Diseases 1995;171(1):198-203.

[159] Abdullah S. El-Madhun RJC, and Lars R. Haaheim. The effect of age and natural priming on the igg and iga subclass responses after parenteral influenza vaccination. The Journal of Infectious Diseases 1999;180(4):1356-60.

[160] Cox RJ, Mykkeltvedt E, Sjursen H, Haaheim LR. The effect of zanamivir treatment on the early immune response to influenza vaccination. Vaccine 2001;19(32):4743-9.

[161] Guthrie T, Hobbs CL, Davenport V, Horton Rachel E, Heyderman Robert S, Williams Neil A. Parenteral influenza vaccination influences mucosal and systemic T cell-mediated immunity in healthy adults. The Journal of Infectious Diseases 2004;190(11):1927-35.

[162] Letter CR, Gravenstein S, McElhaney JE. Influenza vaccination is less effective for stimulating a granzyme B response in older adults. International Congress Series 2001;1219:713-21.

[163] McElhaney JE, Hooton JW, Hooton N, Bleackley RC. Comparison of single versus booster dose of influenza vaccination on humoral and cellular immune responses in older adults. Vaccine 2005;23(25):3294-300.

[164] Treanor JJ, Campbell JD, Zangwill KM, Rowe T, Wolff M. Safety and immunogenicity of an inactivated subvirion influenza a (H5N1) vaccine. New England Journal of Medicine 2006;354(13):1343-51.

[165] Falsey Ann R, Treanor John J, Tornieporth N, Capellan J, Gorse Geoffrey J. Randomized, double blind controlled phase 3 trial comparing the immunogenicity of

high-dose and standard-dose influenza vaccine in adults 65 years of age and older. The Journal of Infectious Diseases 2009;200(2):172-80.

[166] Geeraedts F, Goutagny N, Hornung V, Severa M, de Haan A, Pool J, et al. Superior immunogenicity of inactivated whole virus H5N1 influenza vaccine is primarily controlled by toll-like receptor signalling. PLoS Pathogens 2008;4(8):e1000138.

[167] Bresson J-L, Perronne C, Launay O, Gerdil C, Saville M, Wood J, et al. Safety and immunogenicity of an inactivated split-virion influenza A/Vietnam/1194/2004 (H5N1) vaccine: Phase I randomised trial. The Lancet 2006;367(9523):1657-64.

[168] Nolan T, Richmond PC, Formica NT, Höschler K, Skeljo MV, Stoney T, et al. Safety and immunogenicity of a prototype adjuvanted inactivated split-virus influenza a (H5N1) vaccine in infants and children. Vaccine 2008;26(50):6383-91.

[169] Lin J, Zhang J, Dong X, Fang H, Chen J, Su N, et al. Safety and immunogenicity of an inactivated adjuvanted whole-virion influenza A (H5N1) vaccine: A phase I randomised controlled trial. The Lancet 2006;368(9540):991-7.

[170] Keitel WA, Dekker CL, Mink C, Campbell JD, Edwards KM, Patel SM, et al. Safety and immunogenicity of inactivated, vero cell culture-derived whole virus influenza A/H5N1 vaccine given alone or with aluminum hydroxide adjuvant in healthy adults. Vaccine 2009;27(47):6642-8.

[171] Snyder MH, Betts RF, DeBorde D, Tierney EL, Clements ML, Herrington D, et al. Four viral genes independently contribute to attenuation of live influenza A/Ann Arbor/6/60 (H2N2) cold-adapted reassortant virus vaccines. Journal of Virology 1988;62(2):488-95.

[172] Larson TA, Potter LA. Reviews in medical virology. Journal of the American Medical Association 1994;271(1):73.

[173] Belshe RB, Edwards KM, Vesikari T, Black SV, Walker RE, Hultquist M, et al. Live attenuated versus inactivated influenza vaccine in infants and young children. New England Journal of Medicine 2007;356(7):685-96.

[174] Belshe RB, Gruber WC, Mendelman PM, Cho I, Reisinger K, Block SL, et al. Efficacy of vaccination with live attenuated, cold-adapted, trivalent, intranasal influenza virus vaccine against a variant (A/Sydney) not contained in the vaccine. The Journal of Pediatrics 2000;136(2):168-75.

[175] Halloran ME, Piedra PA, Longini JIM, Gaglani MJ, Schmotzer B, Fewlass C, et al. Efficacy of trivalent, cold-adapted, influenza virus vaccine against influenza A (Fujian), a drift variant, during 2003-2004. Vaccine 2007;25(20):4038-45.

[176] Karron RA, Talaat K, Luke C, Callahan K, Thumar B, DiLorenzo S, et al. Evaluation of two live attenuated cold-adapted H5N1 influenza virus vaccines in healthy adults. Vaccine 2009;27(36):4953-60.

[177] Suguitan AL, Jr., McAuliffe J, Mills KL, Jin H, Duke G, Lu B, et al. Live, attenuated influenza A H5N1 candidate vaccines provide broad cross-protection in mice and ferrets. PLoS Medicine 2006;3(9):e360.

[178] Jin H, Manetz S, Leininger J, Luke C, Subbarao K, Murphy B, et al. Toxicological evaluation of live attenuated, cold-adapted H5N1 vaccines in ferrets. Vaccine 2007;25(52):8664-72.

[179] Rudenko L, Desheva J, Korovkin S, Mironov A, Rekstin A, Grigorieva E, et al. Safety and immunogenicity of live attenuated influenza reassortant H5 vaccine (phase I & II clinical trials). Influenza and Other Respiratory Viruses 2008;2(6):203-9.

[180] Shi J, Wen Z, Guo J, Zhang Y, Deng G, Shu Y, et al. Protective efficacy of an H1N1 cold-adapted live vaccine against the 2009 pandemic H1N1, seasonal H1N1, and H5N1 influenza viruses in mice. Antiviral Research 2012;93(3):346-53.

[181] Jang YH, Byun YH, Lee YJ, Lee YH, Lee K-H, Seong BL. Cold-adapted pandemic 2009 H1N1 influenza virus live vaccine elicits cross-reactive immune responses against seasonal and H5 influenza a viruses. Journal of Virology 2012;86(10):5953-8.

[182] Hoffmann E, Neumann G, Kawaoka Y, Hobom G, Webster RG. A DNA transfection system for generation of influenza A virus from eight plasmids. Proceedings of the National Academy of Sciences of the United States of America 2000;97(11):6108-13.

[183] Neumann G, Watanabe T, Ito H, Watanabe S, Goto H, Gao P, et al. Generation of influenza A viruses entirely from cloned cdnas. Proceedings of the National Academy of Sciences of the United States of America 1999;96(16):9345-50.

[184] Hoffmann E, Krauss S, Perez D, Webby R, Webster RG. Eight-plasmid system for rapid generation of influenza virus vaccines. Vaccine 2002;20(25-26):3165-70.

[185] Subbarao K, Chen H, Swayne D, Mingay L, Fodor E, Brownlee G, et al. Evaluation of a genetically modified reassortant H5N1 influenza a virus vaccine candidate generated by plasmid-based reverse genetics. Virology 2003;305(1):192-200.

[186] Eun-Ju Jung K-HL, and Baik Lin Seong. Reverse genetic platform for inactivated and live-attenuated influenza vaccine. Experimental and Molecular Medicine 2010;42(2):116-31.

[187] Nicolson C, Major D, Wood JM, Robertson JS. Generation of influenza vaccine viruses on vero cells by reverse genetics: An H5N1 candidate vaccine strain produced under a quality system. Vaccine 2005;23(22):2943-52.

[188] Webby RJ, Perez DR, Coleman JS, Guan Y, Knight JH, Govorkova EA, et al. Responsiveness to a pandemic alert: Use of reverse genetics for rapid development of influenza vaccines. The Lancet 2004;363(9415):1099-103.

[189] Howard MK, Kistner O, Barrett PN. Pre-clinical development of cell culture (vero)-derived H5N1 pandemic vaccines. Biological Chemistry 2008;389(5):569-77.

[190] Ozawa M, Goto H, Horimoto T, Kawaoka Y. An adenovirus vector-mediated reverse genetics system for influenza A virus generation. Journal of Virology 2007;81(17):9556-9.

[191] Kistner O, Howard MK, Spruth M, Wodal W, Brühl P, Gerencer M, et al. Cell culture (vero) derived whole virus (H5N1) vaccine based on wild-type virus strain induces cross-protective immune responses. Vaccine 2007;25(32):6028-36.

[192] Webster RG, Webby RJ, Hoffmann E, Rodenberg J, Kumar M, Chu H-J, et al. The immunogenicity and efficacy against H5N1 challenge of reverse genetics-derived H5N3 influenza vaccine in ducks and chickens. Virology 2006;351(2):303-11.

[193] Tian G, Zhang S, Li Y, Bu Z, Liu P, Zhou J, et al. Protective efficacy in chickens, geese and ducks of an H5N1-inactivated vaccine developed by reverse genetics. Virology 2005;341(1):153-62.

[194] Suguitan Jr AL, Marino MP, Desai PD, Chen L-M, Matsuoka Y, Donis RO, et al. The influence of the multi-basic cleavage site of the H5 hemagglutinin on the attenuation, immunogenicity and efficacy of a live attenuated influenza A H5N1 cold-adapted vaccine virus. Virology 2009;395(2):280-8.

[195] Fan S, Gao Y, Shinya K, Li CK, Li Y, Shi J, et al. Immunogenicity and protective efficacy of a live attenuated H5N1 vaccine in nonhuman primates. PLoS Pathogens 2009;5(5):e1000409.

[196] Sharma AK, Khuller GK. DNA vaccines: Future strategies and relevance to intracellular pathogens. Immunology and Cellular Biology 2001;79(6):537-46.

[197] Davis HL, Michel M-L, Whalen RG. DNA-based immunization induces continuous secretion of hepatitis B surface antigen and high levels of circulating antibody. Human Molecular Genetics 1993;2(11):1847-51.

[198] Cohen AD, Boyer JD, Weiner DB. Modulating the immune response to genetic immunization. The Journal of the Federation of American Societies for Experimental Biology (FASEB Journal) 1998;12(15):1611-26.

[199] Kawai T, Akira S. The role of pattern-recognition receptors in innate immunity: Update on toll-like receptors. Nature Immunology;11(5):373-84.

[200] Holt JT. A `senseless' immune response to DNA. Nature Medicine 1995;1(5):407-8.

[201] Shedlock DJ, Weiner DB. DNA vaccination: Antigen presentation and the induction of immunity. Journal of Leukocyte Biology 2000;68(6):793-806.

[202] Shirota H, Petrenko L, Hong C, Klinman DM. Potential of transfected muscle cells to contribute to DNA vaccine immunogenicity. Journal of Immunology 2007;179(1):329-36.

[203] Xiang Z, Ertl HCJ. Manipulation of the immune response to a plasmid-encoded viral antigen by coinoculation with plasmids expressing cytokines. 1995;2(2):129-35.

[204] Okada E, Sasaki S, Ishii N, Aoki I, Yasuda T, Nishioka K, et al. Intranasal immunization of a DNA vaccine with IL-12- and granulocyte- macrophage colony-stimulating factor (GM-CSF)-expressing plasmids in liposomes induces strong mucosal and cell-mediated immune responses against HIV-1 antigens. Journal of Immunology 1997;159(7):3638-47.

[205] Boyle JS, Brady JL, Lew AM. Enhanced responses to a DNA vaccine encoding a fusion antigen that is directed to sites of immune induction. Nature 1998;392(6674):408-11.

[206] Chow Y, Huang W, Chi W, Chu Y, Tao M. Improvement of hepatitis B virus DNA vaccines by plasmids coexpressing hepatitis b surface antigen and interleukin-2. Journal of Virology 1997;71(1):169-78.

[207] de Andrés X, Reina R, Ciriza J, Crespo H, Glaria I, Ramírez H, et al. Use of B7 costimulatory molecules as adjuvants in a prime-boost vaccination against visna/maedi ovine lentivirus. Vaccine 2009;27(34):4591-600.

[208] Logan GJ, Wang L, Zheng M, Ginn SL, Coppel RL, Alexander IE. Antigen-specific humoral tolerance or immune augmentation induced by intramuscular delivery of adeno-associated viruses encoding ctla4-ig-antigen fusion molecules. Gene Therapy 2008;16(2):200-10.

[209] Patel A, Tran K, Gray M, Li Y, Ao Z, Yao X, et al. Evaluation of conserved and variable influenza antigens for immunization against different isolates of H5N1 viruses. Vaccine 2009;27(23):3083-9.

[210] Epstein SL, Kong W-p, Misplon JA, Lo C-Y, Tumpey TM, Xu L, et al. Protection against multiple influenza A subtypes by vaccination with highly conserved nucleoprotein. Vaccine 2005;23(46-47):5404-10.

[211] Chen M-W, Cheng T-JR, Huang Y, Jan J-T, Ma S-H, Yu AL, et al. A consensus-hemagglutinin-based DNA vaccine that protects mice against divergent H5N1 influenza viruses. Proceedings of the National Academy of Sciences 2008;105(36):13538-43.

[212] Rao SS, Kong W-P, Wei C-J, Van Hoeven N, Gorres JP, Nason M, et al. Comparative efficacy of hemagglutinin, nucleoprotein, and matrix 2 protein gene-based vaccination against H5N1 influenza in mouse and ferret. PLoS ONE;5(3):e9812.

[213] Lalor Peggy A, Webby Richard J, Morrow J, Rusalov D, Kaslow David C, Rolland A, et al. Plasmid DNA-based vaccines protect mice and ferrets against lethal challenge with A/Vietnam/1203/04 (H5N1) influenza virus. The Journal of Infectious Diseases 2008;197(12):1643-52.

[214] Xu K, Ling Z-Y, Sun L, Xu Y, Bian C, He Y, et al. Broad humoral and cellular immunity elicited by a bivalent DNA vaccine encoding HA and NP genes from an H5N1 virus. Viral Immunology 2011;24(1):45-56.

[215] Luo M, Qu X, Pan R, Zhu D, Zhang Y, Wu J, et al. The virus-induced signaling adaptor molecule enhances DNA-raised immune protection against H5N1 influenza virus infection in mice. Vaccine 2011;29(14):2561-7.

[216] Laddy DJ, Yan J, Kutzler M, Kobasa D, Kobinger GP, Khan AS, et al. Heterosubtypic protection against pathogenic human and avian influenza viruses via *in vivo* electroporation of synthetic consensus DNA antigens. PLoS ONE 2008;3(6):e2517.

[217] (NIAID) NIoAaID. NIAID DNA vaccine for H5N1 avian influenza enters human trial. In: Services USDoHaH, editor. Bethesda, MD: NIAID News Office, 2007.

[218] Perrone LA, Ahmad A, Veguilla V, Lu X, Smith G, Katz JM, et al. Intranasal vaccination with 1918 influenza virus-like particles protects mice and ferrets from lethal 1918 and H5N1 influenza virus challenge. Journal of Virology 2009;83(11):5726-34

[219] Bright RA, Carter DM, Crevar CJ, Toapanta FR, Steckbeck JD, Cole KS, et al. Cross-clade protective immune responses to influenza viruses with H5N1 HA and NA elicited by an influenza virus-like particle. PLoS ONE 2008;3(1):e1501.

[220] Pandey A, Singh N, Mittal SK. Egg-independent vaccine strategies for highly pathogenic H5N1 influenza viruses. Human Vaccines 2010;6(2):178-88.

[221] Kang S-M, Song J-M, Quan F-S, Compans RW. Influenza vaccines based on virus-like particles. Virus Research 2009;143(2):140-6.

[222] Compans RW, Orenstein WA, Kang SM, Pushko P, Bright RA, Smith G, et al. Influenza virus-like particles as pandemic vaccines. Vaccines for pandemic influenza: Springer Berlin Heidelberg, 2009: 269-89.

[223] Song H, Wittman V, Byers A, Tapia T, Zhou B, Warren W, et al. *In vitro* stimulation of human influenza-specific $CD8^+$ T cells by dendritic cells pulsed with an influenza virus-like particle (VLP) vaccine. Vaccine;28(34):5524-32.

[224] Kang S-M, Yoo D-G, Lipatov AS, Song J-M, Davis CT, Quan F-S, et al. Induction of long-term protective immune responses by influenza H5N1 virus-like particles. PLoS ONE 2009;4(3):e4667.

[225] Tao P, Luo M, Zhu D, Qu S, Yang Z, Gao M, et al. Virus-like particle vaccine comprised of the HA, NA, and M1 proteins of an avian isolated H5N1 influenza virus

induces protective immunity against homologous and heterologous strains in mice. Viral Immunology 2009;22(4):273-81.

[226] Song J-M, Kim Y-C, Lipatov AS, Pearton M, Davis CT, Yoo D-G, et al. Microneedle delivery of H5N1 influenza virus-like particles to the skin induces long-lasting B and T cell responses in mice. Clinical and Vaccine Immunology 2010;17(9):1381-9.

[227] Song J-M, Hossain J, Yoo D-G, Lipatov AS, Davis CT, Quan F-S, et al. Protective immunity against H5N1 influenza virus by a single dose vaccination with virus-like particles. Virology;405(1):165-75.

[228] Quan F-S, Kim Y-C, Vunnava A, Yoo D-G, Song J-M, Prausnitz MR, et al. Intradermal vaccination with influenza virus-like particles by using microneedles induces protection superior to that with intramuscular immunization. Journal of Virology;84(15):7760-9.

[229] Giles BM, Crevar CJ, Carter DM, Bissel SJ, Schultz-Cherry S, Wiley CA, et al. A computationally optimized hemagglutinin virus-like particle vaccine elicits broadly reactive antibodies that protect nonhuman primates from H5N1 infection. Journal of Infectious Diseases 2012;205(10):1562-70.

[230] Park J-K, Lee D-H, Youn H-N, Kim M-S, Lee Y-N, Yuk S-S, et al. Protective efficacy of crude virus-like particle vaccine against HPAI H5N1 in chickens and its application on DIVA strategy. Influenza and Other Respiratory Viruses 2012.

[231] Cornelissen LAHM, de Vries RP, de Boer-Luijtze EA, Rigter A, Rottier PJM, de Haan CAM. A single immunization with soluble recombinant trimeric hemagglutinin protects chickens against highly pathogenic avian influenza virus H5N1. PLoS ONE;5(5):e10645.

[232] Wei C-J, Xu L, Kong W-P, Shi W, Canis K, Stevens J, et al. Comparative efficacy of neutralizing antibodies elicited by recombinant hemagglutinin proteins from avian H5N1 influenza virus. Journal of Virology 2008;82(13):6200-8.

[233] Prabakaran M, Madhan S, Prabhu N, Qiang J, Kwang J. Gastrointestinal delivery of baculovirus displaying influenza virus hemagglutinin protects mice against heterologous H5N1 infection. Journal of Virology;84(7):3201-9.

[234] Guo L, Zheng M, Ding Y, Li D, Yang Z, Wang H, et al. Protection against multiple influenza A virus subtypes by intranasal administration of recombinant nucleoprotein. Archives of Virology:1-11.

[235] Price GE, Soboleski MR, Lo C-Y, Misplon JA, Pappas C, Houser KV, et al. Vaccination focusing immunity on conserved antigens protects mice and ferrets against virulent H1N1 and H5N1 influenza A viruses. Vaccine 2009;27(47):6512-21.

[236] Adar Y, Singer Y, Levi R, Tzehoval E, Perk S, Banet-Noach C, et al. A universal epitope-based influenza vaccine and its efficacy against H5N1. Vaccine 2009;27(15):2099-107.

[237] Shoji Y, Bi H, Musiychuk K, Rhee A, Horsey A, Roy G, et al. Plant-derived hemagglutinin protects ferrets against challenge infection with the A/Indonesia/05/05 strain of avian influenza. Vaccine 2009;27(7):1087-92.

[238] Xie QM, Ji J, Du LQ, Cao YC, Wei L, Xue CY, et al. Preparation and immune activity analysis of H5N1 subtype avian influenza virus recombinant protein-based vaccine. Poultry Science 2009;88(8):1608-15.

[239] Tompkins SM, Zhao Z-S, Lo C-Y, Misplon JA, Liu T, Ye Z, et al. Matrix protein 2 vaccination and protection against influenza viruses, including subtype H5N1. Emerging Infectious Diseases 2007;13(3).

[240] Lin Y, Deng M, Wu S, Chen Y, Cheng H, Chang C, et al. Baculovirus-derived hemagglutinin vaccine protects chickens from lethal homologous virus H5N1 challenge. Journal of Veterinary Medical Science 2008;70(11):1147-52.

[241] Weldon WC, Wang B-Z, Martin MP, Koutsonanos DG, Skountzou I, Compans RW. Enhanced immunogenicity of stabilized trimeric soluble influenza hemagglutinin. PLoS ONE 2010;5(9):e12466.

[242] Lin S-C, Huang M-H, Tsou P-C, Huang L-M, Chong P, Wu S-C. Recombinant trimeric HA protein immunogenicity of H5N1 avian influenza viruses and their combined use with inactivated or adenovirus vaccines. PLoS ONE 2011;6(5):e20052.

[243] Cornelissen LAHM, de Vries RP, de Boer-Luijtze EA, Rigter A, Rottier PJM, de Haan CAM. A single immunization with soluble recombinant trimeric hemagglutinin protects chickens against highly pathogenic avian influenza virus H5N1. PLoS ONE 2010;5(5):e10645.

[244] Cox MM, Patriarca PA, Treanor J. Flublok, a recombinant hemagglutinin influenza vaccine. Influenza and Other Respiratory Viruses 2008;2(6):211-9.

[245] Tobin GJ, Trujillo JD, Bushnell RV, Lin G, Chaudhuri AR, Long J, et al. Deceptive imprinting and immune refocusing in vaccine design. Vaccine 2008;26(49):6189-99.

[246] Garrity R, Rimmelzwaan G, Minassian A, Tsai W, Lin G, de Jong J, et al. Refocusing neutralizing antibody response by targeted dampening of an immunodominant epitope. Journal of Immunology 1997;159(1):279-89.

[247] Nara PL, Roland DS. Deceptive imprinting: Insights into mechanisms of immune evasion and vaccine development. Advances in Veterinary Medicine: Academic Press, 1999: 115-34.

[248] Steel J, Lowen AC, Wang TT, Yondola M, Gao Q, Haye K, et al. Influenza virus vaccine based on the conserved hemagglutinin stalk domain. mBio;1(1):e00018-10-e-10.

[249] Bublot M, Pritchard N, Cruz JS, Mickle TR, Selleck P, Swayne DE. Efficacy of a fowlpox-vectored avian influenza H5 vaccine against Asian H5N1 highly pathogenic avian influenza virus challenge. Avian Diseases 2007;51(s1):498-500.

[250] Swayne DE, Garcia M, Beck JR, Kinney N, Suarez DL. Protection against diverse highly pathogenic H5 avian influenza viruses in chickens immunized with a recombinant fowlpox vaccine containing an H5 avian influenza hemagglutinin gene insert. Vaccine 2000;18(11-12):1088-95.

[251] Mingxiao M, Ningyi J, Zhenguo W, Ruilin W, Dongliang F, Min Z, et al. Construction and immunogenicity of recombinant fowlpox vaccines coexpressing HA of AIV H5N1 and chicken IL18. Vaccine 2006;24(20):4304-11.

[252] Kreijtz JHCM, Suezer Y, van Amerongen G, de Mutsert G, Schnierle BS, Wood JM, et al. Recombinant modified vaccinia virus ankara-based vaccine induces protective immunity in mice against infection with influenza virus H5N1. Journal of Infectious Diseases 2007;195(11):1598-606.

[253] Kyriakis CS, De Vleeschauwer A, Barbe F, Bublot M, Van Reeth K. Safety, immunogenicity and efficacy of poxvirus-based vector vaccines expressing the haemagglutinin gene of a highly pathogenic H5N1 avian influenza virus in pigs. Vaccine 2009;27(16):2258-64.

[254] Van Kampen KR, Shi Z, Gao P, Zhang J, Foster KW, Chen D-T, et al. Safety and immunogenicity of adenovirus-vectored nasal and epicutaneous influenza vaccines in humans. Vaccine 2005;23(8):1029-36.

[255] Toro H, Tang D-cC, Suarez DL, Sylte MJ, Pfeiffer J, Van Kampen KR. Protective avian influenza in ovo vaccination with non-replicating human adenovirus vector. Vaccine 2007;25(15):2886-91.

[256] Gao W, Soloff AC, Lu X, Montecalvo A, Nguyen DC, Matsuoka Y, et al. Protection of mice and poultry from lethal H5N1 avian influenza virus through adenovirus-based immunization. Journal of Virology 2006;80(4):1959-64.

[257] Hoelscher MA, Garg S, Bangari DS, Belser JA, Lu X, Stephenson I, et al. Development of adenoviral-vector-based pandemic influenza vaccine against antigenically distinct human H5N1 strains in mice. The Lancet 2006;367(9509):475-81.

[258] Veits J, Wiesner D, Fuchs W, Hoffmann B, Granzow H, Starick E, et al. Newcastle disease virus expressing H5 hemagglutinin gene protects chickens against newcastle disease and avian influenza. Proceedings of the National Academy of Sciences 2006;103(21):8197-202.

[259] Wang Z, Yu Q, Gao J, Yang Q. Mucosal and systemic immune responses induced by recombinant lactobacillus expressing the hemagglutinin of the avian influenza virus. Clinical and Vaccine Immunology 2011.

[260] Beran J, Abdel-Messih IA, Raupachova J, Hobzova L, Fragapane E. A phase III, randomized, open-label study to assess the tolerability and immunogenicity of an H5N1 influenza vaccine administered to healthy adults with a 1-, 2-, 3-, or 6-week interval between first and second doses. Clinical Therapeutics 2010;32(13):2186-97.

[261] Banzhoff A, Gasparini R, Laghi-Pasini F, Staniscia T, Durando P, Montomoli E, et al. Mf59®-adjuvanted H5N1 vaccine induces immunologic memory and heterotypic antibody responses in non-elderly and elderly adults. PLoS ONE 2009;4(2):e4384.

[262] Bernstein DI, Edwards KM, Dekker CL, Belshe R, Talbot HKB, Graham IL, et al. Effects of adjuvants on the safety and immunogenicity of an avian influenza H5N1 vaccine in adults. Journal of Infectious Diseases 2008;197(5):667-75.

[263] Lopez P, Caicedo Y, Sierra A, Tilman S, Banzhoff A, Clemens R. Combined, concurrent, and sequential administration of seasonal influenza and MF59-adjuvanted A/H5N1 vaccines: A phase II randomized, controlled trial of immunogenicity and safety in healthy adults. Journal of Infectious Diseases 2011;203(12):1719-28.

[264] Vesikari T, Karvonen A, Tilman S, Borkowski A, Montomoli E, Banzhoff A, et al. Immunogenicity and safety of MF59-adjuvanted H5N1 influenza vaccine from infancy to adolescence. Pediatrics 2010;126(4):e762-70.

[265] Galli G, Medini D, Borgogni E, Zedda L, Bardelli M, Malzone C, et al. Adjuvanted H5N1 vaccine induces early $CD4^+$ T cell response that predicts long-term persistence of protective antibody levels. Proceedings of the National Academy of Sciences 2009;106(10):3877-82.

[266] Galli G, Hancock K, Hoschler K, DeVos J, Praus M, Bardelli M, et al. Fast rise of broadly cross-reactive antibodies after boosting long-lived human memory B cells primed by an MF59 adjuvanted prepandemic vaccine. Proceedings of the National Academy of Sciences U S A 2009;106(19):7962-7.

[267] Fragapane E, Gasparini R, Schioppa F, Laghi-Pasini F, Montomoli E, Banzhoff A. A heterologous MF59-adjuvanted H5N1 prepandemic influenza booster vaccine induces a robust, cross-reactive immune response in adults and the elderly. Clinical and Vaccine Immunology 2010;17(11):1817-9.

[268] Ledgerwood JE, Wei CJ, Hu Z, Gordon IJ, Enama ME, Hendel CS, et al. DNA priming and influenza vaccine immunogenicity: Two phase 1 open label randomised clinical trials. Lancet Infectious Diseases 2011;11(12):916-24.

[269] Zangwill KM, Treanor JJ, Campbell JD, Noah DL, Ryea J. Evaluation of the safety and immunogenicity of a booster (third) dose of inactivated subvirion H5N1 influenza vaccine in humans. Journal of Infectious Diseases 2008;197(4):580-3.

[270] Lin JT, Li CG, Wang X, Su N, Liu Y, Qiu YZ, et al. Antibody persistence after 2-dose priming and booster response to a third dose of an inactivated, adjuvanted, whole-virion H5N1 vaccine. Journal of Infectious Diseases 2009;199(2):184-7.

[271] Brady RC, Treanor JJ, Atmar RL, Keitel WA, Edelman R, Chen WH, et al. Safety and immunogenicity of a subvirion inactivated influenza A/H5N1 vaccine with or without aluminum hydroxide among healthy elderly adults. Vaccine 2009;27(37):5091-5.

[272] Beigel JH, Voell J, Huang CY, Burbelo PD, Lane HC. Safety and immunogenicity of multiple and higher doses of an inactivated influenza A/H5N1 vaccine. Journal of Infectious Diseases 2009;200(4):501-9.

[273] Belshe RB, Frey SE, Graham I, Mulligan MJ, Edupuganti S, Jackson LA, et al. Safety and immunogenicity of influenza A H5 subunit vaccines: Effect of vaccine schedule and antigenic variant. Journal of Infectious Diseases 2011;203(5):666-73.

[274] Goji NA, Nolan C, Hill H, Wolff M, Noah DL, Williams TB, et al. Immune responses of healthy subjects to a single dose of intramuscular inactivated influenza A/Vietnam/1203/2004 (H5N1) vaccine after priming with an antigenic variant. Journal of Infectious Diseases 2008;198(5):635-41.

[275] Leroux-Roels I, Van der Wielen M, Kafeja F, Vandermeulen C, Lazarus R, Snape MD, et al. Humoral and cellular immune responses to split-virion H5N1 influenza vaccine in young and elderly adults. Vaccine 2009;27(49):6918-25.

[276] Langley JM, Frenette L, Ferguson L, Riff D, Sheldon E, Risi G, et al. Safety and cross-reactive immunogenicity of candidate AS03-adjuvanted prepandemic H5N1 influenza vaccines: A randomized controlled phase 1/2 trial in adults. Journal of Infectious Diseases 2010;201(11):1644-53.

[277] Nagai H, Ikematsu H, Tenjinbaru K, Maeda A, Drame M, Roman FP. A phase II, open-label, multicentre study to evaluate the immunogenicity and safety of an adjuvanted prepandemic (H5N1) influenza vaccine in healthy japanese adults. BMC Infectious Diseases 2010;10:338.

[278] Schwarz TF, Horacek T, Knuf M, Damman HG, Roman F, Drame M, et al. Single dose vaccination with AS03-adjuvanted H5N1 vaccines in a randomized trial induces strong and broad immune responsiveness to booster vaccination in adults. Vaccine 2009;27(45):6284-90.

[279] Heijmans S, De Meulemeester M, Reynders P, Giet D, Demanet E, Devresse PY, et al. Immunogenicity profile of a 3.75-µg hemagglutinin pandemic rH5N1 split virion AS03a-adjuvanted vaccine in elderly persons: A randomized trial. Journal of Infectious Diseases 2011;203(8):1054-62.

[280] Risi G, Frenette L, Langley JM, Li P, Riff D, Sheldon E, et al. Immunological priming induced by a two-dose series of H5N1 influenza antigen, administered alone or in combination with two different formulations of AS03 adjuvant in adults: Results of a randomised single heterologous booster dose study at 15 months. Vaccine 2011;29(37):6408-18.

[281] Fritz R, Sabarth N, Kiermayr S, Hohenadl C, Howard MK, Ilk R, et al. A vero cell-derived whole-virus H5N1 vaccine effectively induces neuraminidase-inhibiting antibodies. Journal of Infectious Diseases 2012;205(1):28-34.

[282] Rümke HC, Bayas J-M, de Juanes J-R, Caso C, Richardus JH, Campins M, et al. Safety and reactogenicity profile of an adjuvanted H5N1 pandemic candidate vaccine in adults within a phase III safety trial. Vaccine 2008;26(19):2378-88.

[283] Landry N, Ward BJ, Trépanier S, Montomoli E, Dargis M, Lapini G, et al. Preclinical and clinical development of plant-made virus-like particle vaccine against avian H5N1 influenza. PLoS ONE 2010;5(12):e15559.

[284] Cox RJ, Pedersen G, Madhun AS, Svindland S, Sævik M, Breakwell L, et al. Evaluation of a virosomal H5N1 vaccine formulated with matrix m™ adjuvant in a phase I clinical trial. Vaccine 2011;29(45):8049-59.

[285] Levie K, Leroux-Roels I, Hoppenbrouwers K, Kervyn A-D, Vandermeulen C, Forgus S, et al. An adjuvanted, low-dose, pandemic influenza a (H5N1) vaccine candidate is safe, immunogenic, and induces cross-reactive immune responses in healthy adults. Journal of Infectious Diseases 2008;198(5):642-9.

[286] Sambhara S, Poland GA. Breaking the immunogenicity barrier of bird flu vaccines. The Lancet 2007;370(9587):544-5.

[287] Mastelic B, Ahmed S, Egan WM, Del Giudice G, Golding H, Gust I, et al. Mode of action of adjuvants: Implications for vaccine safety and design. Biologicals;38(5):594-601.

[288] Leroux-Roels G. Unmet needs in modern vaccinology: Adjuvants to improve the immune response. Vaccine;28(Supplement 3):C25-C36.

[289] Sahly HE. MF59 as a vaccine adjuvant: A review of safety and immunogenicity. Expert Review of Vaccines;9(10):1135-41.

[290] Ninomiya A, Imai M, Tashiro M, Odagiri T. Inactivated influenza H5N1 whole-virus vaccine with aluminum adjuvant induces homologous and heterologous protective immunities against lethal challenge with highly pathogenic H5N1 avian influenza viruses in a mouse model. Vaccine 2007;25(18):3554-60.

[291] Ruat C, Caillet C, Bidaut A, Simon J, Osterhaus ADME. Vaccination of macaques with adjuvanted formalin-inactivated influenza a virus (H5N1) vaccines: Protection against H5N1 challenge without disease enhancement. Journal of Virology 2008;82(5):2565-9.

[292] Carter NJ, Plosker GL. Prepandemic influenza vaccine H5N1 (split virion, inactivated, adjuvanted) [Prepandrix(tm)]: A review of its use as an active immunization against influenza A subtype H5N1 virus. BioDrugs 2008;22(5):279-92.

[293] Compans RW, Orenstein WA, Atmar RL, Keitel WA. Adjuvants for pandemic influenza vaccines. Vaccines for pandemic influenza: Springer Berlin Heidelberg, 2009: 323-44.

[294] Leroux-Roels I, Borkowski A, Vanwolleghem T, Dramé M, Clement F, Hons E, et al. Antigen sparing and cross-reactive immunity with an adjuvanted rH5N1 prototype pandemic influenza vaccine: A randomised controlled trial. The Lancet 2007;370(9587):580-9.

[295] Leroux-Roels I, Leroux-Roels G. Current status and progress of prepandemic and pandemic influenza vaccine development. Expert Review of Vaccines 2009;8(4):401-23.

[296] Leroux-Roels I, Roman F, Forgus S, Maes C, De Boever F, Dramé M, et al. Priming with AS03a-adjuvanted H5N1 influenza vaccine improves the kinetics, magnitude and durability of the immune response after a heterologous booster vaccination: An open non-randomised extension of a double-blind randomised primary study. Vaccine;28(3):849-57.

[297] Keitel W, Groth N, Lattanzi M, Praus M, Hilbert AK, Borkowski A, et al. Dose ranging of adjuvant and antigen in a cell culture H5N1 influenza vaccine: Safety and immunogenicity of a phase 1/2 clinical trial. Vaccine;28(3):840-8.

[298] Khurana S, Chearwae W, Castellino F, Manischewitz J, King LR, Honorkiewicz A, et al. Vaccines with MF59 adjuvant expand the antibody repertoire to target protective sites of pandemic avian H5N1 influenza virus. Science Translational Medicine;2(15).

[299] Heldens JGM, Glansbeek HL, Hilgers LAT, Haenen B, Stittelaar KJ, Osterhaus ADME, et al. Feasibility of single-shot H5N1 influenza vaccine in ferrets, macaques and rabbits. Vaccine;28(51):8125-31.

[300] Bodewes R, Kreijtz JHCM, van Amerongen G, Geelhoed-Mieras MM, Verburgh RJ, Heldens JGM, et al. A single immunization with covaccine ht-adjuvanted H5N1 influenza virus vaccine induces protective cellular and humoral immune responses in ferrets. Journal of Virology;84(16):7943-52.

[301] Rimmelzwaan GF, Claas ECJ, Van Amerongen G, de Jong JC, Osterhaus ADME. ISCOM vaccine induced protection against a lethal challenge with a human H5N1 influenza virus. Vaccine 1999;17(11-12):1355-8.

[302] Kodihalli S, Sivanandan V, Nagaraja KV, Shaw D, Halvorson DA. A type-specific avian influenza virus subunit vaccine for turkeys: Induction of protective immunity to challenge infection. Vaccine 1994;12(15):1467-72.

[303] Xie Y, Sun H-X, Li D. Platycodin D improves the immunogenicity of Newcastle disease virus-based recombinant avian influenza vaccine in mice. Chemistry & Biodiversity;7(3):677-89.

[304] Steinhagen F, Kinjo T, Bode C, Klinman DM. TLR-based immune adjuvants. Vaccine;29(17):3341-55.

[305] Warshakoon HJ, Hood JD, Kimbrell MR, Malladi S, Wu WY, Shukla N, et al. Potential adjuvantic properties of innate immune stimuli. Human Vaccines 2009;5(6):381-94.

[306] Lahiri A, Das P, Chakravortty D. Engagement of TLR signaling as adjuvant: Towards smarter vaccine and beyond. Vaccine 2008;26(52):6777-83.

[307] Wong JP, Christopher ME, Viswanathan S, Karpoff N, Dai X, Das D, et al. Activation of toll-like receptor signaling pathway for protection against influenza virus infection. Vaccine 2009;27(25-26):3481-3.

[308] Isaka M, Zhao Y, Nobusawa E, Nakajima S, Nakajima K, Yasuda Y, et al. Protective effect of nasal immunization of influenza virus hemagglutinin with recombinant cholera toxin B subunit as a mucosal adjuvant in mice. Microbiology and Immunology 2008;52(2):55-63.

[309] Asahi-Ozaki Y, Itamura S, Ichinohe T, Strong P, Tamura S-i, Takahashi H, et al. Intranasal administration of adjuvant-combined recombinant influenza virus HA vaccine protects mice from the lethal H5N1 virus infection. Microbes and Infection 2006;8(12-13):2706-14.

[310] Ichinohe T, Watanabe I, Ito S, Fujii H, Moriyama M, Tamura S-i, et al. Synthetic double-stranded rna poly(I:C) combined with mucosal vaccine protects against influenza virus infection. Journal of Virology 2005;79(5):2910-9.

[311] Lau Y-F, Tang L-H, McCall AW, Ooi E-E, Subbarao K. An adjuvant for the induction of potent, protective humoral responses to an H5N1 influenza virus vaccine with antigen-sparing effect in mice. Journal of Virology;84(17):8639-49.

[312] Quintilio W, Kubrusly FS, Iourtov D, Miyaki C, Sakauchi MA, Lúcio F, et al. Bordetella pertussis monophosphoryl lipid A as adjuvant for inactivated split virion influenza vaccine in mice. Vaccine 2009;27(31):4219-24.

[313] Sjoblom-Hallen A, Marklund U, Nerstedt A, Schon K, Ekman L, Bergqvist P, et al. Gene expression profiling identifies STAT3 as a novel pathway for immunomodulation by cholera toxin adjuvant. Mucosal Immunology;3(4):374-86.

[314] Prabakaran M, Velumani S, He F, Karuppannan AK, Geng GY, Yin LK, et al. Protective immunity against influenza H5N1 virus challenge in mice by intranasal co-administration of baculovirus surface-displayed HA and recombinant CTB as an adjuvant. Virology 2008;380(2):412-20.

[315] Yang P, Tang C, Luo D, Zhan Z, Xing L, Duan Y, et al. Cross-clade protection against HPAI H5N1 influenza virus challenge in BALB/c mice intranasally administered adjuvant-combined influenza vaccine. Veterinary Microbiology;146(1-2):17-23.

[316] Glenn GM, Thomas DN, Poffenberger KL, Flyer DC, Ellingsworth LR, Andersen BH, et al. Safety and immunogenicity of an influenza vaccine A/H5N1 (A/Vietnam/1194/2004) when coadministered with a heat-labile enterotoxin (LT) adjuvant patch. Vaccine 2009;27(Supplement 6):G60-G6.

[317] Huang M-H, Lin S-C, Hsiao C-H, Chao H-J, Yang H-R, Liao C-C, et al. Emulsified nanoparticles containing inactivated influenza virus and CPG oligodeoxynucleotides critically influences the host immune responses in mice. PLoS ONE;5(8):e12279.

[318] Huang M-H, Huang C-Y, Lin S-C, Chen J-H, Ku C-C, Chou A-H, et al. Enhancement of potent antibody and T-cell responses by a single-dose, novel nanoemulsion-formulated pandemic influenza vaccine. Microbes and Infection;11(6-7):654-60.

[319] Prabakaran M, Madhan S, Prabhu N, Geng GY, New R, Kwang J. Reverse micelle-encapsulated recombinant baculovirus as an oral vaccine against H5N1 infection in mice. Antiviral Research;86(2):180-7.

[320] Meunier I, Pillet S, Simonsen JN, von Messling V. Influenza pathogenesis: Lessons learned from animal studies with H5N1, H1N1 Spanish, and pandemic H1N1 2009 influenza. Critical Care Medicine;38(4 Suppl):e21-9.

[321] Influenza virus transmission: Basic science and implications for the use of antiviral drugs during a pandemic. Infectious Disorders - Drug Targets 2007;7:318-28.

[322] Govorkova EA, Leneva IA, Goloubeva OG, Bush K, Webster RG. Comparison of efficacies of RWJ-270201, Zanamivir, and Oseltamivir against H5N1, H9N2, and other avian influenza viruses. Antimicrobial Agents and Chemotherapy 2001;45(10):2723-32.

[323] Govorkova EA, Ilyushina NA, Boltz DA, Douglas A, Yilmaz N, Webster RG. Efficacy of oseltamivir therapy in ferrets inoculated with different clades of H5N1 influenza virus. Antimicrobial Agents and Chemotherapy 2007;51(4):1414-24.

[324] Le QM, Kiso M, Someya K, Sakai YT, Nguyen TH, Nguyen KHL, et al. Avian flu: Isolation of drug-resistant H5N1 virus. Nature 2005;437(7062):1108-.

[325] Boltz DA, Douangngeun B, Phommachanh P, Sinthasak S, Mondry R, Obert C, et al. Emergence of H5N1 avian influenza viruses with reduced sensitivity to neuraminidase inhibitors and novel reassortants in Lao people's democratic republic. Journal of Genetic Virology;91(4):949-59.

[326] Leneva IA, Goloubeva O, Fenton RJ, Tisdale M, Webster RG. Efficacy of Zanamivir against avian influenza A viruses that possess genes encoding H5N1 internal proteins and are pathogenic in mammals. Antimicrobial Agents and Chemotherapy 2001;45(4):1216-24.

[327] Stittelaar KJ, Tisdale M, van Amerongen G, van Lavieren RF, Pistoor F, Simon J, et al. Evaluation of intravenous zanamivir against experimental influenza A (H5N1) virus infection in cynomolgus macaques. Antiviral Research 2008;80(2):225-8.

[328] Hay AJ, Wolstenholme AJ, Skehel JJ, Smith MH. The molecular basis of the specific anti-influenza action of Amantadine. EMBO Journal 1985;4(11):3021-4.

[329] He G, Qiao J, Dong C, He C, Zhao L, Tian Y. Amantadine-resistance among H5N1 avian influenza viruses isolated in northern China. Antiviral Research 2008;77(1):72-6.

[330] Le MT, Wertheim HF, Nguyen HD, Taylor W, Hoang PV, Vuong CD, et al. Influenza A H5N1 clade 2.3.4 virus with a different antiviral susceptibility profile replaced clade 1 virus in humans in northern Vietnam. PLoS ONE 2008;3(10):e3339.

[331] Van Hoeven N, Belser JA, Szretter KJ, Zeng H, Staeheli P, Swayne DE, et al. Pathogenesis of 1918 pandemic and H5N1 influenza virus infections in a guinea pig model: Antiviral potential of exogenous alpha interferon to reduce virus shedding. Journal of Virology 2009;83(7):2851-61.

[332] Kugel D, Kochs G, Obojes K, Roth J, Kobinger GP, Kobasa D, et al. Intranasal administration of alpha interferon reduces seasonal influenza A virus morbidity in ferrets. Journal of Virology 2009;83(8):3843-51.

[333] Salomon R, Hoffmann E, Webster RG. Inhibition of the cytokine response does not protect against lethal H5N1 influenza infection. Proceedings of the National Academy of Sciences 2007;104(30):12479-81.

[334] Cinatl J, Michaelis M, Doerr HW. The threat of avian influenza A (H5N1). Part III: Antiviral therapy. Medical Microbiology and Immunology 2007;196(4):203-12.

[335] Hui DSC. Influenza A/H5N1 infection: Other treatment options and issues. Respirology 2008;13:S22-S6.

[336] White NJ, Webster RG, Govorkova EA, Uyeki TM. What is the optimal therapy for patients with H5N1 influenza? PLoS Medicine 2009;6(6):e1000091.

[337] O'Hagan DT. MF59 is a safe and potent vaccine adjuvant that enhances protection against influenza virus infection. Expert Review of Vaccines 2007;6(5):699-710.

[338] Podda A, Del Giudice G. MF59-adjuvanted vaccines: Increased immunogenicity with an optimal safety profile. Expert Review of Vaccines 2003;2(2):197-204.

[339] Puig Barbera J, Gonzalez Vidal D. MF59-adjuvanted subunit influenza vaccine: An improved interpandemic influenza vaccine for vulnerable populations. Expert Review of Vaccines 2007;6(5):659-65.

[340] Torres MP, Determan AS, Mallapragada SK, Narasimhan B. Polyanhydrides. In: Lee S, editor. Encyclopedia of Chemical Processing. New York: Marcell Dekker, 2005.

[341] Li X, Petersen L, Broderick S, Narasimhan B, Rajan K. Identifying factors controlling protein release from combinatorial biomaterial libraries via hybrid data mining methods. ACS Combinatorial Science 2011;13(1):50-8.

[342] Lopac SK, Torres MP, Wilson-Welder JH, Wannemuehler MJ, Narasimhan B. Effect of polymer chemistry and fabrication method on protein release and stability from polyanhydride microspheres. Journal of Biomedical Materials Research Part B: Applied Biomaterials 2009;91B(2):938-47.

[343] Ulery B, Phanse Y, Sinha A, Wannemuehler M, Narasimhan B, Bellaire B. Polymer chemistry influences monocytic uptake of polyanhydride nanospheres. Pharmaceutical Research 2009;26(3):683-90.

[344] Carrillo-Conde B, Schiltz E, Yu J, Chris Minion F, Phillips GJ, Wannemuehler MJ, et al. Encapsulation into amphiphilic polyanhydride microparticles stabilizes *Yersinia pestis* antigens. Acta biomaterialia 2010;6(8):3110-9.

[345] Torres MP, Determan AS, Anderson GL, Mallapragada SK, Narasimhan B. Amphiphilic polyanhydrides for protein stabilization and release. Biomaterials 2007;28(1):108-16.

[346] Petersen LK, Phanse Y, Ramer-Tait AE, Wannemuehler MJ, Narasimhan B. Amphiphilic polyanhydride nanoparticles stabilize *Bacillus anthracis* protective antigen. Molecular Pharmaceutics 2012;9(4):874-82.

[347] Torres MP, Wilson-Welder JH, Lopac SK, Phanse Y, Carrillo-Conde B, Ramer-Tait AE, et al. Polyanhydride microparticles enhance dendritic cell antigen presentation and activation. Acta biomaterialia 2011;7(7):2857-64.

[348] Mallapragada SK, Narasimhan B. Immunomodulatory biomaterials. International Journal of Pharmaceutics 2008;364(2):265-71.

[349] Petersen LK, Xue L, Wannemuehler MJ, Rajan K, Narasimhan B. The simultaneous effect of polymer chemistry and device geometry on the in vitro activation of murine dendritic cells. Biomaterials 2009;30(28):5131-42.

[350] Kipper MJ, Shen E, Determan A, Narasimhan B. Design of an injectable system based on bioerodible polyanhydride microspheres for sustained drug delivery. Biomaterials 2002;23(22):4405-12.

[351] Determan AS, Trewyn BG, Lin VSY, Nilsen-Hamilton M, Narasimhan B. Encapsulation, stabilization, and release of BSA-FITC from polyanhydride microspheres. Journal of Controlled Release 2004;100(1):97-109.

[352] Determan AS, Wilson JH, Kipper MJ, Wannemuehler MJ, Narasimhan B. Protein stability in the presence of polymer degradation products: Consequences for controlled release formulations. Biomaterials 2006;27(17):3312-20.

[353] Torres MP, Vogel BM, Narasimhan B, Mallapragada SK. Synthesis and characterization of novel polyanhydrides with tailored erosion mechanisms. Journal of Biomedical Materials Research Part A 2006;76A(1):102-10.

[354] Determan A, Graham JR, Pfeiffer KA, Narasimhan B. The role of microsphere fabrication methods on the stability and release kinetics of ovalbumin encapsulated in polyanhydride microspheres. Journal of Microencapsulation 2006;23(8):832-43.

[355] Kipper MJ, Wilson JH, Wannemuehler MJ, Narasimhan B. Single dose vaccine based on biodegradable polyanhydride microspheres can modulate immune response mechanism. Journal of Biomedical Materials Research Part A 2006;76A(4):798-810.

[356] Ulery BD, Kumar D, Ramer-Tait AE, Metzger DW, Wannemuehler MJ, Narasimhan B. Design of a protective single-dose intranasal nanoparticle-based vaccine platform for respiratory infectious diseases. PLoS ONE 2011;6(3):e17642.

[357] Finkelman FD, Holmes J, Katona IM, Urban JF, Beckmann MP, Park LS, et al. Lymphokine control of in vivo immunoglobulin isotype selection. Annual Review of Immunology 1990;8(1):303-33.

[358] Goodin JL, Powell BS, Enama JT, Raab RW, McKown RL, Coffman GL, et al. Purification and characterization of a recombinant *Yersinia pestis* V-F1 "reversed" fusion protein for use as a new subunit vaccine against plague. Protein Expression and Purification 2011;76(1):136-44.

CHAPTER 3: SINGLE IMMUNIZATION WITH A SUBOPTIMAL ANTIGEN DOSE ENCAPSULATED INTO POLYANHYDRIDE MICROPARTICLES PROMOTES HIGH TITER AND AVID ANTIBODY RESPONSES

Modified from a paper published in *The Journal of Biomedical Materials Research Part B: Applied Biomaterials*

Lucas Huntimer, Jennifer H. Wilson Welder, Kathleen Ross, Brenda Carrillo-Conde, Lynn Pruisner, Chong Wang, Balaji Narasimhan, Michael J. Wannemuehler and Amanda E. Ramer-Tait

Abstract

Microparticle adjuvants based on biodegradable polyanhydrides were used to provide controlled delivery of a model antigen, ovalbumin (Ova), to mice. Ova was encapsulated into two different polyanhydride microparticle formulations to evaluate the influence of polymer chemistry on the nature and magnitude of the humoral immune response following administration of a suboptimal dose. Subcutaneous administration of a single dose of polyanhydride microparticles containing 25 μg of Ova elicited humoral immune responses that were comparable in magnitude to that induced by soluble doses of 400 to 1600 μg Ova, demonstrating at least a 16-fold dose-sparing capability. In contrast, the avidity of the Ova-specific antibodies was greater in mice administered the microparticle formulations in comparison to the higher soluble doses. The increased avidity was maintained throughout the 12 week

time period. Finally, the microparticle delivery system primed an anamnestic immune response as evidenced by the significant increases in Ova-specific antibody when mice were administered an antigenic challenge of 25 μg of Ova at 12 weeks post-vaccination. Together, these results indicate that encapsulation of antigens into polyanhydride microparticles facilitates isotype switching, establishes immunologic memory and the humoral response provides a dosage sparing benefit as characterized by a higher quality antibody response.

1. Introduction

Many current subunit vaccine formulations consist of poorly immunogenic recombinant proteins that require adjuvants to induce humoral and cellular immune responses. Although beneficial, vaccine adjuvants do pose a risk of adverse reactions, which may, in part, explain why only three formulations (the aluminum salts $Al(OH)_3$ and $AlPO_4$, oil-in-water emulsion, and monophosphoryl lipid A) are currently licensed for human use in the United States [1]. Recombinant proteins are also often costly to produce. Reducing the amount of antigen needed to elicit protective immune responses could help eliminate vaccine production shortages similar to those observed during the 2009 H1N1 influenza pandemic [2]. Immunization with subunit vaccines can also fail to induce robust humoral immune responses in which naïve B cells differentiate into antigen-specific, long-lived plasma cells and memory B cells. While these vaccines elicit measurable antibody titers, the quality (i.e., avidity) and kinetics of the antibody response may be less than optimal. Successful vaccines must induce antigen specific memory B cells capable of rapidly

proliferating upon antigen stimulation [3, 4]. In addition, an avid antibody response must be developed through somatic hypermutation and positive selection of high affinity B cell clones. These attributes are all essential factors in determining the quality of antibody-mediated protection against a subsequent pathogen challenge.

To overcome many of the limitations associated with traditional vaccine regimens, antigens have been encapsulated into synthetic, biodegradable polymer micro- and nanoparticles [5-8]. The most extensively studied formulations include the polyesters poly(glycolic acid), poly(lactic acid) and their copolymers (i.e., poly(lactide-co-glycolide) or PLGA). Unfortunately, particles made of PLGA degrade by a bulk erosion mechanism that may negatively affect the stability of proteins susceptible to moisture-induced aggregation [9, 10]. In addition, the acidic microenvironment created by PLGA degradation products (i.e., lactic or glycolic acids) can lead to protein instabilities [11, 12]. Polyanhydrides, another class of well-studied biodegradable polymers, present an alternative for drug and vaccine delivery [13]. These materials exhibit surface erosion characteristics and possess hydrolytically labile anhydride bonds [14]. The most commonly studied polyanhydrides are based on the aliphatic sebacic acid (SA) and the aromatic 1,6-bis(*p*-carboxyphenoxy)hexane (CPH). Encapsulation of proteins into CPH:SA copolymers has been shown to preserve protein and antigenic epitope stability [9, 15, 16]. These surface-erodible polymers also provide sustained protein release [15-17] and possess immune-modulatory capabilities [18-21].

In this present work, we extend our studies of polyanhydride particle-based vaccines by exploring the ability of this platform to enhance the immunogenicity of ovalbumin

(Ova), a model vaccine antigen. We found that a single subcutaneous (SC) administration of a suboptimal dose of Ova encapsulated into polyanhydride microparticles induced an antibody response that was comparable in magnitude to that induced by 16-fold higher doses of soluble Ova or that induced by multiple doses of Alum-adjuvanted OVA [22]. Moreover, this microparticle vaccine regimen successfully primed the humoral immune response for an anamnestic immune response. Together, these results indicate that encapsulation of vaccine antigens into polyanhydride microparticles provides a dosage sparing effect by providing a platform delivery system that can eliciting a mature humoral memory response following a single administration.

2. Materials and Methods

2.1 Materials and polymer synthesis

The chemicals needed for CPH monomer synthesis, 4-*p*-hydroxybenzoic acid, 1,6-dibromohexane, 1-methyl-2-pyrrolidinone, and sebacic acid (99%), were purchased from Sigma Aldrich (St Louis, MO); acetic anhydride, methylene chloride, and ethanol were purchased from Fisher Scientific (Fairlawn, NJ). CPH diacid was synthesized as described previously [23, 24]. Prepolymers of SA and CPH were synthesized by the methods described by Shen et al. [25] and Conix et al [23]. CPH:SA copolymers were synthesized by melt polycondensation as described previously [14]. The purity and degree of polymerization of the copolymers was analyzed using ^{1}H nuclear magnetic resonance (NMR) spectroscopy obtained from a Varian VXR-300 MHz NMR spectrometer (Varian Inc., Palo Alto, CA). NMR spectra

were consistent with previously published data and confirmed the synthesis of the desired copolymer compositions [24]. In addition, polymer molecular weight was determined using gel permeation chromatography (GPC, Waters HPLC System, Milford, MA) using Varian Inc. GPC columns.

2.3 Microparticle fabrication

To eliminate the endotoxin contamination of the Ovalbumin (Ova; Sigma Aldrich) and to prevent unintended enhancement of the immune response caused by contaminating endotoxin, affinityPak Detoxi-Gel endotoxin removal columns (Thermo Scientific, Rockford, IL) were used according to manufacturer's instructions. The recovered Ova contained <10 EU/mg protein and was lyophilized and stored at -20^{o}C. Ova-loaded microparticles were fabricated using cryogenic atomization [5, 9, 26]. The parameters used for each copolymer chemistry were previously specified by Torres et al. [16] and Lopac et al [17]. The obtained microparticles were collected by vacuum filtration and dried under vacuum. Using four replicative samples for each microparticle preparation, microparticle morphology and size distribution were analyzed by using images obtained by scanning electron microscopy (SEM) (JEOL 840 A, JEOL, Peabody, MA), and ImageJ image analysis software (National Institutes of Health, Bethesda, MD). An average of 200 particles per image was analyzed.

2.4 In vitro antigen release

In vitro Ova release kinetics were measured by suspending 15 mg of the Ova-loaded microparticles in 1 mL of phosphate buffered saline (0.1 M, pH 7.4) with 0.01% w/v sodium azide, and incubating at 37°C on a shaker platform at 100 rpm. Aliquots of 750 µL were taken at prescribed time intervals and replaced with fresh buffer. Aliquots were stored at 4°C to measure protein concentration using micro-bicinchoninic acid (BCA) analysis at an absorbance of 570 nm. At least three replicates of each sample were analyzed. After 25 days, the remaining encapsulated protein was extracted by degrading the remaining particles in 17 mM NaOH. Protein concentration was determined with a microBCA assay. Total protein encapsulated in the particles was determined by calculating the protein released at each timepoint as described by Torres et al [16].

2.6 Mice and immunization procedures

Female C3H/HeNHsd (C3H) mice were purchased from Harlan Sprague Dawley (Frederick, MD). All animal procedures were conducted with the approval of the Iowa State University Institutional Animal Care and Use Committee. To evaluate the serum antibody response to non-adjuvanted Ova, twenty milligrams of endotoxin-free Ova was suspended in pyrogen-free saline and diluted to the indicated concentrations. Mice were subcutaneously (SC) immunized with soluble Ova alone at doses of 1600, 400, 100, or 25 µg in 100 µL pyrogen-free saline with 7 mice per treatment group (n=7). Control animals received 100 µL saline alone (n=6). Blood samples were collected from the left saphenous vein prior to immunization

and every four weeks thereafter. Serum was collected after centrifugation and stored at -20°C until assayed for Ova-specific antibody as described below.

Mice were immunized SC with 25 μg of Ova encapsulated into 0.5 mg of either 20:80 CPH:SA or 50:50 CPH:SA microparticles suspended in pyrogen-free saline with 8 mice per treatment group (n=8). Prior to administration, microparticles were sonicated briefly to generate a uniform suspension. A total volume of 100 μL was administered at the injection site. For the antigenic challenge studies, mice that had been immunized 12 weeks prior were immunized SC with 25 μg of endotoxin-free Ova suspended in pyrogen-free saline. Serum samples were collected five days later in order to measure the anamnestic antibody response.

2.7 ELISA for Ova-specific antibody titer and avidity

ELISA plates (Costar Catalog # 3590, EIA/RIA high binding) were coated overnight with 0.5 μg/well Ova. Plates were washed with phosphate buffered saline containing 0.5% Tween 20 at a pH of 7.4 (PBST). Plates were blocked for two hours with 2% gelatin (Difco) in PBST. Plates were washed and serial dilutions of individual serum samples in PBST with 1% heat inactivated normal goat serum (GIBCO) were incubated overnight at 4^{o}C. Plates were washed again with PBST and alkaline phosphatase-conjugated goat anti-mouse IgG (H&L), IgG1, or IgG2a (Jackson ImmunoResearch Laboratories, West Grove, PA) diluted 1:1000 in 1% heat inactivated normal goat serum in PBST was incubated for 2 h. Plates were washed and p-nitrophenyl phosphate (Sigma) substrate (1 mg/mL) in 50 mM Na_2CO_3 and 2 mM $MgCl_2$ buffer (pH 9.3) was added to each well. Changes in optical

density (OD) were measured at 405 nm using a spectrophotometer (Spectra Max 190, Molecular Devices, Sunnyvale CA). Antibody avidity ELISA was performed as described previously to determine antibody binding strength in the presence of a chaotropic agent that disurpts antibody-antigen binding interactions [18]. The molar concentration of NaSCN corresponding to the to 50% percent loss of absorbance was designated as the relative avidity value reported.

2.8 Statistical analysis

Longitudinal data were analyzed using repeated measure analysis of variance (ANOVA) models (with SAS version 9.2). Treatment and time were fixed effects in the statistical model, whereas mouse was the subject of repeated measures. Cross-sectional data were analyzed using one-way ANOVA models with treatment as the explanatory variable. Differences in mean responses among treatments were compared by using Tukey's T-test. Log_{10} transformation was applied to responses with skewed distributions before analyses. Statistical tests with $p \leq 0.05$ were regarded as significant.

3. Results

3.1 Single, soluble doses of Ova require 100 mg or more to elicit significant antibody titers and prime the humoral response to respond to an antigenic challenge.

In order to demonstrate the dose sparing advantages associated with capabilities of a single dose immunization regimen employing a suboptimal dose of Ova encapsulated into polyanhydride microparticles, we first examined the kinetics

of the IgG antibody response of mice immunized subcutaneously once with varying doses of soluble Ova (Figure 1A). Groups of mice that were administered 1600 µg, 400 µg or 100 µg of Ova elicited significantly higher antibody titers in contrast to mice immunized with 25 µg of Ova. The kinetics of the IgG response induced by a single, soluble dose of Ova demonstrated that the peak titer was obtained four weeks post-injection and then began to wane.

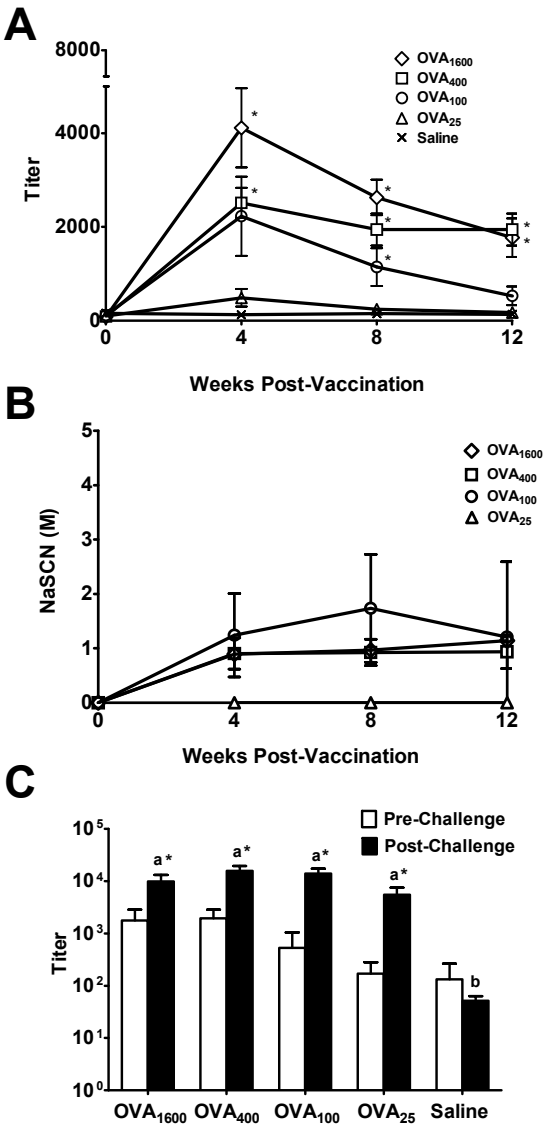

Figure 1. **Single doses of soluble ovalbumin (Ova) required 100 mg or more to elicit significant antibody titers and prime the humoral response to respond to an antigenic challenge.** Separate groups of C3H mice were immunized with a titrating dosage of soluble Ova: 1600 µg (open diamonds), 400 µg (open squares), 100 µg (open circles), 25 µg (open triangles), or saline alone (x). Ova-specific serum antibody titers (A) and antibody avidity (B) were measured over 12 weeks. (C) At 12 weeks post-immunization, the Ova-specific serum antibody titer was measured prior to (open histograms) and five days after (closed histograms) an antigenic challenge administered subcutaneously in the form of 25 µg Ova. All data are presented as the mean ± SEM and are representative of three independent experiments. For panel A, * represents a statistically significant difference from the 25 µg group at $p < 0.05$. For panel C, * indicates a statistically significant difference from treatments prior to boost at $p < 0.05$. Treatments with different letters are significantly different from one another at $p < 0.05$.

Antibody avidity was also assessed as a surrogate marker of vaccine efficacy. Serum samples from the mice immunized with a single dose of 100 μg, 400 μg or 1600 μg of soluble Ova developed a peak antibody avidity at four weeks post-vaccination that was stable through 12 weeks post-immunization (Figure 1B). Serum samples from mice vaccinated with 25 μg of soluble Ova alone did not induce a sufficient antibody titer to measure antibody avidity. To ascertain the generation of antigen-specific memory responses, a 25 μg “antigenic challenge” was administered at 12 weeks post-vaccination. A measurable increase in the secondary humoral antibody response was observed in mice that had received 25 μg or more antigen at the initial vaccination (Figure 1C). A soluble dose of 25 μg of Ova was not sufficient to induce a primary serum antibody (Figure 1C, open bar) response but was able to prime the mice for a secondary immune response (Figure 1C, closed bar), indicating that 25 μg was a suboptimal dose of immunogen.

3.2 Controlled antigen release by polyanhydride microparticles in vivo results in a primed humoral response while sparing antigen.

Ova-loaded 20:80 and 50:50 CPH:SA microparticles were characterized by SEM after fabrication (Figure 2A). Morphologies of the Ova-loaded microparticles were consistent with previous work describing blank microparticles [16, 17]. The diameter of the microparticles ranged between 5 and 21 μm for both 20:80 CPH:SA and 50:50 CPH:SA. While there was a greater initial burst release from the 20:80 CPH:SA formulation (Figure 2B), the release profile of Ova from the two

polyanhydride formulations was shown to be sustained and is consistent with previous work [9, 16, 17].

Figure 2

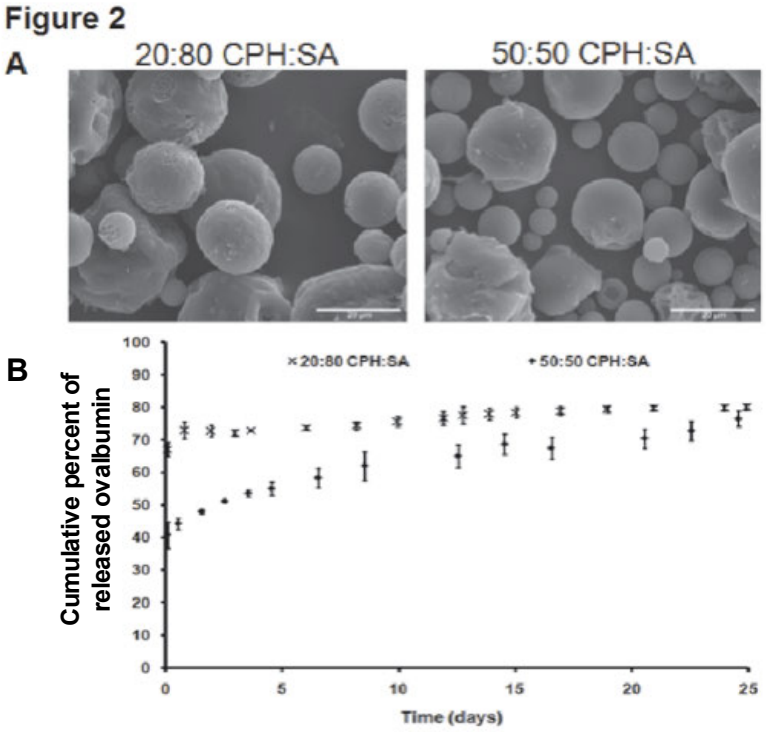

Figure 2. **Morphology and in vitro release kinetics of Ova-loaded polyanhydride microparticles**. Scanning electron photomicrographs of Ova-loaded 20:80 CPH:SA (mean diameter ± SD, 10 ± 5 μm) and 50:50 CPH:SA (12 ± 7 μm). (A) Scale bar: 20 μm. (B) Release kinetics of Ova from 20:80 CPH:SA and 50:50 CPH:SA microparticles. Data are presented as the mean ± SEM and are representative of two independent experiments with duplicate samples analyzed in each experiment.

Using the polyanhydride microparticle vaccine delivery platform, we sought to demonstrate that a significant humoral response could be induced when a suboptimal dose of Ova (25 μg) was encapsulated into one or both of the

microparticle formulations evaluated in this study. The IgG response induced by the administration of 500 μg of either 20:80 CPH:SA or 50:50 CPH:SA containing 25 μg of Ova (i.e., 5% wt/wt) was evaluated for 12 weeks following administration (Figure 3A). Both polyanhydride formulations tested elicited similar Ova-specific antibody titers. Compared to mice receiving 25 μg of soluble Ova, significant antibody titers were demonstrable in microparticle vaccinated groups beginning at week four and were maintained through 12 weeks post-vaccination. Compared to the mice receiving the larger soluble doses (i.e., ≥ 100 μg) of Ova, the anti-Ova serum antibody response of the microparticle vaccinated mice peaked four weeks later (Figure 3A versus Figure 1A). Mice receiving either Ova-encapsulated microparticle vaccine formulation developed a more avid Ova-specific antibody response than did mice receiving much larger doses of soluble Ova (Figure 3B). These more avid antibody responses were sustained over the 12 weeks of the experiment (Figure 3B). After the antigenic challenge (i.e., booster immunization), greater Ova-specific serum antibody responses (i.e., titers ≥ 100,000) were observed in mice administered the Ova-loaded microparticles as compared to the antibody responses (i.e., titers ≤ 10,000) induced by the soluble doses of Ova (Figure 3C compared to Figure 1C). Statistical comparisons of the antibody responses induced after the antigenic challenge (Figures 1C and 3C, solid histograms) demonstrated an adjuvant effect associated with the administration of the microparticles that was consistent with the elevated titers and avidity presented in Figures 3A and 3B.

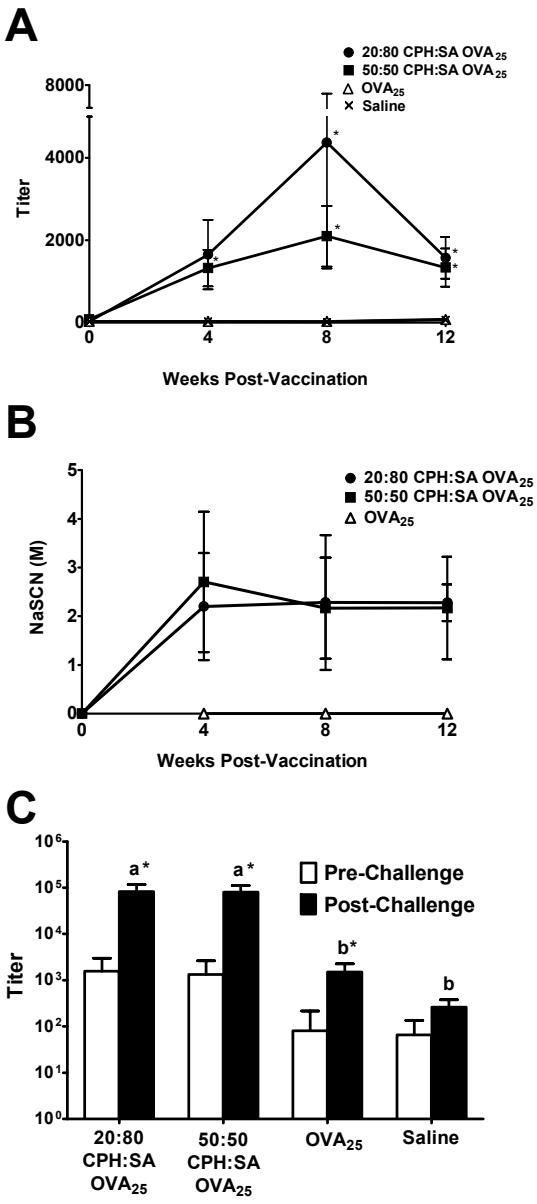

Figure 3. Enhanced serum antibody response in mice immunized with Ova-loaded polyanhydride microparticles. Ova-specific serum antibody titers (A) and antibody avidity (B) for C3H mice immunized with 20:80 CPH:SA Ova-loaded microparticles (closed circles), 50:50 CPH:SA Ova-loaded microparticles (closed squares), 25 μg soluble Ova (open triangles) or saline alone (x). (C) At 12 weeks post-immunization, the anamnestic Ova-specific serum antibody titer was measured prior to (open histograms) and five days after (closed histograms) a subcutaneously administered dose of 25 μg Ova(i.e., antigenic challenge). All data are presented as the mean ± SEM and are representative of three independent experiments. For panel A, * represents a statistically significant difference from the 25 μg soluble Ova group at $p < 0.05$. For panel C, * indicates a statistically significant difference from treatments prior to boost at $p < 0.05$. Treatments with different letters are significantly different from one another at $p < 0.05$.

3.3 Isotype switching of the serum antibody responses suggests immunological memory.

Characteristics of an immune response can be determined by examining the antibody isotype produced. For mice immunized with Ova-loaded microparticles, the secondary serum antibody response was characterized by the presence of both

Ova-specific IgG1 and IgG2a (Figure 4A and 4B, respectively). For mice immunized with single doses of soluble Ova (100 to 1600 μg), there was no demonstrable Ova-specific IgG2a detected after the antigenic-challenge (data not shown). Together, these results indicate that a mature, antigen-specific memory response was obtained with a priming dose of only 25 μg when encapsulated into polyanhydride microparticles.

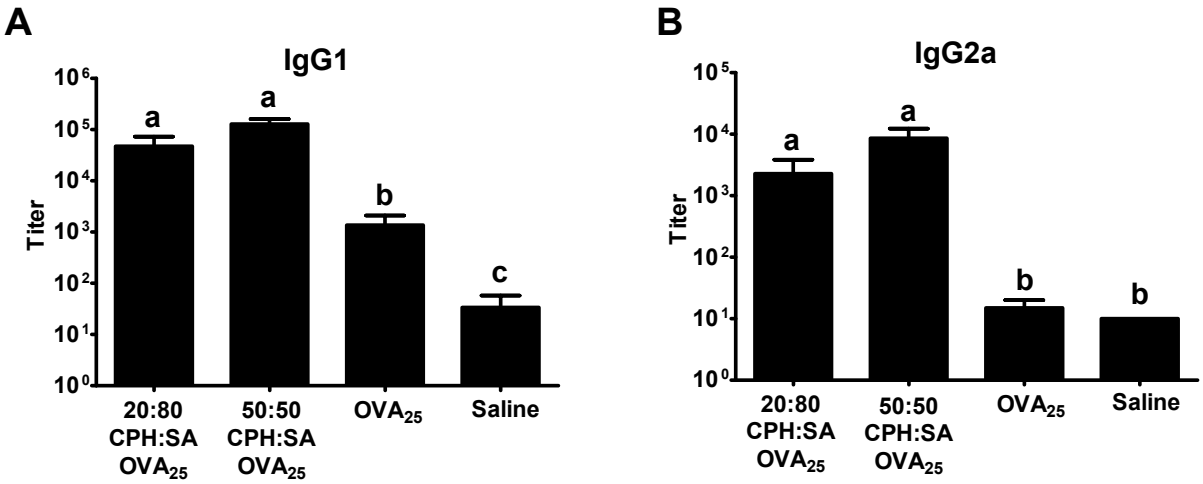

Figure 4. Mice immunized with Ova-loaded polyanhydride microparticles develop an anamnestic humoral response characterized by IgG1 and IgG2a, indicating antibody isotype switching. Ova-specific (A) IgG1 and (B) IgG2a serum antibody titer in mice administered a subcutaneous antigenic challenge of 25 μg Ova in saline 12 weeks after initial immunization with Ova-loaded polyanhydride microparticles. Data are presented as the mean ± SEM and are representative of three independent experiments. Treatments with different letters are significantly different from one another at $p < 0.05$.

4. Discussion

Biodegradable polymers exhibit adjuvant properties, making them ideal delivery platforms for single dose vaccine regimens [27-29]. Specifically, vaccine

formulations based on PLGA, PLA or PGA have been shown to induce immune responses to a variety of immunogens [30, 31]. Several of these studies incorporated monophosphoryl lipid A, a known adjuvant, into the polymer delivery device along with the immunogen, thereby complicating the ability to determine whether or not the polymer itself provides any immune enhancing activity [13, 29, 31]. Other studies have included excipients and/or stabilizers to enhance the immunogenicity of encapsulated proteins [27]. In the current study, no additional immune-enhancers were included during the fabrication of our polyanhydride microparticles loaded with endotoxin-free Ova or administered at the time of immunization. Therefore, any immuno-modulatory properties observed were the direct result of the polymers themselves.

Previously, we have demonstrated that polymer chemistry differentially effects *in vitro* antigen presenting cell (APC) cytokine production, particle uptake, and cell surface marker expression [20, 32]. In contrast to these differential effects demonstrated *in vitro* on APCs, *in vivo* administration of Ova-loaded 20:80 or 50:50 CPH:SA microparticles induced similar serum antibody titers (Figure 3A), avidity (Figure 3B), and recall responses (Figure 3C and 4). A robust antigen-specific humoral response to Ova, a weakly immunogenic protein, was induced using 16- to 64-fold less protein when encapsulated into polyanhydride microparticles as compared to soluble Ova alone (Figure 1 compared to Figure 3). The present studies were performed to demonstrate that immune responses could be induced with a single, suboptimal dose of an immunogen, not to compare the adjuvant capabilities of the microparticles to other adjuvants. However, these studies do infer

that polyanhydride delivery devices provide the adjuvant properties essential for effective implementation of subunit vaccines. Indeed, when a sub-immunogenic dose (e.g., 25 μg) of Ova was encapsulated into the microparticles, both co-polymer formulations were able to induce a robust immune response comparable to that induced by 400 to 1600 μg of soluble Ova. Furthermore, the titers of mice immunized with single dose microparticle formulations were similar to those reported for mice immunized multiple times with Alum-adjuvanted Ova over a range of doses comparable to the 25 μg dose used in this study [22, 33-38]. For example, Pollock et al. reported mean IgG1 titers of 40,000 after two administrations of 100 μg Ova adjuvanted with Alum [22]. In another study, a single immunization with 50 μg Ova adjuvanted with Alum in C57BL/6 mice induced an IgG1 titer of approximately 100, which increased to approximately 10,000 after a second immunization [36]. Sun et al. observed similar antigen-specific IgG titers following administration of 100 μg Ova adjuvanted with Alum [38]. In the present work, the titer values (approximately 1,000) obtained by immunizing mice once with 25 μg of Ova encapsulated in polyanhydride microparticles are similar to those induced by multiple doses of Alum-adjuvanted Ova described in the literature [22, 33-38]. Moreover, these titers increased to approximately 100,000 by boosting with only 25 μg of non-adjuvanted, endotoxin-free Ova (Figure 3C).

Recombinant protein antigens provide excellent purity and safety profiles for vaccines, but may sacrifice potency of the vaccine and lead to less than efficacious immune responses. The peak antibody response of microparticle vaccinated mice appeared four weeks later than in mice vaccinated with large amounts of soluble

antigen. This observation indicates that microparticle controlled antigen release provides a unique microenviroment *in vivo* where antigen persistance facilitates a more avid antibody response . In this regard, the avidity of the antibody response induced by the microparticle formulations was greater than that induced by any of the soluble doses of Ova used in this study. These observations demonstrate the importance of evaluating the magnitude (i.e., titer) and the quality (i.e., avidity) of the antibody response in order to fully appreciate the benefits of novel vaccine delivery platforms.

Persistence of antigen is also known to be critical for inducing long-lived plasma cells and memory B cells [39]. Companion studies from our laboratory indicate the persistence of polyanhydride particles at injection sites up to 12 weeks post-administration (manuscript in preparation). In the present study, the encapsulation, controlled release and subsequent persistence of Ova *in vivo* likely contributed to the induction of long-lived plasma cells and induction of a more avid humoral immune response than that induced by higher doses of soluble Ova. It may be speculated that the increased avidity of the serum antibody response in mice vaccinated with the Ova-loaded microparticles results specifcially from persistence of antigen in germinal centers, possibly mediated by follicular dendritic cells, in secondary lymphoid tissue [40]. An optimal immunization regimen employing both soluble and particle encapsulated antigen likely induces a robust humoral response more rapidly after immunization as well as promotes a sustained antibody response . The single dose of 25 μg Ova encapsulated into the microparticles was sufficient to induce a demonstrable antibody response and to prime the host for a more robust

secondary antibody responses following an antigenic challenge 12 weeks later (Figures 3 and 4). In contrast, there was little evidence of a recall response in mice initially administered 1600 μg Ova. Bioerodible microparticles may be performing similar actions as traditional emulsification vaccine adjuvants by providing an antigenic depot and creating particulate antigen that is more readily recognized by B cells and taken up by APCs [41]. Experimental models employing micro- or nanoparticle vaccination regimen incorporating recombinant immunogens followed by pathogen challenge will demonstrate the full potential of this polymer delivery platform to induce protective immune responses [42].

5. Conclusions

In this work, we demonstrated that robust, long-lived immune responses can be induced by a single, suboptimal dose of a weak immunogen by encapsulation into surface eroding polyanhydride microparticles. Administration of Ova-loaded microparticles facilitated the induction of a more robust humoral immune response with 16- to 64-fold less immunogen than the amount of soluble Ova required to induce a comparable titers. The use of these polymer delivery devices to immunize mice induced an anamnestic antibody response and generated isotype switching, as evidenced by the induction of antigen-specific IgG2a, an antibody isotype indicative of memory T cell development). Lastly, the avidity (i.e., quality) of the serum antibody induced by 25 μg of Ova encapsulated into microparticles was greater than that induced by 1600 μg of soluble Ova. Collectively, the data demonstrate that the use of surface erodible polyanhydride microparticles as a vaccine delivery platform

may enhance the magnitude and quality of the immune response to subunit or recombinant proteins, and thus broaden the arsenal of recombinant immunogens that can be safely, efficaciously, and cost effectively employed in vaccine formulations.

6. Acknowledgments

The authors would like to acknowledge financial support from the Whitaker Foundation, the U.S. Army Medical Research and Materiel Command (Grant Nos. W81XWH-09-1-0386 and W81XWH-10-1-0806) and the National Science Foundation (Grant Nos. EEC 0552584 and EEC 0851519).

7. References

[1] Tritto E, Mosca F, De Gregorio E. Mechanism of action of licensed vaccine adjuvants. Vaccine 2009;27(25-26):3331-4.

[2] Collin N, de Radiguès X. Vaccine production capacity for seasonal and pandemic (H1N1) 2009 influenza. Vaccine 2009;27(38):5184-6.

[3] Sallusto F, Lanzavecchia A, Araki K, Ahmed R. From vaccines to memory and back. Immunity;33(4):451-63.

[4] Bemark M, Bergqvist P, Stensson A, Holmberg A, Mattsson J, Lycke NY. A unique role of the Cholera Toxin A1-DD adjuvant for long-term plasma and memory B Cell development. The Journal of Immunology;186(3):1399-410.

[5] Lam XM, Duenas ET, Daugherty AL, Levin N, Cleland JL. Sustained release of recombinant human insulin-like growth factor-I for treatment of diabetes. Journal of Controlled Release 2000;67(2-3):281-92.

[6] Semete B, Booysen L, Lemmer Y, Kalombo L, Katata L, Verschoor J, et al. In vivo evaluation of the biodistribution and safety of PLGA nanoparticles as drug delivery systems. Nanomedicine: Nanotechnology, Biology and Medicine;6(5):662-71.

[7] Chong CSW, Cao M, Wong WW, Fischer KP, Addison WR, Kwon GS, et al. Enhancement of T helper type 1 immune responses against hepatitis B virus core antigen by PLGA nanoparticle vaccine delivery. Journal of Controlled Release 2005;102(1):85-99.

[8] Jiang W, Gupta RK, Deshpande MC, Schwendeman SP. Biodegradable poly(lactic-co-glycolic acid) microparticles for injectable delivery of vaccine antigens. Advanced Drug Delivery Reviews 2005;57(3):391-410.

[9] Determan AS, Wilson JH, Kipper MJ, Wannemuehler MJ, Narasimhan B. Protein stability in the presence of polymer degradation products: Consequences for controlled release formulations. Biomaterials 2006;27(17):3312-20.

[10] Lu W, Park TG. *In vitro* release profiles of eristostatin from biodegradable polymeric microspheres: protein aggregation problem. Biotechnology Progress 1995;11(2):224-7.

[11] Schwendeman S, Costantino H, Gupta R, Langer R. Peptide, protein, and vaccine delivery from implantable polymeric systems. In: Park K, editor. Controlled Drug Delivery: Challenges and Strategies. Washington, DC: ACS Books, 1997: 229-67.

[12] Shenderova A, Burke T, Schwendeman SP. The acidic microclimate in poly(lactide-co-glycolide) microspheres stabilizes camptothecins. Pharmaceutical Research 1999;16(2):241-8.

[13] Kumar N, Langer RS, Domb AJ. Polyanhydrides: an overview. Advanced Drug Delivery Reviews 2002;54(7):889-910.

[14] Torres MP, Determan AS, Mallapragada SK, Narasimhan B. Polyanhydrides. In: Lee S, editor. Encyclopedia of Chemical Processing. New York: Marcell Dekker, 2005.

[15] Determan AS, Trewyn BG, Lin VSY, Nilsen-Hamilton M, Narasimhan B. Encapsulation, stabilization, and release of BSA-FITC from polyanhydride microspheres. Journal of Controlled Release 2004;100(1):97-109.

[16] Torres MP, Determan AS, Anderson GL, Mallapragada SK, Narasimhan B. Amphiphilic polyanhydrides for protein stabilization and release. Biomaterials 2007;28(1):108-16.

[17] Lopac SK, Torres MP, Wilson-Welder JH, Wannemuehler MJ, Narasimhan B. Effect of polymer chemistry and fabrication method on protein release and stability from polyanhydride microspheres. Journal of Biomedical Materials Research Part B: Applied Biomaterials 2009;91B(2):938-47.

[18] Kipper MJ, Wilson JH, Wannemuehler MJ, Narasimhan B. Single dose vaccine based on biodegradable polyanhydride microspheres can modulate immune response mechanism. Journal of Biomedical Materials Research Part A 2006;76A(4):798-810.

[19] Torres MP, Wilson-Welder JH, Lopac SK, Phanse Y, Carrillo-Conde B, Ramer-Tait AE, et al. Polyanhydride microparticles enhance dendritic cell antigen presentation and activation. Acta biomaterialia 2011;7(7):2857-64.

[20] Petersen LK, Xue L, Wannemuehler MJ, Rajan K, Narasimhan B. The simultaneous effect of polymer chemistry and device geometry on the in vitro activation of murine dendritic cells. Biomaterials 2009;30(28):5131-42.

[21] Petersen LK, Ramer-Tait AE, Broderick SR, Kong C-S, Ulery BD, Rajan K, et al. Activation of innate immune responses in a pathogen-mimicking manner by amphiphilic polyanhydride nanoparticle adjuvants. Biomaterials 2011;32(28):6815-22.

[22] Pollock KGJ, Conacher M, Wei X-Q, Alexander J, Brewer JM. Interleukin-18 plays a role in both the alum-induced T helper 2 response and the T helper 1 response induced by alum-adsorbed interleukin-12. Immunology 2003;108(2):137-43.

[23] Conix A. Poly[1,3-bis(p-carboxyphenoxy)-propane anhydride]. Macro Synth 1966;2:95-8.

[24] Kipper MJ, Shen E, Determan A, Narasimhan B. Design of an injectable system based on bioerodible polyanhydride microspheres for sustained drug delivery. Biomaterials 2002;23(22):4405-12.

[25] Shen E, Pizsczek R, Dziadul B, Narasimhan B. Microphase separation in bioerodible copolymers for drug delivery. Biomaterials 2001;22(3):201- 10.

[26] Carrasquillo KG, Stanley AM, Aponte-Carro JC, De Jesus P, Costantino HR, Bosques CJ, et al. Non-aqueous encapsulation of excipient-stabilized spray-freeze dried BSA into poly(lactide-co-glycolide) microspheres results in release of native protein. Journal of Controlled Release 2001;76(3):199-208.

[27] Gupta RK, Chang AC, Siber GR. Biodegradable polymer microspheres as vaccine adjuvants and delivery systems. Development of Biological Standardization 1998;92:63-78.

[28] Gupta RK, Singh M, O'Hagan DT. Poly(lactide-co-glycolide) microparticles for the development of single-dose controlled-release vaccines. Advanced Drug Delivery Reviews 1998;32(3):225-46.

[29] Lutsiak ME, Kwon GS, Samuel J. Biodegradable nanoparticle delivery of a Th2-biased peptide for induction of Th1 immune responses. Journal of Pharmaceutical Pharmacology 2006;58(6):739-47.

[30] Conway MA, Madrigal-Estebas L, McClean S, Brayden DJ, Mills KH. Protection against *Bordetella pertussis* infection following parenteral or oral immunization with antigens entrapped in biodegradable particles: effect of formulation and route of immunization on induction of Th1 and Th2 cells. Vaccine 2001;19(15-16):1940-50.

[31] McNeela EA, Mills KH. Manipulating the immune system: humoral versus cell-mediated immunity. Advanced Drug Delivery Reviews 2001;51(1-3):43-54.

[32] Ulery B, Phanse Y, Sinha A, Wannemuehler M, Narasimhan B, Bellaire B. Polymer chemistry influences monocytic uptake of polyanhydride nanospheres. Pharmaceutical Research 2009;26(3):683-90.

[33] Flach TL, Ng G, Hari A, Desrosiers MD, Zhang P, Ward SM, et al. Alum interaction with dendritic cell membrane lipids is essential for its adjuvanticity. Nature Medicine 2011;17(4):479-87.

[34] Kool M, Soullié T, van Nimwegen M, Willart MAM, Muskens F, Jung S, et al. Alum adjuvant boosts adaptive immunity by inducing uric acid and activating inflammatory dendritic cells. The Journal of Experimental Medicine 2008;205(4):869-82.

[35] Kool M, Pétrilli V, De Smedt T, Rolaz A, Hammad H, van Nimwegen M, et al. Cutting edge: Alum adjuvant stimulates inflammatory dendritic cells through

activation of the NALP3 inflammasome. The Journal of Immunology 2008;181(6):3755-9.

[36] Huang H, Ostroff GR, Lee CK, Specht CA, Levitz SM. Robust stimulation of humoral and cellular immune responses following vaccination with antigen-loaded ß-Glucan particles. mBio 2010;1(3).

[37] Brewer JM, Conacher M, Satoskar A, Bluethmann H, Alexander J. In interleukin-4-deficient mice, alum not only generates T helper 1 responses equivalent to Freund's complete adjuvant, but continues to induce T helper 2 cytokine production. European Journal of Immunology 1996;26(9):2062-6.

[38] Sun H-X, Pan H-J. Immunological adjuvant effect of *Glycyrrhiza uralensis* saponins on the immune responses to ovalbumin in mice. Vaccine 2006;24(11):1914-20.

[39] Ochsenbein AF, Pinschewer DD, Sierro S, Horvath E, Hengartner H, Zinkernagel RM. Protective long-term antibody memory by antigen-driven and T help-dependent differentiation of long-lived memory B cells to short-lived plasma cells independent of secondary lymphoid organs. Proceedings of the National Academy of Sciences of the United States of America 2000;97(24):13263-8.

[40] Elgueta R, De Vries VC, Noelle RJ. The immortality of humoral immunity. Immunological Reviews 2010;236(1):139-50.

[41] Bachmann MF, Jennings GT. Vaccine delivery: a matter of size, geometry, kinetics and molecular patterns. Nature Reviews Immunology;10(11):787-96.

[42] Ulery BD, Petersen LK, Phanse Y, Kong CS, Broderick SR, Kumar D, et al. Rational design of pathogen-mimicking amphiphilic materials as nanoadjuvants. Scientific Reports 2011;1.

CHAPTER 4: EVALUATION OF BIOCOMPATIBILITY AND ADMINISTRATION SITE REACTOGENICITY OF POLYANHYDRIDE PARTICLE-BASED PLATFORM FOR VACCINE DELIVERY

Modified from a paper accepted to be published in *Advanced Healthcare Materials*

Lucas Huntimer, Amanda E. Ramer-Tait, Latrisha K. Petersen, Kathleen A. Ross, Katherine A. Walz, Chong Wang, Jesse Hostetter, Balaji Narasimhan, and Michael J. Wannemuehler

Abstract

Efficacy, purity, safety, and potency are important attributes of vaccines. Polyanhydride particles represent a novel class of vaccine adjuvants and delivery platforms that have demonstrated the ability to enhance the stability of protein antigens as well as elicit protective immunity against bacterial pathogens. This work aims to elucidate the biocompatibility, inflammatory reactions, and particle effects on mice injected with a 5 mg dose of polyanhydride nanoparticles via common parenteral routes (subcutaneous and intramuscular). Independent of polymer chemistry, nanoparticles more effectively disseminated away from the injection site as compared to microparticles, which exhibited a depot effect. Using fluorescent probes, the *in vivo* distribution of three formulations of nanoparticles, following subcutaneous administration, indicated migration away from the injection site. Less inflammation was observed at the injection sites of mice administered nanoparticles as compared to Alum and incomplete Freund's adjuvant. Furthermore, histological

evaluation revealed minimal adverse injection site reactions and minimal toxicological effects associated with the administration of nanoparticles at 30 days post-administration. Collectively, these results demonstrate that polyanhydride nanoparticles do not induce inflammation as a cumulative effect of particle persistence or degradation and are therefore a viable candidate for a vaccine delivery platform.

1. Introduction

Next generation vaccine design aims to recapitulate the positive effects of enhancing immune responses to the immunogen of interest while avoiding the detrimental side-effects often caused by adjuvants [2]. While efficacy is an essential outcome of vaccine design, biocompatibility is critical for ensuring patient compliance and ultimately developing protective immunity [3]. Adverse injection site reactions that cause either pain or tissue damage are major hurdles in the development and licensure of vaccines containing immunostimulatory adjuvants. These adjuvants are often necessary vaccine components, as they enhance immune responses against poorly immunogenic antigens. Specifically, adjuvants often comprise particulate material that is readily taken up by antigen presenting cells, activates innate immunity, and provides an antigenic depot to sustain immune responses [4]. The most common adjuvants used in human and veterinary medicine consist of aluminum salts, modified Toll-like receptor ligands, oil-water emulsions, or combinations thereof [5]. The majority of adjuvanted vaccines approved for human use contain potassium aluminum sulfate (Alum), MF59 (a squalene oil-in-water

emulsion), or ASO4 (monophosphoryl lipid A and Alum). Unfortunately, administration of vaccines containing these adjuvants often induces clinical signs of pain, redness, rash, swelling, and fever [6-8].

Polyanhydrides are a class of biodegradable polymers that have been studied for more than three decades as carriers for drugs, proteins, and vaccines [9]. The degradation products of polyanhydrides are metabolized and either released as carbon dioxide or excreted through urine and feces as carboxylic acids and were found to have no significant impact on kidney or liver functions [10, 11]. Additionally, polyanhydride wafer implants comprised of 1,3-bis-(*p*-carboxyphenoxy)pentane (CPP) and sebacic acid (SA) have been successfully used in humans to deliver chemotherapeutic drugs to treat glioblastoma multiforme [12-15]. Recently, amphiphilic polyanhydride nanoparticles based upon copolymers of SA, 1,6-bis-(*p*-carboxyphenoxy)hexane (CPH), and 1,8-bis-(*p*-carboxyphenoxy)-3,6-dioxaoctane (CPTEG) have been explored as a vaccine delivery platform with inherent adjuvant and antigen stabilization properties [16, 17]. These particles provide amphiphilic environments for release of conformationally and functionally stable protein antigens [17, 18] and demonstrate a combination of bulk and surface erosion kinetics that create a controlled release of encapsulated payload, making them ideal candidates for delivery of single-dose vaccines. Recent studies have shown that these polyanhydride nanoparticles exhibit pathogen-mimicking properties in terms of their effect on immune activation, cellular uptake, and cellular persistence [19-23]. Moreover, single dose vaccination with these particles has induced long-lasting, high titer, and avid antibody responses against multiple immunogens. For example,

administration of a single-dose of CPH:SA microparticles encapsulating tetanus toxoid to mice created antibody titers that persisted for at least 26 weeks post-vaccination [24]. Additionally, immunization of mice with a single dose of ovalbumin-loaded polyanhydride microparticles elicited humoral responses comparable to those induced by a 40-fold greater dose of soluble ovalbumin [25]. We have also demonstrated the ability of the polyanhydride nanoparticle vaccine platform to induce, in a single intranasal administration, long-lived protective immunity in mice for up to 280 days after an otherwise lethal challenge by *Yersinia pestis*, the causative agent of pneumonic plague [21, 23].

However, the toxicological effects of these novel polyanhydride nanoparticles, especially when administered via various routes, need to be determined. To complement our previous findings of efficacy, we demonstrate here that polyanhydride nanoparticles result in deposition characteristics similar to those of traditional adjuvants. However, in contrast to traditional adjuvants, immunization with polyanhydride nanoparticles induced minimal inflammatory reactions and little to no tissue damage at sites of injection. Together with previous results, these data demonstrate the biocompatibility and limited reactogenicity of this nanoparticle delivery platform.

2. Materials and Methods

2.1 Synthesis and characterization of copolymers

CPH and CPTEG monomers were synthesized using the chemicals listed: 4-p-hydroxybenzoic acid, 1,6-dibromohexane, 1-methyl-2-pyrrolidinone, and tri-

ethylene glycol. All these chemicals and sebacic acid (99%) were purchased from Sigma Aldrich (St. Louis, MO); 4-p-fluorobenzonitrile was obtained from Apollo Scientific (Cheshire, UK); potassium carbonate, dimethyl formamide, toluene, sulfuric acid, acetic acid, acetonitrile, acetic anhydride, methylene chloride, and petroleum ether were purchased from Fisher Scientific (Fairlawn, NJ). Synthesis of CPH and CPTEG diacids was performed as previously described [17, 26] and pre-polymers of SA and CPH were synthesized using previously described methods [26, 27]. Copolymers (20:80 and 50:50 CPH:SA and 20:80 and 50:50 CPTEG:CPH) were synthesized using a melt polycondensation process as detailed by Kipper et al. and Torres et al., [17, 24] respectively. The degree of polymerization, molecular weight, chemical structure, and polymer purity were determined using ^{1}H nuclear magnetic resonance (NMR) spectroscopy (Varian VXR-300 MHz, Palo Alto, CA).

2.2 Fabrication and characterization of particles

Microparticles were fabricated using a cryogenic atomization method as described in Kipper et al [24]. Blank and dye-loaded (Kodak X-Sight 640 LSS Dye, NHS Ester Carestream Health, Rochester, NY) nanoparticles (0.5% w/w loading) were fabricated using the anti-solvent nanoencapsulation method outlined in Ulery et al [20]. Briefly, the copolymer was dissolved in methylene chloride at a concentration of 25 mg/mL at 4˚C. The dye was added to the dissolved copolymer and the solution was sonicated for uniform dispersal of the dye within the copolymer. The dissolved dye and copolymer (dye-loaded) or copolymer (blank) solution was rapidly transferred into chilled pentane (-20°C) at a non-solvent to solvent ratio of 80:1, and

this solution was vacuum filtered to recover the nanoparticles. Shape and size of the resulting nanoparticles were characterized using scanning electron microscopy (SEM) (JEOL 840 A, JEOL, Peabody, MA). The particle size distribution was obtained from SEM images using Image J version 1.44 image analysis software [28]. An average of 200 particles per image was analyzed.

2.3 Mice

Female BALB/c mice were purchased from Harlan Laboratories (Indianapolis, IN). Female SKH1-E (hairless) mice were purchased from Charles River Laboratories (Wilmington, MA). All mice were housed under specific pathogen-free conditions where all bedding, caging, water, and feed were sterilized prior to use. Animal procedures were conducted with the approval of the Iowa State University Institutional Animal Care and Use Committee.

2.4 Mouse treatments

2.4.1 Microparticle and nanoparticle biodistribution

Separate groups of BALB/c mice received a subcutaneous (SC) injection of either 0.5 mg of microparticles or 0.5 mg nanoparticles loaded with LSS 640 in 250 μL of saline at the nape of the neck (Figure 1).

2.4.2 Nanoparticle and adjuvant in vivo imaging

To avoid the auto-fluorescence often associated with animal fur, immunocompetent, hairless SKH1-E mice were employed for these studies and

assigned to one of six treatment groups: 1.5 mL of sterile saline, 5 mg of nanoparticles (of three different chemistries) loaded with LSS 640 suspended in 1.5 mL of sterile saline, 200 µL of 1:1 sterile saline batched with Imject® Alum (Pierce Rockford, IL) or 200 µL of 1:1 sterile saline emulsified in incomplete Freund's adjuvant (IFA). To administer the same amount of fluorescent dye as present in the polyanhydride particles, LSS 640 was solubilized in saline (6.25 µg/mL). Each mouse was injected SC at the nape of the neck with 2.5 mg of particles in 330 µL saline, 1.75 mg of particles in 230 µL of saline in the left rear flank intramuscularly (IM) and 0.75 mg in 100 µL of saline IM in the right rear flank. The three nanoparticle formulations used for these studies were 20:80 CPH:SA, 50:50 CPTEG:CPH, and 20:80 CPTEG:CPH. IFA and Alum injections consisted of 100 µL SC at the nape of the neck, 75 µL IM in the left rear flank, and 25 µL IM in the right rear flank. The regimen for the administration of sterile saline with LSS 640 employed the same volumes as the nanoparticle injections. Rotational image capture was performed daily for 7 days after the injection with a Multimodal Animal Rotation System (Carestream Multispectral FX, Rochester, NY). *In vivo* images were captured while mice were anesthetized with 2% isoflurane in 100% O_2, at 2.5 L/min. Images were captured using 60-second exposures with an excitation filter of 630 nm and emission filter of 790 nm. Rotational images consisted of exposures taken every 25^o from 0° to 400^o to provide sufficient overlap and create a full 360^o rotational image of each mouse. All image analysis was performed using Image J software version 1.44.[27] Raw images were inverted and background subtracted via a rolling ball radius of 150 pixels. The ImageJ lookup table "thal" was applied to the data in Figures 1 and 2. A

region of interest (ROI) was constructed and used to analyze mean fluorescence intensity (MFI) at the injection site of all mice for every image. The MFI of the ROI at the injection site of mice receiving particles was compared to the MFI of the ROI at the injection site measured immediately after administration of nanoparticles and the data is expressed as percent of initial fluorescence intensity.

2.4.3 Nanoparticle and adjuvant inflammation

SKH1-E mice were injected with blank nanoparticles as outlined in the treatment groups described above. To evaluate the *in vivo* inflammatory response, mice were intravenously administered 2 nmol of ProSense® 750 (VisEn Medical, Woburn, MA) 8 h prior to imaging on days 3 and 7 after the administration of the nanoparticles. ProSense® 750 is an activatable fluorescent reagent that is optically visible when the dye is cleaved by degradative enzymes, including cathepsin B, L, S, or plasminogen, that are common at sites of inflammation [29]. After 8 h, *in vivo* images were captured while mice were kept under anesthesia with 2% isoflurane in 100% O_2, at 2.5 L/min. Images were captured using 30-second exposures with an excitation filter of 730 nm and an emission filter of 790 nm. All image analysis was performed using ImageJ version 1.44 [28]. Raw images were inverted and background subtracted via a rolling ball radius of 150 pixels. The ImageJ lookup table “smart” was applied to the data in Figure 3. ROI analysis of injections sites was performed and mean fluorescence intensity (MFI) was quantified.

2.4.4 Nanoparticle and adjuvant histological and biomarker examination

BALB/c mice were injected with a total of 5 mg of nanoparticles as described above. Other treatments included mice injected with Alum, IFA, or saline. Serum samples were collected from all mice prior to the administration of the nanoparticles and on days 3, 7, and 28 after administration. Serum samples were obtained via saphenous vein bleeds. Serum, tissue, and urine samples were collected at necropsy.

2.5 Serum cytokine analysis

Serum samples obtained from BALB/c mice were analyzed using a 22-plex chemokine and cytokine antibody array (Millipore, Billerica, MA) measuring the following analytes: G-CSF, GM-CSF, IFN-γ, IL-10, IL-12p70, IL-13, IL-15, IL-17, IL-1α, IL-1β, IL-2, IL-2, IL-4, IL-5, IL-6, IL-7, IL-9, IP-10, KC, MCP-1, MIP-1α, RANTES, and TNF-α. Assays were performed according to the manufacturer's recommendations; data were acquired and analyzed using a Bio-Plex 200 (Bio Rad, Hercules, CA).

2.6 Biomarker analysis

Serum and urinary biomarkers of kidney and liver function were analyzed using Vitros 5.1 Chemistry Analyzer. Toxicological biomarker values were compared to those reported in Mazzaccara et al [1].

2.7 Histological evaluation

Formalin-fixed tissues from BALB/c mice were embedded, sectioned, stained with hematoxylin and eosin (H&E), and blindly evaluated by a board-certified veterinary pathologist (JM Hostetter) for indications of toxicity in liver and kidney and adverse injection site reactions in muscle as well as in the epidermal and dermal tissue. A twenty-point histopathological scoring system for adverse reactions at injection sites was created in which scores of 0-5 were assigned to four independent parameters: inflammation, distribution of inflammatory cell infiltrate, muscle degeneration, and fibrosis. A fifteen-point histopathological scoring system for toxicological damage in liver and kidneys was created in which scores of 0 to 5 were assigned to three independent parameters: inflammation, distribution of inflammatory cell infiltrate, and tissue necrosis.

2.8 Statistical analysis

Repeated measured cytokine variables were $\log_{10}$ transformed and analyzed using repeated measure Analysis of Variance (ANOVA) models. Treatment and time were fixed effects in this model, while mouse was the subject of repeated measures. Histological, weight, and biomarker data were analyzed using one-way ANOVA models with treatment as an explanatory variable. Differences in mean responses among treatments were tested with an overall F-test followed by a post-hoc Tukey's t-test. Statistical tests with p values ≤ 0.05 were regarded as significant.

3. Results

3.1 Nanoparticles disseminated away from the injection site whereas microparticles formed a depot

The estimated mean diameter of the LSS 640 fluorophore-loaded microparticles was 10 μm (± 400 nm) (Figure 1A) and that of the LSS 640 fluorophore-loaded nanoparticles was 400 nm (± 100 nm) (Figure 1B). These sizes were consistent between particles of all chemistries and with previously published studies [21-24, 30-34]. The polymers were characterized by ^{1}H NMR and the molecular weights were determined to be within published ranges [30].

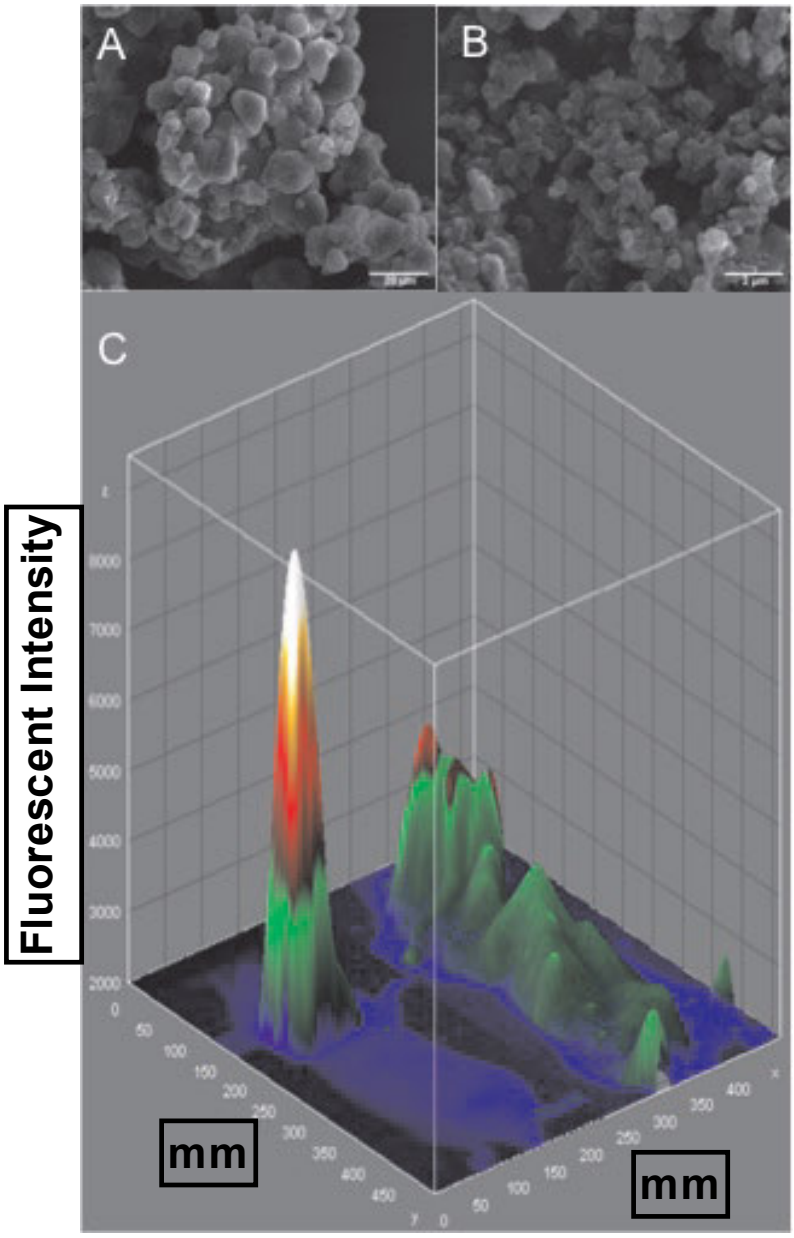

Figure 1. Nanoparticles disseminated away from the injection site whereas microparticles formed a depot. Scanning electron photomicrographs of 50:50 CPH:SA (A) micro- (scale bar 20 μm) or (B) nanoparticles (scale bar 2 μm). (C) Representative three-dimensional surface plot for a BALB/c mouse 4 days after SC administration of 500 μg of 50:50 CPH:SA micro- (left) or nanoparticles (right) graphed as a function of platform location (X- and Y- axes) and fluorescent intensity (Z-axis). X- and Y- axes represent size (in millimeters) of field of view; Z-axis represents fluorescence intensity.

The effect of size on particle biodistribution was investigated following SC administration of 50:50 CPH:SA nanoparticles or microparticles using live animal *in vivo* imaging. At four days post-administration, nanoparticles were more widely disseminated in contrast to the microparticles (Figure 1C). Specifically, three dimensional image analysis revealed a single, more intense peak of fluorescence at the injection site of mice receiving microparticles (Figure 1C). In contrast, multiple sites of discrete fluorescence were detected at tissue sites distal to the site of administration for mice receiving nanoparticles. This pattern of distribution observed following administration of the nanoparticles is not associated with the release of the tracer dye because at no time point after administration of the soluble tracer dye was a discrete pattern of fluorescence detected.

3.2 In vivo persistence of nanoparticles mimicked that of traditional adjuvants when administered via parenteral routes

Traditional vaccine adjuvants, including Alum, are thought to elicit immune-enhancing effects partly by forming antigenic depots [4]. In these studies, live animal *in vivo* imaging was employed to compare the deposition and persistence of polyanhydride nanoparticle adjuvants to those of traditional adjuvants. SKH1-E mice were administered a total of 5 mg of nanoparticles at three different injection sites as outlined in the methods (Figure 2A). Control mice were administered saline containing the fluorescent dye (LSS 640), and other mice were administered the LSS 640 dye adsorbed onto Alum or emulsified into IFA. Rotational images of mice

were captured at 7-day intervals; a representative image of a mouse from each treatment group is shown in Figure 2B. Mice administered Alum or IFA exhibited depot effects as demonstrated by the focal fluorescence present at the injection site after 7 days (Figure 2B). Each of the nanoparticle formulations provide a depot, however, there were lower amounts of fluorescence emanating from the injection sites, suggesting dissemination and/or erosion of the nanoparticles. Image analysis of injection site regions of interest (ROI) revealed chemistry-dependent effects on particle persistence (Figure 2C). Fluorescence intensity diminished most rapidly (by 2 weeks post-injection) for 20:80 CPH:SA nanoparticles. Based on the fluorescence intensity, 50:50 CPTEG:CPH nanoparticles persisted for 6 weeks post-injection, while the fluorescent signal was detectable at the injection site for 12 weeks post-administration for the 20:80 CPTEG:CPH nanoparticle formulation.

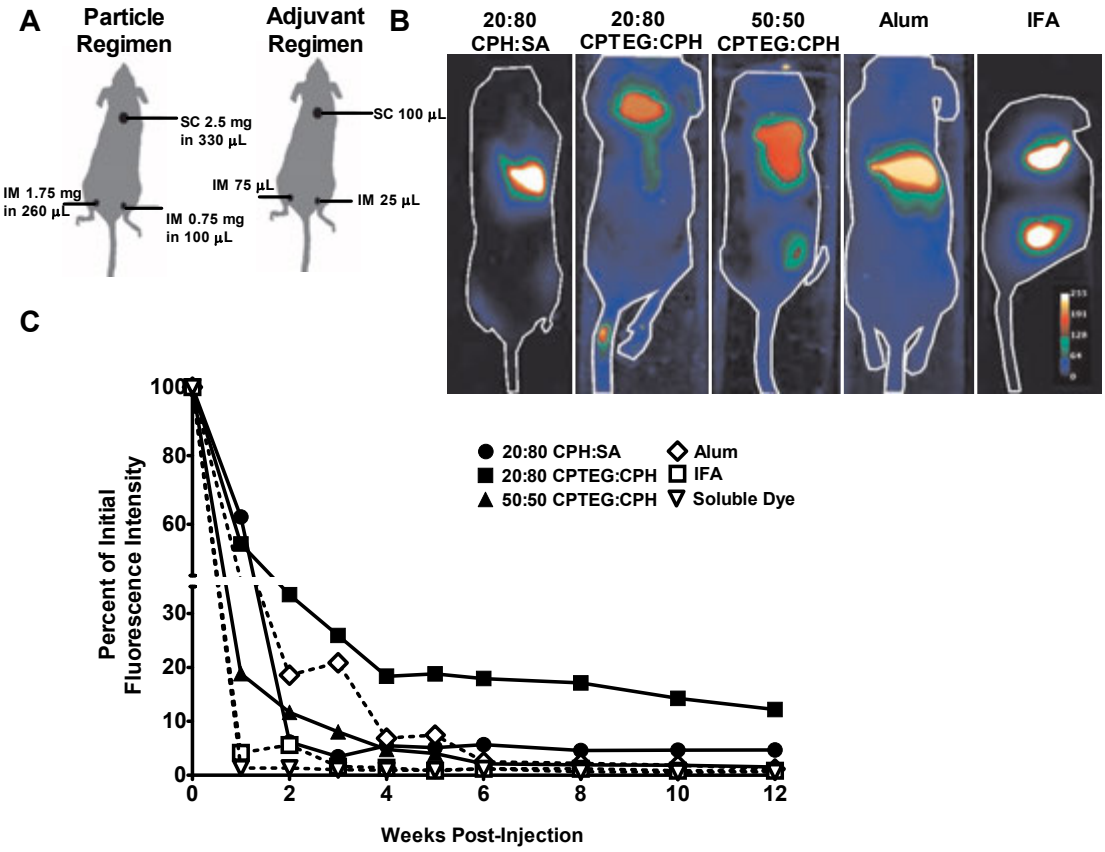

Figure 2. *In vivo* persistence of nanoparticles mimicked that of traditional adjuvants when administered via parenteral routes. (A) Schematic of dosing regimen for mice injected with either polyanhydride nanoparticles or traditional adjuvants. (B) *In vivo* imaging of mice injected with a total of 5 mg of 20:80 CPH:SA, 20:80 CPTEG:CPH, or 50:50 CPTEG:CPH nanoparticles loaded with fluorescent dye or administered with the fluorescent dye adsorbed onto Alum or emulsified into incomplete Freund's adjuvant (IFA). Images were captured at 7 days post-injection. Fluorescence intensity calibration bar is located in bottom right corner. (C) Fluorescence extinction of dye at injection sites. Data depict the percent of fluorescence intensity of the SC region of interest (ROI) at the nape of the neck as compared to the fluorescence intensity of the initial image taken immediately after administration. n = 2 mice per group.

3.3 Polyanhydride nanoparticle formulations did not induce deleterious injection site reactions

To assess the biocompatibility and phlogistic properties of polyanhydride nanoparticles, the magnitude of the host inflammatory response to each nanoparticle formulation was compared to that induced by Alum or IFA. Local tissue inflammation was visualized in SKH1-E mice using ProSense® 750, a fluorescent probe activated by enzymes released by inflammatory cells [35]. At 3 days post-injection, the magnitude of the inflammation induced at the SC (nape of the neck) site of administration was significantly greater in IFA treated mice than in mice administered Alum or any formulation of polyanhydride nanoparticles (Figure 3). The IM injection of Alum (left flank) induced a more severe inflammatory reaction than that induced by nanoparticles or IFA. At 7 days post-injection, the relative intensity of the local inflammatory reactions at sites of nanoparticle administration was significantly lower ($p \leq 0.05$) than that observed in mice receiving Alum or IFA. These results indicate that the nanoparticles did not induce inflammation as a cumulative effect of particle persistence or degradation (Supplemental Figure 1). Furthermore, there was little to no evidence of local inflammation at 30 days post-injection for any of the treatment groups, even though the nanoparticles persisted *in vivo* for up to twelve weeks post-injection (data not shown).

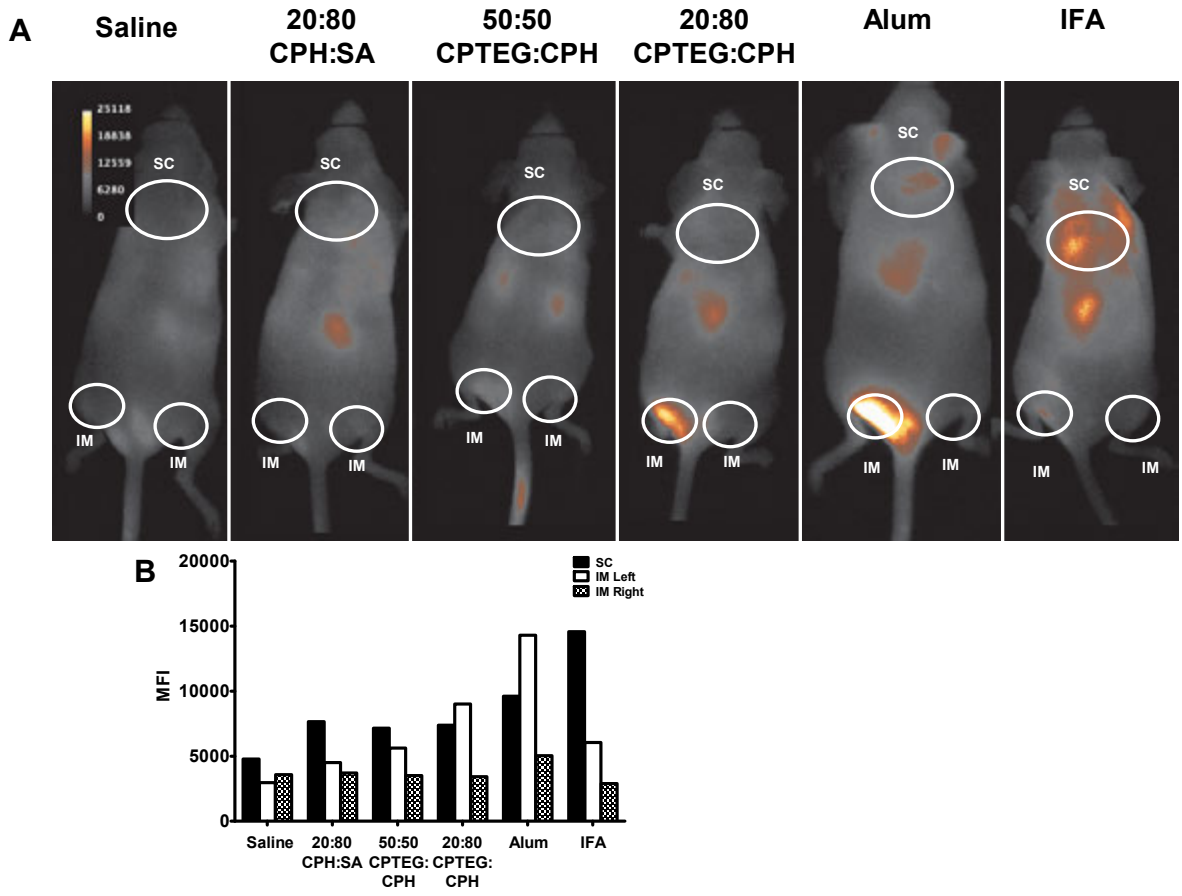

Figure 3. Polyanhydride nanoparticles induced less inflammation-associated enzymatic activity than traditional adjuvants. At 3 days post-injection, mice were administered ProSense® 750, a protease activatable fluorescent imaging agent activated by cathepsins B, L, S and Plasmin at sites of inflammation. ProSense® 750 is optically silent in its inactivated state and becomes highly fluorescent following protease-mediated activation. Images were captured 8 hours after ProSense® 750 administration. Data depict the mean of the fluorescence intensity of the ROI's of the three injection sites. n = 2 mice per group.

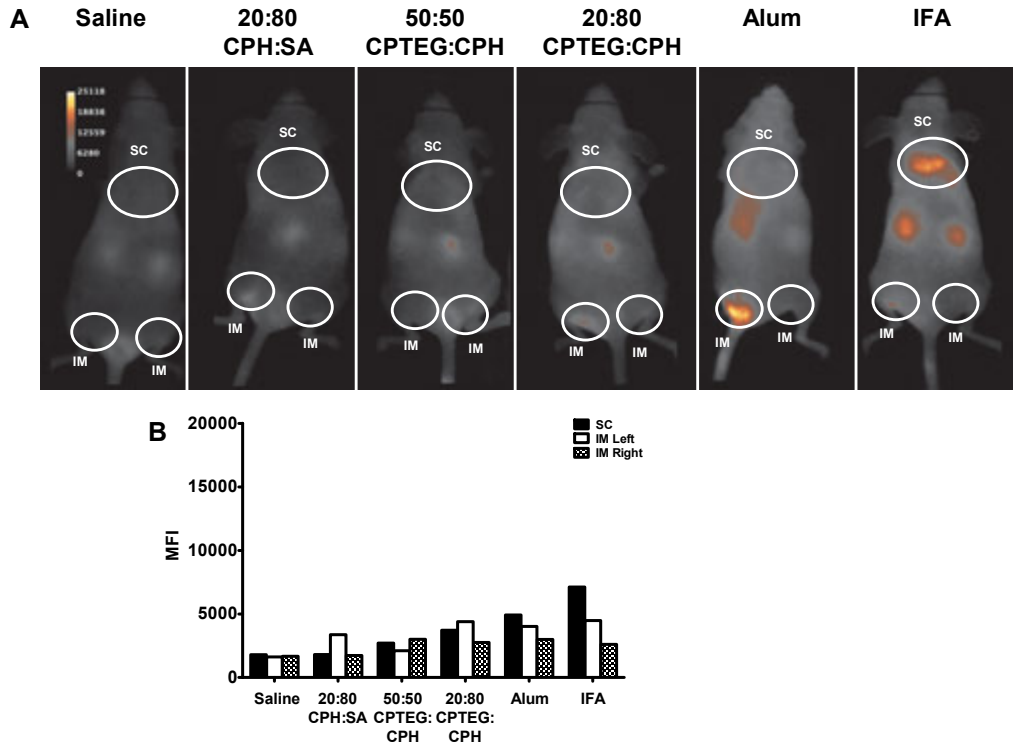

Supplemental Figure 1. Polyanhydride nanoparticles induce less inflammation-associated enzymatic activity than traditional adjuvants. At 7 days post-injection, mice were administered ProSense® 750, a protease activatable fluorescent imaging agent activated by cathepsins B, L, S and Plasmin at sites of inflammation. ProSense® 750 is optically silent in its inactivated state and becomes highly fluorescent following protease-mediated activation. Images were captured 8 hours after ProSense® 750 administration. n = 2

The systemic inflammatory response of mice administered Alum, IFA, or nanoparticles was examined by assaying for inflammatory chemokines and cytokines in the serum at 3, 7, and 30 days post-injection. At 3 days post-injection, levels of the monocyte-recruiting chemokines IP-10 and MCP-1 were elevated in the serum of mice administered CPTEG:CPH nanoparticles, Alum, or IFA compared to saline controls (Figure 4A-B). Of note, the MCP-1 and IP-10 levels remained elevated in mice administered Alum on day 7 post-injection while the levels for mice

receiving other treatments were similar to the saline controls (Figure 4 C-D). At 30 days post-immunization, all cytokine levels were basal (data not shown).

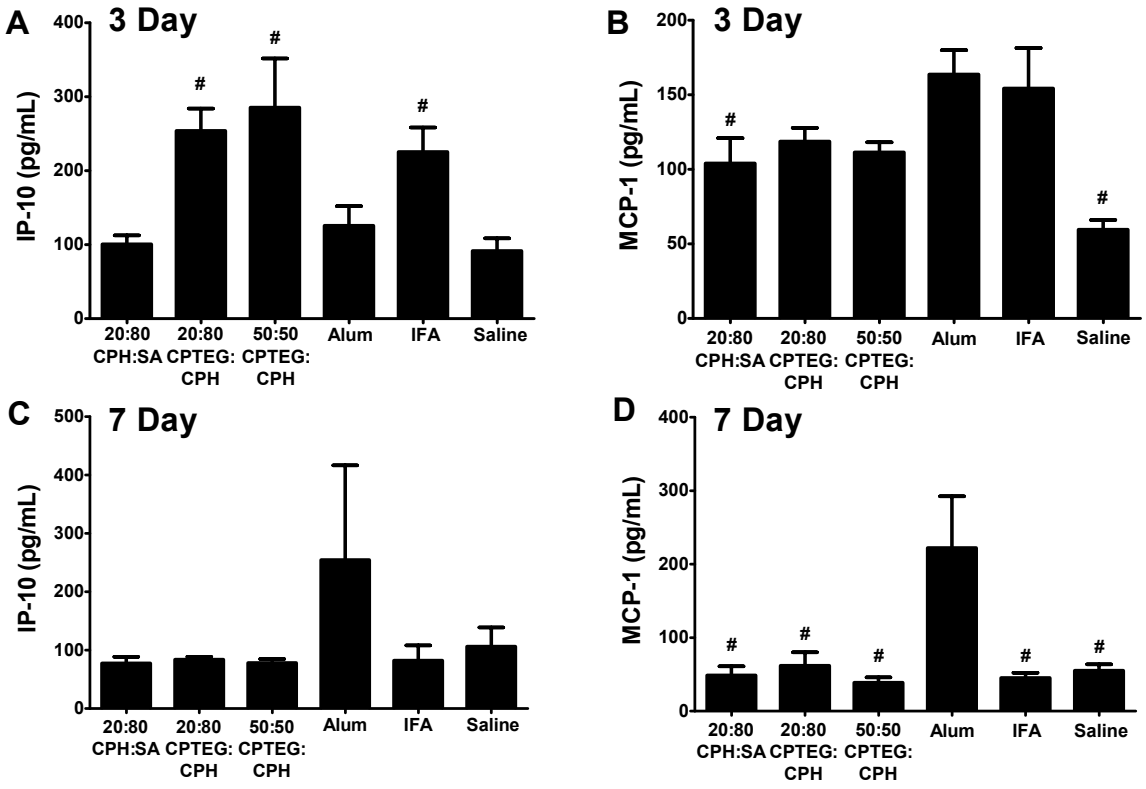

Figure 4. Increased levels of the monocyte-recruiting chemokines IP-10 and MCP-1 in the serum of mice administered either nanoparticles, Alum, or IFA. Concentrations of (A-B) IP-10 and (C-D) MCP-1 in the serum of mice administered a 5.0 mg dose of 20:80 CPH:SA, 20:80 CPTEG:CPH, or 50:50 CPTEG:CPH nanoparticles, Alum, IFA or saline at 3 (A and C) or 7 days post-injection (B and D). Treatment groups marked with # are significantly different from those mice treated with Alum at $p < 0.05$. n = 6-7 mice per group.

Because polyanhydride nanoparticles persist *in vivo,* tissues from SC and IM injection sites were harvested at 30 days post-injection and evaluated for microscopic evidence of tissue damage and inflammation. The highest dosages of

adjuvant were administered at the SC immunization site, and it was observed that the tissue response induced by Alum was histopathologically more severe than that induced by the nanoparticles or IFA (Figure 5A). Statistical differences were observed in only the 20:80 CPH:SA groups for both IM tissues sites indicating more inflammation associated with CPTEG:CPH chemistries (Figure 5B-C). Mice immunized with Alum had marked injection site reactions, characterized by muscle degeneration, inflammatory cell infiltrate, and fibrosis. Macrophage infiltrate was observed in all groups at the SC injection site; however, polymorphonuclear cell infiltrate was only noted in tissue recovered from mice treated with Alum, IFA, or 50:50 CPTEG:CPH nanoparticles. Granuloma formation was recorded in five of the six Alum treated mice at the SC injection site. In contrast, only one mouse (50:50 CPTEG:CPH) was found to have granuloma formation across all the nanoparticle-treated mice.

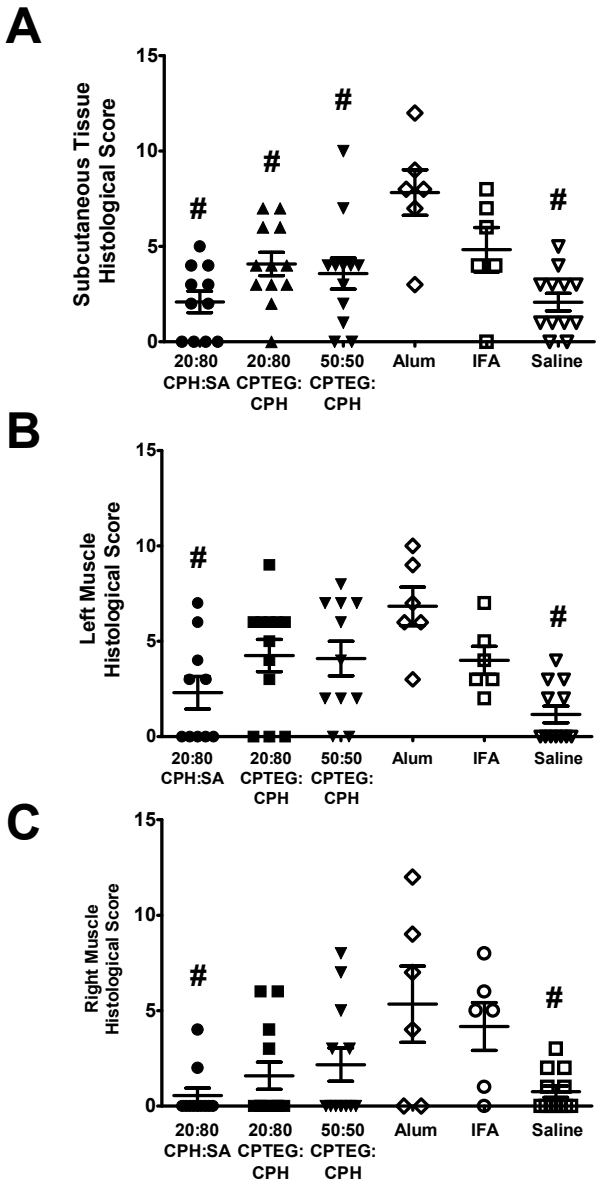

Figure 5. Polyahnhydride nanoparticle formulations did not induce deleterious injection site reactions. Composite histopathological scores of injection site subcutaneous tissue (A), left muscle (B), and right muscle (C) from mice administered 20:80 CPH:SA, 20:80 CPTEG:CPH, 50:50 CPTEG:CPH nanoparticles, Alum, IFA, or saline at 30 days post-administration. Treatments with # are significantly different from Alum at $p < 0.05$. n = 6-13 per group.

3.4 Minimal toxicological effects on kidney and liver function following immunization with polyanhydride nanoparticles

Although enhanced tissue distribution of polyanhydride nanoparticles may provide immunological benefits, accumulation of CPTEG:CPH or CPH:SA

nanoparticles in the liver or kidney could prove detrimental to normal physiological processes. Therefore, separate groups of mice were administered one of the three nanoparticle formulations, Alum or IFA and the appearance of serological biomarkers of liver or kidney damage was subsequently evaluated.

To measure liver function, total bilirubin, alanine aminotransferase (ALT) aspartate aminotransferase (AST) ratios, albumin, and lactate dehydrogenase were assayed using serum from mice at seven and 30 days post-treatment. Kidney function was evaluated by measuring changes in blood urea nitrogen (BUN), serum creatinine, and albumin in serum samples. For all parameters evaluated, no statistical differences were observed between nanoparticle treated mice in comparison to saline controls (Table 1). Similar results were observed at both 7 and 30 days post-injection, indicating that there was no evidence of adverse responses at acute or chronic times post-treatment (Supplementary Table 1).

Table 1. No elevated biomarkers of liver or kidney damage in serum of mice 30 days after injections with polyanhydride nanoparticles.

Test	Synopsis	Normal Range*	Treatment Results (Mean ± SEM)						Units
			20:80 CPH:SA	20:80 CPTEG:CPH	50:50 CPTEG:CPH	Alum	IFA	Saline	
Liver Function									
Total Bilirubin	High levels of total bilirubin indicated diminished liver function due to liver being incapable of sufficiently removing bilirubin.	0.1-0.9	0.46 ± 0.08	0.44 ± 0.09	0.42 ± 0.07	0.32 ± 0.06	0.54 ± 0.16	0.52 ± 0.07	Milligrams per deciliter (mg/dL)
Alanine Aminotransferase (ALT)	Used to detect liver injury and/or diagnose liver disease. Elevation of ALT levels may be elevated when exposed to substances that are toxic and/or decrease blood flow.	29-191	36.2 ± 6.50	37.73± 3.89	30.88 ± 3.10	31.67± 3.35	30.33 ± 3.13	38.0 ± 6.87	International Units per Liter (IU/L)
Albumin	Low albumin levels suggest liver disease.	2.5-4.8	2.49 ± 0.13	2.43 ± 0.09	2.30 ± 0.11	2.15 ± 0.08	2.40 ± 0.10	2.5 ± 0.05	gm/dL
Aspartate Aminotransferase (AST/)ALT Ratio	Used in conjunction with ALT measurement for diagnosis of diminished liver function. AST/ALT ratios can be calculated to detect liver disease or decreased function and AST/ALT <1.0 may indicate damage.	>1.0	5.25 ± 0.84	4.35 ± 0.51	5.55 ± 0.67	5.83 ± 0.28	7.09 ± 0.79	7.38 ± 1.54	Ratio
Lactate Dehydrogenase (LDH)	High levels of total LDH may be an indicator of acute or chronic tissue injury.	843-3150	2248.7 ± 192.8	2065.6 ± 204.8	2092.5 ± 105.6	2100.2 ± 129.6	2735.5 ± 356.9	2626.7 ± 429.4	IU
Kidney Function									
Blood Urea Nitrogen (BUN)	Increased BUN is suggestive of impaired kidney function or excessive catabolism.	18-29	15.36 ± 0.59	14.50 ± 0.82	13.38 ± 0.63	12.25 ± 0.56	13.5 ± 0.62	14.86 ± 0.67	mg/dL
Serum Creatinine	Used in conjunction with BUN to assess kidney function. Combination of blood and urine creatinine can be used to assess how well kidneys are filtering small molecules out of blood.	0.1-0.4	0.26 ± 0.02	0.25 ± 0.02	0.23 ± 0.02	0.23 ± 0.02	0.22 ± 0.04	0.24 ± 0.02	mg/dL

Table 1.
Enzymatic tests, synopsis of test and normal ranges are indicated in the first three columns. Values are presented as the mean ± SEM. *Normal range values are acquired from Mazzacara et al [1] and from Iowa State University Clinical Pathology.

Supplementary Table 1. No elevated biomarkers of liver or kidney damage in serum of mice 7 days after injections with polyanhydride nanoparticles.

Test	Synopsis	Normal Range*	Treatment Results (Mean ± SEM)				Units
			20:80 CPH:SA	20:80 CPTEG:CPH	50:50 CPTEG:CPH	Saline	
Liver Function							
Total Bilirubin	High levels of total bilirubin indicated diminished liver function due to liver being incapable of sufficiently removing bilirubin.	0.1-0.9	0.56 ± 0.14	0.70 ± 0.13	0.60 ± 0.28	0.64 ± 0.24	Milligrams per deciliter (mg/dL)
Alanine Aminotransferase (ALT)	Used to detect liver injury and/or diagnose liver disease. Elevation of ALT levels may be elevated when exposed to substances that are toxic and/or decrease blood flow.	29-191	73.0 ± 8.4	135.0 ± 38.7	87.0 ± 4.7	103.0 ± 20.8	International Units per Liter (IU/L)
Albumin	Low albumin levels suggest liver disease.	2.5-4.8	1.9 ± 0.20	2.5 ± 0.05	2.6 ± 0.19	2.7 ± 0.08	gm/dL
Aspartate Aminotransferase (AST/)ALT Ratio	Used in conjunction with ALT measurement for diagnosis of diminished liver function. AST/ALT ratios can be calculated to detect liver disease or decreased function and AST/ALT <1.0 may indicate damage.	>1.0	407 ± 45.6	654 ± 92.8	476 ± 30.7	616 ± 92.0	Ratio
Lactate Dehydrogenase (LDH)	High levels of total LDH may be an indicator of acute or chronic tissue injury.	843-3150	4885 ± 399.3	7001 ± 643.3	5776 ± 444.6	7116 ± 794.3	IU
Kidney Function							
Blood Urea Nitrogen (BUN)	Increased BUN is suggestive of impaired kidney function or excessive catabolism.	18-29	17 ± 1.5	19 ± 1.2	17 ± 0.7	16 ± 1.1	mg/dL
Serum Creatinine	Used in conjunction with BUN to assess kidney function. Combination of blood and urine creatinine can be used to assess how well kidneys are filtering small molecules out of your blood.	0.1-0.4	0.4 ± 0.05	0.6 ± 0.06	0.5 ± 0.04	0.6 ± 0.06	mg/dL

Supplementary Table 1.
Enzymatic tests, synopsis of test and normal ranges are indicated in the first three columns. Values are presented as the mean ± SEM. *Normal range values are acquired from Mazzacara et al [1] and from Iowa State University Clinical Pathology.

Liver and kidney tissues were also examined both macroscopically and microscopically to identify structural or histological damage. No statistical differences in liver and kidney weights were observed for any adjuvant-treated mice as compared to controls (Figure 6A and B). Histopathological analysis revealed no significant indications of toxicity, inflammation, or necrosis in livers and kidneys from nanoparticle-treated mice (Figure 6C and D). While one mouse administered 20:80 CPTEG:CPH particles did present with focal signs of hepatic necrosis, the pathologist interpreted this lesion as being consistent with commonly observed

tissue changes within the liver of BALB/c mice. Altogether, tissues analyzed from all mice, regardless of treatment group, revealed normal histological features similar to those observed in the saline treated controls.

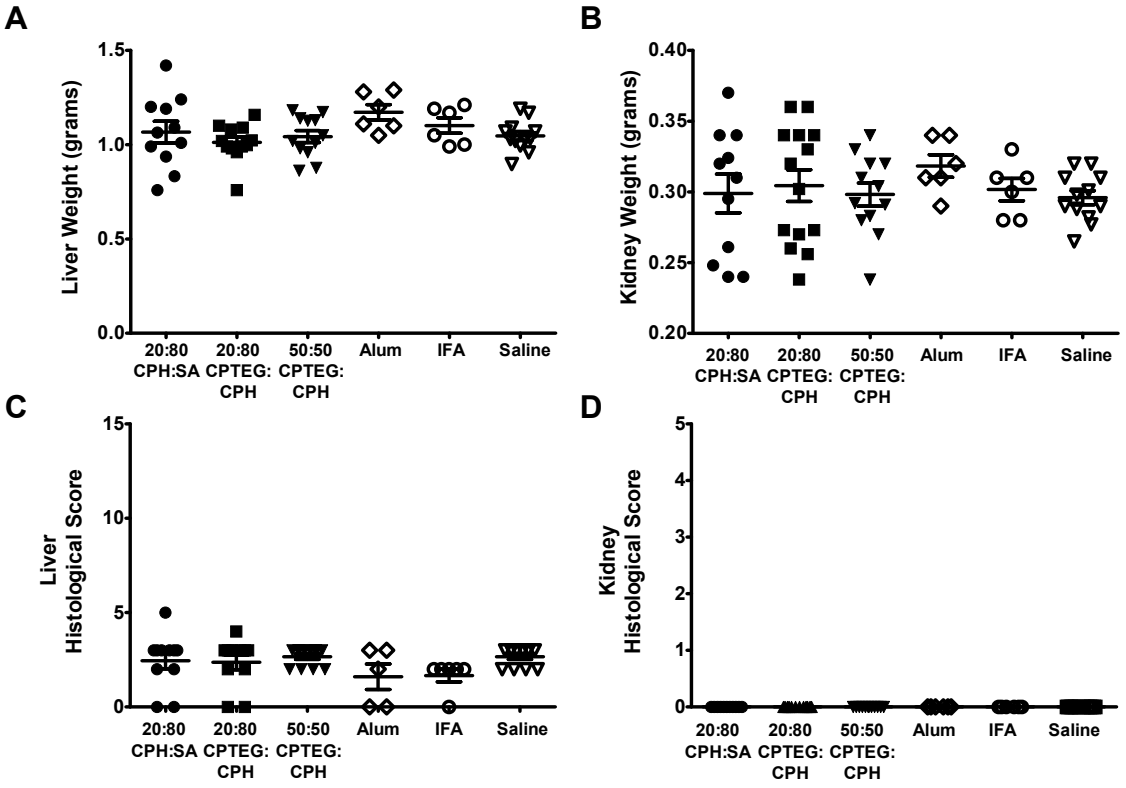

Figure 6. **Minimal toxicological effects on kidney and liver function following immunization with polyanhydride nanoparticles.** (A and B) Livers and kidneys from immunized mice were weighed at 30 days post-injection; no significant differences among treatments were observed. (C and D) Composite histopathological scores of liver and kidney tissues from mice administered 20:80 CPH:SA, 20:80 CPTEG:CPH, 50:50 CPTEG:CPH nanoparticles, Alum, IFA, or saline at 30 days post-administration; no significant differences from healthy controls were observed. n = 6-13 per group.

4. Discussion

Vaccine adjuvants must maintain a delicate balance between eliciting a robust antigen-specific immune response and inducing an adverse reaction at the site of administration [4, 5, 36-39]. When administered subcutaneously, polyanhydride nanoparticles persisted at the injection site, providing an antigenic depot similar to that provided by Alum and IFA (Figure 2). However, unlike the traditional adjuvants, the nanoparticles provided the added advantage of disseminating throughout the body (Figure 1 and 2). Based on companion studies and the injection of soluble tracer dye, the distinct biodistribution observed was not a result of detecting tracer dye released from the nanoparticles but the dissemination of the nanoparticles themselves. Similar to the systemic spread of a pathogen, the capacity to distribute or disseminate throughout the body further supports the pathogen-mimicking potential of the polyanhydride nanoparticles [19, 23]. Measuring the presence of the dye-loaded nanoparticles over time demonstrated that polyanhydride nanoparticles persisted for up to 12 weeks *in vivo*, with polymer chemistry influencing the degree of persistence (Figure 2). Additional analyses evaluated the biocompatibility of the polyanhydride nanoparticle platform by comparing the inflammatory responses, injection site tissue responses, and liver and kidney functions from nanoparticle-treated mice to those of mice administered Alum or IFA (Figures 3 to 6). No indications of inflammation or adverse reactions associated with administration or degradation of the nanoparticles were observed.

In combination with our previous reports of nanoparticle-based vaccine potency and efficacy [20-22, 24, 30] the reactogenicity profile presented in this work

further supports the *in vivo* use of polyanhydride nanoparticle adjuvants in vaccine formulations. Independent of chemistry, the nanoparticles presented unique biodistribution characteristics not observed with the microparticles, including their ability to disperse from the injection site. We hypothesize that particle size and chemistry influences both dissemination to distal tissues and more efficient uptake by phagocytic cells that would contribute to tissue distribution and/or persistence of the nanoparticles [20, 40]. The observed persistence of the nanoparticles at injection sites resembles that of Alum and IFA; however, CPTEG:CPH nanoparticle chemistries appear to more readily disperse throughout the body and mimic the distribution patterns of pathogens [41-43].

To date, the majority of *in vivo* immunization studies in murine models performed in our laboratories have employed a single 0.5 mg dose of the polyanhydride nanoparticles [21, 24]. The data presented herein demonstrated negligible inflammatory and adverse biological responses in mice subsequent to the administration of 5.0 mg (i.e., 10-fold higher amount) of polyanhydride nanoparticles as compared to Alum or IFA. IP-10, thought to be the chemokine primarily responsible for the efficacy of the yellow fever vaccine [44], was elevated in the nanoparticle-treated mice, indicating monocytic recruitment. Collectively, our results indicate that although polyanhydride nanoparticles may mimic pathogens with respect to tissue distribution and phagocytic uptake [19, 20, 22], they do not, however, induce detrimental tissue destruction caused by extensive inflammatory cell infiltrate.

The surface erosion characteristics of the polyanhydride nanoparticles enables them to persist *in vivo* as long or longer than other vaccine formulations. It is, therefore, critical that polyanhydride delivery systems be evaluated for the induction of both acute and chronic adverse toxicological reactions. In the present study, we observed no significant elevation of physiological biomarkers of liver or kidney damage in mice administered a 5 mg dose of nanoparticles (Table 1), suggesting that neither the nanoparticles nor their degradation products were adversely accumulating or altering liver or kidney functions. This finding is in agreement with previous studies where liver and kidney functions were fully preserved after implantation of a polyanhydride wafer used to treat human brain cancer [11, 45]. Together, these results demonstrate the non-toxic and biocompatible characteristics of polyanhydride nanoparticle-based vaccine carriers and support the hypothesis that their inherent physicochemical properties (e.g., degradation kinetics and pathogen-mimicking ability, leading to dissemination and persistence) positively affect the immune response by inducing long-lived, protective immunity [23].

5. Conclusions

Developing adjuvants that balance enhancing innate and adaptive immune responses while simultaneously limiting the induction of non-specific adverse events are a challenge for vaccinology. The results of this study indicate that administration of larger doses of polyanhydride nanoparticles are more biocompatible than nominal doses of traditional adjuvants such as Alum and IFA. The nanoparticles

disseminated rapidly into tisssues distal to the administration site, and persisted for as long as 12 weeks, potentially providing a basis for the induction of long-lived immunity. Furthermore, administration of a 5 mg dose of polyanhydride particles resulted in no adverse effects as evidenced by the lack of biomarkers of liver and kidney damage and/or dysfunction, affirming the biocompatibility of these materials. The data herein also outline the inherent adjuvant activity of polyanhydride nanoparticles that stimulates immune responses with minimal lesion development at the site of administration. These data offer an initial standard for translating polyanhydride nanomaterials into use as a vaccine delivery platform for humans and animals.

6. References:

[1] Mazzaccara C, Labruna G, Cito G, Scarfo M, De Felice M, Pastore L, et al. Age-related reference intervals of the main biochemical and hematological parameters in C57BL/6J, 129SV/EV and C3H/HeJ mouse strains. PLoS ONE 2008;3(11):e3772.

[2] Petrovsky N, Aguilar JC. Vaccine adjuvants: Current state and future trends. Immunology and Cell Biology 2004;82(5):488-96.

[3] USDHHS. Guidance for industry: General principles for the development of vaccines to protect against global infectious diseases. In: Services USDoHaH, editor. Rockville, 2008.

[4] Tritto E, Mosca F, De Gregorio E. Mechanism of action of licensed vaccine adjuvants. Vaccine 2009;27(25-26):3331-4.

[5] Wilson-Welder JH, Torres MP, Kipper MJ, Mallapragada SK, Wannemuehler M, Narasimhan B. Vaccine adjuvants: Current challenges and future approaches. Journal of Pharmaceutical Sciences 2009;98(4):1278-316.

[6] Rivera Medina DM, Valencia A, de Velasquez A, Huang L-M, Prymula R, Garcia-Sicilia J, et al. Safety and immunogenicity of the HPV-16/18 AS04-adjuvanted vaccine: A randomized, controlled trial in adolescent girls. Journal of Adolescent Health 2010;46(5):414-21.

[7] Carmona A, Omenaca F, Tejedor JC, Merino JM, Vaman T, Dieussaert I, et al. Immunogenicity and safety of AS03-adjuvanted 2009 influenza A H1N1 vaccine in children 6-35 months. Vaccine 2010;28(36):5837-44.

[8] Harro CD, Pang Y-YS, Roden RBS, Hildesheim A, Wang Z, Reynolds MJ, et al. Safety and immunogenicity trial in adult volunteers of a human papillomavirus 16 L1 virus-like particle vaccine. Journal of the National Cancer Institute 2001;93(4):284-92.

[9] Mallapragada SK, Narasimhan B. Immunomodulatory biomaterials. International Journal of Pharmaceutics 2008;364(2):265-71.

[10] Kumar N, Langer RS, Domb AJ. Polyanhydrides: an overview. Advanced Drug Delivery Reviews 2002;54(7):889-910.

[11] Katti DS, Lakshmi S, Langer R, Laurencin CT. Toxicity, biodegradation and elimination of polyanhydrides. Advanced Drug Delivery Reviews 2002;54(7):933-61.

[12] Brem H. Polymers to treat brain tumours. Biomaterials 1990;11(9):699-701.

[13] Brem H, Mahaley MS, Vick NA, Black KL, Schold SC, Burger PC, et al. Interstitial chemotherapy with drug polymer implants for the treatment of recurrent gliomas. Journal of Neurosurgery 1991;74(3):441-6.

[14] Dang W, Daviau T, Brem H. Morphological Characterization of Polyanhydride biodegradable implant Gliadel during *in vitro* and *in vivo* erosion using scanning electron microscopy. Pharmaceutical Research 1996;13(5):683-91.

[15] Olivi A, Ewend MG, Utsuki T, Tyler B, Domb AJ, Brat DJ, et al. Interstitial delivery of carboplatin via biodegradable Polymers is effective against experimental glioma in the rat. Cancer Chemotherapy and Pharmacology 1996;39(1):90-6.

[16] Torres MP, Determan AS, Mallapragada SK, Narasimhan B. Polyanhydrides. In: Lee S, editor. Encyclopedia of Chemical Processing. New York: Marcell Dekker, 2005.

[17] Torres MP, Vogel BM, Narasimhan B, Mallapragada SK. Synthesis and characterization of novel polyanhydrides with tailored erosion mechanisms. Journal of Biomedical Materials Research Part A 2006;76A(1):102-10.

[18] Carrillo-Conde B, Schiltz E, Yu J, Chris Minion F, Phillips GJ, Wannemuehler MJ, et al. Encapsulation into amphiphilic polyanhydride microparticles stabilizes *Yersinia pestis* antigens. Acta biomaterialia 2010;6(8):3110-9.

[19] Petersen LK, Ramer-Tait AE, Broderick SR, Kong C-S, Ulery BD, Rajan K, et al. Activation of innate immune responses in a pathogen-mimicking manner by amphiphilic polyanhydride nanoparticle adjuvants. Biomaterials 2011;32(28):6815-22.

[20] Ulery B, Phanse Y, Sinha A, Wannemuehler M, Narasimhan B, Bellaire B. Polymer chemistry influences monocytic uptake of polyanhydride nanospheres. Pharmaceutical Research 2009;26(3):683-90.

[21] Ulery BD, Kumar D, Ramer-Tait AE, Metzger DW, Wannemuehler MJ, Narasimhan B. Design of a protective single-dose intranasal nanoparticle-based vaccine platform for respiratory infectious diseases. PLoS ONE 2011;6(3):e17642.

[22] Torres MP, Wilson-Welder JH, Lopac SK, Phanse Y, Carrillo-Conde B, Ramer-Tait AE, et al. Polyanhydride microparticles enhance dendritic cell antigen presentation and activation. Acta biomaterialia 2011;7(7):2857-64.

[23] Ulery BD, Petersen LK, Phanse Y, Kong CS, Broderick SR, Kumar D, et al. Rational design of pathogen-mimicking amphiphilic materials as nanoadjuvants. Scientific Reports 2011;1.

[24] Kipper MJ, Wilson JH, Wannemuehler MJ, Narasimhan B. Single dose vaccine based on biodegradable polyanhydride microspheres can modulate immune response mechanism. Journal of Biomedical Materials Research Part A 2006;76A(4):798-810.

[25] Huntimer L, Wilson Welder J, Ross K, Carrillo-Conde B, Pruisner L, Wang C, et al. Single immunization with a suboptimal antigen dose encapsulated into polyanhydride microparticles promotes high titer and avid antibody responses. Journal of Biomedical Materials Research Part B: Applied Biomaterials 2012

[26] Conix A. Poly[1,3-bis(p-carboxyphenoxy)-propane anhydride]. Macro Synth 1966(2):95-8.

[27] Shen E, Pizsczek R, Dziadul B, Narasimhan B. Microphase separation in bioerodible copolymers for drug delivery. Biomaterials 2001;22(3):201-10.

[28] Rasband WS. ImageJ. 1.44 ed. Bethesda, Maryland, USA: U. S. National Institutes of Health.

[29] Nahrendorf M, Sosnovik DE, Waterman P, Swirski FK, Pande AN, Aikawa E, et al. Dual channel optical tomographic imaging of leukocyte recruitment and protease activity in the healing myocardial infarct. Circulation Research 2007;100(8):1218-25.

[30] Kipper MJ, Shen E, Determan A, Narasimhan B. Design of an injectable system based on bioerodible polyanhydride microspheres for sustained drug delivery. Biomaterials 2002;23(22):4405-12.

[31] Determan AS, Trewyn BG, Lin VSY, Nilsen-Hamilton M, Narasimhan B. Encapsulation, stabilization, and release of BSA-FITC from polyanhydride microspheres. Journal of Controlled Release 2004;100(1):97-109.

[32] Determan AS, Wilson JH, Kipper MJ, Wannemuehler MJ, Narasimhan B. Protein stability in the presence of polymer degradation products: Consequences for controlled release formulations. Biomaterials 2006;27(17):3312-20.

[33] Lopac SK, Torres MP, Wilson-Welder JH, Wannemuehler MJ, Narasimhan B. Effect of polymer chemistry and fabrication method on protein release and stability from polyanhydride microspheres. Journal of Biomedical Materials Research Part B: Applied Biomaterials 2009;91B(2):938-47.

[34] Carrillo-Conde B, Ramer-Tait A, Wannemuehler M, Narasimhan B. Chemistry-dependent adsorption of serum proteins onto polyanhydride microparticles differentially influences dendritic cell uptake and activation. Acta Biomater 2012.

[35] Gounaris E, Tung CH, Restaino C, Maehr R, Kohler R, Joyce JA, et al. Live imaging of cysteine-cathepsin activity reveals dynamics of focal inflammation, angiogenesis, and polyp growth. PLoS ONE 2008;3(8):e2916.

[36] Halperin SA, Van Nest G, Smith B, Abtahi S, Whiley H, Eiden JJ. A phase I study of the safety and immunogenicity of recombinant hepatitis B surface antigen co-administered with an immunostimulatory phosphorothioate oligonucleotide adjuvant. Vaccine 2003;21(19-20):2461-7.

[37] Scheifele DW, Halperin SA, Ferguson AC. Assessment of injection site reactions to an acellular pertussis-based combination vaccine, including novel use of skin tests with vaccine antigens. Vaccine 2001;19(32):4720-6.

[38] Miliauskas JR, Mukherjee T, Dixon B. Postimmunization (vaccination) injection-site reactions: A report of four cases and review of the literature. The American Journal of Surgical Pathology 1993;17(5):516-24.

[39] Korsholm KS, Petersen RV, Agger EM, Andersen P. T-helper 1 and T-helper 2 adjuvants induce distinct differences in the magnitude, quality and kinetics of the early inflammatory response at the site of injection. Immunology;129(1):75-86.

[40] Bachmann MF, Jennings GT. Vaccine delivery: a matter of size, geometry, kinetics and molecular patterns. Nature Reviews Immunology;10(11):787-96.

[41] Doyle TC, Burns SM, Contag CH. Technoreview: *In vivo* bioluminescence imaging for integrated studies of infection. Cellular Microbiology 2004;6(4):303-17.

[42] Garside P, Brewer J. *In vivo* imaging of infection immunology—4I's! Seminars in Immunopathology 2010;32(3):289-96.

[43] Hutchens M, Luker GD. Applications of bioluminescence imaging to the study of infectious diseases. Cellular Microbiology 2007;9(10):2315-22.

[44] Querec TD, Akondy RS, Lee EK, Cao W, Nakaya HI, Teuwen D, et al. Systems biology approach predicts immunogenicity of the yellow fever vaccine in humans. Nature Immunology 2009;10(1):116-25.

[45] Leong KW, Kost J, Mathiowitz E, Langer R. Polyanhydrides for controlled release of bioactive agents. Biomaterials 1986;7(5):364-71.

CHAPTER 5: POLYANHYDRIDE PARTICLE VACCINE PLATFORM ENHANCES EARLY ANTIGEN-SPECIFIC CYTOTOXIC T CELL RESPONSES

Lucas Huntimer, Kathleen Ross, Ross Darling, Balaji Narasimhan, Amanda Ramer-Tait, and Michael J. Wannemuehler

To be submitted to Biomaterials

Abstract

Vaccination remains the paramount preventive intervention against many different pathogens. Designing new vaccines against pathogens for which there is no current vaccine that are efficacious and induce minimal adverse side effects associated is one of the greatest challenges in medicine. Recent efforts have been focused on the use of biomaterials to enhance immune responses following immunization. Recently, polyanhydride nanoparticles have been shown to have the ability to provide controlled release of and stabilize protein antigens, enhance innate immune activation of antigen presenting cells, and elicit protective immunity against a respiratory bacterial pathogen. However, there is limited direct evidence of cell mediated immune activation when mice were immunized using polyanhydride nanoparticles. Using the transgenic ovalbumin (Ova) specific T cell (OT) model, we report the enhanced expansion of antigen specific cytotoxic $CD8^+$ T cells expressing an effector memory phenotype ($CD44^{high}$ $CD62L^{low}$) at early time points when antigen is encapsulated into polyanhydride nanoparticles. A significant population of the Ova-specific $CD8^+$ T cells is maintained at seven days post-injection indicating

that controlled and sustained release of Ova contributed to the maintenance of the Ova-specific T cell population. Using the high frequency adoptive transfer of bioluminescent reporter Ova-specific T cells (3×10^6 cells), it was shown that mice vaccinated with Ova-loaded polyanhydride nanoparticles induced the expansion of significantly more Ova-specific $CD8^+$ T cells than mice immunized with Alum adjuvanted Ova or Ova alone. The $CD8^+$ T cells induced by the polyanhydride nanoparticle vaccine were cytotoxic as evidenced by the ability to prevent the growth of EG7-Ova tumor cells. A low frequency adoptive transfer model, which better represents a naïve antigen specific T cell precursor frequency, was utilized to measure induction of $CD8^+$ T cell memory phenotypes following immunization with multiple formulations of nanoparticles. Polyanhydride nanoparticles were able to significantly ($p \leq 0.05$) expand Ova-specific $CD8^+$ T cells that included cells characterized as memory effector cells (cell surface markers) and central memory (cell surface markers) T cells. These data indicate that subunit vaccine regimens designed using the polyanhydride nanoparticle platform can induce cytotoxic cell-mediated immunity to target antigens using biocompatible and biodegradable materials.

1. Introduction

The use of preventive vaccines to curb disease remains the most effective public health intervention strategy to decrease morbidity and mortality associated with infectious diseases. Challenges associated with the development of next

generation vaccines include eliciting effective cell mediated immune responses towards the target antigen and inducing long-lived immunologic memory towards that antigen while minimizing severe adverse events (SAEs) following vaccination. The yellow fever vaccine remains the most successful vaccine in the human population due to its ability to elicit cell mediated ($CD4^+$ and $CD8^+$) T cell responses within the first two weeks of immunization and subsequently a long-lived protective antibody response that can last 45 years [1-3]. Engagement of multiple pattern recognition receptors (PRRs) on antigen presenting cells (APCs) by the antigens of yellow fever vaccine leads to pro-inflammatory cytokines IL-1β, TNF-α, and IFN-α/β, stimulating migration of mature dendritic cells to the draining lymph nodes and the subsequent induction of a robust adaptive immune response.

The effectiveness of the yellow fever vaccine can be attributed to its engagement of the innate immune system as well as its attributes as a live attenuated virus establishing a mild subclinical infection, persisting (i.e., replicating) for a period of time and effectively establishing immunological memory [3]. Next generation vaccine design is subsequently hindered if an organism is unable to be attenuated. This hinderence of design is further compounded with concerns regarding the presence of the phlogistic components associated with whole cell vaccines. Subunit (i.e., recombinant proteins) vaccines are a viable alternative due to elimination of phlogistic components and technological capabilities that are readily available for the production of recombinant immunogens. However, recombinant proteins are often poorly immunogenic requiring the addition of excipients or adjuvants to the vaccine formulation in order to enhance immune responses.

Altering the kinetics of antigen availability has been a favorable attribute associated with generating cellular immunity [4]. Human cytomegalovirus (HCMV) infection and the subsequent establishment of cellular immune memory present an interesting model for immunologists to consider when designing an efficacious vaccine. Low level infection of HCMV and persistent virus presence induces a robust T cell population that includes both effector (i.e., cytotoxic) and memory T cells [5]. Induction of cytotoxic T cells necessary for mediating immune responses against virally infected cells or tumor-specific cells is often difficult to achieve with purified subunit vaccines.

Polyanhydride copolymers based on sebacic acid (SA), 1,6-bis(*p*-carboxyphenoxy) hexane (CPH), and 1,8-bis(*p*-carboxyphenoxy)-3,6-dioxaoctane (CPTEG) have been shown to enhance the stability of encapsulated immunogens and provide adjuvant activities that enhance the benefits associated with controlled and sustained release of the immunogen [6, 7]. Polyanhydride microparticles also enhance in vitro dendritic cell activation and increase cell surface marker expression, cytokine production, and proliferation of antigen-specific $CD4^+$ and $CD8^+$ T cells [8]. Dosage sparing capabilities of the polyanhydride particle platform have been demonstrated in the context of a single parenteral vaccination resulting in sustained antibody titers of high avidity (Chapter 3).

Little analysis has been performed regarding cell-mediated immune responses elicited by the polyanhydride platform. Here, we expand our analysis of the cell-mediated immune responses elicited by polyanhydride particle vaccination. Specifically, we utilize adoptive transfer of ovalbumin (Ova)-specific transgenic T

cells to mice receiving a combination vaccine regimen of soluble and encapsulated Ova as previously described and a tumor challenge model expressing the model antigen Ova [9].

We demonstrate that encapsulation of antigen in polyanhydride nanoparticles enhances antigen-specific $CD8^+$ T cells in a high frequency adoptive transfer. Memory phenotypes of high frequency transfers showed $CD8^+$ effector and central memory characteristics. Using an ovalbumin secreting tumor model, we are able to show delayed progression of tumor growth using the polyanhydride nanoparticle platform as well as significantly increased circulating Ova-specific $CD8^+$ T cells post-tumor challenge compared to that induced by Ova adjuvanted with Alum. Low frequency adoptive transfer was utilized to examine antigen specific T cell responses in a less contrived system to capitulate actual naïve T cell precursor frequency. $CD8^+$ central effector and central memory phenotypes were examined and show that, in low frequency transfer, 20:80 CPH:SA (C:S) and 20:80 CPTEG:CPH (C:C) polyanhydride chemistries significantly expand Ova-specific $CD8^+$ T cells leading to higher frequencies of memory precursor effector cells and central memory $CD8^+$ T cells.

2. Materials and Methods

2.1 Synthesis and characterization of copolymers

Polyanhydrides were synthesized using the chemicals listed: 4-p-hydroxybenzoic acid, 1,6-dibromohexane, 1-methyl-2-pyrrolidinone, N,N-dimethylacetamide, and tri-ethylene glycol. All these chemicals and sebacic acid

(99%) were purchased from Sigma Aldrich (St. Louis, MO); 4-p-fluorobenzonitrile was obtained from Apollo Scientific (Cheshire, UK); potassium carbonate, dimethyl formamide, toluene, sulfuric acid, acetic acid, acetonitrile, acetone, acetic anhydride, methylene chloride, chloroform, sodium hydroxide, hexane, ethyl ether, and petroleum ether were purchased from Fisher Scientific (Fairlawn, NJ). Synthesis of CPH and CPTEG diacids was performed as previously described [10, 11] and pre-polymers of SA and CPH were synthesized using previously described methods [11, 12]. Copolymers (20:80 CPH:SA (C:S) and 20:80 and 50:50 CPTEG:CPH (C:C)) were synthesized using a melt polycondensation process as detailed by Kipper et al. and Torres et al.[10, 13] The molecular weight, and polymer purity were determined using ^{1}H nuclear magnetic resonance (NMR) spectroscopy (Varian VXR-300 MHz, Palo Alto, CA).

2.2 Fabrication and characterization of particles

Nanoparticles encapsulating ovalbumin (Ova) (Sigma-Aldrich, St. Louis, MO) (5.0% w/w loading) were fabricated using the anti-solvent nanoencapsulation method outlined in Ulery et al. [7] Briefly, the copolymer was dissolved in methylene chloride at a concentration of 20 mg/mL at 4˚C. Lyophilized Ova was added to the dissolved copolymer and the solution was sonicated for uniform dispersal of the protein within the copolymer. The Ova-loaded copolymer (Ova-loaded) or copolymer (blank) solution was poured into chilled pentane (-20°C) at a non-solvent to solvent ratio of 250:1, and this suspension was vacuum filtered to recover the nanoparticles. Shape and size of the resulting nanoparticles were characterized using scanning

electron microscopy (SEM) (JEOL 840 A, JEOL, Peabody, MA). The particle size distribution was obtained from SEM images using Image J version 1.46 image analysis software[14]. An average of 200 particles per image was analyzed.

2.3 Mice

Recipient female C57BL/6 Thy 1.1^+, recipient albino C57BL/6, OTI, and OTII mice were purchased from Jackson Laboratories (Bar Harbor, MN). C57BL/6 mice were obtained from Harlan Laboratories (Indianopolis, IN). T-lux mice were a kind gift from the lab of Casey Weaver at University of Alabama. T-lux breeding colony was established at Iowa State University. Heterozygous breeding between T-lux and OT mice was established to produce T-lux/OT offspring. Phenotyping of offspring for T cell receptor rearrangement (Vα2 Clone B20.1 Vβ5 Clone MR9-4 (eBioscience San Diego, CA)) and luciferase positive status was examined to establish which mice were the desired T cell donors (e.g., OT I^+:T-Lux^+). All mice were housed under specific pathogen-free conditions where all bedding, caging, water, and feed were sterilized prior to use. Animal procedures were conducted with the approval of the Iowa State University Institutional Animal Care and Use Committee.

2.4 Mouse treatments

2.4.1 Adoptive transfer of antigen-specific T cells

High frequency adoptive transfer of 3.0×10^6 donor OTI Thy 1.2^+ cells was performed by tail vein injection on day -1. For in vivo imaging studies, high frequency adoptive transfer of 5×10^5 OTI:T-lux cells were transferred into albino C57BL/6

recipients performed on day -1. For the low frequency adoptive transfer studies, 3 x 10^3 OTI Thy 1.2^+ 5-(and-6)-carboxyfluorescein diacetate, succinimidyl ester (CFSE) (Molecular Probes/Life Technologies, Grand Island, NY) labeled cells were adoptively transferred to each recipient mouse.

2.4.2 Immunization Regimens

On day 0 mice were immunized with 1.75 mg of soluble Ova and 5 mg of Ova-loaded (5 %) polyanhydride nanoparticles 20:80 CPH:SA, 20:80 CPTEG:CPH, 50:50 CPTEG:CPH, 2.0 mg of soluble ova (sOVA), or 2.0 mg of Ova adjuvanted 1:1 with Imject Alum (ThermoFisher, Rockford, IL).

2.4.3 Tumor challenge

EG7 ovalbumin expressing tumor cells (2.5 x 10^6) were subcutaneously administered in the left rear flank on day 35 post-immunization. Tumor measurements were recorded using a digital caliper and tumor volume was calculated using ellipsoid volume equation where volume = (4/3)* π * length * width * height. Per criteria outlined in consultation with the attending veterinarian, animals were removed from the study when tumor volume reached 1000 mm^3. Prosense® 750 was administered (2 nmol) via tail vein injection 7 days post-tumor challenge to visualize the inflammation associated with the tumor and to quantify changes in tumor size. ProSense® 750 is an activatable fluorescent reagent that is optically visible when the dye is cleaved by degradative enzymes, including cathepsin B, L, S, or plasminogen, that are common at sites of tumor growth [15]. After 24 h, *in vivo* images were captured while mice were kept under anesthesia using 2 % isoflurane

in 100 % O_2, at 2.5 L/min. Images were captured using 30 second exposures with an excitation filter of 730 nm and an emission filter of 790 nm.

2.4.4 In vivo imaging of T-lux cells

Five minutes prior to imaging for the presence of T-lux positive T cells, mice were administered D-luciferin (215 µg/g body weight) via intraperitoneal injection. In vivo images (Carestream Multispectral FX Rochester, NY) were captured while mice were anesthetized as described above. Bioluminescent images were captured using 10-minute exposures with high amounts of binning for increasing sensitivity. All image analyses were performed using Image J software version 1.46 [14]. Raw fluorescence images were inverted and background subtracted via a rolling ball radius of 150 pixels. The mean luminescence intensity (MLI) of the region of interest (ROI) of 0.39 mm x 0.32 mm were quantified via ImageJ and presented thereto. Composite images of luminescent channel (lookup table “16 colors” Figure 2 for bioluminescence, lookup table “blue ” Figure 4) for bioluminescence, fluorescence channel (lookup table “red ”), and white light image were created using Image J software.

2.5 Assaying for ex vivo T cell phenotype and activity

At multiple time points post-immunization, mice were euthanized and draining lymph nodes were excised and single cell suspensions were created using a glass homogenizer. Half of the excised spleens were placed in 10 % buffered formalin. The other half of spleen was homogenized to prepare single cell suspensions. Red blood cells were lysed using ACK lysis buffer. Cell numbers and phenotype were

quantified using flow cytometry (BD FACS Aria III). For low frequency adoptive transfer experiments, positive selection for donor T cells was accomplished using biotinylated anti-CD90.2 (Thy 1.2 Clone 53-2.1) (eBioscience, San Diego, CA) and streptavidin magnetic microbeads (Miltenyi Biotech, Auburn, CA). Positive magnetic bead selection was performed via methods outlined by Moon et al [16] (AutoMACS Pro Milteny Biotech). Cell suspensions were blocked for non-specific antibody binding using 0.1 mg/mL Rat IgG (Sigma Aldrich, St. Louis, MO) and 10 µg/mL mouse anti-CD16/32 (eBioscience, San Diego, CA). For T cell assays, fluorescently conjugated antibodies specific for CD4 (PE-Cy7, Clone GK1.5, eBioscience), CD8β (APC, Clone eBioH35-17.2, eBioscience), CD62L (PE, Clone 2G8, eBioscience), Thy 1.2 (APC-eFluor 780, Clone 53-2.1, eBioscience), Thy 1.1 (PerCP-Cy 5.5, Clone HIS51, eBioscience), IL-2 (FITC, Clone JES6-5H4, eBioscience) CD19 (PerCP-Cy5.5, clone eBio1D3, eBioscience), CD11c (PerCP-Cy5.5, clone N418, eBioscience), CD11b (PerCP-Cy5.5, clone M1/70, eBioscience), F4/80 (PerCP-Cy5.5, BM8, eBioscience), IL-7R (eFluor 450, Clone 4B12, eBioscience), CD197 (eFluor 450, Clone 4B12, eBioscience), KLRG1 (PE-Texas Red, Clone 145-2C11, eBioscience), or CD44 (v500, clone IM7, BD Franklin Lakes, NJ) were diluted in FACS buffer and used to label the cells in order to quantify donor antigen-specific cell populations. Abs were used in appropriate combination of fluorochromes.

2.6 Analysis of cytokines in serum and culture supernatants

Serum or cell culture supernatant samples were analyzed using a 32-plex chemokine and cytokine antibody array (Millipore, Billerica, MA) measuring the

following analytes: Eotaxin, G-CSF, GM-CSF, M-CSF, IFN-γ, IL-10, IL-12p40, IL-12p70, IL-13, IL-15, IL-17, IL-1α, IL-1β, IL-2, IL-3, IL-4, IL-5, IL-6, IL-7, IL-9, IP-10, KC, MCP-1, MIG, MIP-1α, MIP-1β, MIP-2, LIF, LIX, VEGF, RANTES, and TNF-α. Assays were performed according to the manufacturer's recommendations; data were acquired and analyzed using a Bio-Plex 200 (Bio Rad, Hercules, CA). Type I interferon was assayed using Verikine Mouse Interferon alpha ELISA kit (PBL, Piscataway, NJ) and IL-33 was assayed using IL-33 ELISA Ready-Set-Go (eBioscience).

2.7 Bone marrow macrophage gene changes and cytokine release

Bone marrow macrophages were derived via methods outlined in Weischenfeldt et al. [17]. Briefly, bone marrow was isolated from long bones of donor C57BL/6 mice and plated in 125 x 25 mm plates tissue culture plates in complete bone marrow macrophage medium containing dulbelcco's modified eagle medium (DMEM) with L-glutamine supplemented with 40 % fetal bovine serum (FBS) and L929 cell conditioned medium from L929 cells serving as a source of GM-CSF. Cells were incubated for 6 days, and characterized using flow cytometry for the expression of macrophage markers CD11b clone: M1/70 (eBioscience, San Diego, CA) and F4/80 clone: BM8 (eBioscience, San Diego, CA) After confirming the macrophage phenotype of the cells, the cells were harvested and inoculated into the wells of a 24 well culture plates at a density of 1.0×10^6 cells/mL in complete tissue culture medium consisting of DMEM with L-glutamine supplemented with 10 % FBS. Nanoparticles were suspended in complete tissue culture medium at a concentration of 0.25 mg/mL translating to 250 μg per well for each treatment, sonicated briefly,

and added to the macrophages. Culture supernatant fluid was collected 8 hours after particle addition, aliquoted, and frozen for cytokine analysis.

Cells were collected and total RNA isolated using a RNeasy Mini Kit (SABiosciences/Qiagen, Valencia, CA) according to manufacturers instructions. RNA quality and concentration was analyzed via Agilent 2100 Bioanalyzer (Agilent, Santa Clara, CA) and reported RNA integrity numbers (RIN) were above 7.0. RT2 cDNA first strand kit (SABiosciences/Qiagen, Valencia, CA) was used for cDNA synthesis according to manufacturer's instructions. Converted cDNA was added to RT2 master mix and added to NF-κB signaling pathway PCR array plate (SABiosciences/Qiagen, Valencia, CA) and RT-PCR was performed using Applied Biosystems 5700 thermocycler.

2.8 Statistical analysis

Differences in mean responses among treatment groups were tested with either unpaired T test with Welch's correction or one-way ANOVA F-test followed by a post-hoc Tukey's t-test using Graph Pad Prism version 5. Statistical tests with p values ≤ 0.05 were regarded as significant. Data was log transformed when variances were not equal.

3. Results

Induction of antigen specific cell mediated responses to cognate antigen happens early after antigen induction. An initial expansion of antigen specific T cells occurs and these cells either leave the secondary lymphoid tissue to respond to the antigen or are programmed to reside in the lymphoid tissue to respond to antigen

later (memory). High frequency adoptive transfer of Ova-specific T cells (OT) was utilized to enhance the detection of antigen-specific T cells after immunization. Previous studies that have evaluated the use of the polyanhydride platform to immunize mice have shown that optimal immune responses are induced using a combination of soluble protein administered with protein encapsulated into the polyanhydride nanoparticles [9]. Mice were adoptively transferred with 3 x 10^6 OTI ($CD8^+$) T cells prior to immunization. A polyanhydride nanoparticle vaccine consisting of 1.75 mg of soluble Ova and 0.25 mg of Ova encapsulated in 50:50 CPTEG:CPH nanoparticles showed differences in magnitude expansion and contraction of Ova-specific T cells compared to soluble OVA alone (Figure 1A). For the mice immunized using the nanoparticle regimen, there was a significantly greater number of Ova-specific $CD8^+$ T cells observed in the draining lymph nodes at day 3 post-immunization that was maintained through day 7 (Figure 1B). At day 14 post-immunization, a small proportion of the Ova-specific T cells was still detectable although there was no statistically significant differences.

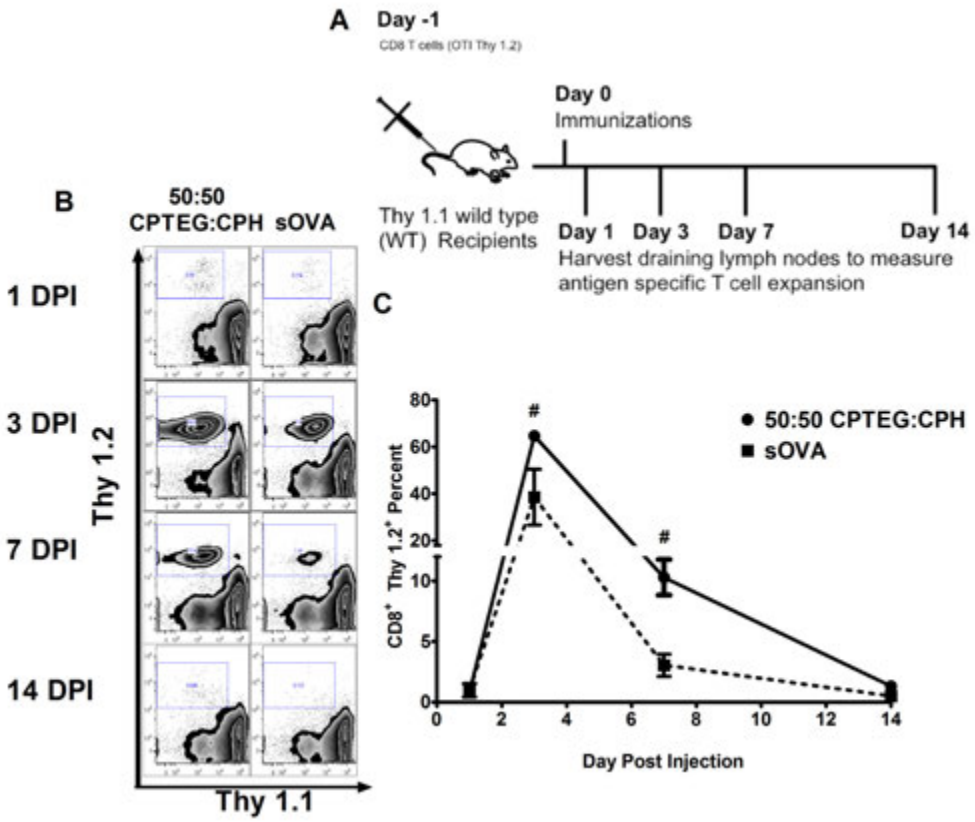

Figure 1. Encapsulation of antigen in 50:50 CPTEG:CPH nanoparticles expands greater numbers of antigen specific T cells and maintain higher numbers of T cells at later time points. The adoptive transfer and immunization schedule showing the time points of tissues obtained (A). Representative flow histograms of gated $CD8^+$ T cells at the four time points (B). X-axis represents the recipient congenic marker Thy 1.1 and the y-axis represents the donor Thy 1.2 congenic marker. Quantification of the percentage of $CD8^+$ Thy 1.2^+ (donor OTI cells) obtained at the four time-points. N = 4-5 per group and # indicates a significant difference at $p < 0.05$.

Serum samples obtained at 3 days post-immunization DPI were evaluated to determine the monocyte chemokine expression patterns in the nanoparticle immunization group as compared to the mice immunized with Ova alone. As can be seen in Table 1, there was a statistically significant ($P \leq 0.05$) increase in the serum

levels of IP-10, MCP-1 and IFN-γ in the mice immunized with the nanoparticle formulation.

Table 1. Nanoparticle immunization increases monocyte chemokine activity.

Group	IFN-γ (pg/mL)	IP-10	MCP-1
50:50 CPTEG:CPH	39.28[a]	961.36[a]	696.13[a]
sOVA	18.23[ab]	171.94[b]	104.18[ab]
PBS	3.77[b]	86.88[b]	203.62[b]

Table 1.
Serum samples from mice immunized with 50:50 CPTEG:CPH, soluble Ova (sOVA), or PBS euthanized at 3 days post-immunization were evaluated for monocyte chemokines via 22-plex multiplex assay. IFN-γ, interferon gamma inducible protein (IP-10), and monocyte chemotactic protein (MCP-1) show statistical differences. Numbers expressed are mean concentrations of the analyte in pg/mL. N = 4-5 per group and superscript letters indicate significant difference at $p < 0.05$ using one-way ANOVA with Tukey's post test.

The activation phenotype of the expanded Ova-specific $CD8^+$ T cell populations was examined by measuring the expression levels of cell surface markers CD44 and CD62L, as well as, IL-2 production after in vitro antigen stimulation. The phenotype of the T cell population induced following immunization with the nanoparticle formulation was characterized by the appearance of short-lived effector memory T cells ($CD44^{high}$ $CD62L^{low}$) at 3 DPI (data not shown). At the 7 DPI,

a shift in the percentage of effector memory ($CD44^{high}$ $CD62L^{low}$) and central memory ($CD44^{high}$ $CD62L^{high}$) was observed in the nanoparticle immunized groups (Figure 2A). When quantified the subtle shift in surface markers was not statistically significant (Figure 2B). T cells from the nanoparticle immunized mice that were stimulated in vitro with Ova produced a greater amount of IL-2 production than mice immunized with Ova alone indicating induction of a central memory T cell population in the draining lymph node (Figure 2C-D). PBS immunized mice showed little IL-2 production (data not shown).

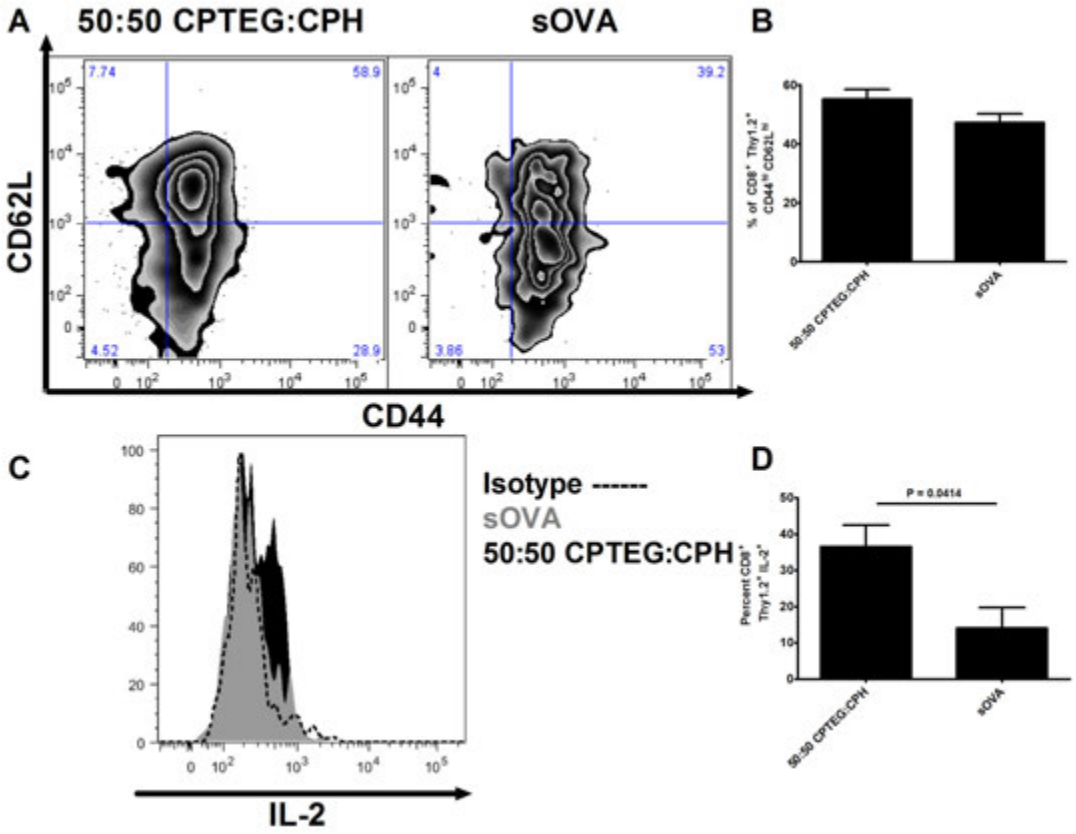

Figure 2. A greater number of antigen-specific T cells from nanoparticle immunized mice demonstrate a central memory phenotype. (A) Representative contour plots showing cell surface marker analysis of donor T cells ($CD8^+$ Thy 1.2^+) for expression of CD44 and CD62L at 7 days post-immunization. (B) Quantified analysis of the percentage of donor T cells (Thy 1.2^+) expressing a central memory phenotype ($CD8^+$, $CD44^{high}$, and $CD62L^{high}$). (C) Representative histograms of depicting the induction of $CD8^+$ Thy 1.2^+ IL-2^+ cells following immunization. Dotted histogram indicates isotype control, gray histogram indicates Th 1.2^+ T cells from sOva immunized mice, and black histogram indicates the IL-2 producing cells present in mice immunized with the Ova-loaded 50:50 CPTEG:CPH. (D) Percentage of $CD8^+$Thy 1.2^+ cells that were positive for IL-2. N = 4 to 5 mice per treatment group. P value obtained via unpaired T test with Welch's correction.

In order to efficiently ascertain the capability of multiple polyanhydride

nanoparticle chemistries to induce $CD8^+$ T cells expressing a memory phenotype, we adoptively transferred OTI T cells that also expressed T cell specific luciferase to facilitate visualization of Ova-specific T cells in vivo. Mice were immunized with one of three separate Ova-loaded polyanhydride nanoparticle formulations. The formulations were prepared, namely, 20:80 CPH:SA, 20:80 CPTEG:CPH, and 50:50 CPTEG:CPH (Figure 3A). Separate groups of mice were also immunized with Ova adjuvanted with Alum or soluble Ova (sOVA) alone to examine differences in T cell expansion (Figure 3). Antigen release profiles show a release of Ova from the 20:80 CPH:SA, 20:80 CPTEG:CPH, and 50:50 CPTEG:CPH nanoparticles (Figure 3B). After immunization, cohorts from each treatment group were imaged at 1, 3, 5, 7, and 10 days. Greater numbers of $CD8^+$ T cell were observed at the site of administration and draining lymph nodes for mice immunized with the Ova-loaded 20:80 and 50:50 CPTEG:CPH nanoparticle formulations (Figure 3C-D). 20:80 CPH:SA, Alum and sOVA groups also demonstrate expansion of the antigen specific T cells although in less magnitude attributable to the high dose of antigen used in these studies (Figure 3D).

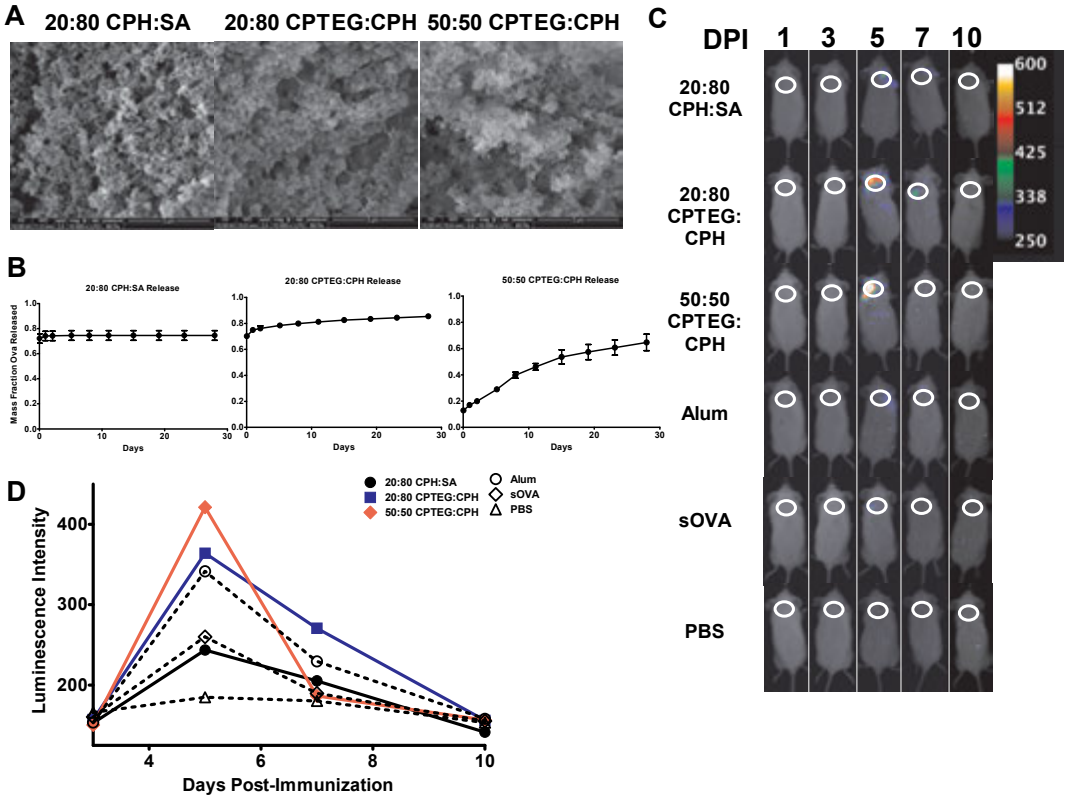

Figure 3. CPTEG:CPH polyanhydride nanoparticle immunized groups elicit CD8$^+$ T cell expansion at the immunization site. (A) Scanning electron microscopy images of Ova-loaded nanoparticles of the three chemistries (20:80 CPH:SA, 20:80 CPTEG:CPH, and 50:50 CPTEG:CPH) evaluated. (B) In vitro release kinetics of Ova from three separate formulations of Ova-loaded nanoparticles over time. (C) Representative images of albino C57BL/6 mice receiving transfer of OTI$^+$ T-lux$^+$ cells from immunized groups (20:80 CPH:SA, 20:80 CPTEG:CPH, 50:50 CPTEG:CPH, Alum, MPLA, sOVA, or PBS) at 1, 3, 5, 7, or 10 days post-immunization (DPI) examining bioluminescent CD8 T cell activity. (D) Regions of interest of equal area were drawn at immunization site to measure intensity of T cell luminescence and quantified over time.

To test if polyanhydride nanoparticle immunizations were able to elicit cytotoxic $CD8^+$ T cells capable of responding to challenge, albino C57BL/6 mice receiving adoptive transfer of OTI+ T-lux+ cells and immunized with the regimens outlined previously were injected with 2.5 x 10^6 Ova expressing EG-7 lymphoma cells into the right rear flank at 35 DPI. Additionally, at seven days post-tumor challenge, Prosense® 750 was administered to cohorts of tumor challenged mice to examine fluorescence intensity differences that will indicate differences in tumor size and progression. Mice immunized with either Ova-loaded CPTEG:CPH nanoparticle formulation effectively inhibited tumor growth resulting from an enhanced Ova-specific T cell response as evidenced by the decreased fluorescence intensity as well as increased luminescence signal at the tumor challenge site, respectively (Figure 4A). Mice immunized with Alum, Ova-loaded 20:80 CPH:SA, or sOVA alone show little luminescence activity at the challenge site. At eight days post-tumor implantation, analysis of peripheral blood samples demonstrated that there was a statistically significant increases in V-$\alpha 2^+$ V-$\beta 5^+ CD8^+$ $CD44^{high}$ T cells (i.e., Ova specific) in all mice immunized with the polyanhydride nanoparticle formulations when compared to cells recovered from mice immunized with Ova adjuvanted with Alum, Ova alone, and PBS (Figure 4B). Quantitative analysis of the T cell response (i.e, luminescence intensity) at the site of tumor implantation indicated that the more robust $CD8^+$ T cell responses correlated with those mice that demonstrated the greatest primary T cell expansion after immunization (Figure 4C). These cells were also examined for increases in the surface marker CD107a and intracellular

Granzyme B, markers of cytotoxic activity, but no statistical differences between polyanhydrides and control immunizations were reported (data not shown).

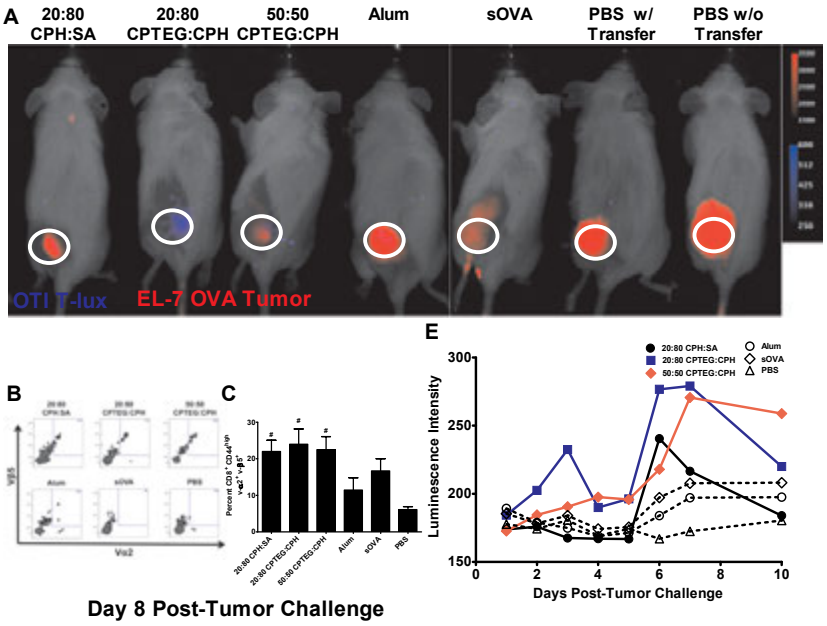

Figure 4. Polyanhydride nanoparticle immunized groups demonstrated cellular recall responses capable of controlling tumor growth with significant increases in peripheral CTL's at 8 days post-tumor challenge. (A) Representative images of albino C57BL/6 mice receiving transfer of OTI^{+} T-lux^{+} cells from immunized groups (20:80 CPH:SA, 20:80 CPTEG:CPH, 50:50 CPTEG:CPH, Alum, MPLA, sOVA, or PBS) challenged with EL-7 tumor cells visualizing OT-I T-lux cells (Blue) and tumor size (ProSense® 750, Red) at the site of tumor implantation. (B) Representative FACS histograms of peripheral blood samples were obtained at 8 days post-tumor challenge and the percentage of total CD8^{+} T cells that were V-α2^{+} V-β5^{+} CD8ß$^{+}$ CD44^{high} T cells were quantified. (C) Numbers of V-α2^{+} V-β5^{+} CD8ß$^{+}$ CD44^{high} T cells quantified via flow cytometry (n = 12 per group). (D) Regions of interest of equal area were drawn at the tumor challenge site and luminescent intensity of T cell luminescence was quantified post-tumor challenge (n = 4). Mean tumor volume measurements of each immunized group recorded over time post-tumor challenge (n = 12). Survival curve of immunized groups post-tumor challenge (n = 12) (E). # indicates statistical difference from PBS at a p value < 0.05 value obtained via one-way ANOVA with Tukey's post-test. Data presented from one experiment.

All immunization groups were able to delay tumor progression throughout the study. The passive transfer of a large number of naïve Ova-specific T cells was able to provide some protective benefit in regard to tumor progression as evidenced by the slower tumor progression compared to naïve animals receiving no adoptive transfer of OTI T-lux T cells (Figure 5 A-B).

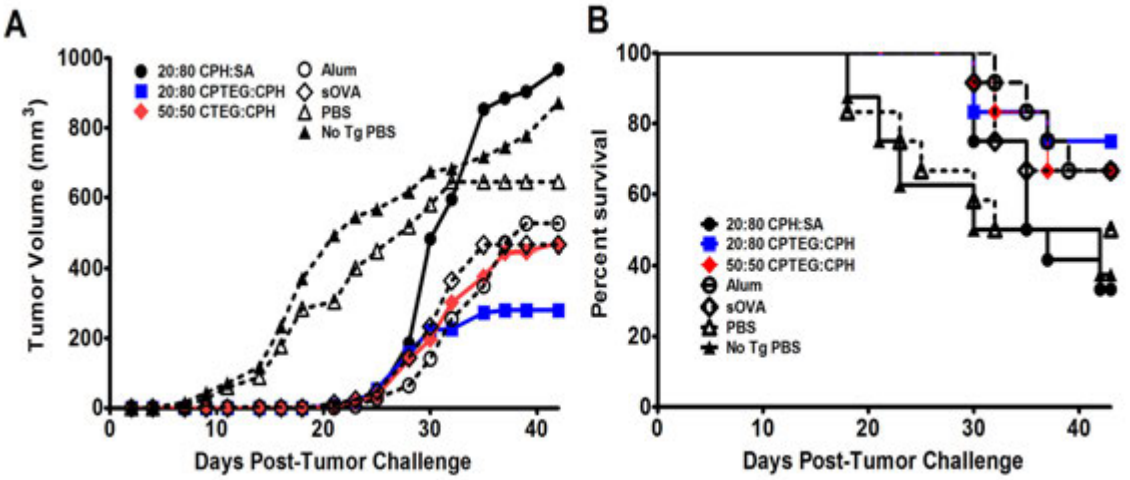

Figure 5. 20:80 CPTEG:CPH immunized mice slowed tumor progression and increased survival (A) Mean tumor volume measurements of each immunized group recorded over time post-tumor challenge (n = 12). (B) Survival curve of immunized groups post-tumor challenge (n = 12). Data presented from one experiment.

High frequency adoptive transfer of OTI T cells allowed us to assess the capability of various NP formulations to enhance the activation of Ova-specific $CD8^+$ T cells during the early stages of an immune response. In order to more closely model a naturally occuring immune response, a low frequency adoptive transfer (3×10^3 OTI Thy 1.2^+ cells) model was utilized to examine the expansion and contraction phases of $CD8^+$ T cells early after immunization and the induction of effector versus memory phenotypes being elicited. 20:80 CPH:SA or 20:80 CPTEG:CPH

polyanhydride nanoparticles significantly ($p \leq 0.05$) increased the numbers of Ova-specific $CD8^+$ T cells in the draining lymph nodes at 7 DPI compared to the other treatment groups (Figure 5A-B). The donor OTI T cells populations were further examined for phenotypic indications of memory precursor effector cells ($CD44^{high}$ $CD62L^{high}$ and $KLRG1^{low}$ $CD127^{low}$) and for central memory phenotypes ($CD44^{high}$ $CD62L^{high}$ $CCR7^+$). CCR7 is a lymph node homing integrin that is up-regulated for retention in the secondary lymph tissue [18, 19]. The numbers of precursor central memory $CD44^{high}$ $CD62L^{high}$ T cells is significantly greater ($p \leq 0.05$) in the 20:80 CPH:SA and 20:80 CPTEG:CPH immunization groups than Alum and sOVA controls (Figure 6C-D). These groups show greater numbers of memory precursor effector cells (MPEC) as defined by expression of $KLRG1^{low}$ $CD127^{low}$ surface marker expression (Figure 6E-F) and evidence of establishing Ova-specific, central memory T cells defined by expression of $CD44^{high}$ $CD62L^{high}$ $CCR7^+$ although neither were statistically significant.

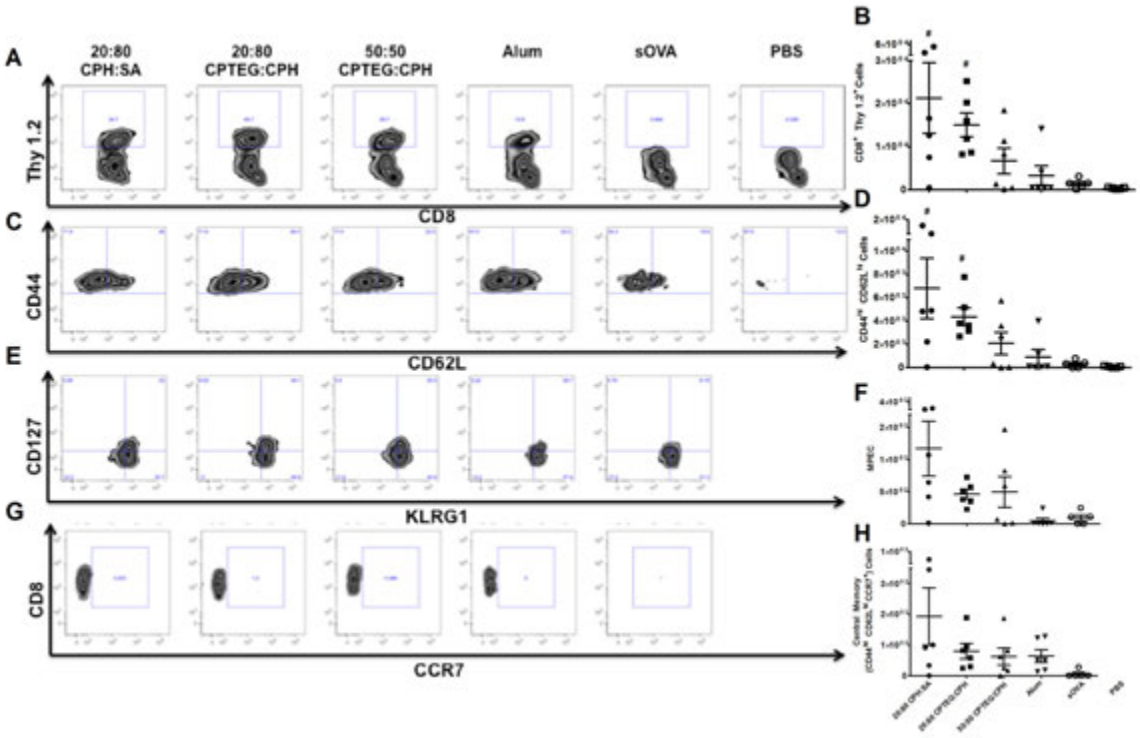

Figure 6. Polyanhydride nanoparticle immunization expands antigen specific T cells early after immunization and promotes central memory development. (A) Representative flow cytometric histograms of donor OTI Thy 1.2^+ (y-axis) $CD8^+$ (x-axis) T cell expansion from draining lymph nodes seven days post-immunization (DPI). (B) Total $CD8^+$ Thy 1.2^+ T cells recovered from the axial and brachial LN at seven DPI . (C) Representative flow cytometric histograms of OTI Thy 1.2^+ $CD8^+$ T cells analyzed for expression of CD44 (y-axis) and CD62L (x-axis). (D) Total numbers of $CD8^+$ Thy 1.2^+ $CD44^{high}$ $CD62L^{high}$ T cells recovered from the axial and brachial LN at seven DPI. (E) Representative flow cytometric histograms of gated OTI Thy 1.2^+ $CD8^+$ T cells for surface markers CD127 (y-axis) and KLRG1 (x-axis). (F) Total numbers of $CD8^+$ Thy 1.2^+ $CD127^{low}$ $KLRG1^{low}$ (MPEC) T cells recovered from the axial and brachial LN. Representative flow cytometric histograms of gated OTI Thy 1.2^+ $CD8^+$ $CD44^{high}$ $CD62L^{high}$ T cells for surface marker CCR7 (x-axis) (G). Total numbers of Thy 1.2^+ $CD8^+$ $CD44^{high}$ $CD62L^{high}$ $CCR7^+$ T cells quantified by gating percentage multiplied by total cell numbers obtained from flow cytometric counting beads (H). # indicates statistical difference from PBS at a p value < 0.05 value obtained via one-way ANOVA with Tukey's post-test. Data is from a single experiment.

The 20:80 CPTEG:CPH vaccine regimen provided the most consistent T cell

expansion and induction of precursor memory cell formation. This particular chemistry is the slowest eroding polyanhydride polymer providing the longest bioavailability in vivo (Chapter 4). The in vitro release kinetics of Ova from 20:80 CPH:SA and 20:80 CPTEG:CPH were largely similar while Ova was released from 50:50 CPTEG:CPH NPs much more slowly in vitro (Figure 3B). Thus, the burst release of Ova from of the 20:80 CPH:SA and 20:80 CPTEG:CPH may have contributed to the expanded T cell responses.

The Ova release kinetics from the particles may contribute to the enhanced T cell responses however since the vaccine was administered with such a large dose of bolus antigen the more likely contributing factor is the immunomodulatory signaling effects of the polyanhydride nanoparticles on APCs. The inflammatory cytokine milieu presented by APC's also contributes to T cell expansion and phenotype polarization [20]. The evidence of increases in monocyte chemotactic cytokines as well as the dominant macrophage infiltrate at the administration site as seen in histopathology (Chapter 4) led us to examine the inflammatory profile of macrophages administered polyanhydride nanoparticles.

The three polyanhydride chemistries were administered to bone-marrow derived macrophages and gene changes of those macrophages were analyzed via an array examining NF-κB signaling pathways (Table 2). As hypothesized, the CPTEG:CPH containing chemistries led to the largest genetic up-regulation of *tnf* and increases in expression of TNF associated receptors and signaling genes (*cd27, tnfrsf1a, tnfrsf1b, tnfsf10,* and *stat1*). The CPTEG:CPH chemistries also up-regulated expression of pattern recognition receptors (*tlr1, tlr2, tlr3, tlr4, tlr6, tlr9* and

nod1) and downstream signaling with the greatest increases in *tlr3* and *nod1*. Large up-regulation of the co-stimulatory molecule gene *cd40* also occurred which is consistent with previous work examining dendritic cell and alveolar macrophage activation with the polyanhydride particle platform [8, 21, 22].

Table 2. Nanoparticle immunization increases monocyte chemokine activity.

Gene	Descriptor (fold regulation above or below No Stimulation)	20:80 CPH:SA	20:80 CPTEG:CPH	50:50 CPTEG:CPH
Agt	Angiotensinogen (serpin peptidase inhibitor, clade A, member 8)	4.05	3.20	1.18
Akt1	Thymoma viral proto-oncogene 1	1.07	16	9.38
Atf1	Activating transcription factor 1	-6.41	-1.79	-1.8
Atf2	Activating transcription factor 2	-5.54	1.36	-1.21
Bcl10	B-cell leukemia/lymphoma 10	-2.08	10.20	8.11
Bcl2a1a	B-cell leukemia/lymphoma 2 related protein A1a	-1.26	6.02	5.39
Bcl2l1	Bcl2-like 1	-3.18	4.23	3.66
Bcl3	B-cell leukemia/lymphoma 3	3.12	177.29	134.36
Birc3	Baculoviral IAP repeat-containing 3	-2.10	5.54	7.46
Card10	Caspase recruitment domain family, member 10	4.96	2.38	1.16
Card11	Caspase recruitment domain family, member 11	3.14	17.88	19.70
Casp1	Caspase 1	1.60	1.27	5.03
Casp8	Caspase 8	-78.79	-10.27	-5.54
Ccl2	Chemokine (C-C motif) ligand 2 (MCP-1)	2.20	2.93	4.56
Ccl5	Chemokine (C-C motif) ligand 5 (RANTES)	51.98	372.22	699.41
Cd27	CD27 antigen	-1.29	7.26	8.57
Cd40	CD40 antigen	39.67	474.41	729.11
Cflar	CASP8 and FADD-like apoptosis regulator	1.16	14.12	21.41
Chuk	Conserved helix-loop-helix ubiquitous kinase	-6.32	-2.19	-2.60
Crebbp	CREB binding protein	-6.63	1.83	1.72
Csf1	Colony stimulating factor 1 (macrophage) M-CSF	1.37	16.34	11.71
Csf2	Colony stimulating factor 2 (granulocyte-macrophage)	22.63	491.14	340.14
Csf3	Colony stimulating factor 3 (granulocyte) G-CSF	5.46	54.19	385.34
Egfr	Epidermal growth factor receptor	1.66	11.08	6.77
Egr1	Early growth response 1	-4.35	1.77	1.41
Eif2ak2	Eukaryotic translation initiation factor 2-alpha kinase 2	1.59	11.47	12.21
Elk1	ELK1, member of ETS oncogene family	-2.06	7.21	5.28
F2r	Coagulation factor II (thrombin) receptor	1.99	11.31	10.85
Fadd	Fas (TNFRSF6)-associated via death domain	-1.03	7.46	5.24
Fasl	Fas ligand (TNF superfamily, member 6)	2.27	3.05	6.06
Fos	FBJ osteosarcoma oncogene	-6.68	3.84	2.04
Hmox1	Heme oxygenase (decycling) 1	-2.79	6.23	5.17
Icam1	Intercellular adhesion molecule 1	1.89	61.39	37.53
Ifng	Interferon gamma	8	37.27	140.07

Table 2 (Continued)

Ikbkb	Inhibitor of kappaB kinase beta	1.07	14.32	11
Ikbke	Inhibitor of kappaB kinase epsilon	-1.13	13.18	13.45
Ikbkg	Inhibitor of kappaB kinase gamma	-3.03	-1.66	-1.14
Il10	Interleukin 10	2.41	17.15	229.13
Il1a	Interleukin 1 alpha	-1379.56	-202.25	-56.89
Il1b	Interleukin 1 beta	3.18	35.75	119.43
Il1r1	Interleukin 1 receptor, type I	1.56	6.15	4.50
Irak1	Interleukin-1 receptor-associated kinase 1	-1.89	6.11	4.44
Irak2	Interleukin-1 receptor-associated kinase 2	1.28	27.10	24.76
Irf1	Interferon regulatory factor 1	2.33	37.27	32.22
Jun	Jun oncogene	-1.92	7.01	4.69
Lta	Lymphotoxin A	9.51	73.52	81.01
Ltbr	Lymphotoxin B receptor	1.16	11	5.66
Map3k1	Mitogen-activated protein kinase kinase kinase 1	-2.57	3.29	1.59
Mapk3	Mitogen-activated protein kinase 3	-1.80	2.48	2.28
Myd88	Myeloid differentiation primary response gene 88	9.85	205.07	110.66
Nfkb1	Nuclear factor of kappa light polypeptide gene enhancer in B-cells 1, p105	-1.03	9.92	10.56
Nfkb2	Nuclear factor of kappa light polypeptide gene enhancer in B-cells 2, p49/p100	1.44	14.42	19.16
Nfkbia	Nuclear factor of kappa light polypeptide gene enhancer in B-cells inhibitor, alpha	1.16	12.30	23.10
Nod1	Nucleotide-binding oligomerization domain containing 1	4.92	79.89	70.03
Raf1	V-raf-leukemia viral oncogene 1	-1.25	8.46	7.62
Rel	Reticuloendotheliosis oncogene	-2.31	3.73	3.86
Rela	V-rel reticuloendotheliosis viral oncogene homolog A (avian)	8.82	127.16	81.57
Relb	Avian reticuloendotheliosis viral (v-rel) oncogene related B	14.83	179.77	111.43
Ripk1	Receptor (TNFRSF)-interacting serine-threonine kinase 1	-2.77	8.34	10.93
Ripk2	Receptor (TNFRSF)-interacting serine-threonine kinase 2	-2.64	1.19	1.95
Slc20a1	Solute carrier family 20, member 1	-1.62	3.86	2.93
Smad3	MAD homolog 3 (Drosophila)	1.60	14.62	7.46
Stat1	Signal transducer and activator of transcription 1	2.95	36	45.25
Tbk1	TANK-binding kinase 1	-1.62	6.15	7.52
Tlr1	Toll-like receptor 1	-2.68	5.13	4.66
Tlr2	Toll-like receptor 2	-2.43	10.78	8.40
Tlr3	Toll-like receptor 3	18.64	156.50	288.02
Tlr4	Toll-like receptor 4	-5.66	3.34	2.20
Tlr6	Toll-like receptor 6	-1.15	7.46	6.36
Tlr9	Toll-like receptor 9	-1.16	10.63	9.19
Tnf	Tumor necrosis factor	13.55	352.14	433.53
Tnfaip3	Tumor necrosis factor, alpha-induced protein 3	-227.54	-31.56	-6.82
Tnfrsf10b	Tumor necrosis factor receptor superfamily, member 10b	-1.42	5.28	1.30
Tnfrsf1a	Tumor necrosis factor receptor superfamily, member 1a	5.86	65.34	27.67
Tnfrsf1b	Tumor necrosis factor receptor superfamily, member 1b	2.57	50.91	42.81
Tnfsf10	Tumor necrosis factor (ligand) superfamily, member 10	2.41	32.22	28.05
Tnfsf14	Tumor necrosis factor (ligand) superfamily, member 14	-3.71	1.56	1.40
Tollip	Toll interacting protein	-1.74	4.50	4
Tradd	TNFRSF1A-associated via death domain	-2.85	-1.35	-1.41
Traf2	Tnf receptor-associated factor 2	1.60	11.71	10.06
Traf3	Tnf receptor-associated factor 3	-1.30	8.46	4.29

Table 2 (Continued)

Traf5	Tnf receptor-associated factor 5	3.25	21.86	19.56
Traf6	Tnf receptor-associated factor 6	2.17	8.63	9.13
Zap70	Zeta-chain (TCR) associated protein kinase	3.07	13.36	12.91

Table 2. CPTEG:CPH nanoparticles cause up-regulation of mRNA leading to greater NF-κB transcription**.** RNA changes from bone marrow derived macrophages cultured in the presence of 0.25 mg of 20:80 CPH:SA, 20:80 CPTEG:CPH, or 50:50 CPTEG:CPH nanoparticles as compared to no stimulation controls. Total RNA was harvested 8 hours after addition of treatments to the macrophages. Numbers indicated fold regulation above (in red) or below (in blue) the non-stimulated controls cells. Array data is from a single experiment.

In addition to the genetic changes we tested if the treated macrophages resulted in increased production of inflammatory cytokines associated with these genes. We examined the culture supernatants of the treated bone marrow-derived macrophages against a panel of inflammatory cytokines and chemokines. Coinciding with the gene expression data presented in Table 2, increases in cytokines TNF-α, IFN-γ, IL-1β, IL-10, and chemokines MCP-1, G-CSF, GM-CSF, M-CSF, and RANTES (Figure 6 A-J) were observed in the culture supernatant validating the gene changes from the PCR array. Because of the *MyD88* and *stat1* upregulation we also examined if type I interferons and IL-33 (an IL-1 cytokine family member) were also increased. No type I interferon or IL-33 (an IL-1 cytokine family member) secretion was identified by ELISA (data not shown).

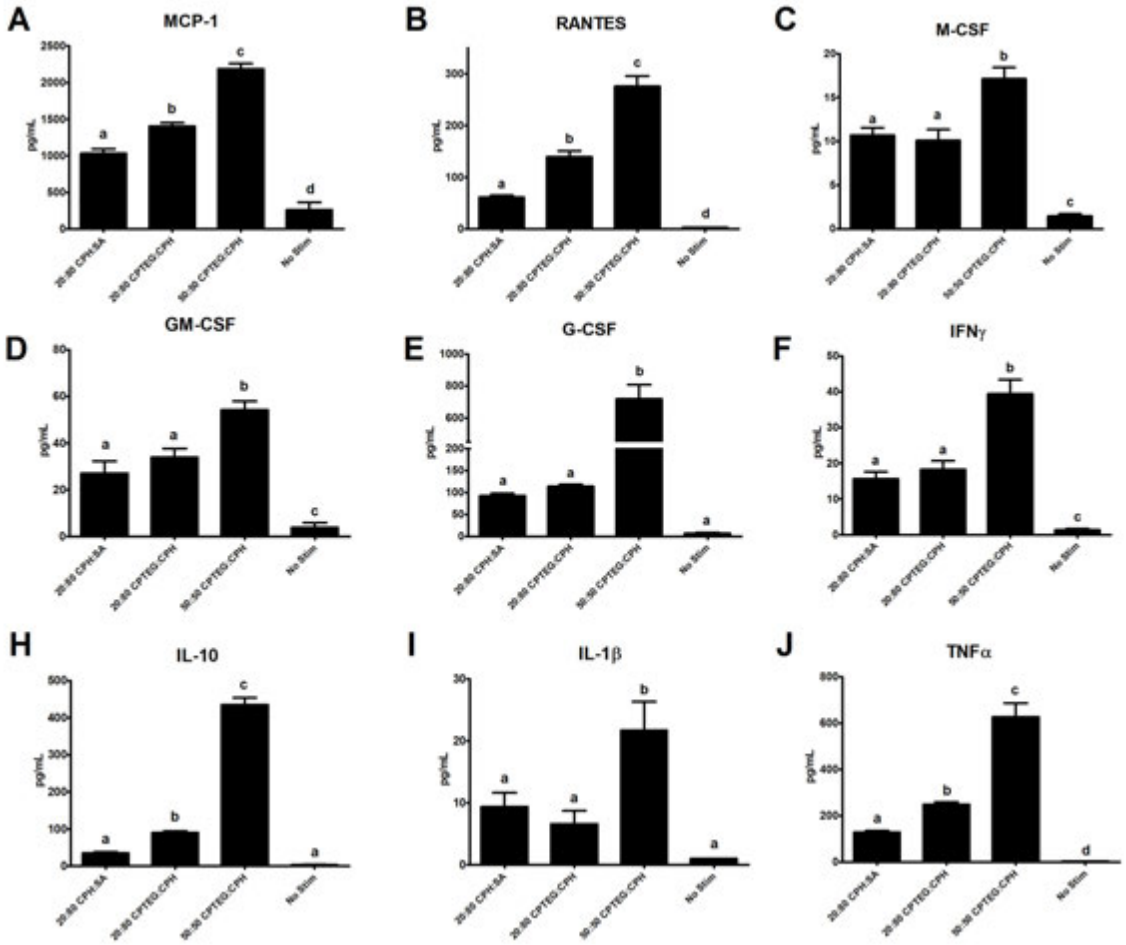

Figure 6. CPTEG:CPH nanoparticles cause increased secretion of inflammatory cytokines and chemokines coinciding with gene profile changes from bone-marrow derived macrophages. Culture supernatant fluid was assayed for the secretion of cytokines and chemokines from bone-marrow derived macrophages stimulated with 0.25 mg of 20:80 CPH:SA, 20:80 CPTEG:CPH, or 50:50 CPTEG:CPH or MPLA (0.5 μg) and compared to supernatant fluid collected from cultures of non stimulated macrophages. MCP-1 (A), RANTES (B), M-CSF (C), GM-CSF (D), G-CSF (E), IFNγ (F), IL-10 (G), IL-1β (H) and TNFα (J) were quantified using multiplex immunoassay procedures. N = 12 for each treatment group. Different letters indicate statistical difference at a p value < 0.05 value obtained via one-way ANOVA with Tukey's post-test.

4. Discussion:

Generation of cell mediated immunity in vaccination remains a major obstacle in vaccine design especially considering the more stringent purity and safety requirements outlined by governmental licensing institutions. The ability to expand cytotoxic T cells and generate memory T cells using immunization is largely biased towards replicating viral vectors or DNA vaccines expressing targeted antigens which provide both the innate viral stimulatory mechanisms as well as extended presence of antigen as would be provided by a replicating viral vector [23, 24]. Targeting the small number of antigen-specific, naïve T cells that would be available for a given T cell epitope, expanding that population of T cells and creating stable central memory populations capable of responding to a subsequent pathogen with subunit immunizations appears to rely on immunizations capable of recreating the aspects of a pathogenic infection and providing shifted or prolonged antigen kinetics [25-28]. These principles of pathogen mimicry by imitating size and particulate structure of pathogens as well as attempting to continuously provide antigen similarly to a replicating pathogen provides the basic principle advantages of the polyanhydride nanoparticle vaccine delivery platform. Encapsulation of antigen into 50:50 CPTEG:CPH nanoparticles provides an enhanced expansion of Ova-specific $CD8^+$ T cells that peaked at 3 DPI in the draining lymph node and that T cell population shows a delayed contraction compared to that observed in mice immunized with soluble Ova alone specific T cell precursor frequency is high (Figure 1). This enhanced expansion of antigen-specific $CD8^+$ T cells could be attributable to the presumed influx of antigen presenting cell precursor monocytes due to increased

monocyte chemokines being elicited by the polyanhydride nanoparticle vaccine (Table 1 and Chapter 4). We employed a similar combination of soluble Ova with encapsulated Ova in this study with the hypothesis being that the soluble protein will rapidly drain to the lymph nodes proximal to the injection site and initiate the immune response [29, 30]. The encapsulated protein in polyanhydride particles is then trafficked to the lymph nodes at later time points (1-3 days) and continues the maintenance of the antigen specific immune response started by the soluble protein [31].

Different nanoparticle chemistries can persist from 2-12 weeks in vivo depending on copolymer chemistry (Chapter 4). Nanoparticle immunization theoretically provides extended antigen kinetics in vivo and this may translate to numbers of antigen specific CD8 T cells at 7 DPI as well as promoting a central memory phenotype ($CD44^{high}$ $CD62L^{high}$ and increased IL-2 production upon antigen restimulation) (Figure 1 and 2). Continued antigen presence is key towards driving memory populations as naïve T cells activated as the antigen load is waning acquire more central memory characteristics needed for retention in the secondary lymph tissue such as decreased ability to down-regulate CD62L and less proliferative capacity [32-34]. IL-2 production is also critical for establishing a stable memory pool [35].

Simultaneous evaluation of antigen-specific $CD8^+$ T cell responses induced using vaccine regimen that included one of three different polyanhydride chemistries was accomplished using adoptive transfer of a transgenic luciferase reporter mouse line (T-lux) under the control of the T cell integrin CD2 promoter [36] crossed with

the transgenic OTI antigen specific line. The three chemistries evaluated showed differential antigen release kinetics in vitro with 20:80 CPH:SA and 20:80 CPTEG:CPH providing a large burst release of antigen while 50:50 CPTEG:CPH show a slower and more sustained release (Figure 3B). CPTEG:CPH polyanhydride nanoparticles enhance $CD8^+$ T cell expansion at the immunization site based on bioluminescence signal increases (Figure 3). Peak expansion of T cells occurred early (5 DPI) and contracted to baseline levels by 10 DPI. Based on anatomical location of the bioluminescent signal, magnitude, and dominant effector cell phenotype exhibited in Figure 2, it can be postulated that a majority of these cells were short-lived effector cells migrating to the immunization site. The EL-7 Ova expressing T cell lymphoma cell line was used to assess the presence of cytotoxic effector $CD8^+$ T cells in the immunized mice. In vivo imaging of bioluminescent Ova-specific T cells showed that MPLA and CPTEG:CPH immunized mice showed earlier measurable T cell infiltrate than mice in other immunization groups (Figure 4). The T cell infiltrate in all immunizations demonstrates T cell memory as no measurable increases in luminescence is detected in sham immunized (PBS) mice until 14 days post-tumor challenge time point (Figure 4C). Tumor challenge was largely controlled in all groups receiving immunization compared to sham immunized mice as well indicating the high frequency adoptive transfer of naïve T cells demonstrates a protective advantage against this tumor model (Figure 5 D-E). The kinetics of the response to the tumor challenge and the statistically significant amount of antigen specific $CD8^+$ T cells in the periphery are indicative of the levels

of memory T cells developed from immunization that were capable of responding rapidly to challenge.

The high frequency adoptive transfer model illuminated the ability of polyanhydride nanoparticle immunizations to activate Ova-specific T cells and gave indications that an effector memory $CD8^+$ T cell response can be enhanced by the inclusion of Ova-containing nanoparticles as part of the vaccine regimen. The high frequency transfer model is somewhat unrealistic however, in that the precursor frequency of the antigen-specific T cells was skewed in the favor of detecting a positive response after administration of a high dose of Ova that would be sufficient to stimulate a large number of antigen-specific naïve T cells. To outline the capabilities of the polyanhydride nanoparticle-based vaccine regimen to elicit T cell responses in an environment more closely resembling the frequency of antigen-specific naïve T cells while still maintaining the ability to examine an antigen specific cell population we utilized a low frequency adoptive transfer technique outlined by Moon et al [16]. Examinations of the draining lymph nodes for expansion of Ova-specific T cells at 7 DPI show that polyanhydride nanoparticle immunizations significantly increase the numbers of Ova-specific $CD8^+$ T cells (Figure 6A-B) with 20:80 CPTEG:CPH demonstrating the greatest ability to expand $CD8^+$ T cells with the least variability.

The kinetics of antigen exposure to naïve T cells entering the draining lymph node is crucial in programming memory T cells as this stage in the maturation of the antigen-specific response is more likely to occur during the times of limited antigen availability [37]. Naïve T cells that arrive later or during reduced antigen lead to a

differential programming resulting in the development of more central memory T cells rather than a short-lived effector cells (SLEC) [26, 34, 38, 39]. This increased memory conversion can be dictated by naïve precursor frequency with increased naïve precursor frequency leading to higher memory T cells so it was important to both control for that frequency by utilizing low frequency transfer [34, 38]. Longer periods of antigen exposure lead to more opportunity for late-coming naïve $CD8^+$ T cells to arrive and be programmed. The greater expansion of $CD8^+$ antigen specific T cells also leads to higher amounts of precursor memory T cells (MPEC) characterized by decreased expression of CD127 (IL-7Rα) and KLRG1 surface markers (Figure 6E-F) [19]. $KLRG1^{low}$ $CD127^{low}$ T cells have demonstrated greater ability to effectively convert into central memory T cells [19, 40]. Previously MPEC definitions of $KLRG1^{low}$ $CD127^{high}$ T cells gave rise to memory T cells [41] but more recent evidence supports the concepy/hypothesis that memory precursor cells to be focused on the low KLRG1 marker. Nevertheless, the polyanhydride nanoparticle immunizations were able to induce greater numbers of the MPEC at 7 DPI. As such, greater numbers of central memory T cells are also elicited by the polyanhydride nanoparticle immunizations at this early time-point (Figure 6G-H) indicating that in a pathogen-like manner, the nanoparticle formulations facilitate the induction of a cellular immune response.

Antigen kinetics appear to play a greater role in memory programming in support of the “decreasing-potential model” proposed in Ahmed and Gray [37]. Exogenous inflammatory stimuli did not support greater memory population generation in a lymphocytic choriomeningitis virus (LCMV) infection model but

antigen load dictated memory conversion [19]. Prolonged antigen exposure does not increase the memory T cell pool but rather decreases it as more of the MPEC and antigen experienced effector cells are programmed to short-lived effector phenotypes [42, 43]. Therefore the controlled release kinetics of encapsulation of antigen in polyanhydride nanoparticles appears to potentiate the “decreasing-potential” exposure window leading to more memory precursors and memory T cell pools (Figure 2B, Figure 6)

Inflammation associated with the initiation of the immune response dictates aspects of memory pool generation. Increasing amounts of IL-12 drives T-bet transcription factor expression leading to larger central memory pools [41]. As such we identified changes in gene expression and secretion of cytokines by bone marrow derived macrophages treated with the three different polyanhydride chemistries. Polyanhydride particles increased the secretion of IL-12p40 and IL-6 from bone marrow derived dendritic cells indicating the cytokine milieu that may drive programming [8].

Activation of naïve $CD8^+$ T cells is not only limited to DCs but macrophages can also activate naïve $CD8^+$ T cells and influence effector and memory functions [44]. The in vivo evidence of enhancing antigen specific T cell expansion (Figure 1, 3, and 5) as well as increases in monocyte chemokines and cytokines (Chapter 4 and Table 1) and the dominant monocyte/macrophage infiltrate at the administration site (Chapter 4), led us to examine the genetic and inflammatory chemokine/cytokine profile of macrophages administered nanoparticles in vitro. We observed the CPTEG:CPH polyanhydride chemistries to induce the largest NF-κB associated

signaling gene changes as well as the greatest inflammatory cytokine production as compared to 20:80 CPH:SA which seemed similar in genetic changes to un-stimulated cells (Table 2). The genetic up-regulation of stat1 has been shown to be critical for IP-10 production from macrophages [45] which may be a major indicator of the polyanhydride specific IP-10 production in vivo (Chapter 4 and Table 1). The increases in transcription of intracellular PRRs TLR3 and NOD1 and to a lesser extent TLR9 all indicate that nanoparticles are perceived as intracellular pathogens by the BM-MØ [46-49]. Most relevant to the expanded T cell responses, however, was the large up-regulation of CD40 (Table 2). CD40-CD40L ligation is needed for optimal expansion of T cell responses and one can theorize that sustained antigen presentation occurring from APCs continually processing slowly eroding nanoparticles benefits from sustained expression of CD40 for greater increases in T cell expansion. We speculated that the 20:80 CPTEG:CPH chemistry would be the most immunomodulatory in these in vitro assays based on the in vivo inflammatory response induced at the site of injection (Chapter 4). However, the 50:50 CPTEG:CPH chemistry appeared the most immunomodulatory according to the genetic profiles and cytokines secreted. This could be a function of timing of the assay as these in vitro data reported were examined at 8 hours. The 20:80 CPTEG:CPH polymer is the slowest eroding polymer and, therefore, may provide stronger signals later and/or more sustained immunomodulatory signals leading to the best in vivo responses. This data, the T cell activation data, and the T cell localization data correlates with observations that macrophages are more capable of activating naïve $CD8^+$ T cells and forming multiple immunological synapses than are

DCs. These BM-MØ:naive T cell interactions may occur at the administration site as well as within the draining lymph tissue [50].

The data reported herein coincides with meta-analysis of previous publications examining the immunomodulatory potential of the polyanhydride platform indicating that the CPTEG:CPH chemistries appear “pathogen-like” in the ability to induce innate immune functions [8, 51, 52]. These “pathogen-like” properties most likely are a synergistic combination of the particulate structures of the nanoparticles mimicking pathogen size, the controlled release of encapsulated antigen mimicking the antigen kinetics of replicating pathogen being resolved by the immune system leading to immune memory, and interaction of conserved innate immune receptors responding to the polymeric strands of degrading particles and the oxygenated hydrophobic backbones of the polymers. Therefore, the polyanhydride nanoparticle platform performs as both an effective particulate vaccine delivery system as well as a potent immunopotentiator capable of activating APCs leading to enhanced CD8 T cell immunity.

5. References:

[1] Hepburn MJ, Kortepeter MG, Pittman PR, Boudreau EF, Mangiafico JA, Buck PA, et al. Neutralizing antibody response to booster vaccination with the 17d yellow fever vaccine. Vaccine 2006;24(15):2843-9.

[2] Querec TD, Akondy RS, Lee EK, Cao W, Nakaya HI, Teuwen D, et al. Systems biology approach predicts immunogenicity of the yellow fever vaccine in humans. Nature Immunology 2009;10(1):116-25.

[3] Barrett ADT, Teuwen DE. Yellow fever vaccine - how does it work and why do rare cases of serious adverse events take place? Current Opinion in Immunology 2009;21(3):308-13.

[4] Tritto E, Mosca F, De Gregorio E. Mechanism of action of licensed vaccine adjuvants. Vaccine 2009;27(25-26):3331-4.

[5] O Hara GA, Welten SPM, Klenerman P, Arens R. Memory T cell inflation: understanding cause and effect. Trends in Immunology 2012;33(2):84-90.

[6] Carrillo-Conde B, Schiltz E, Yu J, Chris Minion F, Phillips GJ, Wannemuehler MJ, et al. Encapsulation into amphiphilic polyanhydride microparticles stabilizes *Yersinia pestis* antigens. Acta biomaterialia 2010;6(8):3110-9.

[7] Ulery B, Phanse Y, Sinha A, Wannemuehler M, Narasimhan B, Bellaire B. Polymer chemistry influences monocytic uptake of polyanhydride nanospheres. Pharmaceutical Research 2009;26(3):683-90.

[8] Torres MP, Wilson-Welder JH, Lopac SK, Phanse Y, Carrillo-Conde B, Ramer-Tait AE, et al. Polyanhydride microparticles enhance dendritic cell antigen presentation and activation. Acta biomaterialia 2011;7(7):2857-64.

[9] Ulery BD, Kumar D, Ramer-Tait AE, Metzger DW, Wannemuehler MJ, Narasimhan B. Design of a protective single-dose intranasal nanoparticle-based vaccine platform for respiratory infectious diseases. PLoS ONE 2011;6(3):e17642.

[10] Torres MP, Vogel BM, Narasimhan B, Mallapragada SK. Synthesis and characterization of novel polyanhydrides with tailored erosion mechanisms. Journal of Biomedical Materials Research Part A 2006;76A(1):102-10.

[11] Conix A. Poly[1,3-bis(p-carboxyphenoxy)-propane anhydride]. Macro Synth 1966(2):95-8.

[12] Shen E, Pizsczek R, Dziadul B, Narasimhan B. Microphase separation in bioerodible copolymers for drug delivery. Biomaterials 2001;22(3):201-10.

[13] Kipper MJ, Wilson JH, Wannemuehler MJ, Narasimhan B. Single dose vaccine based on biodegradable polyanhydride microspheres can modulate immune response mechanism. Journal of Biomedical Materials Research Part A 2006;76A(4):798-810.

[14] Rasband WS. ImageJ. 1.44 ed. Bethesda, Maryland, USA: U. S. National Institutes of Health.

[15] Nahrendorf M, Sosnovik DE, Waterman P, Swirski FK, Pande AN, Aikawa E, et al. Dual channel optical tomographic imaging of leukocyte recruitment and

protease activity in the healing myocardial infarct. Circulation Research 2007;100(8):1218-25

[16] Moon JJ, Chu HH, Hataye J, Pagan AJ, Pepper M, McLachlan JB, et al. Tracking epitope-specific T cells. Nature Protocols 2009;4(4):565-81.

[17] Weischenfeldt J, Porse B. Bone marrow-derived macrophages (BMM): isolation and applications. Cold Spring Harbor Protocols 2008;2008(13):pdb.prot5080-.

[18] Sallusto F, Geginat J, Lanzavecchia A. Central memory and effector memory T cell subsets: Function, generation, and maintenance. Annual Review of Immunology 2004;22(1):745-63.

[19] Fousteri G, Dave A, Juedes A, Juntti T, Morin B, Togher L, et al. Increased memory conversion of naïve CD8 T cells activated during late phases of acute virus infection due to decreased cumulative antigen exposure. PLoS ONE 2011;6(1):e14502.

[20] Cockburn IA, Chen Y-C, Overstreet MG, Lees JR, van Rooijen N, Farber DL, et al. Prolonged antigen presentation is required for optimal CD8+ T cell responses against malaria liver stage parasites. PLoS Pathogens 2010;6(5):e1000877.

[21] Chavez-Santoscoy AV, Huntimer LM, Ramer-Tait AE, Wannemuehler M, Narasimhan B. Harvesting murine alveolar macrophages and evaluating cellular activation induced by polyanhydride nanoparticles. Journal of Visual Experiments 2012(64):e3883.

[22] Chavez-Santoscoy AV, Roychoudhury R, Pohl NL, Wannemuehler MJ, Narasimhan B, Ramer-Tait AE. Tailoring the immune response by targeting C-type lectin receptors on alveolar macrophages using "pathogen-like" amphiphilic polyanhydride nanoparticles. Biomaterials 2012;33(18):4762-72.

[23] Gilbert SC. T-cell-inducing vaccines – what's the future. Immunology 2012;135(1):19-26.

[24] Foged C, Hansen J, Agger EM. License to kill: Formulation requirements for optimal priming of CD8+ CTL responses with particulate vaccine delivery systems. European Journal of Pharmaceutical Sciences 2012;45(4):482-91.

[25] Lipford GB, Bauer M, Blank C, Reiter R, Wagner H, Heeg K. CpG-containing synthetic oligonucleotides promote B and cytotoxic T cell responses to protein

antigen: A new class of vaccine adjuvants. European Journal of Immunology 1997;27(9):2340-4.

[26] Harty JT, Badovinac VP. Shaping and reshaping CD8+ T-cell memory. Nature Reviews Immunology 2008;8(2):107-19.

[27] Bachmann MF, Beerli RR, Agnellini P, Wolint P, Schwarz K, Oxenius A. Long-lived memory CD8+ T cells are programmed by prolonged antigen exposure and low levels of cellular activation. European Journal of Immunology 2006;36(4):842-54.

[28] Bachmann MF, Jennings GT. Designing recombinant vaccines with viral properties: a rational approach to more effective vaccines. Current Molecular Medicine 2007;7(2):143-55.

[29] Pape KA, Catron DM, Itano AA, Jenkins MK. The humoral immune response is initiated in lymph nodes by B cells that acquire soluble antigen directly in the follicles. Immunity 2007;26(4):491-502.

[30] Catron DM, Itano AA, Pape KA, Mueller DL, Jenkins MK. Visualizing the first 50 hr of the primary immune response to a soluble antigen. Immunity 2004;21(3):341-7.

[31] Catron DM, Pape KA, Fife BT, van Rooijen N, Jenkins MK. A Protease-Dependent mechanism for initiating T-Dependent B cell responses to large particulate antigens. The Journal of Immunology 2010;184(7):3609-17.

[32] Kaech SM, Ahmed R. Memory CD8+ T cell differentiation: initial antigen encounter triggers a developmental program in naive cells. Nature Immunology 2001;2(5):415-22.

[33] van Faassen H, Saldanha M, Gilbertson D, Dudani R, Krishnan L, Sad S. Reducing the stimulation of CD8+ T Cells during infection with intracellular bacteria promotes differentiation primarily into a central ($CD62L^{high}CD44^{high}$) subset. The Journal of Immunology 2005;174(9):5341-50.

[34] D'Souza WN, Hedrick SM. Cutting edge: Latecomer CD8 T cells are imprinted with a unique differentiation program. The Journal of Immunology 2006;177(2):777-81.

[35] Williams MA, Tyznik AJ, Bevan MJ. Interleukin-2 signals during priming are required for secondary expansion of CD8+ memory T cells. Nature 2006;441(7095):890-3.

[36] Chewning J, Dugger K, Chaudhuri T, Zinn K, Weaver C. Bioluminescence-based visualization of CD4 T cell dynamics using a T lineage-specific luciferase transgenic model1. BMC Immunology 2009;10(1):44.

[37] Ahmed R, Gray D. Immunological memory and protective immunity: Understanding their relation. Science 1996;272(5258):54-60.

[38] Obar JJ, Khanna KM, Lefrançois L. Endogenous naive CD8+ T cell precursor frequency regulates primary and memory responses to infection. Immunity 2008;28(6):859-69.

[39] Badovinac VP, Haring JS, Harty JT. Initial T cell receptor transgenic cell precursor frequency dictates critical aspects of the CD8+ T cell response to infection. Immunity 2007;26(6):827-41.

[40] Mitchell DM, Ravkov EV, Williams MA. Distinct roles for IL-2 and IL-15 in the differentiation and survival of CD8+ effector and memory T cells. The Journal of Immunology 2010;184(12):6719-30.

[41] Joshi NS, Cui W, Chandele A, Lee HK, Urso DR, Hagman J, et al. Inflammation directs memory precursor and short-lived effector CD8+ T cell fates via the graded expression of T-bet transcription factor. Immunity 2007;27(2):281-95.

[42] Mescher MF, Curtsinger JM, Agarwal P, Casey KA, Gerner M, Hammerbeck CD, et al. Signals required for programming effector and memory development by CD8+ T cells. Immunological Reviews 2006;211(1):81-92.

[43] Jelley-Gibbs DM, Dibble JP, Brown DM, Strutt TM, McKinstry KK, Swain SL. Persistent depots of influenza antigen fail to induce a cytotoxic CD8 T cell response. The Journal of Immunology 2007;178(12):7563-70.

[44] Pozzi LA, Maciaszek JW, Rock KL. Both dendritic cells and macrophages can stimulate naive CD8 T cells in vivo to proliferate, develop effector function, and differentiate into memory cells. Journal of Immunology 2005;175(4):2071-81.

[45] Ohmori Y, Hamilton TA. Requirement for STAT1 in LPS-induced gene expression in macrophages. Journal of Leukocyte Biology 2001;69(4):598-604.

[46] Gerold G, Zychlinsky A, de Diego JL. What is the role of Toll-like receptors in bacterial infections? Seminars in Immunology 2007;19(1):41-7.

[47] Moreira LO, Zamboni DS. NOD1 and NOD2 Signaling in Infection and Inflammation. Frontiers in Immunology 2012;3:328.

[48] Bhatt K, Salgame P. Host innate immune response to *Mycobacterium tuberculosis*. Journal of Clinical Immunology 2007;27(4):347-62.

[49] Kim YG, Park JH, Reimer T, Baker DP, Kawai T, Kumar H, et al. Viral infection augments Nod1/2 signaling to potentiate lethality associated with secondary bacterial infections. Cell Host Microbe 2011;9(6):496-507.

[50] Olazabal IM, Martin-Cofreces NB, Mittelbrunn M, Martinez del Hoyo G, Alarcon B, Sanchez-Madrid F. Activation outcomes induced in naive CD8 T-cells by macrophages primed via "phagocytic" and nonphagocytic pathways. Molecular Biology of the Cell 2008;19(2):701-10.

[51] Petersen LK, Ramer-Tait AE, Broderick SR, Kong C-S, Ulery BD, Rajan K, et al. Activation of innate immune responses in a pathogen-mimicking manner by amphiphilic polyanhydride nanoparticle adjuvants. Biomaterials 2011;32(28):6815-22.

[52] Ulery BD, Petersen LK, Phanse Y, Kong CS, Broderick SR, Kumar D, et al. Rational design of pathogen-mimicking amphiphilic materials as nanoadjuvants. Scientific Reports 2011;1.

CHAPTER 6: HUMORAL IMMUNE RESPONSES ELICITED BY THE POLYANHYDRIDE PARTICLE VACCINE PLATFORM ARE FACILITATED BY ENHANCED T FOLLICULAR HELPER CELL PHENOTYPE

Lucas Huntimer, Kathleen Ross, Balaji Narasimhan, Amanda Ramer-Tait, and Michael J. Wannemuehler

To be submitted to Vaccine

Abstract:

The polyanhydride nanoparticle vaccine platform provides innate immunomodulatory activity while also controlling antigen release kinetics to enhance humoral immunity. The increased humoral responses by adjuvanting vaccines with polyanhydride nanoparticles is indicative of activating T helper cell responses early after immunization that provide the necessary help for B cells to secrete antibody. Here we identify the mechanisms of $CD4^+$ T cell expansion and phenotypes observed after immunizing with three different polyanhydride nanoparticle formulations using the transgenic Ovalbumin specific T cell (OTII) system. Statistically increased expansion of $CD4^+$ T cells occurs with 20:80 CPH:SA and 20:80 CPTEG:CPH chemistries. These T cells show T follicular helper cells ($CXCR5^{high}$ $PD\text{-}1^{high}$) phenotypes important for initiating and maintaining germinal centers in similar percentages as traditional Alum and MPLA adjuvants. The polyanhydride nanoparticle vaccines display enhanced IgG1 antibody responses as compared to antigen alone and the mice were effectively primed to respond with

robust IgG1 and IgG2c isotype antibody after antigenic challenge 35 days post immunization. The polyanhydride nanoparticles show enhanced amounts of $V\alpha2^+$ $V\beta5^+$ $CD4^+$ T cells of the Tfh phenotype as well as enhanced PNA^+ activated B cells indicative germinal centers.

1. Introduction

Protective humoral immunity elicited by preventive immunization is provided by long-lived plasma cells and memory B cells, leading to the production of antibody that inhibits bacterial growth or colonization, provides immune exclusion, opsonizes bacteria, activates complement activation, or neutralizes toxins or viral entry into cells [1]. Germinal centers are elegant B cell training grounds where initial activation of B cells occurs as well as affinity maturation of the antibody response, and development of memory B cells that ultimately maintain humoral immune responses. Competition of high affinity antigen receptors against immune complexes of antibody and antigen maintained by follicular dendritic cells occur in the germinal center [2]. Subsequent studies into germinal center formation have shown that competition for cytokines provided by a unique $CD4^+$ T cell phenotype, namely T follicular helper cells (Tfh), is an important cellular mechanism for optimal B cell responses after immunization [3-5]. In particular, Tfh cells are critical sources of cytokines IL-4 and IL-21 which are important for B cell activation, proliferation, and isotype switching [3]. Co-stimulatory ligation of CD40, T cell co-stimulatory molecule-ligand (ICOSL), and CD80/86 are also critical components of T cell help that augment B cell activation during germinal center formation.

Biodegradable polyanhydride biomaterials represent a unique next generation vehicle delivery platform that can be used to design efficacious vaccine regimen for poorly immunogenic subunit (i.e., recombinant) proteins [6, 7]. Polyanhydride copolymers based on sebacic acid (SA), 1,6-bis(*p*-carboxyphenoxy) hexane (CPH), and 1,8-bis(*p*-carboxyphenoxy)-3,6-dioxaoctane (CPTEG) formed into particulate carriers can be tailored to meet the desired controlled release profile of encapsulated immunogens as well as providing innate immunomodulatory functions such as activating dendritic cells [8-11]. A polyanhydride nanoparticle vaccine regimen was used to induce protective immunity against *Yersinia pestis.* The resultant antibody response was characterized by the presence of avid high titer F1-V-specific IgG1 after a single intranasal immunization consisting of soluble recombinant F1-V and polyanhydride nanoparticles encapsulating F1-V [12].

Herein, we identify the cellular responses important in generation of the high titer antibody responses elicited by vaccine regimen incorporating the polyanhydride nanoparticle vaccine platform by utilizing transgenic $CD4^+$ T cells (OT II) responsive to ovalbumin (Ova). Immunization with Ova-loaded polyanhydride nanoparticles after high frequency adoptive transfer of OTII T cells induced the expansion and contraction kinetics of OTII T cells that was similar to soluble antigen alone. In contrast, a more significant expansion of OTII T cells was observed when mice were immunized with Ova adjuvanted with Alum. Following high frequency transfer of OTII T cells, the induction of Ova-specific IgG1 antibody responses at 14 days post-immunization (DPI) was greater in mice immunized with Ova-loaded 50:50 CPTEG:CPH nanoparticles. To mimic the in vivo environment where antigen-specific

naïve T cell precursor frequency ≥ 0.1 % , a low frequency adoptive transfer of OTII T cells was utilized and the polyanhydride nanoparticle platform exhibited expanded $CD4^+$ T cells highlighted by increases in $CD4^+$ T cells with a Tfh phenotype. Antibody responses in the low frequency adoptive transfer model also indicate augmentation of antibody responses when antigen is encapsulated in each of the three polyanhydride nanoparticle chemistries examined compared to unadjuvanted Ova. Strong IgG1 antigen specific antibody was generated and these nanoparticle immunized mice were primed to respond strongly with IgG1 when antigenically challenged 35 DPI. Polyanhydride nanoparticle vaccine regimens show statistically increased numbers of V-$\alpha 2^+$ V-$\beta 5^+$ $CD4^+$ Tfh at 42 DPI as well as increased percentage of $B220^+$ $CD23^{high}$ PNA^+ B cells. These early indications of GC formation outline the cellular mechanisms responsible for the immune phenotype observed after immunization with vaccines utilizing the polyanhydride nanoparticle platform.

2. Materials and Methods

2.1 Synthesis and characterization of copolymers

CPH and CPTEG monomers were synthesized using the chemicals listed: 4-p-hydroxybenzoic acid, 1,6-dibromohexane, 1-methyl-2-pyrrolidinone, and tri-ethylene glycol. All these chemicals and sebacic acid (99%) were purchased from Sigma Aldrich (St. Louis, MO); 4-p-fluorobenzonitrile was obtained from Apollo Scientific (Cheshire, UK); potassium carbonate, dimethyl formamide, toluene, sulfuric acid, acetic acid, acetonitrile, acetic anhydride, methylene chloride, and petroleum ether were purchased from Fisher Scientific (Fairlawn, NJ). Synthesis of

CPH and CPTEG diacids was performed as previously described [13, 14] and pre-polymers of SA and CPH were synthesized using previously described methods [14, 15]. Copolymers (20:80 and 50:50 CPH:SA and 20:80 and 50:50 CPTEG:CPH) were synthesized using a melt polycondensation process as detailed by Kipper et al. and Torres et al [6, 13]. The degree of polymerization, molecular weight, chemical structure, and polymer purity were determined using ^{1}H nuclear magnetic resonance (NMR) spectroscopy (Varian VXR-300 MHz, Palo Alto, CA).

2.2 Fabrication and characterization of particles

Nanoparticles encapsulating Ova (Sigma-Aldrich, St. Louis, MO) (5.0% w/w loading) were fabricated using the anti-solvent nanoencapsulation method outlined in Ulery et al [9]. Briefly, the copolymer was dissolved in methylene chloride at a concentration of 20 mg/mL at 4˚C. Ova was added to the dissolved copolymer and the solution was sonicated for uniform dispersal of the protein within the copolymer. The dissolved ova loaded copolymer (ova-loaded) or copolymer (blank) solution was poured into chilled pentane (-20°C) at a non-solvent to solvent ratio of 250:1, and was vacuum filtered to recover the nanoparticles. Shape and size of the resulting nanoparticles were characterized using scanning electron microscopy (SEM) (FEI Quanta 250, FEI, Hillsboro, OR). The particle size distribution was obtained from SEM images using Image J version 1.46 image analysis software [16]. An average of 200 particles per image was analyzed.

2.3 Mice

Recipient female C57BL/7 Thy 1.1, recipient albino C57BL/6, OTII mice were purchased from Jackson Laboratories (Bar Harbor, MN). All mice were housed under specific pathogen-free conditions where all bedding, caging, water, and feed were sterilized prior to use. Animal procedures were conducted with the approval of the Iowa State University Institutional Animal Care and Use Committee.

2.4 Mouse treatments

2.4.1 Adoptive transfer of antigen-specific T cells

For the high frequency adoptive transfer experiments, 3.0×10^6 donor OTII Thy 1.2^+ cells were transferred by tail vein injection on day -1. For the low frequency adoptive transfer experiments, 3×10^3 OTII Thy 1.2^+ cells were transferred via the tail vein on day -1. For in vivo imaging studies, low frequency adoptive transfer of 3.0×10^3 OTII cells was performed on day -1.

2.4.2 Immunization Regimens

On day 0, mice were immunized subcutaneously (SC) with 1.75 mg of soluble Ova and 5 mg of 5 % Ova loaded polyanhydride nanoparticles (20:80 C:S, 20:80 C:C, 50:50 C:C), 2.0 mg of soluble Ova (sOVA), or 2.0 mg of Ova adjuvanted 1:1 with Imject Alum (Alum) (ThermoFisher, Rockford, IL). For the low frequency adoptive transfer experiments, 25 µg of Ova was administered as an antigenic challenge at 37 DPI.

2.5 Assaying for ex vivo T cell phenotype and activity

At three, five, seven, fourteen, and forty-five days post-immunization (DPI), draining lymph nodes were excised and single cell suspensions were created using a glass homogenizer. Half of each spleen was homogenized to prepare single cell suspensions and the red blood cells were lysed using ACK lysis buffer. The numbers of T cells recovered from the splenic tissue and their phenotype were quantified using flow cytometry (BD FACS Aria III). For low frequency adoptive transfer experiments, positive selection for donor T cells was accomplished using biotinylated anti-CD90.2 (Thy 1.2 Clone 53-2.1) (eBioscience, San Diego, CA) and streptavidin conjugated magnetic microbeads (Miltenyi Biotech, Auburn, CA). Positive magnetic bead selection was performed via methods outlined by Moon et al (AutoMACS Pro Milteny Biotec) [17]. Prior to the addition of the monoclonal antibodies used for selection or cell surface marker analysis, cell suspensions were blocked for non-specific antibody binding using 0.1 mg/mL Rat IgG (Sigma Aldrich) and 10 µg/mL mouse anti-CD16/32 (eBioscience). For T cell assays, fluorescently conjugated antibodies for CD4 (PE-Cy7, Clone GK1.5, eBioscience), CD8ß (APC, Clone eBioH35-17.2, eBioscience), CD62L (PE, Clone 2G8, eBioscience), PD-1 (eFluor 450, Clone 4B12, eBioscience), Thy 1.2 (APC-eFluor 780, Clone 53-2.1, eBioscience), Thy 1.1 (PerCP-Cy 5.5, Clone HIS51, eBioscience), CD19 (PerCP-Cy5.5, clone eBio1D3, eBioscience), CD11c (PerCP-Cy5.5, clone N418, eBioscience), CD11b (PerCP-Cy5.5, clone M1/70, eBioscience), F4/80 (PerCP-Cy5.5, BM8, eBioscience), CXCR5 (PE, clone 2G8, BD, Franklin Lakes, NJ), and CD44 (v500, clone IM7, BD) were used to label the cells, to establish analytical

gates, and to quantify donor Thy 1.2^+ cells. Abs were used in appropriate combination of fluorochromes. The population of B cells was analyzed using fluorescently conjugated antibodies for CD19 (PerCP-Cy5.5, clone eBio1D3, eBioscience), B220 (PE-eFluor 780, clone RA3-682, eBioscience), and CD23 (PE-Cy7, clone B384, eBioscience), and FITC PNA (Vector Labs, Burlingame, CA) to quantify germinal center responses.

2.6 Serum cytokine analysis

Serum samples obtained from C57BL/6 Thy 1.1 recipient mice were analyzed using a 22-plex chemokine and cytokine antibody array (Millipore, Billerica, MA) measuring the following analytes: G-CSF, GM-CSF, IFN-γ, IL-10, IL-12p70, IL-13, IL-15, IL-17, IL-1α, IL-1β, IL-2, IL-4, IL-5, IL-6, IL-7, IL-9, IP-10, KC, MCP-1, MIP-1α, RANTES, and TNF-α. Assays were performed according to the manufacturer's recommendations; data were acquired and analyzed using a Bio-Plex 200 (Bio Rad, Hercules, CA).

2.7 Antigen Specific Antibody Analysis

Serum was generated from blood samples taken from saphenous vein bleeds or collected by cardiac puncture after the mice were euthanized. Serum was clarified by centrifugation at 1000 x g for 10 minutes. The serum samples were then stored at -20 °C until used. ELISA plates (Costar Catalog # 3590, EIA/RIA high binding) were coated overnight with 0.5 µg/well Ova. Plates were washed with phosphate buffered saline (PBS, 0.05 M, pH 7.4) containing 0. 5 % Tween 20 at a (PBST). Plates were

blocked for two hours with 2 % fish gelatin (Difco) in PBST. Plates were washed and serial dilutions of individual serum samples in PBST supplemented with 1% heat inactivated normal goat serum (GIBCO) were incubated overnight at 4 ^{o}C. Plates were washed again with PBST and alkaline phosphatase-conjugated goat anti-mouse IgG (H&L), IgG1, or IgG2c (Jackson ImmunoResearch Laboratories, West Grove, PA) diluted 1:1000 in 1 % heat inactivated normal goat serum in PBST was incubated for 2 h. Plates were washed and p-nitrophenyl phosphate (Sigma) substrate (1 mg/mL) in 50 mM Na_2CO_3 and 2 mM $MgCl_2$ buffer (pH 9.3) was added to each well. Changes in optical density (OD) were measured at 405 nm using a spectrophotometer (Spectra Max 190, Molecular Devices, Sunnyvale CA).

The avidity of the Ova-specific IgG1 was measured as described previously to determine antibody binding strength in the presence of a chaotropic agent that disurpts antibody-antigen binding interactions [6]. The relative avidity percentage was calculated by dividing the OD405 nm of 1:3000 diluted serum treated with 0.625 M NaSCN by the OD405nm of 0 M NaSCN treated wells and the percentage was reported.

2.8 Statistical analysis

Differences in mean responses among treatments were tested with one-way ANOVA F-test followed by a post-hoc Tukey's t-test using Graph Pad Prism version 5. Values were log transformed for equal variance where needed. Statistical tests with p values ≤ 0.05 were regarded as significant.

3. Results

3.1 Nanoparticle immunization in high frequency adoptive transfer expands less $CD4^+$ antigen specific T cells compared to Alum

Measures of vaccine efficacy for vaccines designed with the polyanhydride nanoparticle platform exhibit high titer IgG1 antibody of high avidity [7]. Little evidence of T cell recall responses were observed in these studies other than the protection from challenge. We hypothesized that encapsulation of antigen in polyanhydride nanoparticles leads to an expansion of T helper cells that exceeds soluble antigen and would be similar to traditional adjuvants such as Alum. C57BL/6 Thy 1.1 recipients were adoptively transferred high amounts of purified OTII $CD4^+$ T cells and immunized with 2.0 mg of Ova as a soluble dose (sOVA), encapsulated regimen of 1.75 mg of soluble Ova and 0.25 mg encapsulated in 50:50 CPTEG:CPH particles or adsorbed to Alum. The expansion of antigen specific T cells was quantified via the donor specific congenic marker Thy 1.2. The expansion kinetics of polyanhydride nanoparticle immunizations mimicked the expansion and contraction of a soluble dose immunization alone (Figure 1). The main differences observed were in the heightened expansion of antigen specific $CD4^+$ T cells at five DPI with

the Alum adjuvanted immunization.

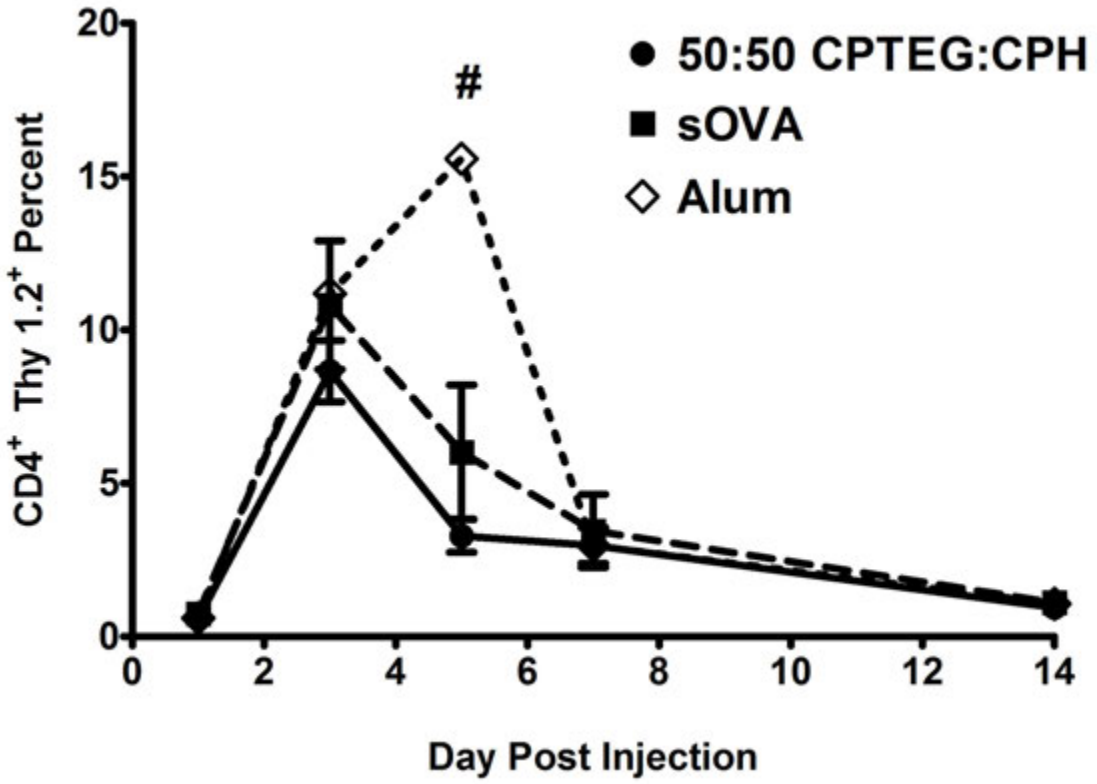

Figure 1. Nanoparticle immunization regimen leads to less $CD4^+$ antigen specific T cell expansion compared to Alum. High frequency adoptive transfer of OTII Thy 1.2^+ T cells (3×10^6 cells/mouse) was performed one day prior to immunization with Ova-loaded 50:50 CPTEG:CPH nanoparticles, adsorbed to Alum, or soluble Ova (sOVA) alone. Percentages of Thy1.2^+ T cells present in the draining lymph nodes were examined at the time points indicated and donor T cells were identified by donor congenic marker Thy 1.2^+ compared to Thy 1.1^+ recipient markers. Each time point is mean percentage of $CD4^+$ Thy 1.2^+ cells for cohorts of 4 to 5 mice per time point ($N \geq 4$). # indicates a significant difference from other groups at $p < 0.05$.

3.2 Nanoparticle immunization elicits less serum inflammatory in a high frequency adoptive transfer model

We hypothesized that the lower amounts of inflammation associated with a nanoparticle regimen as compared to Alum contributed to differences in expansion of antigen specific $CD4^+$ T cells (Chapter 4). Examining the serum cytokine and

chemokine responses from mice at one DPI shows an increase in the neutrophil chemotactic pro-inflammatory cytokine KC (mouse analog of IL-8) (Figure 2A). IL-6 was also increased in the serum of immunized mice although there was no significant differences between groups observed (Figure 2B).

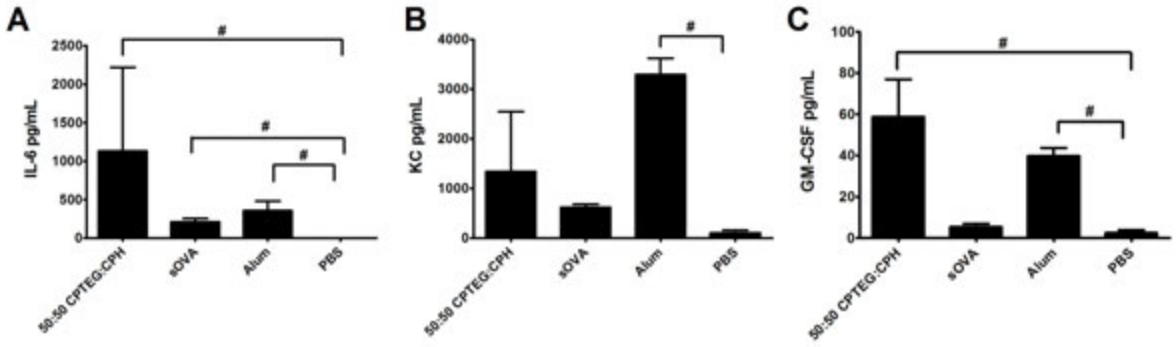

Figure 2. Inflammatory cytokines IL-6, KC, and GM-CSF are increased after immunization. Concentrations of (A) KC, (B) IL-6, and (C) GM-CSF in the serum of mice immunized with the polyanhydride nanoparticle vaccine (50:50 CPTEG:CPH, soluble Ova (sOVA), Alum adjuvanted Ova (Alum), or saline one day post-immunization. Treatment groups marked with # are significantly different from those mice treated with saline at $p < 0.05$. n = 4-5 mice per group.

3.3 Nanoparticle immunization leads to greater Ova-specific antibody

We hypothesized that the Alum adjuvanted groups, because of the increased expansion of $CD4^+$ T cells at 5 DPI, would exhibit enhanced Ova-specific antibody as compared to the 50:50 CPTEG:CPH and sOva groups. At 14 DPI, the Thy 1.2^+CD4^+ T cells had all but contracted to baseline levels in the mice receiving 3 x 10^6 Thy 1.2^+ OTII T cells. (Figure 1). The IgG1 Ova-specific antibody response was enhanced in the polyanhydride nanoparticle groups at 14 DPI (Figure 3). no Ova-specific IgG2c antibody was observed at this time point (data not shown).

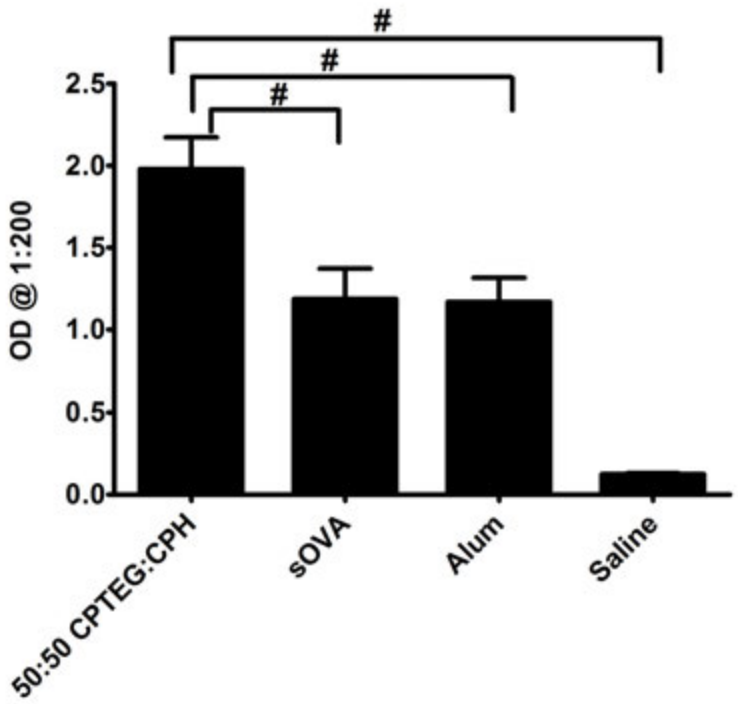

Figure 3. Nanoparticle vaccine enhances antigen specific IgG1 antibody responses following high frequency adoptive transfer of OTII T cells. Ova specific antibody responses were quantified via ELISA at 14 days post-immunization with 50:50 CPTEG:CPH nanoparticles, soluble Ova (sOVA), Ova adsorbed to Alum, or PBS. IgG1 isotype specific secondary antibody was used to identify isotype specific antibodies. N = 4-5 mice per group. # indicates a significant difference from other groups at $p < 0.05$. Data presented from one experiment.

3.4 Nanoparticle immunizations expand CD4$^+$ T cells in low precursor frequency adoptive transfer

The high frequency adoptive transfer model allowed us to enhance and magnify the in vivo expansion kinetics of CD4$^+$ T cells after polyanhydride nanoparticle adjuvanted vaccines. The high frequency adoptive transfer model is unconventional in that it artificially inflates the pool of naïve antigen-specific CD4$^+$ T cells. To examine antigen-specific T cell responses while maintaining a more natural level of naïve antigen-specific T cells, 3 x 10^3 Thy1.2$^+$ OTII T cells were adoptively

transferred into recipient mice. The expansion and the phenotype of OTII T cells was monitored after immunization by flow cytometry.

Adoptive transfer was performed one day prior to immunization. Immunizations consisted of three formulations of polyanhydride nanoparticles, 20:80 CPH:SA, 20:80 CPTEG:CPH, and 50:50 CPTEG:CPH, as well as two positive control vaccines consisting of Ova adsorbed to Alum or co-administered. Statistically significant antigen specific $CD4^+$ T cell expansion was observed in the mice receiving the 20:80 CPH:SA, and 20:80 CPTEG:CPH, vaccine formulations (Figure 4A-B). The phenotype of these antigen experienced ($CD4^+$ $CD44^{high}$) expanded T cells shows a shift in Tfh cell phenotype (PD-1^{high} $CXCR5^{high}$) in percent and total cell numbers when the antigen is adjuvanted by encapsulation into polyanhydrides or by Alum (Figure 4C-E).

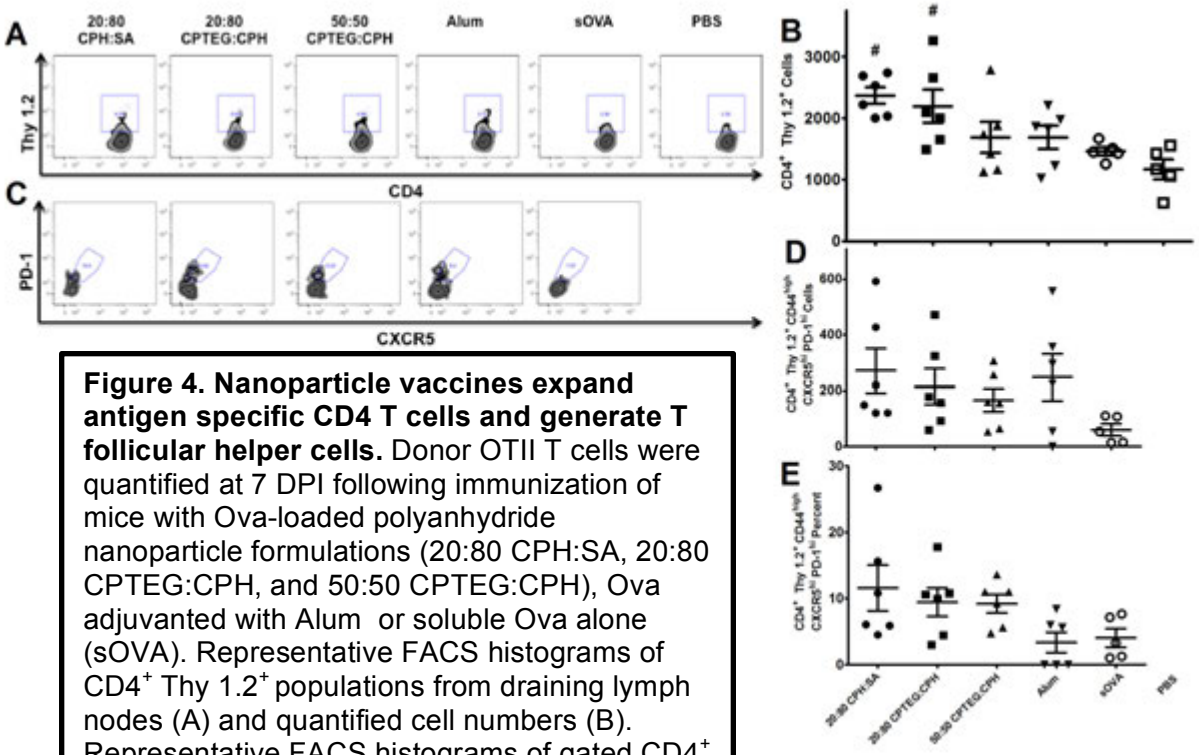

Figure 4. Nanoparticle vaccines expand antigen specific CD4 T cells and generate T follicular helper cells. Donor OTII T cells were quantified at 7 DPI following immunization of mice with Ova-loaded polyanhydride nanoparticle formulations (20:80 CPH:SA, 20:80 CPTEG:CPH, and 50:50 CPTEG:CPH), Ova adjuvanted with Alum or soluble Ova alone (sOVA). Representative FACS histograms of $CD4^+$ Thy 1.2^+ populations from draining lymph nodes (A) and quantified cell numbers (B). Representative FACS histograms of gated $CD4^+$ Thy 1.2^+ $CD44^{high}$ cells gated for $PD\text{-}1^{high}$ $CXCR5^{high}$ populations (Tfh cells) (C), quantified cell numbers (D) and percentage of gated cells (E). N = 5 to 6 mice per group. # indicates a significant difference from PBS groups at $p < 0.05$.

3.5 Nanoparticle immunizations enhance antibody responses in low frequency adoptive transfer models by sustaining germinal centers

To test the hypothesis that an increase in Tfh cells would correlate with a greater humoral immune responses, the kinetics of the Ova-specific antibody response was evaluated for a period of 35 DPI (Figure 5A-D). We observed that enhanced IgG1 antibody responses were generated by all adjuvanted vaccines as compared to sOva alone. Higher sustained IgG1 antibody titers were maintained, as compared to the titers induced by sOVA, through 35 DPI (Figure 5A-D). There was no evidence that Ova-specific IgG2c and IgG3 was induced by any vaccine

formulation after the initial immunization (data not shown). At 37 DPI, a 25 μg antigenic challenge was administered to the immunized groups to examine the anamnestic Ova specific antibody responses. All groups receiving antigen were effectively primed and displayed robust IgG1 responses (Figure 5D). Antigen specific IgG2c responses were also expanded in all groups receiving antigen though no statistical differences were identified

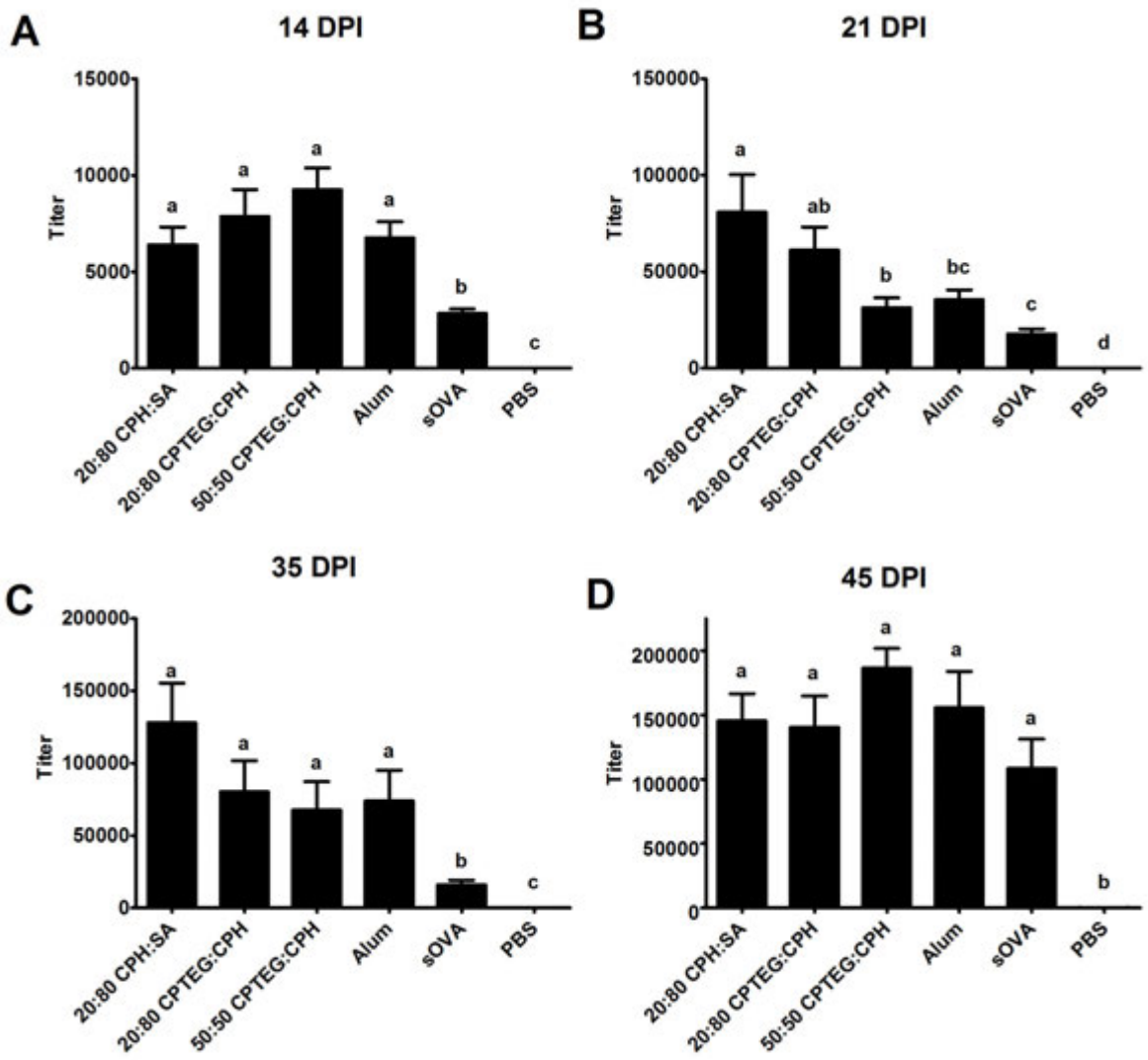

Figure 5. Nanoparticle vaccines expand antigen specific antibody responses similar to common adjuvants Alum. Ova specific antibody responses elicited from mice receiving low frequency transfer of OTII T cells and Ova immunizations adjuvanted with 20:80 CPH:SA, 20:80 CPTEG:CPH, 50:50 CPTEG:CPH polyanhydride nanoparticles, Alum, or soluble Ova (sOVA) were quantified to examine IgG1 isotype. A 25 μg antigenic challenge of Ova was administered on 37 DPI. Antibody titers reported as mean titer values at 14 (A), 21 (B), 35 (C), and 45 (D) N = 9 mice per group. Different letters above indicate significant difference at $p < 0.05$. Results are from one experiment

To examine if the enhanced antibody responses observed were due to sustained Ova specific T cells, the draining lymph nodes from the immunized mice were examined for $CD4^+$ T cells ($V\alpha2^+$, $V\beta5^+$) that displayed the Tfh phenotype (Figure 6A). OTII T cells recovered from mice immunized with polyanhydride nanoparticle vaccines showed a greater numbers of Tfh $V\alpha2^+$ $V\beta5^+$ T cells. The presence of larger numbers of Tfh cells also correlated with larger germinal center B cell populations ($B220^+$ $CD23^{high}$ PNA^+) with polyanhydride nanoparticle vaccines (Figure 6C). MPLA adjuvanted vaccines show high CD4 T^+ cell responses early (Figure 4) however T cell populations are not identified later (Figure 6A) and correlating PNA^+ B cell populations were not identified (Figure 6B). The strength of the antibody responses at this late time point indicated that immunization with the polyanhydride nanoparticles facilitated the maintenance of germinal center cell populations and more avid antigen-specific antibodies.

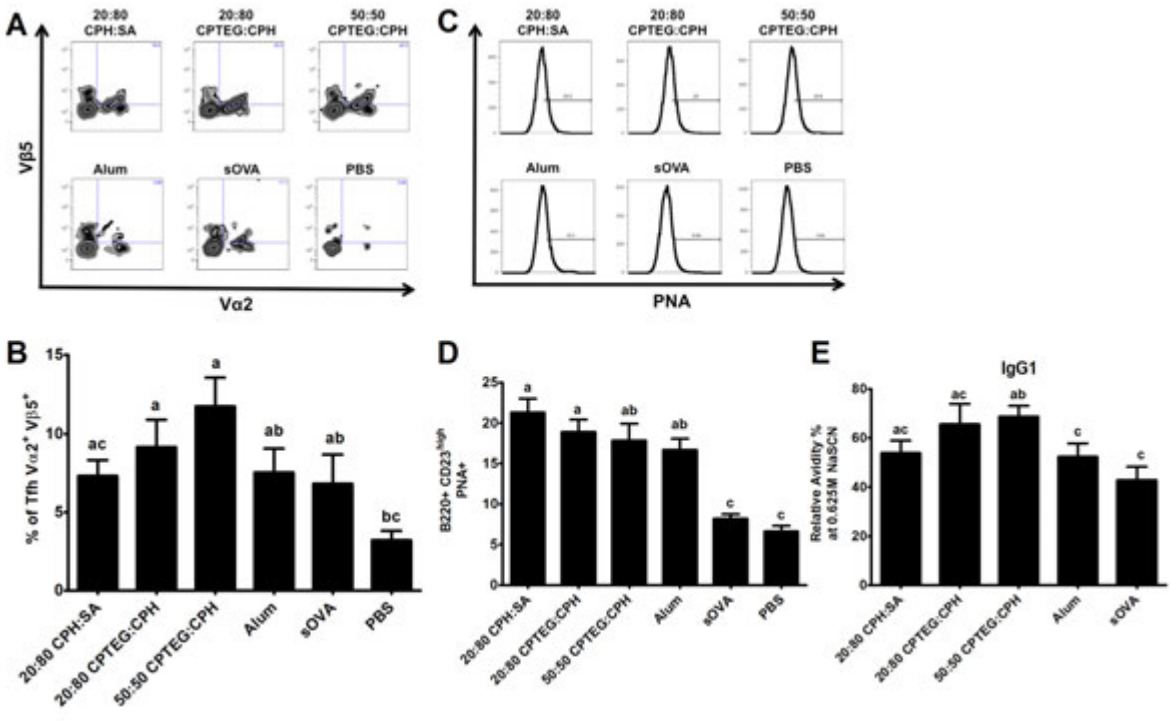

Figure 6. Nanoparticle vaccines maintain Tfh cell populations correlating to more sustained germinal centers at 45 days post-immunization. Single cell suspensions of draining lymph nodes of mice immunized with Ova adjuvanted with 20:80 CPH:SA, 20:80 CPTEG:CPH, or 50:50 CPTEG:CPH polyanhydride nanoparticles, Alum, or soluble Ova (sOVA) protein at 45 DPI were labeled with anti-CD4, anti-CD44, anti-PD-1, anti-CXCR5, anti-Vα2, and anti-Vβ5. Representative FACS histograms of $CD4^+$ $CD44^{high}$ $CXCR5^{high}$ $PD\text{-}1^{high}$ cells that are $V\text{-}\alpha2^+$ (x-axis) and $V\text{-}\beta5^+$ (y-axis) (A). Percent of $CD4^+$ $CD44^{high}$ $CXCR5^{high}$ $PD\text{-}1^{high}$ cells that are $V\text{-}\alpha2^+$ $V\text{-}\beta5^+$ (Ova specific) in the draining lymph nodes (B). Lymph node cells labeled with anti-B220, anti-CD23, and PNA. Representative FACS histograms of gated $B220^+$ $CD23^{high}$ with PNA on the x-axis (C). Quantified $B220^+$ $CD23^{high}$ PNA^+ percent of total cells in the spleen of immunized mice (D). Relative avidity percentage (OD405nm at 0.625M NaSCN divided by 0M NaSCN) of Ova specific IgG1 antibody at 45 DPI (E). N = 9 mice per group. Different letters above histograms indicate significant differences between groups at $p < 0.05$. Data is from one experiment.

4. Discussion

Induction of protective immune responses via immunization is one of the most effective preventive medicinal measures for decreasing infectious disease in at-risk populations. Designing efficacious vaccines while minimizing safety and purity

concerns by implementing the use of subunit immunogens (e.g., recombinant proteins) is a foundation of next generation vaccine design. Adjuvants are often employed to boost immunostimulatory activity and skew antigen availability to bolster the efficacy of subunit vaccines.

Polyanhydride particles provide a particulate context for APCs for optimal phagocytosis as well as increases in the expression of co-stimulatory molecules (e.g., CD86, CD40) on APC [9, 10, 12, 18]. Encapsulation of antigen in polyanhydride particles enhances humoral immune responses with low doses of antigen while eliciting less inflammation in vivo than traditional adjuvants such as alum or Freund's incomplete adjuvant (Chapter 3 and 4). Designing vaccines consisting of a soluble portion of antigen as well as a portion of F1-V antigen encapsulated in polyanhydrides nanoparticles led to high-affinity IgG1 antibody induction and protection from *Yersinia pestis* challenge utilizing a single dose regimen [7, 12]. We hypothesized that the polyanhydride nanoparticles may augment antigen-specific $CD4^+$ T cell expansion similar to that described for Alum. In contrast, the results of the present study indicated that the expansion and contraction kinetics of Ova-specific $CD4^+$ OTII T cells followed the kinetics of that induced by immunization with soluble Ova alone compared to an Alum adjuvanted vaccine in mice receiving 3×10^6 naïve OTII T cells by adoptive transfer (Figure 1). These observations would be consistent with the decreased inflammation induced following administration of the various polyanhydride nanoparticle formulations (Chapter 4) and measured in the serum may contribute to the differential expansion and contraction kinetics (Figure 2). Antigen-specific IgG1 antibody responses were

enhanced in mice immunized with the polyanhydride vaccines compared to those vaccinated with Ova adjuvanted with Alum (Figure 3) indicating that the increased CD4 expansion at 5 DPI was not sufficient to enhance IgG1 antibody secretion. No measurable antigen specific IgG2c was identified at this time point. What is evident is that the magnitude of $CD4^+$ T cell expansion did not directly translate to more antibody production. How naïve T cells are influenced during antigen presentation to commit to a lineage important for B cell help and antibody production appears to be of vital importance.

Optimal high-affinity antibody responses are dependent on $CD4^+$ T cell help in the context of cytokines and co-stimulatory ligation towards antigen-specific B cells in the germinal centers formed in the secondary lymphoid tissue [4, 19-23]. The $CD4^+$ T cell subset critical for germinal center formation and maintenance are the T follicular helper cells defined by increased expression of CXCR5, allowing for follicle localization, and PD-1 [4, 19, 24]. We employed low frequency adoptive transfer techniques to examine the Ova-specific $CD4^+$ T cells of the Tfh phenotype ($CXCR5^{high}$ $PD\text{-}1^{high}$) at an early time point post-immunization of polyanhydride nanoparticle vaccines. All polyanhydride nanoparticles induced a shift towards Tfh lineage commitment compared to soluble antigen alone both in a percentage of gated donor $CD4^+$ T cells as well as total Tfh cell numbers (Figure 4). Alum adjuvanted vaccines, although demonstrating robust T cell expansion in the high frequency transfer model (Figure 1), show little difference from soluble antigen groups in terms of $CD4^+$ T cell expansion, as well as Tfh commitment (Figure 4),

most likely due to the differences in naïve precursor frequency between the two models.

T follicular helper cell differentiation is largely dependent on cytokine influence and prolonged antigen presentation by APCs. Disruption in type I IFNs, IL-6, and IL-12 leads to impaired Tfh cell generation as well as impaired humoral immune responses [20, 21, 25-27]. Prolonged antigen presentation either by continuous dendritic cell presentation in cases of abundant antigen or by B cells in the T-B border of the germinal center in cases of sparse antigen drive the differentiation of Tfh [22, 24]. Interesting hypotheses emerge when relating the controlled release antigen kinetics of the polyanhydride nanoparticles and how that controlled release of antigen may be allowing for continuous DC presentation or by providing a continuous antigen immune complex directly ligating B cells in the follicle. The latter hypothesis may also answer why the humoral phenotype of polyanhydride nanoparticle vaccines show a dominant antigen specific IgG1 isotype with lesser amounts of IgG2c (Figure 5) indicating greater amounts of IL-4 than IFN-γ [28]. Tfh cells produce abundant amounts of IL-4 again reinforcing the Tfh lineage commitment of $CD4^+$ T helper cells by polyanhydride nanoparticle vaccines [23]. These antigen specific $CD4^+$ Tfh cells are present in the secondary lymphoid tissue in greater amounts at 45 DPI in those mice receiving nanoparticle regimens translating to greater and more sustained activated ($CD23^{high}$) B cells that are PNA^+ (Figure 6). These sustained T cell and B cell GC interactions translate to stronger IgG1 antibody populations post-primary immunization (Figure 5 and 6C) as compared to equivalent protein unadjuvanted. The antibody avidity of the

polyanhydride nanoparticle vaccines was greater at 45 DPI, indicating stronger and longer GC kinetics and a better quality of antibody generated from polyanhydride nanoparticle vaccines.

5. Conclusions

The work presented herein outlines the $CD4^+$ T cell responses that are modulated by the polyanhydride nanoparticle platform leading to the long-lived IgG1 antibody titers characteristic of the polyanhydride platform. These mechanistic understandings of the platform will translate to improved vaccine design when utilizing the polyanhydride nanoparticle platform for vaccines against viral and bacterial pathogens.

6. References

[1] Murphy K, Travers P, Walport M. Janeway's Immunobiology. In: Lawrence E, editor. Janeway's Immunobiology. Seventh ed. New York, NY: Garland Science, 2008: 111-77.

[2] Allen CDC, Okada T, Cyster JG. Germinal-center organization and cellular dynamics. Immunity 2007;27(2):190-202.

[3] Reinhardt RL, Liang H-E, Locksley RM. Cytokine-secreting follicular T cells shape the antibody repertoire. Nature Immunology 2009;10(4):385-93.

[4] King C, Tangye SG, Mackay CR. T follicular helper (TFH) cells in normal and dysregulated immune responses. Annual Review of Immunology 2008;26(1):741-66.

[5] Schwickert TA, Lindquist RL, Shakhar G, Livshits G, Skokos D, Kosco-Vilbois MH, et al. In vivo imaging of germinal centres reveals a dynamic open structure. Nature 2007;446(7131):83-7.

[6] Kipper MJ, Wilson JH, Wannemuehler MJ, Narasimhan B. Single dose vaccine based on biodegradable polyanhydride microspheres can modulate immune response mechanism. Journal of Biomedical Materials Research Part A 2006;76A(4):798-810.

[7] Ulery BD, Kumar D, Ramer-Tait AE, Metzger DW, Wannemuehler MJ, Narasimhan B. Design of a protective single-dose intranasal nanoparticle-based vaccine platform for respiratory infectious diseases. PLoS ONE 2011;6(3):e17642.

[8] Carrillo-Conde B, Schiltz E, Yu J, Chris Minion F, Phillips GJ, Wannemuehler MJ, et al. Encapsulation into amphiphilic polyanhydride microparticles stabilizes *Yersinia pestis* antigens. Acta biomaterialia 2010;6(8):3110-9.

[9] Ulery B, Phanse Y, Sinha A, Wannemuehler M, Narasimhan B, Bellaire B. Polymer chemistry influences monocytic uptake of polyanhydride nanospheres. Pharmaceutical Research 2009;26(3):683-90.

[10] Torres MP, Wilson-Welder JH, Lopac SK, Phanse Y, Carrillo-Conde B, Ramer-Tait AE, et al. Polyanhydride microparticles enhance dendritic cell antigen presentation and activation. Acta biomaterialia 2011;7(7):2857-64.

[11] Petersen LK, Ramer-Tait AE, Broderick SR, Kong C-S, Ulery BD, Rajan K, et al. Activation of innate immune responses in a pathogen-mimicking manner by amphiphilic polyanhydride nanoparticle adjuvants. Biomaterials 2011;32(28):6815-22.

[12] Ulery BD, Petersen LK, Phanse Y, Kong CS, Broderick SR, Kumar D, et al. Rational design of pathogen-mimicking amphiphilic materials as nanoadjuvants. Scientific Reports 2011;1.

[13] Torres MP, Vogel BM, Narasimhan B, Mallapragada SK. Synthesis and characterization of novel polyanhydrides with tailored erosion mechanisms. Journal of Biomedical Materials Research Part A 2006;76A(1):102-10.

[14] Conix A. Poly[1,3-bis(p-carboxyphenoxy)-propane anhydride]. Macro Synth 1966(2):95-8.

[15] Shen E, Pizsczek R, Dziadul B, Narasimhan B. Microphase separation in bioerodible copolymers for drug delivery. Biomaterials 2001;22(3):201-10.

[16] Rasband WS. ImageJ. 1.44 ed. Bethesda, Maryland, USA: U. S. National Institutes of Health.

[17] Moon JJ, Chu HH, Hataye J, Pagan AJ, Pepper M, McLachlan JB, et al. Tracking epitope-specific T cells. Nature Protocols 2009;4(4):565-81.

[18] Chavez-Santoscoy AV, Huntimer LM, Ramer-Tait AE, Wannemuehler M, Narasimhan B. Harvesting murine alveolar macrophages and evaluating cellular activation induced by polyanhydride nanoparticles. Journal of Visualized Experiments 2012(64):e3883.

[19] Fazilleau N, Mark L, McHeyzer-Williams LJ, McHeyzer-Williams MG. Follicular helper T cells: lineage and location. Immunity 2009;30(3):324-35.

[20] Eddahri F, Denanglaire S, Bureau F, Spolski R, Leonard WJ, Leo O, et al. Interleukin-6/STAT3 signaling regulates the ability of naive T cells to acquire B-cell help capacities. Blood 2009;113(11):2426-33.

[21] Ma CS, Suryani S, Avery DT, Chan A, Nanan R, Santner-Nanan B, et al. Early commitment of naive human CD4(+) T cells to the T follicular helper (T(FH)) cell lineage is induced by IL-12. Immunology and Cell Biology 2009;87(8):590-600.

[22] Deenick EK, Chan A, Ma CS, Gatto D, Schwartzberg PL, Brink R, et al. Follicular helper T cell differentiation requires continuous antigen presentation that is independent of unique B cell signaling. Immunity 2010;33(2):241-53.

[23] Vijayanand P, Seumois Gg, Simpson LJ, Abdul-Wajid S, Baumjohann D, Panduro M, et al. Interleukin-4 production by follicular helper T cells requires the conserved Il4 enhancer hypersensitivity site V. Immunity 2012;36(2):175-87.

[24] Deenick EK, Ma CS, Brink R, Tangye SG. Regulation of T follicular helper cell formation and function by antigen presenting cells. Current Opinion in Immunology 2011;23(1):111-8.

[25] Cucak H, Yrlid U, Reizis B, Kalinke U, Johansson-Lindbom B. Type I interferon signaling in dendritic cells stimulates the development of lymph-node-resident T follicular helper cells. Immunity 2009;31(3):491-501.

[26] Suto A, Kashiwakuma D, Kagami S, Hirose K, Watanabe N, Yokote K, et al. Development and characterization of IL-21-producing $CD4^+$ T cells. Journal of Experimental Medicine 2008;205(6):1369-79.

[27] Dienz O, Eaton SM, Bond JP, Neveu W, Moquin D, Noubade R, et al. The induction of antibody production by IL-6 is indirectly mediated by IL-21 produced by CD4+ T cells. Journal of Experimental Medicine 2009;206(1):69-78.

[28] Deenick EK, Hasbold J, Hodgkin PD. Decision criteria for resolving isotype switching conflicts by B cells. European Journal of Immunology 2005;35(10):2949-55.

CHAPTER 7: POLYANYHYDRIDE NANOPARTICLE H5N1 VACCINE ELICITS VIRAL NEUTRALIZING TITERS AND CELLULAR IMMUNITY

Lucas Huntimer, Kathleen A. Ross, Wuwei Wu, Susan Carpenter, Balaji Narasimhan, and Michael J. Wannemuehler

To be submitted to the Journal of Virology

Abstract

Influenza virus infections remain one of the most common and costly illnesses throughout the world. Because of the high mutation rates and possibilities for co-infections with different strains of influenza virus leading to genetic reassortment, global pandemics of influenza infection are an alarming possibility. One potential influenza strain that could lead to global pandemics, due to the human naivety to the virus, is H5N1. Therefore, development of efficacious vaccines designed against H5N1 which are safe and induce protective immunity are of incredible import. Bio-erodible polyanhydride nanoparticles provide a particulate structural context for delivery of encapsulated subunit immunogens as well as innate immunomodulatory activities in vivo. Herein, we characterize H5-specific humoral and cellular immune responses induced following vaccination with polyanhydride nanoparticles based vaccines. Immunizations consisted of combinations of soluble and encapsulated recombinant trimeric H5 (influenza A*/Whooper Swan/Mongolia/*244/05) protein and encapsulated synthetic innate immunostimulatory ligands to activate the

inflammasome pathway (poly dA:dT) or TLR 3 (Poly I:C). The results of these studies show that vaccines utilizing encapsulated H5-Trimer with encapsulated Poly I:C generated viral neutralizing antibody titers as well as significant H5-specific $CD4^+$ T cell recall responses when administered subcutaneously or intranasally. Collectively, these studies demonstrate the successful design of a polyanhydride-based anti-H5 nanoparticle vaccine with balanced humoral and cellular immune efficacy.

1. Introduction

The 2009 H1N1 influenza pandemic demonstrated that a novel influenza virus can efficiently spread worldwide by unwittingly infected international travelers [1]. Less than a year after identification of the novel triple re-assortment (human, swine, and avian) H1N1 virus, it had spread to 215 countries and resulted in 18,000 reported deaths [2]. Epidemiological studies following the pandemic reinforced the impact that efficacious preventive therapies, mainly immunization, have in controlling spread and severity of infections [3, 4]. The CDC estimates seasonal influenza infections leads to $10 billion in direct healthcare costs annually [5].

Highly pathogenic avian influenza (HPAI) H5N1 has long been monitored because of its potential as a pandemic influenza strain to which humans are relatively immunologically naïve. HPAI H5N1 is an avian virus demonstrating hemagglutinin (HA) binding specificity to α 2-3 sialic acid receptors found in high density in the avian respiratory tract and very low density in the human respiratory tract (mostly α 2-6 sialic acid receptors present). The greater concern with HPAI is

the clinical severity of humans with confirmed infection. Hyper-cytokinemia as well as viral replication in tissue sites beyond the lung are attributes of the pathogenesis associated with human infection with H5N1 influenza [6-8].

Although the immune-pathology of HPAI infected individuals is severe mammalian viral transfer does not occur. Currently, mammalian viral transfer has only been demonstrated in ferret models driving the adaptation of H5N1 virus [9, 10]. However, if sufficient pressure to push the virus to evolve towards mammalian viral transfer occurs, the pandemic potential of HPAI H5N1 dramatically increases. Therefore, great emphasis has been placed on the development and implementation of pre-pandemic therapeutic interventions against H5N1, in particular, safe and efficacious vaccines [11-21].

Polyanhydrides based on copolymer combinations of aromatic polyanhydrides 1,6-bis(*p*-carboxyphenoxy) hexane (CPH), and 1,8-bis(*p*-carboxyphenoxy)-3,6-dioxaoctane (CPTEG) are unique biomaterials that can provide a protein stablizing amphiphilic environment as well as provide for the controlled release of protein immunogens [22-25]. These materials can be tailored to generate particulate structures for optimizing uptake by innate phagocytic cells [26-28]. The polyanhydride particles exhibit inherent immunomodulatory activity in vitro by activating antigen presenting cells (APCs) [27, 29] and in vivo by increasing monocyte chemotactic cytokine production (MCP-1 and IP-10) as well as by inducing mild inflammatory reactivity while minimizing tissue damage at the administration site (Chapter 4). Encapsulation of antigen into polyanhydride microparticles resulted in an enhanced antibody titer when vaccinating with an

otherwise suboptimal dose of protein (Chapter 3) and increased the antibody titer and antibody avidity to tetanus toxoid [30]. The use of a single dose nanoparticle vaccine induced protective immunity from *Yersinia pestis* challenge after intranasal (IN) administration of soluble plus encapsulated F1-V antigen [31]. In addition, studies using the model antigen ovalbumin (Ova) and transgenic T cells specific for Ova (OTI and OTII) revealed the ability to significantly increase the numbers antigen-specific cytotoxic T cell (Chapter 4) as well as T follicular helper cells (Chapter 6) when mice were immunized with vaccine formulations containing antigen-loaded polyanhydride nanoparticles.

Herein, we outline the evaluation of nanoparticle vaccine regimen using a stabilized trimeric form of the recombinant H5 hemagglutinin from the A*/Whooper Swan/Mongolia/*244/05 strain of influenza virus (Wu et al., Appendix). The adaptability of the platform is demonstrated by the ability to increase $CD4^+$ and $CD8^+$ T cell memory populations in the draining lymph nodes by including pattern recognition receptor (PRR) ligands in the vaccine formulation. Viral neutralizing anti-H5 antibody responses were elicited using single and multiple dose immunization strategies. These data indicate the effectiveness of the polyanhydride nanoparticle platform to enhance both antigen-specific cellular immune responses as well as elicit viral neutralizing antibody against a potentially pandemic strain of influenza virus.

2. Materials and Methods

2.1 Synthesis and characterization of copolymers

CPH and CPTEG monomers were synthesized using the chemicals listed: 4-p-hydroxybenzoic acid, 1,6-dibromohexane, 1-methyl-2-pyrrolidinone, and tri-ethylene glycol. All these chemicals and sebacic acid (99%) were purchased from Sigma Aldrich (St. Louis, MO); 4-p-fluorobenzonitrile was obtained from Apollo Scientific (Cheshire, UK); potassium carbonate, dimethyl formamide, toluene, sulfuric acid, acetic acid, acetonitrile, acetic anhydride, methylene chloride, and petroleum ether were purchased from Fisher Scientific (Fairlawn, NJ). Synthesis of CPH and CPTEG diacids was performed as previously described [24, 32]. 20:80 CPTEG:CPH was synthesized using a melt polycondensation process as detailed by Kipper et al. and Torres et al., [24, 30] respectively. The degree of polymerization, molecular weight, and polymer purity were determined using ^{1}H nuclear magnetic resonance (NMR) spectroscopy (Varian VXR-300 MHz, Palo Alto, CA).

2.2 Particle fabrication and characterization

Antigen-loaded nanoparticles (4.0 % w/w) were fabricated using a modified anti-solvent nanoencapsulation method outlined in Ulery et al [28]. Particles functionalized with poly I:C or poly dA:dT (Invivogen San Diego, CA) were loaded at (1.0 % w/w). Briefly, H5-T was concentrated into 100 µL of nanopure water (20 mg/mL) and homogenized for 90 seconds with the copolymer dissolved in methylene chloride at 4˚C. The copolymer solution was rapidly transferred into chilled pentane (-20 °C) at a non-solvent to solvent ratio of 250:1, and the suspension of nanoparticles was vacuum filtered to recover the nanoparticles. Shape and size of

the resulting nanoparticles were characterized using scanning electron microscopy (SEM) (FEI Quanta 250, FEI, Hillsboro, OR). The particle size distribution was obtained from SEM images using Image J version 1.44 image analysis software [33]. An average of 200 particles per image was analyzed.

2.3 Mice and immunization procedures

BALB/c mice were purchased from Harlan Sprague Dawley (Frederick, MD). All animal procedures were conducted with the approval of the Iowa State University Institutional Animal Care and Use Committee. To evaluate the serum antibody responses to H5-T induced by administration of polyanhydride nanoparticle vaccines and control vaccines adjuvanted with MPLA or unadjuvanted sH5-T diluted in pyrogen-free saline. H5-T is a recombinant protein of the full length H5 (A*/Whooper Swan/Mongolia/*244/05) hemagluttinin (HA) minus the cytoplasmic tail. This construct was stabilized with an isoleucine zipper motif as described in Wu et al (Appendix). Prior to administration, nanoparticles were sonicated briefly to generate a uniform suspension. A total volume of 250 μL was administered at the subcutanous (SC) injection site (nape of the neck) and a total volume of 50 μL was administered intranasally (IN). Separate groups of mice (n=12, multiple immunizations n=6 and single immunizations n=6) were immunized as outlined in Table 1. Control animals received saline alone (n=8). Blood samples were collected from the left saphenous vein prior to immunization and at indicated time points thereafter. Serum was collected after centrifugation and stored at -20 °C until assayed for H5-T-specific antibody as described below. At termination of the study,

bronchioalveolar lavage fluid (BAL) was collected via methods outlined in Chavez-Santoscoy et al [34].

2.4 Flow cytometric bead assay for antigen specific antibody

Carboxylated xMAP magnetic beads (Luminex, Austin, TX) were conjugated with 10 µg of H5-T per 1.25 x 10^6 (037 fluorescent signature) beads according to manufacturer's instructions. Serum samples were diluted 1:200 in blocking-storeage buffer supplemented with Tween 20 (BST) (PBS with 1% bovine serum albumin, 0.05% sodium azide, 0.05% Tween 20). BAL protein concentrations were normalized to 0.5 mg/mL with PBS supplemented with 0.05 % Tween 20 prior to assay and this was considered a "neat" concentration. Diluted serum samples or neat BAL (50 µL) was then incubated for 1 h at RT with 6000 beads conjugated with H5-T per well. Beads were washed with BST and incubated for 1 h at RT with 0.5 µg/well of biotinylated anti-mouse IgG antibody or biotinylated anti-mouse IgA heavy chain (eBioscience, San Diego, CA) antibody diluted in BST. Beads were washed and incubated for 30 min at RT with 0.5 µg/mL of streptavidin-phycoerythrin (eBioscience). Beads were washed once more and then fluorescence was quantified using the Bio-Plex Pro 200 (Bio-Rad, Hercules, CA).

2.5 Assaying for memory T and B cell proliferative populations

Draining lymph nodes (e.g., brachial and axilary) from individual mice were harvested at 63 days post-immunization and homogenized into single cell suspensions. Single cell populations were labeled with 2.5 µM 5-(and-6)-carboxyfluorescein diacetate, succinimidyl ester (5(6)-CFDA, SE) (CFSE) (Life Technologies, Grand Island, NY). Cells (2.5 x 10^5/well) were incubated for 96 h at 37

°C in 5 % CO_2 in 96 well U-bottom plates along with 0.5 µg/well of H5-T . Cells were aspirated and lymphocyte proliferation was quantified using flow cytometry (BD FACScanto). Cell suspensions were blocked to prevent non-specific antibody binding using 0.1 mg/mL rat IgG (Sigma Aldrich, St. Louis, MO) and mouse anti-CD16/32 (10 µg/mL , eBioscience, San Diego, CA). Fluorescently conjugated antibodies for CD4 ((PE-Cy7, Clone GK1.5, eBioscience), CD8ß (APC, Clone eBioH35-17.2, eBioscience), and CD19 (PerCP Cy5.5, eBio H35-17.2, eBioscience), to delineate T cells and B cells, were used to stain in FACS buffer, gate, and quantify specific cell populations.

2.6 Neutralizing antibody quantification using pseudovirus

Influenza H5-pseudotyped retroviral vectors carrying a luciferase (Luc) reporter gene were produced in 293T cells by co-transfecting 5 µg of pEV-53B and 5.5 µg of plgSIN6.1Luc with 1 µg of HA expression plasmid DNA containing the H5 gene from H5N1 influenza strains A/Vietnam/1203/2004 (clade1) or A/Whooper Swan/244/Mongolia/ 05 (clade 2.2). At 18h post-transfection, cells were fed with fresh medium containing 7 mU/ml of bacterial nucleic acid (*Vibrio cholera* Type II, Sigma, St. Louis, MO) and 1M NaB to induce the release of H5-pseudovirions (H5-VietnamLuc and H5-WhooperLuc).Supernatants were collected 48 h post-transfection, clarified by centrifugation at 3000 rpm for 10 min, and the viral stocks were then stored frozen at −80^{o}C.

Sera samples were heat inactivated at 56^{o}C for 30 min, serially diluted threefold in culture medium containing 16 µg/ml of polybrene (Sigma, St. Louis, MO), and mixed with an equal volume of diluted pseudoviruses containing 5 × 10^4 relative

light units (RLU)/mL. After incubation at 37°C for 1h, virus and serum mixtures were added into 96-well plates containing 2 x 10^4 293T cells per well. Infectivity was evaluated 48 h after infection using One-Glo Luciferase assay system (Promega, Fitchburg, WI).

2.7 Statistical analysis

Longitudinal data were analyzed using repeated measure analysis of variance (ANOVA) models (with Graphpad Prism 5.0). Treatment and time were fixed effects in the statistical model, whereas mouse was the subject of repeated measures. Cross-sectional data were analyzed using one-way ANOVA models with treatment as the explanatory variable. Differences in mean responses among treatments were compared by using Tukey's T-test. Log_{10} transformation was applied to responses with skewed distributions before analyses. Statistical tests with $p \leq 0.05$ were regarded as significant.

3. Results

3.1 Neutralizing antibody responses are elicited following single dose and prime/boost immunization regimens administered subcutaneously.

Using polyanhydride nanoparticles encapsulating either poly dA:dT or poly I:C, three formulations of an H5N1 influenza subunit vaccine were fabricated using a stable trimer of recombinant H5 HA. The nanoparticles were loaded with the H5-T at 0.4 % (w/w) The immunization regimens (Table 1) were designed based on the protection results elicited by a ratio combination soluble antigen and encapsulated regimen demonstrated in a *Yersinia pestis* challenge model [31]. Additional particles

encapsulating poly I:C and poly dA:dT were included to evaluate the benefits associated with increased innate signaling relative to enhancing the induction of neutralizing serum antibody response with a single primary immunization as compared to the multiple dose regimens (primary dose day 0, second immunization day 21, third immunization day 42). As a positive control, mice were immunized with 10 μg H5-T adjuvanted with MPLA given as a single dose or administered as a multiple dose regimen consistent with previously published reports [35] .

Table 1. H5N1 polyanhydride and control vaccine formulations.

Group	Abbreviation	Total 20:80 CPTEG:CPH Nanoparticles (μg)	Soluble antigen dose (H5-T in μg)	Encapsulated antigen dose (H5-T)	PRR Ligand	PRR Ligand Dose (μg)
Soluble H5-T + H5-T encapsulated in 20:80 CPTEG:CPH + 250 μg unloaded 20:80 CPTEG:CPH	**20:80 C:C**	300	8.0	2.0	----------	----------
Soluble H5-T + H5-T encapsulated in 20:80 CPTEG:CPH + 250 μg 1% Poly I:C loaded 20:80 CPTEG:CPH	**20:80 C:C Poly I:C**	300	8.0	2.0	Poly I:C	2.5
Soluble H5-T + H5-T encapsulated in 20:80 CPTEG:CPH + 250 μg 1% Poly dA:dT loaded 20:80 CPTEG:CPH	**20:80 C:C Poly dA:dT**	300	8.0	2.0	Poly dA:dT	2.5
Soluble H5-T + MPLA	**MPLA**	----------	10	----------	MPLA	10
Soluble H5-T	**sH5-T**	----------	10	----------	----------	----------
PBS	**PBS**	----------	----------	----------	----------	----------

Table 1.
Table describes the details of the immunization regimens designed using the polyanhydride nanoparticle platform and control immunzations MPLA, sH5-T, and PBS.

Following a single immunization, the 20:80 CPTEG:CPH polyanhydride nanoparticle platform alone significantly enhanced the induction of H5-specific

antibody at 42 DPI (Figure 1A) when compared to the response induced by soluble H5-T alone (sH5-T). Inclusion of poly I:C encapsulated particles in the vaccine regimen also enhanced antibody to near equivalent levels to those induced in mice immuniced with H5-T adjuvanted with MPLA. At day 63 post-primary immunization the same trends in antibody responses were observed as compared to the day 42 data (Figure 1C). Multiple dose immunization regimens provided strong serum antibody responses throughout all groups at 42 days post-immunization (Figure 1B) with little statistical differences between groups other than MPLA providing the best response. The same results were observed at 63 DPI with no statistical differences between immunization groups other than statisical differences above the sham (PBS) vaccine (Figure 1D).

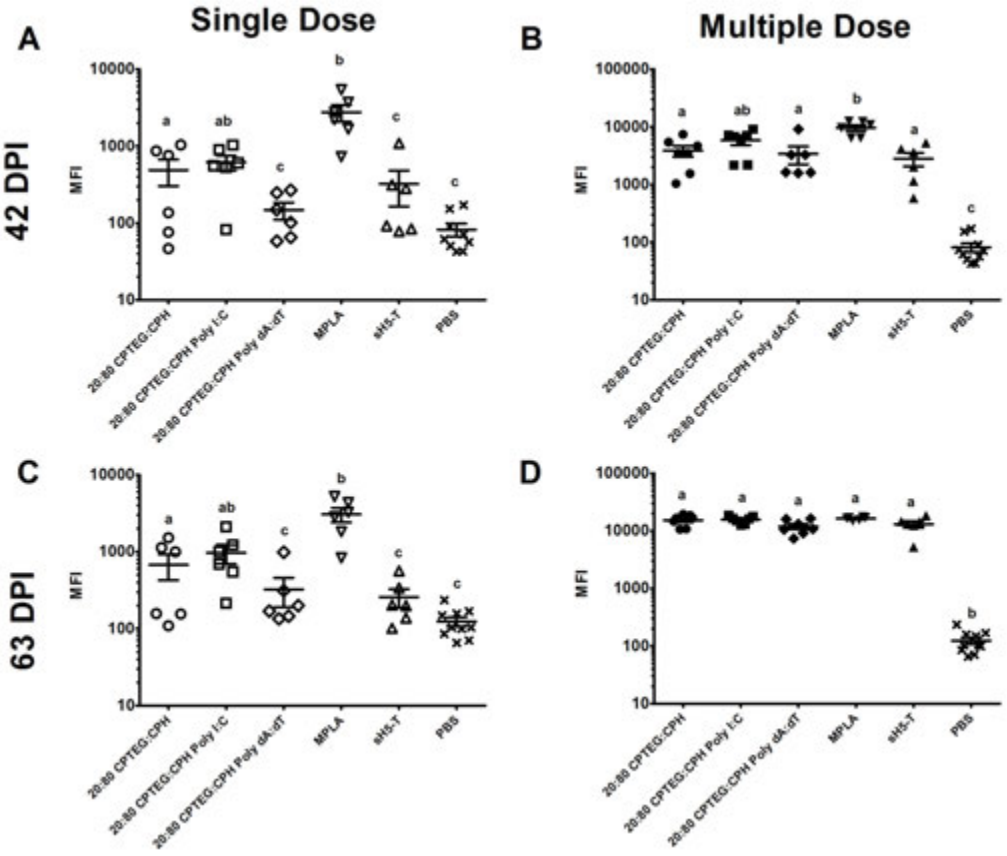

Figure 1. Subunit anti-H5 influenza vaccines show strong antibody responses in multiple dose regimens. H5-T specific antibody quantified using Luminex based system expressed in mean fluorescence intensity of bead at day 42 post subcutaneous immunization (A-B) and day 63 (C-D). Serum was diluted 1:200 in PBS-T prior to assay. Mice were immunized with immunization regimens described in table 1: 20:80 CPTEG:CPH, 20:80 CPTEG:CPH Poly I:C, 20:80 CPTEG:CPH Poly dA:dT, MPLA, sH5-T, and PBS. Six mice per group were immunized with a single dose and followed for antigen specific antibody responses at 42 days post-immunization (A) and 63 DPI (B). Six mice per group were immunized with multiple immunizations at day 0, 21, and 42 DPI and followed for antigen specific antibody responses at 42 DPI (C) and 63 DPI (D). Values were log transformed for statistical analysis. Different letters above each set of data points indicates statistical difference from groups at a P value < 0.05 value obtained via one-way ANOVA with Tukey's post-test. Results are from a single experiment.

Viral neutralizing titers were assayed via pseudovirus expression system using homologous HA. The multiple dose immunizations show generally higher antibody responses in magnitude and neutralizing antibody titers at day 42 than were induced by the single dose regimen (Figure 2A-B). Little neutralizing antibody titers were elicited from any single dose immunization regimen other than MPLA at day 42 and day 63 (Figure 2A and C). By day 63 after multiple immunizations, all groups have effectively mounted robust neutralizing antibody titer (Figure 2D).

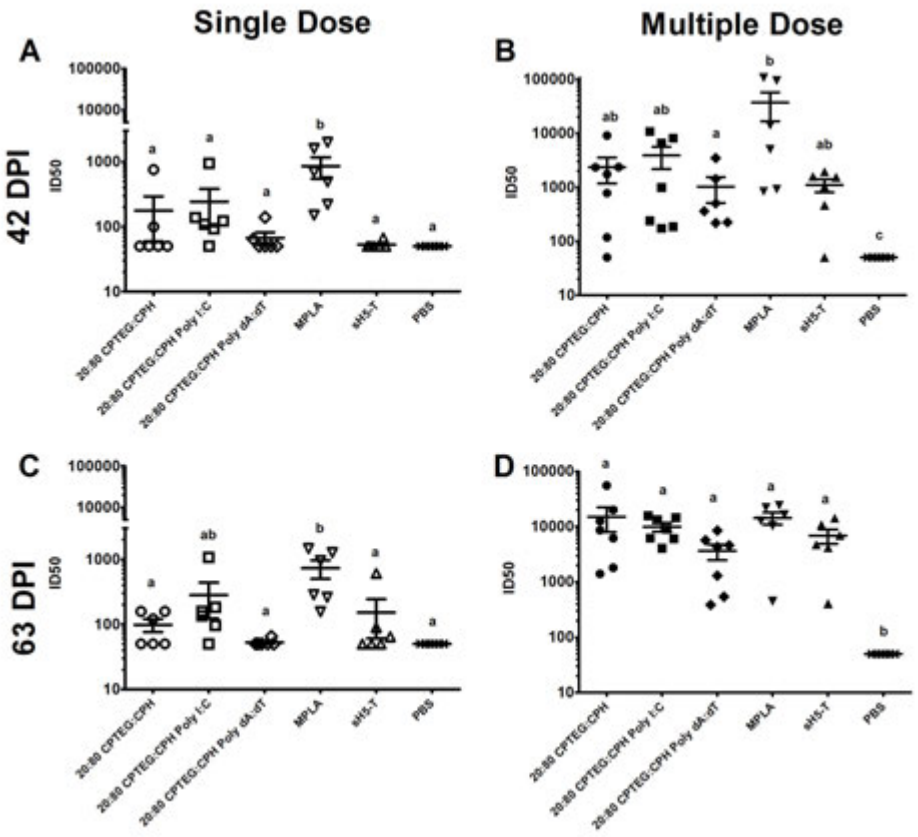

Figure 2. Subunit anti-H5 influenza vaccines show strong neutralizing antibody responses in multiple dose regimens. H5-T specific neutralizing antibody responses were evaluated using a H5 HA pseudotyped reporter virus and results reported as the inverse serum dilution that neutralized 50% of virus infectivity (ID50). Mice were immunized with immunization regimens described in table 1: 20:80 CPTEG:CPH, 20:80 CPTEG:CPH Poly I:C, 20:80 CPTEG:CPH Poly dA:dT, MPLA, sH5-T, and PBS. Six mice per group were immunized with a single dose and followed for antigen specific antibody responses at 42 days post-immunization (A) and 63 DPI (B). Six mice per group were immunized with multiple immunizations at day 0, 21, and 42 DPI and followed for antigen specific antibody responses at 42 DPI (C) and 63 DPI (D). Values were log transformed for statistical analysis. Different letters above each set of data points indicates statistical difference from groups at a P value < 0.05 value obtained via one-way ANOVA with Tukey's post-test. Results are from a single experiment.

3.2 $CD4^+$ T cell memory is enchanced by prime/boost immunization of anti-H5N1 with Poly I:C encapsulated in polyanhydride nanoparticles

On day 63, draining lymph nodes were extracted from the immunized mice, homogenized to a single cell suspension, labeled with CFSE, and incubated with H5-T antigen for 96 hours to measure antigen-specific proliferative responses indicative of memory populations. We identified that multiple immunizations induced more robust T cell memory responses, but more $CD4^+$ T cells capable of proliferating to the cognate antigen were observed in the T cell populations recovered from H5-T immunized mice also treated with the 20:80 C:C poly I:C multidose polyanhydride vaccine (Figure 3A). Similar antigen-specific proliferative responses were demonstrable when assessing $CD8^+$ T cell recall responses in the 20:80 C:C Poly I:C multidose group as well (Figure 3B).

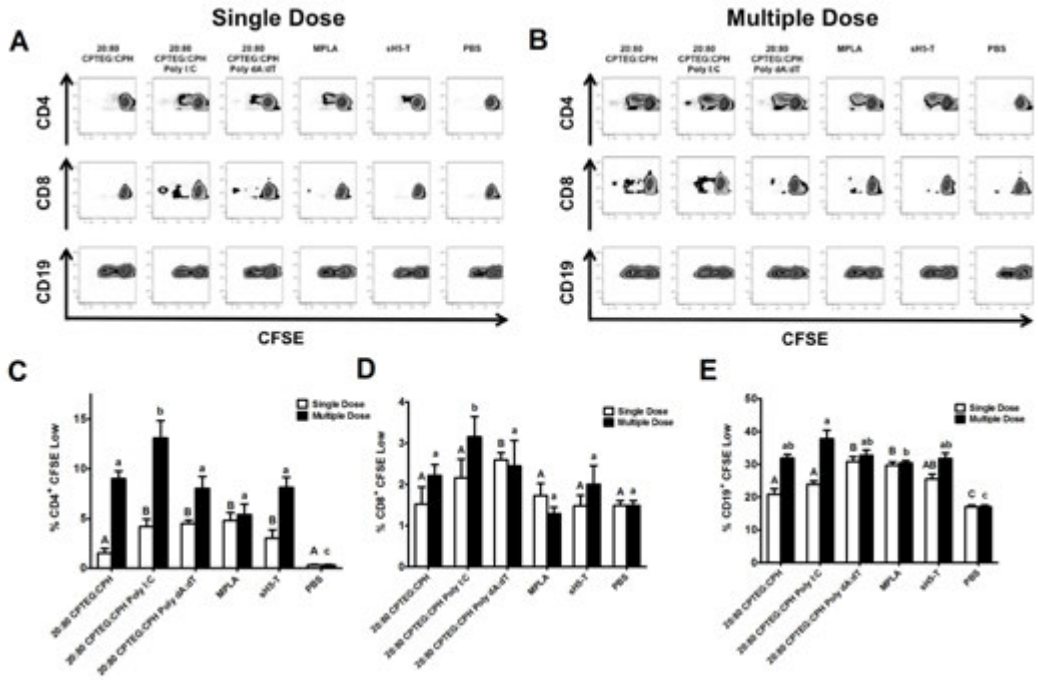

Figure 3. Robust cellular memory responses are obtained by inclusion of encapsulated Poly I:C in anti-H5 influenza polyanhydride nanoparticle vaccines. Single cell suspensions of draining lymph nodes cells were CFSE labeled and incubated with H5-T antigen for 96 hours. Cells were then aspirated and labeled with anti-CD4, anti-CD8, and anti-CD19 antibodies for FACS analysis. Representative FACS histograms draining lymph node cells labeled with cell marker (CD4, CD8, or CD19) on y-axis and of CFSE on x-axis of mice immunized with single dose immunizations (A) or multiple dose immunizations (B). Histograms are mean results of CFSE low gated cell populations indicating proliferation of single immunized groups (open histogram) or multiple dose immunizations (black histograms). Mean CFSE low populations of gated $CD4^+$ T cells (A), $CD8^+$ T cells (B) and $CD19^+$ B cells (C). Different letters above indicates statistical difference between the treatment groups (n = 6) within the single dose (upper case letter) or multiple dose (lower case letters) treatment groups. Data was analyzed using a one-way ANOVA with Tukey's post-test and significance was defined as $P \leq 0.05$. Results are from a single experiment.

3.3 Single dose intranasal adjuvanted vaccine formulations show strong short-lived antibody responses

After evaluating the immune responses following administration of the various H5 vaccine formulations by the subcutaneous route, the efficacy of these same vaccine formulations following intranasal (mucosal) administered was evaluated. Previously our group has demonstrated the ability to induce protective immunity against *Yersinia pestis* using an intranasal vaccine based on the polyanhydride nanoparticle platform [31]. It was hypothesized that the antibody responses of the H5 vaccine designed using the 20:80 CPTEG:CPH nanoparticles would be enhanced by immunizing via a mucosal route in comparison to a systemic route.

The same vaccine regimen were employed as outlined in Table 1 with the only change being the route of administration. In the absence of poly I:C or poly dA:dT nanoparticles, a single administration of the H5 polyanhydride nanoparticle formualtion alone failed to induce a demonstrable anti-H5 specific antibody response (Figure 4A and C). All other single dose immunizations show strong antibody responses compared to sham vaccines in contrast to subcutaneous immunizations (Figure 1 and 2) which show little induction of antibody with single doses. For the single dose vaccine regimen used, the peak antibody responses occurred at 42 DPI with antibody magnitude waning at 63 DPI. While not optimal, the multiple dose regimen of the H5-loaded nanoparticles did induce measurable HA-specific antibody at 42 DPI and remained strong at 63 DPI (Figure 4B and D). Little differences in magnitude of the antibody responses were elicited by adjuvanted and non-adjuvanted vaccines other than the 20:80 CPTEG:CPH group showing lower

antibody responses either in single doses (Figure 4A and C) or multiple doses (Figure 4B and D).

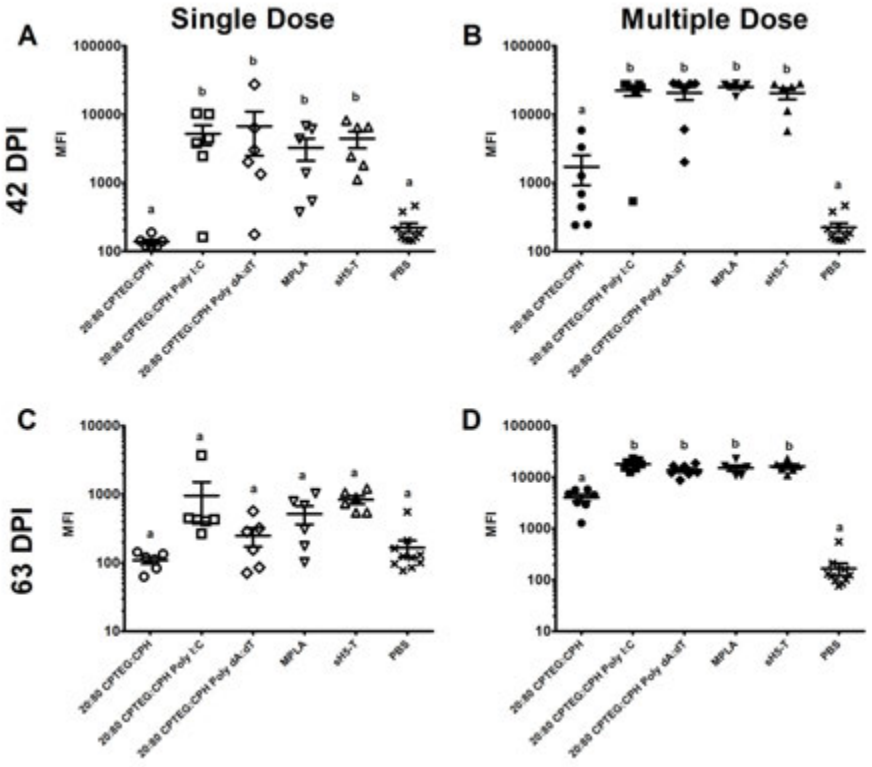

Figure 4. Single dose intranasal immunizations induce strong short lived antibody responses. H5 specific antibody quantified using Luminex based system expressed in mean fluorescence intensity of bead at day 42 post intranasal immunization (A-B) and day 63 (C-D). Serum was diluted 1:200 in PBS-T prior to assay. Mice were immunized with immunization regimens described in table 1: 20:80 CPTEG:CPH, 20:80 CPTEG:CPH Poly I:C, 20:80 CPTEG:CPH Poly dA:dT, MPLA, sH5-T, and PBS. Six mice per group were immunized with a single dose and followed for antigen specific antibody responses at 42 days post-immunization (A) and 63 DPI (B). Six mice per group were immunized with multiple immunizations at day 0, 21, and 42 DPI and followed for antigen specific antibody responses at 42 DPI (C) and 63 DPI (D). Values were log transformed for statistical analysis. Different letters above each set of data points indicates statistical difference from groups at a P value < 0.05 value obtained via one-way ANOVA with Tukey's post-test. Results are from a single experiment.

H5-specific cellular immune responses were evaluated using lymphocytes recovered from the cervical and mediastinal lymph nodes following intranasal immunization. Contrary to the results observed following SC immunization (Figure 2), there was little evidence of enhanced T cell memory was identified (Figure 5A-B). H5-T-specific proliferation of B cells was demonstrated in lymphocytes recovered from mice immunized with MPLA plus H5-T and sH5-T alone.

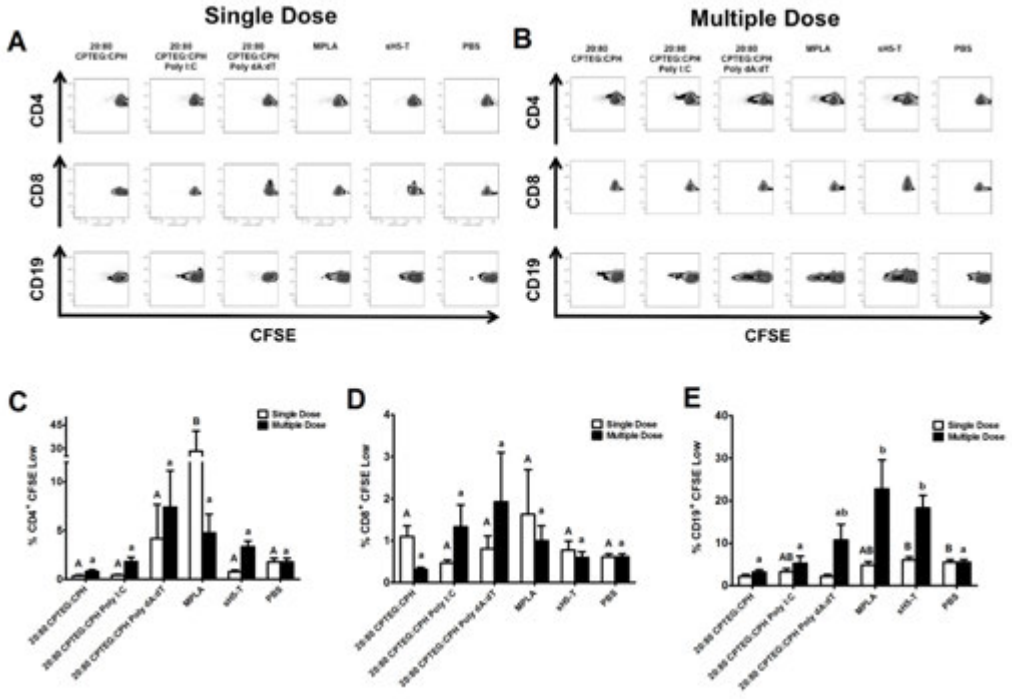

Figure 5. Intranasal H5 polyanhydride nanoparticle formulations elicit little cellular memory in cervical and mediastinal lymph nodes. Single cell suspensions of draining lymph nodes cells were CFSE labeled and incubated with H5-T antigen for 96 hours. Cells were then aspirated and labeled with anti-CD4, anti-CD8, and anti-CD19 antibodies for FACS analysis. Representative FACS histograms draining lymph node cells labeled with cell marker (CD4, CD8, or CD19) on y-axis and of CFSE on x-axis of mice immunized with single dose immunizations (A) or multiple dose immunizations (B). Histograms are mean results of CFSE low gated cell populations indicating proliferation of single immunized groups (open histogram) or multiple dose immunizations (black histograms). Mean CFSE low populations of gated $CD4^+$ T cells (A), $CD8^+$ T cells (B) and $CD19^+$ B cells (C). Different letters above indicates statistical difference between the treatment groups (n = 6) within the single dose (upper case letter) or multiple dose (lower case letters) treatment groups. Data was analyzed using a one-way ANOVA with Tukey's post-test and significance was defined as $P \leq 0.05$. Results are from a single experiment.

3.4 Multiple dose vaccine regimens elicit mucosal IgA in bronchioalveolar lavage fluids Bronchioalveolar lavage (BAL) fluids were evaluated for the presence of antigen-specific IgA. Single dose regimens elicit no demonstrable H5-T-specific antibody in BAL at 63 DPI (Figure 6A). Multiple dose IgA magnitude correlated with systemic antibody magnitude from Figure 3 (Figure 6B).

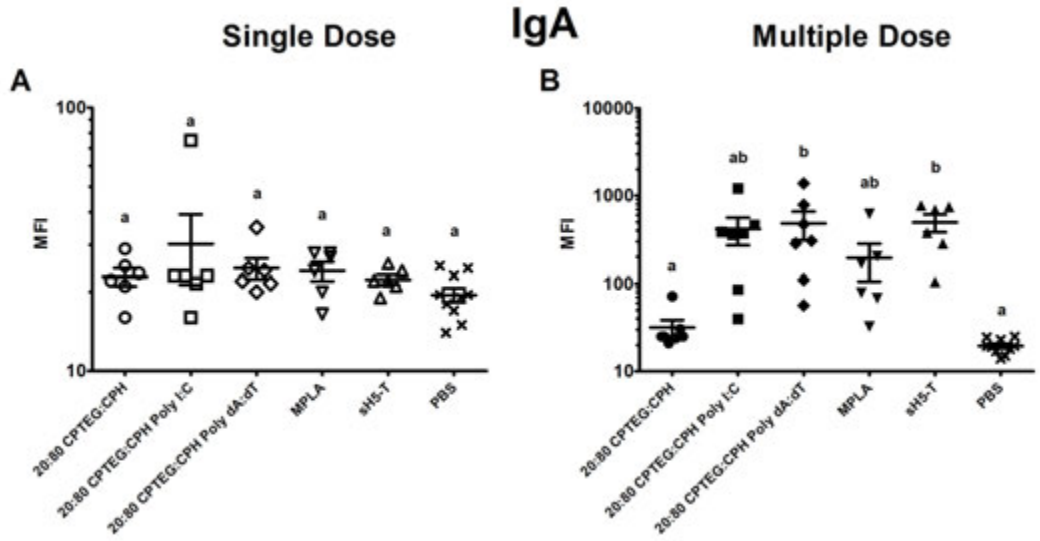

Figure 6. Multiple dose vaccine regimens elicit significant levels of mucosal IgA in bronchioalveolar lavage fluids. H5-T specific antibody quantified using Luminex based system expressed in mean fluorescence intensity of bead at day 63 post single intranasal immunization (A) and multiple dose regimens (B). BAL protein concentrations were normalized to 0.1 mg/mL using PBS prior to sample evaluation. Values were log transformed prior to statistical analysis. Data was analyzed using a one-way ANOVA with Tukey's post-test and significance was defined as $P \leq 0.05$. Results are from a single experiment.

4. Discussion

The need for novel vaccine formulations that increase purity and safety requirements while simultaneosly maintaining or increasing immune efficacy is paramount for next generation vaccine design. The polyanhydride nanoparticle platform combines favorable and unique attributes of adjuvanticity, materials based engineering, and vaccinological design of subunit vaccines. The polyanhydride chemistries used in these studies are readily producible from inexpensive “off the shelf” materials [36]. These polyanhydride biomaterials create a protein favorable environment that maintains immunogenicity of encapsulated protein (subunit) antigens and provides controlled release of those antigens [24, 25, 37-42]. Fabrication techniques of these materials can be altered to create particulate structures that mimic pathogen size crucial for providing a particulate antigenic structure needed for phagocytic antigen presenting cells or bystander cells to take up particles and initiate antigen presentation [27-29, 43]. In vivo profiles of three formulations of polyanhydrides indicate differential inflammation between chemistries with CPTEG:CPH. CPTEG:CPH containing chemistries are more inflammatory as well as being able to elicit more monocyte chemokine activity (Chapter 4 and 5) [44].

Nanoparticles consisting of 20:80 CPTEG:CPH copolymers, which exhibit the slowest in vitro and in vivo degradation kinetics, also elicit inflammatory cytokine secretion in vivo (Chapter 4 and 5). Polyanhydride nanoparticle designed vaccines based on the 20:80 CPTEG:CPH chemistry including the viral PAMP poly I:C were able to elicit neutralizing antibody responses with single doses (Figure 1); however,

these responses were not statistically different from those induced when mice were subcutaneously immunized with H5-T adjuvanted with MPLA. We also examined multiple dose immunization strategies to further expand the cellular and humoral immune responses elicited by the nanoparticle vaccines as the literature and clinical trial data indicate that this regimen is necessary due to the relatively immunologically naivety of the population to the H5 influenza hemagglutinin [7, 8, 45, 46]. The HA immunogen when administered subcutaneously was a weak immunogen and multiple dose regimens were needed to elicit strong neutralizing antibody (Figure 2). The nanoparticle platform release kinetics and immunomodulatory effects were not able to overcome this deficit in single doses. Increased dosages of immunogen and particles should be evaluated. When employing the prime/boost/boost strategy, neutralizing antibody responses were strong throughout all immunized groups (Figure 1 and 2). The best neutralizing antibody responses at 42 DPI (prime/boost) were generated from the 20:80 CPTEG:CPH Poly I:C group and MPLA (Figure 2). At 63 DPI (prime/boost/boost) no difference in antibody and neutralizing antibody between groups was identified.

The greatest changes in adaptive immune responses occurred when examining the T cell recall responses to antigen in the polyanhydride nanoparticle subcutaneous immunization groups that included poly I:C. Statistically significant increases in $CD4^+$ T cell recall responses were observed (Figure 3) as well as significant increases in $CD8^+$ T cell recall responses demonstrating stronger T cell memory populations being elicited from the 20:80 CPTEG:CPH Poly I:C vaccine formulation. The other subcutaneous immunization regimens also show strong $CD4^+$

T cell proliferation so the differences may be slight. Therefore, the benefits of encapsulation of antigen in the polyanhydride platform had more effects on cellular immunity while eliciting strong neutralizing antibody responses when administered subcutaneously.

When evaluating the response profile induced by these polyanhydride vaccines given via a mucosal route (intranasal) the advantages of adjuvanting the protein either with the polyanhydride nanoparticle formulations or with MPLA seemed to have been lost. Interestingly, the 20:80 CPTEG:CPH formulations induced the poorest response especially when compared to soluble H5-T antigen alone. This observation could be the result of high levels of IL-10 elicited by the 20:80 CPTEG:CPH nanoparticles (Chapter 4) and introducing this immune modulation into the lung which is already a highly regulated environment may have resulted in little adaptive immune responses being elicited. The inclusion of PAMPs in the polyanhydride nanoparticle regimens overcame the regulatory effect. The beneficial attributes of enhanced cellular immunity from adjuvanting with polyanhydride nanoparticles appears to be dependent on parenteral routes of immunization (Chapter 4, Figure 3 and 6).

The practical design of subunit influenza vaccines using the polyanhydride platform shown herein demonstrates the malleability of the platform to be adapted to increase immune responses. The H5 influenza vaccines designed for this study showed little differences from adjuvanted vaccines and un-adjuvanted vaccines (sH5-T) though. Encapsulating the antigen into polyanhydride nanoparticles did not lead to detrimental effects as compared to soluble antigen. Alum adjuvanted H5-T

vaccines induced lower antibody responses compared to soluble antigen (Wu et al Appendix). Follow up studies examining dose titrations of antigen and adjuvants need to be performed to truly examine if variable immune responses can be elicited using the nanoparticle platform. Future work should focus on examining efficacy of these designed vaccines within influenza challenge models to truly examine the protective effect of the balanced humoral and cellular responses identified here. Boosting efficacy of influenza vaccines by using inexpensive novel biocompatible technologies can have profound epidemiological effects in controlling pandemic influenza outbreaks worldwide. The platform examined here benefits from being openly accessible to any recombinant antigen or other synthetic patterns needed for optimizing the immune response output. The studies presented herein provide a base evaluation of influenza vaccines designed using the polyanhydride platform even though little differences between designed vaccines were observed. Past work has shown the platform to enhance protein stability, further studies need to examine the glycosylated hemagglutinin protein particle interactions to better understand the platform's capabilities to improve vaccine design.

5. Conclusions:

Influenza vaccines designed using the polyanhydride nanoparticle platform were able to elicit viral neutralizing antibody titers and cellular immunity in multiple dose immunization regimens given subcutaneously. No strong differences from un-adjuvanted protein were identified however. Single dose intranasal immunizations show stronger responses as compared to subcutaneous regimens however the

antibody response waned at later time points. Further evaluation of dosages of these designed vaccines are warranted in conjunction with influenza challenge models.

6. References

[1] Khan K, Arino J, Hu W, Raposo P, Sears J, Calderon F, et al. Spread of a novel influenza A (H1N1) virus via global airline transportation. New England Journal of Medicine 2009;361(2):212-4.

[2] Zhao X, Sun Y, Pu J, Fan L, Shi W, Hu Y, et al. Characterization of an artificial swine-origin influenza virus with the same gene combination as H1N1/2009 Virus: A genesis clue of pandemic strain. PLoS ONE 2011;6(7):e22091.

[3] Lee C-Y, Chuang Y-F, Huang W-Y, Cheng S-H, Pei J-S. Epidemiology, clinical features, treatment, and outcomes of cases of influenza A infection during the 2009 influenza pandemic in northern Taiwan. Pediatrics & Neonatology 2012;53(4):257-63.

[4] Tang JW, Shetty N, Lam TTY, Hon KLE. Emerging, novel, and known influenza virus infections in humans. Infectious Disease Clinics of North America 2010;24(3):603-17.

[5] Molinari N-AM, Ortega-Sanchez IR, Messonnier ML, Thompson WW, Wortley PM, Weintraub E, et al. The annual impact of seasonal influenza in the US: Measuring disease burden and costs. Vaccine 2007;25(27):5086-96.

[6] de Jong MD, Cam BV, Qui PT, Hien VM, Thanh TT, Hue NB, et al. Fatal avian influenza A (H5N1) in a child presenting with diarrhea followed by coma. New England Journal of Medicine 2005;352(7):686-91.

[7] de Jong MD, Simmons CP, Thanh TT, Hien VM, Smith GJD, Chau TNB, et al. Fatal outcome of human influenza A (H5N1) is associated with high viral load and hypercytokinemia. Nature Medicine 2006;12(10):1203-7.

[8] Peiris JSM, de Jong MD, Guan Y. Avian influenza virus (H5N1):A threat to human health. Clinical Microbiology Reviews 2007;20(2):243-67.

[9] Morens DM, Subbarao K, Taubenberger JK. Engineering H5N1 avian influenza viruses to study human adaptation. Nature 2012;486(7403):335-40.

[10] Herfst S, Schrauwen EJA, Linster M, Chutinimitkul S, de Wit E, Munster VJ, et al. Airborne transmission of influenza A/H5N1 virus between ferrets. Science 2012;336(6088):1534-41.

[11] Keitel W, Groth N, Lattanzi M, Praus M, Hilbert AK, Borkowski A, et al. Dose ranging of adjuvant and antigen in a cell culture H5N1 influenza vaccine: Safety and immunogenicity of a phase 1/2 clinical trial. Vaccine;28(3):840-8.

[12] Leroux-Roels I, Roman F, Forgus S, Maes C, De Boever F, Dramé M, et al. Priming with AS03A-adjuvanted H5N1 influenza vaccine improves the kinetics, magnitude and durability of the immune response after a heterologous booster vaccination: An open non-randomised extension of a double-blind randomised primary study. Vaccine;28(3):849-57.

[13] Kistner O, Howard MK, Spruth M, Wodal W, Brühl P, Gerencer M, et al. Cell culture (Vero) derived whole virus (H5N1) vaccine based on wild-type virus strain induces cross-protective immune responses. Vaccine 2007;25(32):6028-36.

[14] Ninomiya A, Imai M, Tashiro M, Odagiri T. Inactivated influenza H5N1 whole-virus vaccine with aluminum adjuvant induces homologous and heterologous protective immunities against lethal challenge with highly pathogenic H5N1 avian influenza viruses in a mouse model. Vaccine 2007;25(18):3554-60.

[15] (NIAID) NIoAaID. NIAID DNA vaccine for H5N1 avian influenza enters human trial. In: Services USDoHaH, editor. Bethesda, MD: NIAID News Office, 2007.

[16] Nolan T, Richmond PC, Formica NT, Höschler K, Skeljo MV, Stoney T, et al. Safety and immunogenicity of a prototype adjuvanted inactivated split-virus influenza A (H5N1) vaccine in infants and children. Vaccine 2008;26(50):6383-91.

[17] Ehrlich HJ, Muller M, Oh HML, Tambyah PA, Joukhadar C, Montomoli E, et al. A clinical trial of a whole-virus H5N1 vaccine derived from cell culture. New England Journal of Medicine 2008;358(24):2573-84.

[18] Carter NJ, Plosker GL. Prepandemic influenza vaccine H5N1 (Split Virion, Inactivated, Adjuvanted) [Prepandrix(TM)]: A review of its use as an active immunization against influenza A subtype H5N1 virus. BioDrugs 2008;22(5):279-92.

[19] Fan S, Gao Y, Shinya K, Li CK, Li Y, Shi J, et al. Immunogenicity and protective efficacy of a live attenuated H5N1 vaccine in nonhuman primates. PLoS Pathogens 2009;5(5):e1000409.

[20] Xie QM, Ji J, Du LQ, Cao YC, Wei L, Xue CY, et al. Preparation and immune activity analysis of H5N1 subtype avian influenza virus recombinant protein-based vaccine. Poultry Science 2009;88(8):1608-15.

[21] Palache B, Krause R. Progress with human H5N1 vaccines: a perspective from industry. Expert Review of Vaccines 2009;8(4):391-400.

[22] Torres MP, Determan AS, Mallapragada SK, Narasimhan B. Polyanhydrides. In: Lee S, editor. Encyclopedia of Chemical Processing. New York: Marcell Dekker, 2005.

[23] Jain JP, Modi S, Domb AJ, Kumar N. Role of polyanhydrides as localized drug carriers. Journal of Controlled Release 2005;103(3):541-63.

[24] Torres MP, Vogel BM, Narasimhan B, Mallapragada SK. Synthesis and characterization of novel polyanhydrides with tailored erosion mechanisms. Journal of Biomedical Materials Research Part A 2006;76A(1):102-10.

[25] Torres MP, Determan AS, Anderson GL, Mallapragada SK, Narasimhan B. Amphiphilic polyanhydrides for protein stabilization and release. Biomaterials 2007;28(1):108-16.

[26] Torres MP, Wilson-Welder JH, Lopac SK, Phanse Y, Carrillo-Conde B, Ramer-Tait AE, et al. Polyanhydride microparticles enhance dendritic cell antigen presentation and activation. Acta biomaterialia 2011;7(7):2857-64.

[27] Petersen LK, Ramer-Tait AE, Broderick SR, Kong C-S, Ulery BD, Rajan K, et al. Activation of innate immune responses in a pathogen-mimicking manner by amphiphilic polyanhydride nanoparticle adjuvants. Biomaterials 2011;32(28):6815-22.

[28] Ulery B, Phanse Y, Sinha A, Wannemuehler M, Narasimhan B, Bellaire B. Polymer chemistry influences monocytic uptake of polyanhydride nanospheres. Pharmaceutical Research 2009;26(3):683-90.

[29] Ulery BD, Petersen LK, Phanse Y, Kong CS, Broderick SR, Kumar D, et al. Rational design of pathogen-mimicking amphiphilic materials as nanoadjuvants. Scientific Reports 2011;1.

[30] Kipper MJ, Wilson JH, Wannemuehler MJ, Narasimhan B. Single dose vaccine based on biodegradable polyanhydride microspheres can modulate immune response mechanism. Journal of Biomedical Materials Research Part A 2006;76A(4):798-810.

[31] Ulery BD, Kumar D, Ramer-Tait AE, Metzger DW, Wannemuehler MJ, Narasimhan B. Design of a protective single-dose intranasal nanoparticle-based vaccine platform for respiratory infectious diseases. PLoS ONE 2011;6(3):e17642.

[32] Conix A. Poly[1,3-bis(p-carboxyphenoxy)-propane anhydride]. Macro Synth 1966(2):95-8.

[33] Rasband WS. ImageJ. 1.44 ed. Bethesda, Maryland, USA: U. S. National Institutes of Health.

[34] Chavez-Santoscoy AV, Huntimer LM, Ramer-Tait AE, Wannemuehler M, Narasimhan B. Harvesting murine alveolar macrophages and evaluating cellular activation induced by polyanhydride nanoparticles. Journal of Visualized Experiments 2012(64):e3883.

[35] Lin S-C, Huang M-H, Tsou P-C, Huang L-M, Chong P, Wu S-C. Recombinant trimeric HA protein immunogenicity of H5N1 avian influenza viruses and their combined use with inactivated or adenovirus vaccines. PLoS ONE 2011;6(5):e20052.

[36] Kumar N, Langer RS, Domb AJ. Polyanhydrides: an overview. Advanced Drug Delivery Reviews 2002;54(7):889-910.

[37] Kipper MJ, Shen E, Determan A, Narasimhan B. Design of an injectable system based on bioerodible polyanhydride microspheres for sustained drug delivery. Biomaterials 2002;23(22):4405-12.

[38] Determan AS, Trewyn BG, Lin VSY, Nilsen-Hamilton M, Narasimhan B. Encapsulation, stabilization, and release of BSA-FITC from polyanhydride microspheres. Journal of Controlled Release 2004;100(1):97-109.

[39] Determan AS, Wilson JH, Kipper MJ, Wannemuehler MJ, Narasimhan B. Protein stability in the presence of polymer degradation products: Consequences for controlled release formulations. Biomaterials 2006;27(17):3312-20.

[40] Lopac SK, Torres MP, Wilson-Welder JH, Wannemuehler MJ, Narasimhan B. Effect of polymer chemistry and fabrication method on protein release and stability

from polyanhydride microspheres. Journal of Biomedical Materials Research Part B: Applied Biomaterials 2009;91B(2):938-47.

[41] Carrillo-Conde B, Schiltz E, Yu J, Chris Minion F, Phillips GJ, Wannemuehler MJ, et al. Encapsulation into amphiphilic polyanhydride microparticles stabilizes Yersinia pestis antigens. Acta biomaterialia 2010;6(8):3110-9.

[42] Petersen LK, Phanse Y, Ramer-Tait AE, Wannemuehler MJ, Narasimhan B. Amphiphilic polyanhydride nanoparticles stabilize *Bacillus anthracis* protective antigen. Molecular Pharmaceutics 2012;9(4):874-82.

[43] Wilson-Welder JH, Torres MP, Kipper MJ, Mallapragada SK, Wannemuehler M, Narasimhan B. Vaccine adjuvants: Current challenges and future approaches. Journal of Pharmaceutical Sciences 2009;98(4):1278-316.

[44] Huntimer L, Ramer-Tait A, Petesen L, Ross K, Walz K, Wang C, et al. Evaluation of biocompatibility and administration site reactogenicity of polyanhydride-particle based platform for vaccine delivery. Advanced Healthcare Materials 2012;In Press.

[45] Buchy P, Mardy S, Vong S, Toyoda T, Aubin J-T, Miller M, et al. Influenza A/H5N1 virus infection in humans in Cambodia. Journal of Clinical Virology 2007;39(3):164-8.

[46] Writing Committee of the Second World Health Organization Consultation on Clinical Aspects of Human Infection with Avian Influenza A Virus. Update on avian influenza A (H5N1) virus infection in humans. New England Journal of Medicine 2008;358(3):261-73.

CHAPTER 8: CONCLUSIONS

Lucas Huntimer

Conclusions:

The polyanhydride particle vaccine platform *displays characteristics associated* with efficacious adjuvanted vaccines. The particle platform provides a particulate context facilitating phagocytosis by antigen presenting cells (APCs) [1-4]. The encapsulation of protein in the polyanhydride materials results in a profile that can be tuned using chemistry to increase or decrease rate of protein release [5-11]. Polyanhydride materials possess abilities to non-specifically activate APCs leading to inflammatory cytokine secretion and costimulatory receptor upregulation [1-4, 11-14]. Those innate activating abilities could theoretically be attributed to repetitive structures of the copolymer materials used to fabricate the materials [15]. The platform also exhibits depot effects after parenteral administration in vivo allowing for extended persistence (Chapter 4).

Those requisites of vaccine design have evolved in parallel with biomaterials applicability for vaccine delivery options. Refinement in fabrication techniques have allowed for fabrication of particles of various sizes and diameters ranging from micrometers to nanometers (Chapter 3 and 4). Unless specifically prepared, these particle preparations are generally polydispersed populations relative to particle diameters. Monodisperse particles may provide a tighter phagocytosis target for APCs. Monodisperse populations will allow for greater insight into the in vivo intracellular and extracellular dynamics. Ongoing efforts in the laboratory to refine

monodisperse fabrication processes and study these particles in the context of intranasal delivery are ongoing. Efficacy studies comparing monodisperse versus polydisperse particle preparations are needed to determine if polydisperse sizes contribute to increased cellular and humoral immune responses or if monodisperse size populations do. Specifically testing the hypothesis of different sizes and chemistries affecting uptake allowing for generation of cellular immunity (Chapter 5) compared to chemistries with less uptake (50:50 CPTEG:CPH) leading to greater humoral immunity to do ability to persist in extracellular environments and ligate surface receptors in the lymph node (Chapter 6).

The aspect of repetitive structure between polydispersed and monodispersed particle preparations also needs to be examined. As of yet, all repetitive structure aspects associated with the particles have been theoretical. Dependent on molar combinations, that the copolymer combinations of CPH, SA, and CPTEG would create a particle of repetitive structure. Combined with that principle is the aspect of antigen encapsulation and surface modifications creating a repetitive structure that may lead to increased receptor ligation thus translating to phagocytosis by APCs or activation of B cells via crosslinking of surface B cell receptors. Additionally, scanning electron microscopy of degrading particles and visualizing the surface is needed

Design of vaccines incorporating the encapsulation of subunit (I.e., recombinant) immunogens in polyanhydride nanpoparticles needs to be refined. Early studies examining the immune response of vaccines with the total amount of antigen encapsulated into the nanoparticles revealed that the onset and peak titer of

the resultant antibody response was delayed [16, 17]. For studies involving design of an efficacious vaccine against *Yersinia pestis*, the most efficacious vaccines were combination vaccines of soluble antigen plus encapsulated antigen at a ratio of 4:1, respectively This ratio dictated design of the vaccines in this thesis. When designing vaccines, the pathogenesis of the target pathogen and the antigen should be the first factors in dictating dosages. Host factors such as age, health, and population susceptibility also need to be considered. The inclusion of encapsulated portions of the antigen dose and how encapsulation may reduce dosages after that needs to be examined both in model antigens and pathogen antigens. In turn, exact antigen availability in vivo must be identified using sensitive protein labeling techniques. The studies outlined in Chapter 4 demonstrate the presence of particles in vivo and how the different chemistries influence degradation in vivo. This does not account for antigen encapsulated in the particles, however.

Enhancement of immune responses from nanoparticle vaccines is most likely due to multiple attributes of the particles. While encapsulation of the antigen will alter the kinetics of the interaction between the host and the antigen and persistence in vivo, the particles also possess innate immunomodulatory activity associated with activation of dendritic cells and macrophages (Chapter 5 and [1-3, 13, 14, 18]). The contribution of the immunomodulation of the innate immune system and how this influences cellular and humoral immune responses should be characterized with experiments involving multiple doses of particles in a fixed antigen regimen. These experiments can also involve examining gene changes at the sites of administration using multiple gene arrays to correlate with the in vitro gene changes in

macrophages presented in Chapter 5. Specifically the innate immune receptor interactions that are upregulated (TLRs) and STAT1 signaling that may contribute to understanding of how innate immune cells interact with particles in vivo.

Particulate antigen delivery and how the particles are trafficked to draining lymph nodes also warrant examination as improving or dictating trafficking can be a mechanism of improving immune responses to polyanhydride particle immunizations. Preliminary microscopy studies attempting to stain for antigen in the lymph nodes at different time points early after immunization provided insight into particle localization within the structure of the lymph node but those experiments need refinement although staining for donor congenic receptors verified the antigen specific T cell expansion identified by FACS (Chapter 5 and 6) and thus allowing for localization in the context of overall structure in the lymph node. Also having built genetic reporter populations of mice (Chapter 5) and using those animals to examine localization of T cells to particles in vivo using multi-photon microscopy or confocal microscopy will provide answers to hypothesis posed involving particle and antigen availability allowing test hypothesis regarding antigen persistence being increased in the lymph nodes by polyanhydride particles, interactions of APCs to the particles in the lymph nodes, and further expansion of antigen specific populations following polyanhydride particle immunizations in secondary lymphoid organs.

In summation, the data presented within this dissertation describes the adaptive immune responses, cellular and humoral, elicited by vaccines designed using the polyanhydride particle platform as the delivery system. Using those principles, we designed H5 influenza nanoparticle-based vaccines containing the

recombinant H5 hemagglutinin from the influenza virus (H5 A/Whooper Swan/244/Mongolia/05 and characterized the resultant immune responses induced by these vaccine regimen. Humoral responses were strong throughout all groups including unadjuvanted antigen vaccines suggesting the polyanhydride particles show the ability to elicit humoral immunity while simultaneously increasing cellular immunity following parenteral administration with a TLR receptor agonist (Chapter 7). Finally, challenge studies involving influenza virus expressing heterologous and homologous hemagglutinin sequences are warranted to fully examine the protection elicited from the polyanhydride nanoparticle vaccines. The studies here and future studies will build the portfolio needed for this platform to be used in translational medicine.

References:

[1] Ulery B, Phanse Y, Sinha A, Wannemuehler M, Narasimhan B, Bellaire B. Polymer Chemistry Influences Monocytic Uptake of Polyanhydride Nanospheres. Pharmaceutical Research 2009;26(3):683-90.

[2] Petersen LK, Xue L, Wannemuehler MJ, Rajan K, Narasimhan B. The simultaneous effect of polymer chemistry and device geometry on the in vitro activation of murine dendritic cells. Biomaterials 2009;30(28):5131-42.

[3] Torres MP, Wilson-Welder JH, Lopac SK, Phanse Y, Carrillo-Conde B, Ramer-Tait AE, et al. Polyanhydride microparticles enhance dendritic cell antigen presentation and activation. Acta biomaterialia 2011;7(7):2857-64.

[4] Petersen LK, Ramer-Tait AE, Broderick SR, Kong C-S, Ulery BD, Rajan K, et al. Activation of innate immune responses in a pathogen-mimicking manner by

amphiphilic polyanhydride nanoparticle adjuvants. Biomaterials 2011;32(28):6815-22.

[5] Determan AS, Trewyn BG, Lin VSY, Nilsen-Hamilton M, Narasimhan B. Encapsulation, stabilization, and release of BSA-FITC from polyanhydride microspheres. Journal of Controlled Release 2004;100(1):97-109.

[6] Torres MP, Determan AS, Mallapragada SK, Narasimhan B. Polyanhydrides. In: Lee S, editor. Encyclopedia of Chemical Processing. New York: Marcell Dekker, 2005.

[7] Determan A, Graham JR, Pfeiffer KA, Narasimhan B. The role of microsphere fabrication methods on the stability and release kinetics of ovalbumin encapsulated in polyanhydrice microspheres. Journal of Microencapsulation 2006;23(8):832-43.

[8] Torres MP, Determan AS, Anderson GL, Mallapragada SK, Narasimhan B. Amphiphilic polyanhydrides for protein stabilization and release. Biomaterials 2007;28(1):108-16.

[9] Lopac SK, Torres MP, Wilson-Welder JH, Wannemuehler MJ, Narasimhan B. Effect of polymer chemistry and fabrication method on protein release and stability from polyanhydride microspheres. Journal of Biomedical Materials Research Part B: Applied Biomaterials 2009;91B(2):938-47.

[10] Carrillo-Conde B, Schiltz E, Yu J, Chris Minion F, Phillips GJ, Wannemuehler MJ, et al. Encapsulation into amphiphilic polyanhydride microparticles stabilizes Yersinia pestis antigens. Acta biomaterialia 2010;6(8):3110-9.

[11] Ulery BD, Petersen LK, Phanse Y, Kong CS, Broderick SR, Kumar D, et al. Rational Design of Pathogen-Mimicking Amphiphilic Materials as Nanoadjuvants. Sci Rep 2011;1.

[12] Carrillo-Conde B, Ramer-Tait A, Wannemuehler M, Narasimhan B. Chemistry-dependent adsorption of serum proteins onto polyanhydride microparticles differentially influences dendritic cell uptake and activation. Acta Biomater 2012.

[13] Chavez-Santoscoy AV, Huntimer LM, Ramer-Tait AE, Wannemuehler M, Narasimhan B. Harvesting Murine Alveolar Macrophages and Evaluating Cellular Activation Induced by Polyanhydride Nanoparticles. J Vis Exp 2012(64):e3883.

[14] Chavez-Santoscoy AV, Roychoudhury R, Pohl NL, Wannemuehler MJ, Narasimhan B, Ramer-Tait AE. Tailoring the immune response by targeting C-type lectin receptors on alveolar macrophages using "pathogen-like" amphiphilic polyanhydride nanoparticles. Biomaterials 2012;33(18):4762-72.

[15] Albertsson A-c, Karlsson S. Macromolecular Architecture-Nature as a Model for Degradable Polymers. Journal of Macromolecular Science, Part A 1996;33(10):1565-70.

[16] Kipper MJ, Wilson JH, Wannemuehler MJ, Narasimhan B. Single dose vaccine based on biodegradable polyanhydride microspheres can modulate immune response mechanism. Journal of Biomedical Materials Research Part A 2006;76A(4):798-810.

[17] Huntimer L, Wilson Welder JH, Ross K, Carrillo-Conde B, Pruisner L, Wang C, et al. Single immunization with a suboptimal antigen dose encapsulated into polyanhydride microparticles promotes high titer and avid antibody responses. J Biomed Mater Res B Appl Biomater 2013;101(1):91-8.

[18] Mallapragada SK, Narasimhan B. Immunomodulatory biomaterials. International Journal of Pharmaceutics 2008;364(2):265-71.

APPENDIX

Harvesting Alveolar Macrophages and Evaluating Cellular Activation Induced by Polyanhydride Nanoparticles

Ana V. Chavez-Santoscoy, Lucas M. Huntimer, Amanda E. Ramer-Tait, Michael Wannemuehler, and Balaji Narasimhan

Published in the Journal of Visualized Experiments

Abstract:

Technological aspects of vaccine design are undergoing a revolution. New information regarding the molecular and cellular processes of innate immune cells is providing important insight as to how immune responses towards pathogens are generated. In order to elucidate the mechanisms regulating the activation of innate immunity following intranasal mucosal vaccination, one must evaluate alveolar macrophage responses. These cells are a critical antigen presenting cell type in the lung [1]. Alveolar macrophages are frontline innate defenders of the pulmonary mucosa and are highly efficient in clearing the lungs of microbial pathogens and cell debris[2, 3]. In addition, alveolar macrophages transport microbial antigens to the draining lymph nodes, which is an important first step in the initiation of an adaptive immune response[4].

In this context, biodegradable nanoparticles have emerged as a versatile platform for the design and implementation of new intranasal vaccines against respiratory infectious diseases. Specifically, polyanhydride nanoparticles composed of the aliphatic sebacic acid (SA), the aromatic 1,6-bis(p-carboxyphenoxy)hexane (CPH),

or the amphiphilic 1,8-bis(p-carboxyphenoxy)-3,6-dioxaoctane (CPTEG) display unique bulk and surface erosion kinetics [5, 6]. These particles can be exploited to slowly release functional biomolecules (e.g., protein antigens, immunoglobulins) in vivo [7-9]. Alveolar macrophages are highly phagocytic, have increased amounts of innate pattern recognition and scavenger receptors, and secrete pro-inflammatory mediators when engaged[2, 10]. The population of alveolar macrophages is greater than 80% of the total cells obtained by lung lavage. Resident alveolar macrophages harvested from immune competent animals provide a representative macrophage phenotype of the cells that will encounter the particle-based vaccine in vivo. Herein, we describe the protocols used to harvest and culture alveolar macrophages from mice and examine the phenotype of the macrophages after treatment with polyanhydride nanoparticles in vitro with the purpose of evaluating the cellular activation of these cells.

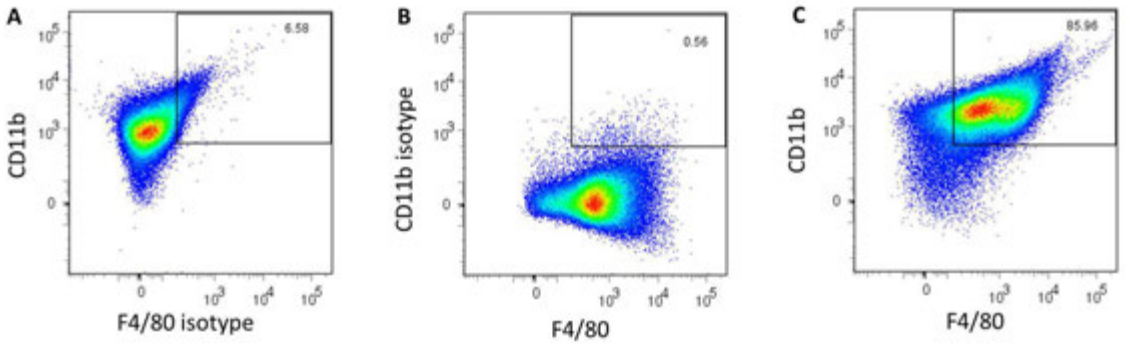

Figure 2. Flow cytometric analysis of harvested alveolar macrophages labeled with (A) Alexa Fluor 700 anti-CD11b and the PE-Cy7 FMO Control, (B) Alexa Fluor 700 FMO Control and the PE-Cy7 anti-F4/80 and (C) Alexa Fluor 700 anti-CD11b and PE-Cy7 anti-F4/80. The number in the top right corner represents the percentage of double-positive cells.

Combinatorial Evaluation of In Vivo Distribution of Polyanhydride Particle-based Platforms for Vaccine Delivery

Latrisha K. Petersen, Lucas Huntimer, Katharine Walz, Amanda Ramer-Tait, Michael J. Wannemuehler, and Balaji Narasimhan

Submitted to Nanomedicine

Abstract

Several challenges are associated with current vaccine strategies, including repeated immunizations, poor patient compliance, and limited approved routes for delivery, which may hinder induction of protective immunity. Thus, there is a need for new vaccine adjuvants capable of multi-route administration and prolonged antigen release at the site of administration by providing a depot within tissue. In this work, we designed a combinatorial platform to investigate the *in vivo* distribution, depot effect, and localized persistence of polyanhydride nanoparticles as a function of nanoparticle chemistry and administration route. Our observations indicated that the route of administration differentially affected tissue residence times. All nanoparticles rapidly dispersed when delivered intranasally but provided a depot when administered parenterally. When amphiphilic and hydrophobic nanoparticles were administered intranasally, they persisted within lung tissue. These results provide insights into the chemistry- and route-dependent distribution and tissue-specific association of polyanhydride nanoparticle-based vaccine adjuvants.

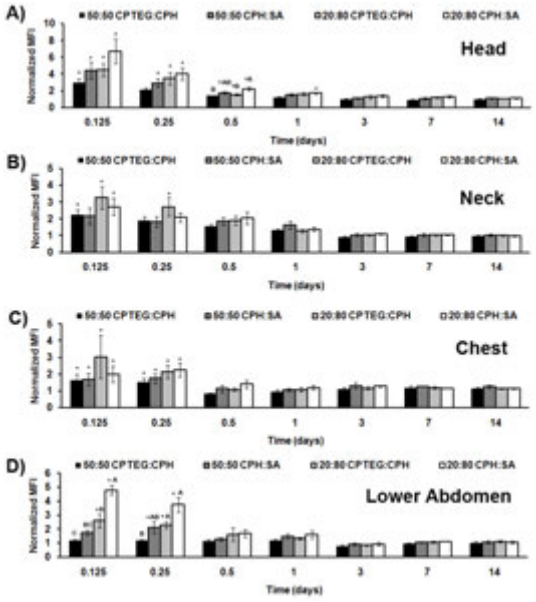

Figure 5. Chemistry played an important role in nanoparticle distribution throughout the body. ROI analysis is depicted in Figure 4 for (A) nasal passage, (B) neck, (C) chest, and (D) abdomen. The 20:80 CPH:SA nanoparticles show significantly greater fluorescence in the lower abdomen at initial time points (3 h). MFI values for all treatment groups were normalized to the saline control (saline normalized MFI = 1). Letters indicate statistical significance between each treatment group and asterisks indicate statistical significance (p-value < 0.05) from the saline control, n = 3 for all groups.

Impact of antibiotics on the susceptibility to inflammatory insults: lessons from defined and conventional microbiota mice

Anne-Marie C. Overstreet, Amanda E. Ramer-Tait, Jesse Hostetter, Chong Wang, Lucas M. Huntimer, Michael J. Wannemuehler

Abstract

The gastrointestinal tract harbors bacteria on which the body depends on for a variety of functions such as vitamin production and energy storage. This community is susceptible to changes from environmental factors such as antibiotics. The effect of the antibiotic on the microbial community lasts longer than the duration of treatment and in some cases the community may never fully re-establish itself. When the community deviates from normal it becomes dysbiotic, which may lead to the development of diseases such as inflammatory bowel disease. We report here the study of two intestinal microbial communities to identify differences in disease severity in response to a DSS-induced model of murine colitis. ASF and CONV mice were given 4 mg/mL of ampicillin for nine days. Mice were then colonized with *Helicobacter bilis* for two weeks. Then either a 1.5 % (ASF) or 2.5 % (CONV) dextran sulfate sodium solution was added to their drinking water for five days followed by a 4 day restitution period. The results of this study revealed major differences in the inflammatory response after the induction of colitis. The administration of ampicillin caused the ASF mice to gain significantly less weight during the study compared to their CONV counterparts. Macropscopic and microscopic lesions within the two communities showed no change in score when

comparing ampicillin *H. bilis* DSS (AhbD) and *H. bilis* DSS (Hbd). Ampicillin administration modulated the microbiota of the ASF mice much more drastically compared to the CONV mice. In the ASF mice, 4 of the 8 species present in the community were significantly reduced at the end of the study. ASF mice produced significantly higher levels of pro-inflammatory cytokines compared to the CONV mice and also produced significantly more antibody against members of the microbiota. CONV mice had an increased concentration of several diabetes biomarkers, something not seen in the ASF mice.

The results of this study reveal that the severity of the immune response to colitic insults is microbiota specific. Mice with a simplified microbiota had increased antibody responses to the microbiota and increased pro-inflammatory cytokine/chemokine production. CONV mice, which had only a minimal inflammatory response, had an increase in diabetic biomarkers indicating that these mice were entering into a metabolic syndrome-like state.

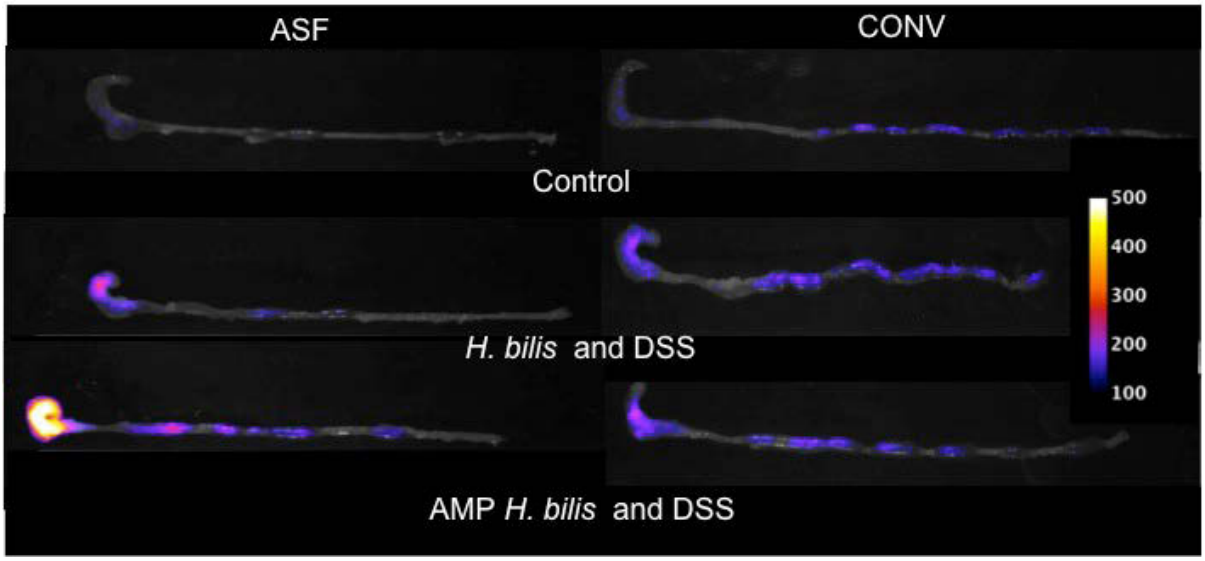

Figure 6. Both ASF and CONV mice have increased inflammation when given the colitic insult of *H. bilis* and DSS. Giving ampicillin preceding the inflammatory insult increases inflammation in the ASF mice only.This is revealed by increased fluorescence intensity present only in the cecum of the ASF mice given ampicillin, colonized with *H.bilis* and treated with DSS.

The effects of *Prunella vulgaris* and *Hypericum gentianoides* whole extract on DSS induced colitis in C3H/HeN mice

Anne-Marie C. Overstreet, Amanda E. Ramer-Tait, Jesse Hostetter, Lucas M. Huntimer, Cathy Hauck, Pat Murphy, Michael J. Wannemuehler

Abstract

The morbidity and expense of traditional inflammatory bowel disease (IBD) treatments have led patients to explore alternative therapeutic options. Over 50 % of IBD patients have used alternative or complementary prebiotic treatments. Botanical supplements represent a subset of alternative therapies of potential value for IBD patients. Additional research is needed to identify the potential biological activity and

safety of these products. Ethanolic extracts of the botanicals *Prunella vulgaris* and *Hypericum gentianoides* possess anti-inflammatory and/or anti-microbial activities; however, limited information exists regarding its efficacy as a treatment for IBD. Using mice with a defined microbiota (the altered Schaedler flora or ASF), we have established a colitis model that mimics human IBD and enables us to elucidate the roles of both the host and its microbiota in the progression of disease and the response to nutraceutical treatment. Despite the purported anti-inflammatory effects of *P. vulgaris* and *H. gentianoides*, neither extract was able to significantly lessen disease severity. There was no significant difference in microscopic lesion scores between any of the treatment groups. Use of an inflammatory probe to measure inflammation *in situ* also revealed no significant difference between the groups, but there was a decrease in the fluorescence intensity in mice treated with *H. gentianoides* indicating the potential for an anti-inflammatory effect with that botanical. Increased production of the pro-inflammatory cytokines and chemokines, KC, IL-5, LIX, and RANTES in mice given *P. vulgaris* was not observed in the mice treated with *H. gentianoides.* Mice administered *H. gentianoides* did have a substantial modulation of their gastrointestinal microbial community as *H. gentianoides* treatment resulted in a significant decrease in four of the eight members of the ASF. *P. vulgaris* had no effect on the bacterial population. In summary, there was no significant amelioration of disease severity in this mouse model of colitis. The presented data do suggest, however, that there may be benefit to the use for *H. gentianoides* in the modulation of the gastrointestinal microbial

community. Further studies are warranted to determine the specific compounds associated with this anti-bacterial activity.

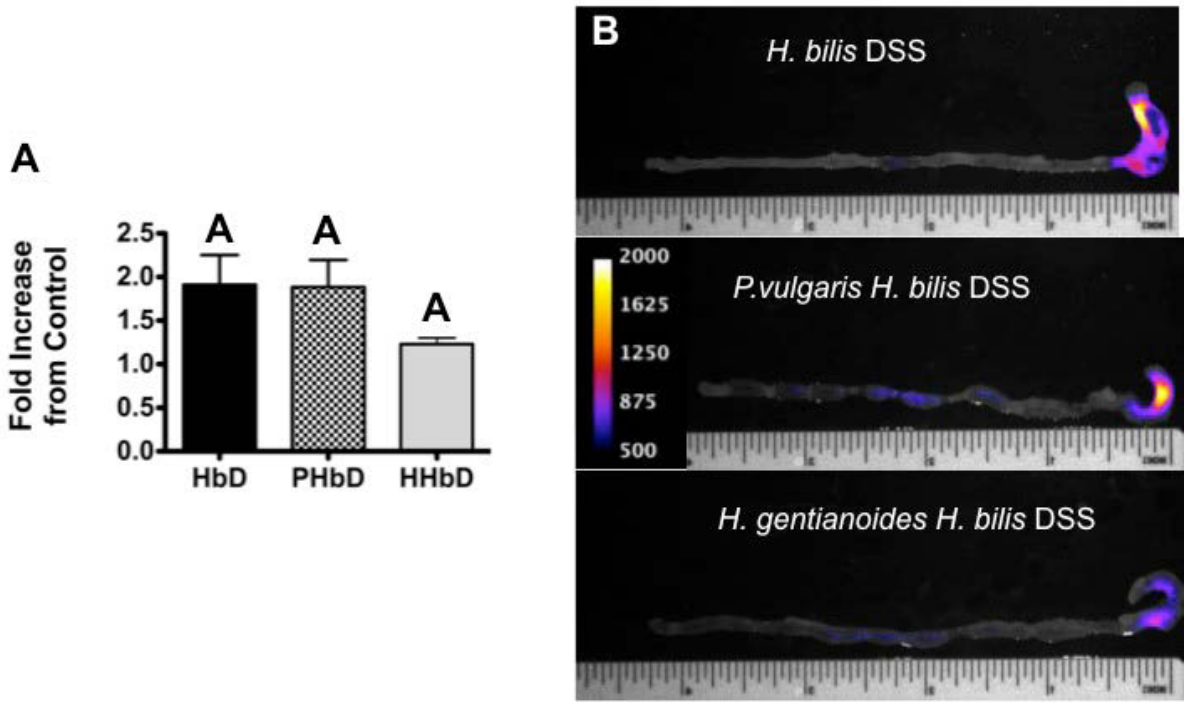

Figure 3. Mice treated with botanical have no difference in cecal inflammation compared to *H. bilis* DSS mice. A) Fold increase of mean fluorescence intensity of treatment compared to naïve control who received no treatment. B) *Ex vivo* images of representative ceca from the three treatment groups analyzed during the study. Data are expressed as mean + SEM. Dissimilar letters indicate $p < 0.05$, while similar letter indicate no significant difference.

Untitled project involving antibiotic delivery using the polyanhydride nanoparticle delivery platform

Antibiotics effective in combating *Brucella* infection were encapsulated into polyanhydride nanoparticles as well as a fluorescent marker to track tissue

distribution in vivo. At time of necropsy we utilized in vivo imaging of ex vivo tissues to quantify biodistribution of the particles given in therapeutic regimens in mice infected with *Brucella*.

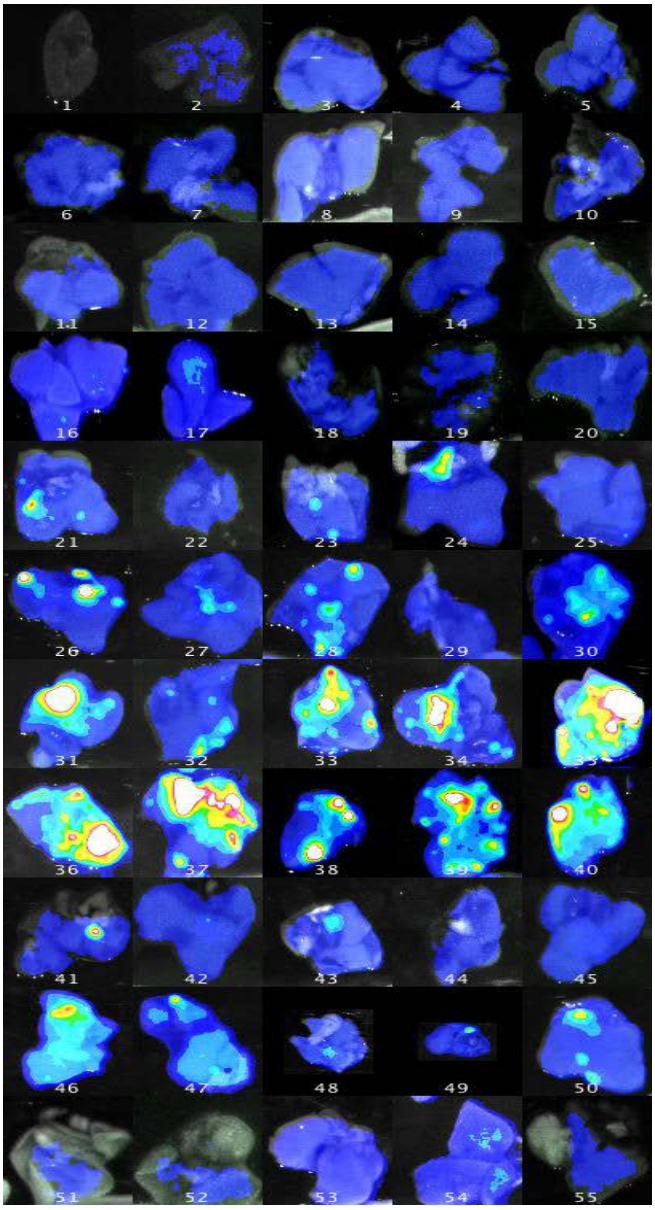

Figure 1. Ex vivo liver images of co-administration of antibiotic with Rhodamine Red either given in a soluble form or encapsulated in polyanhydride nanoparticles. Mice infected with Brucella were given high doses of doxycycline antibiotic either in a soluble form (Images 11-20), encapsulated in multiple polayanhydride nanoparticle chemistries (21-55). Livers were excised and imaged using in vivo imaging techniques. Fluorescence was spectrally unmixed from negative controls. Fluorescent images were overlayed onto white light images for localization.

Untitled project involving dual hit model of colitis using H. bilis or E. coli and DSS to examine inflammation in distinct tissues

A dual hit model of colitis was developed utilizing colonization of mice with E. coli and then adding an inflammatory insult of an epithelial toxin. These mice were administered an inflammatory probe that was optically active in sites of inflammation. Excised cecum and colon tissues at 3 weeks or 12 weeks post colonization were examined using in vivo imaging to localize points of inflammation at the end points of the study.

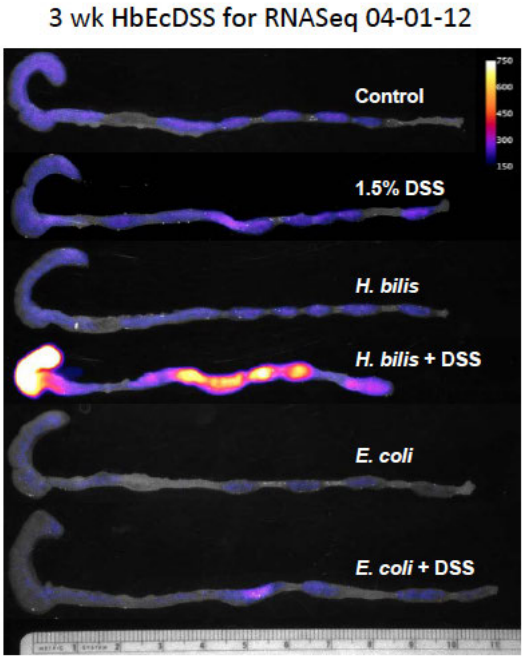

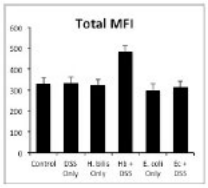

Mouse #s: 3, 8, 14, 15, 23, 26

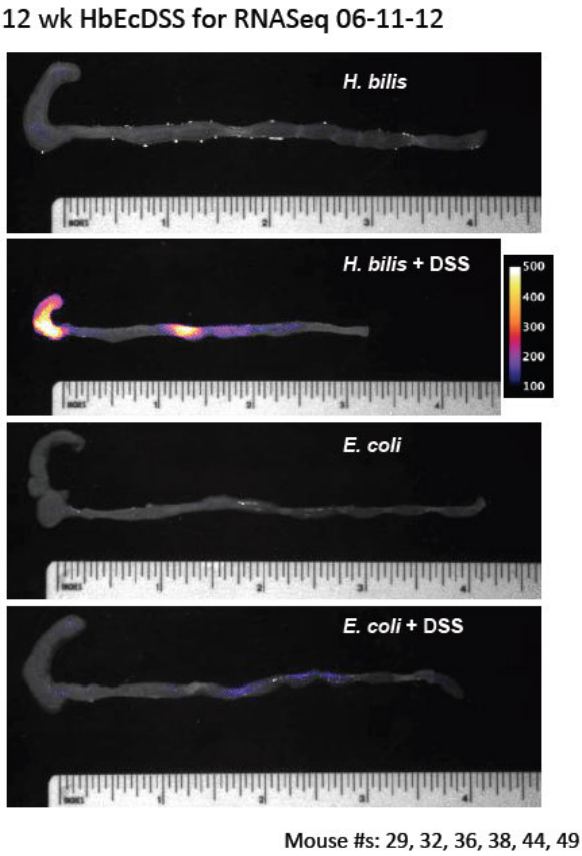

Recombinant trimeric influenza hemagglutinin elicits high level neutralization antibody

Wuwei Wu, Lucas Huntimer, Kathleen Ross, Balaji Narasimhan, Michael Wannemuehler, and Susan Carpenter

Immunization against the influenza virus remains the paramount preventive therapeutic measure to decrease morbidity and mortality in a population while minimizing economic impact at the same time [11, 12]. Influenza A virus is a single stranded, segmented, negative sense RNA virus that is highly susceptible to genetic

drift of its surface glycoproteins hemagglutinin (HA) and neuraminidase (NA) due to low fidelity RNA polymerase proofreading [13]. Therefore seasonal influenza A virus vaccines consist of multiple antigenic preparations of stains of virus that are predicted to be predominant in the upcoming influenza season [14]. Influenza viruses also possess the ability to genetically shift genetic components when different strains of virus co-infect a susceptible mammal. This particular genetic shift scenario presents global health implications in novel recombinations of influenza virus that the human population is naïve to as compared to traditional seasonal strains of the virus. In particular, human infection with highly pathogenic avian influenza virus (HPAI) H5N1 in which nearly 60% of hospitalized cases resulted in mortality attributed to hypercytokinemia [15-17]. Debate wages on the exact lethality of human infections with this predominantly avian circulating virus as proper immune surveillance of exposed humans in the areas where H5N1 is present is still incomplete [18]. Human to human transmission of the virus is limited due to the receptor fidelity towards the α 2-3 linked sialic acid motifs of avian species where the HA of influenza binds. Multiple passages of HPAI in a ferret model can lead to sufficient evolutionary pressure to force the virus to mutate towards ferret to ferret transmission [19, 20].

The surface glycoproteins HA and NA are the key antigenic targets of the immune response wherein an appropriate humoral response directed towards these targets can result in protective immunity. The lack of preexisting immunity against H5N1 as well as the potential morbidity and mortality of the virus point to the importance of efficacious vaccine preparations against the virus to prevent pandemic

spread. Typical seasonal influenza vaccine preparations require prediction of seasonal H1 and H3 strains that may be the most prominent during the particular influenza season. The viruses used for antigen are often propagated in embryonated eggs which require multiple passages as well 3- 6 months of lead time to prepare [21]. The efficacy of these vaccines are reliant on both preexisting immunity to previous H1 and H3 strains as wells as being the correct strains. The luxury of predicting which strains of H5N1 virus that would be dominant during a pandemic is difficult to gauge as the virus is predominantly of avian origin.

Recombinant production of the key HA antigens of H5N1 can effectively limit the production time of antigen production depending on scaling factors. Mammalian and insect cell culture production systems also add the benefit of glycosylation of the proteins important for neutralizing epitope generation [22]. Recombinant production of antigens also allows for ease in manipulation of antigens to create the proper context of the antigens that would recapitulate the structures identified by the immune system during a pathogenic infection. In particular HA exists as trimer on the virion surface of influenza therefore creating a complex where antibodies can be generated. Herein we identify production of a stabilized trimeric form of the HA of H5 A/Whooper Swan/244/Mongolia/ 05 (clade 2.2) in a baculovirus insect cell expression system using the GCN isoleucine zipper motif. The stabilized H5 trimer was successfully able to elicit neutralizing antibody titers using common human approved adjuvants in both a parenteral and a mucosal immunization route indicating efficacy of this antigenic production method for stockpiling of H5N1 pandemic vaccines.

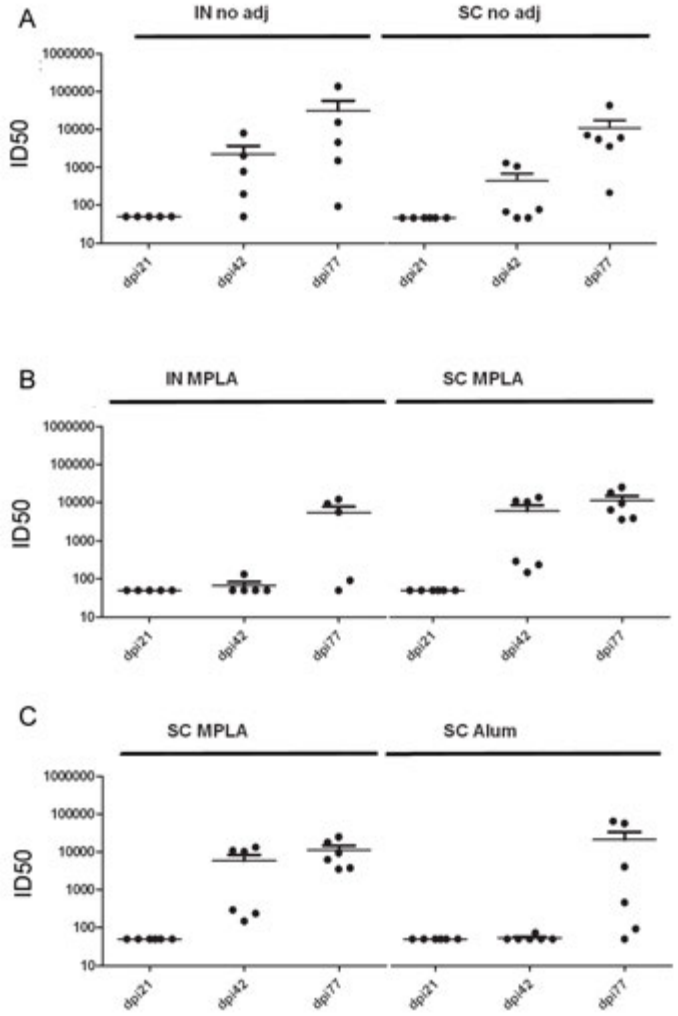

Figure 5. Serum neutralizing antibody titer from mice vaccinated with recombinant H5-T proteins through intranasal (IN) or subcutaneously (SC) at different days post-immunization (DPI) Pseudoviruses H5-WhooperLuc were used to titrate the serum neutralizing antibodies (NAbs) from vaccinated mice. A. Neutralizing antibody titer of serum NAbs from mice vaccinated with H5-T protein without adjuvant. B. Neutralizing antibody titer of serum NAbs from mice vaccinated with H5-T protein with MPLA adjuvant. C. Neutralizing antibody titer of serum NAbs from mice subcutaneously vaccinated with H5-T protein and different adjuvants.

Next Generation Pulmonary Adjuvants Integrating Biological Principles with New Technology for Improving Vaccines

Shannon Haughney, Tim Brenza, Lucas Huntimer, Michael Wannemuehler, Amanda Ramer-Tait, and Balaji Narasimhan

Abstract

Beginning vaccine design by Edward Jenner is centered on the principle of introducing or mimicking a mild pathogenic infection to train the immune system to protect against a subsequent severe pathogenic infection. As such, the optimal training regimen for the immune system against pathogens of different tissue tropisms is to mimic a pathogenic infection in that same tissue site. Respiratory pathogens remain the number one target to design preventive therapeutics against because of their ease of transmission, population dynamics of infection, and the social and economic impact. Constructing pulmonary vaccines that elicit immune responses in respiratory tissues while minimizing reactogenicity remains a lofty goal of biomedical research. Adjuvants provide the enhanced immune function against the antigen of interest but must straddle the line between engaging the immune system without over engagement leading to detrimental immunopathology. Insight into immunological mechanisms of innate and adaptive immunity has led to a myriad of different applications in pulmonary adjuvant design. Herein we attempt to outline, albeit non-exhaustively, and review advances in pulmonary adjuvants.

References:

[1] Rubins JB. Alveolar macrophages: wielding the double-edged sword of inflammation. American Journal of Respiratory and Critical Care Medicine 2003;167(2):103-4.

[2] Sun K, Gan Y, Metzger DW. Analysis of murine genetic predisposition to pneumococcal infection reveals a critical role of alveolar macrophages in maintaining the sterility of the lower respiratory tract. Infection and Immunity 2011;79(5):1842-7.

[3] Morimoto K, Amano H, Sonoda F, Baba M, Senba M, Yoshimine H, et al. Alveolar macrophages that phagocytose apoptotic neutrophils produce hepatocyte growth factor during bacterial pneumonia in mice. American Journal of Respiratory Cellular and Molecular Biology 2001;24(5):608-15.

[4] Kirby AC, Coles MC, Kaye PM. Alveolar macrophages transport pathogens to lung draining lymph nodes. The Journal of Immunology 2009;183(3):1983-9.

[5] Mallapragada SK, Narasimhan B. Immunomodulatory biomaterials. International Journal of Pharmacology 2008;364(2):265-71.

[6] Torres MP, Vogel BM, Narasimhan B, Mallapragada SK. Synthesis and characterization of novel polyanhydrides with tailored erosion mechanisms. Journal of Biomedical Materials Research: Part A 2006;76(1):102-10.

[7] Lopac SK, Torres MP, Wilson-Welder JH, Wannemuehler MJ, Narasimhan B. Effect of polymer chemistry and fabrication method on protein release and stability from polyanhydride microspheres. Journal of Biomedical Materials Research Part B: Applied Biomaterials 2009;91B(2):938-47.

[8] Torres MP, Determan AS, Anderson GL, Mallapragada SK, Narasimhan B. Amphiphilic polyanhydrides for protein stabilization and release. Biomaterials 2007;28(1):108-16.

[9] Ulery BD, Kumar D, Ramer-Tait AE, Metzger DW, Wannemuehler MJ, Narasimhan B. Design of a protective single-dose intranasal nanoparticle-based vaccine platform for respiratory infectious diseases. PLoS ONE 2011;6(3):e17642.

[10] Gordon S, Taylor PR. Monocyte and macrophage heterogeneity. Nature Reviews Immunology 2005;5(12):953-64.

[11] Cox NJ, Subbarao K. Global epidemiology of influenza: Past and present. Annual Review of Medicine 2000;51(1):407-21.

[12] Cox NJ, Subbarao K. Influenza. The Lancet 1999;354(9186):1277-82.

[13] Palese P, Shaw ML. Orthomyxoviridae: the viruses and their replication. In: Knipe DM, Howley PM, editors. Fields Virology. 5th ed. Philadelphia, PA: Lippincott-Raven Publishers, 2007: 1647-89.

[14] Cox RJ, Brokstad KA, Ogra P. Influenza virus: Immunity and vaccination strategies. Comparison of the immune response to inactivated and live, attenuated influenza vaccines. Scandinavian Journal of Immunology 2004;59(1):1-15.

[15] de Jong MD, Cam BV, Qui PT, Hien VM, Thanh TT, Hue NB, et al. Fatal avian influenza A (H5N1) in a child presenting with diarrhea followed by coma. New England Journal of Medicine 2005;352(7):686-91.

[16] de Jong MD, Simmons CP, Thanh TT, Hien VM, Smith GJD, Chau TNB, et al. Fatal outcome of human influenza A (H5N1) is associated with high viral load and hypercytokinemia. Nature Medicine 2006;12(10):1203-7.

[17] Peiris JSM, de Jong MD, Guan Y. Avian influenza virus (H5N1):A threat to human health. Clinical Microbiology Reviews 2007;20(2):243-67.

[18] Racaniello VR. Science Should Be in the Public Domain. mBio 2012;3(1).

[19] Morens DM, Subbarao K, Taubenberger JK. Engineering H5N1 avian influenza viruses to study human adaptation. Nature 2012;486(7403):335-40.

[20] Herfst S, Schrauwen EJA, Linster M, Chutinimitkul S, de Wit E, Munster VJ, et al. Airborne transmission of influenza A/H5N1 virus between ferrets. Science 2012;336(6088):1534-41.

[21] Fleming D. Influenza pandemics and avian flu. BMJ 2005;331(7524):1066-9.

[22] Cox MM, Patriarca PA, Treanor J. FluBlok, a recombinant hemagglutinin influenza vaccine. Influenza and Other Respiratory Viruses 2008;2(6):211-9.